МИСИС
УНИВЕРСИТЕТ

eISSN 2500-0632

Mining Science and Technology

Горные науки и технологии

Vol. / Том 9 № 4
2024

https://mst.misis.ru/
https://t.me/MinSciTech

MINING SCIENCE AND TECHNOLOGY (Russia)

Горные науки и технологии

SCIENTIFIC AND PRACTICAL E-JOURNAL

eISSN 2500-0632

2024

Vol. 9, no. 4

https://mst.misis.ru/

Activities of the ***Mining Science and Technology (Russia) (Gornye nauki i tekhnologii)*** international journal are aimed at developing international scientific and professional cooperation in the field of mining.
The journal target audience comprises researchers, specialists in the field of mining, representatives of academic and professional communities.
The journal publishes original papers describing research findings, experience in the implementation of projects in mining industry, review publications.
The journal seeks to develop interdisciplinary areas that contribute to progress in mining, for example, technological and environmental safety, project organization and management in mining industry, development of territories, legal aspects of natural resource use, and other areas studied by researchers and practitioners. The journal always welcomes new developments. Papers are accepted in English or Russian.

QUARTERLY

FOUNDED in 2016

REGISTRATION

The journal science and applied research journal is registered by the Federal Service for Communication, IT and Mass Communication Control on August 10, 2015.
Registration Certificate E-No. ФС77-62652

INDEXATION

Scopus, CAS, EBSCO, DOAJ, РИНЦ, ВИНИТИ РАН, Dimensions, BASE, J-Gate, Jisc Library Hub Discover.

FOUNDER AND PUBLISHER

MISIS UNIVERSITY University of Science and Technology MISIS

CONTACT

4 Leninsky Prospect, Moscow 119049, Russian Federation
Phone: +7 (495) 955-00-77
e-mail: send@misis.ru

ГОРНЫЕ НАУКИ И ТЕХНОЛОГИИ

Mining Science and Technology (Russia)

ЭЛЕКТРОННЫЙ НАУЧНО-ПРАКТИЧЕСКИЙ ЖУРНАЛ

eISSN 2500-0632

2024

Т. 9, № 4

https://mst.misis.ru/

Деятельность научно-практического журнала «Горные науки и технологии» (Mining Science and Technology (Russia)) направлена на развитие международного научного и профессионального сотрудничества в области горного дела.

Целевая аудитория журнала – исследователи, специалисты в области горного дела, представители академического и профессионального сообществ.

В журнале публикуются оригинальные статьи, описывающие результаты исследований, опыт реализации проектов в горнопромышленном комплексе, обзорные публикации.

Журнал стремится развивать такие междисциплинарные направления, как технологическая и экологическая безопасность, организация и управление проектами в горной промышленности, развитие территорий, правовые аспекты использования природных ресурсов и другие, которые способствуют прогрессу в горном деле и реализуются исследователями и практиками.

ПЕРИОДИЧНОСТЬ 4 раза в год

ОСНОВАН в 2016 году

РЕГИСТРАЦИЯ

Зарегистрирован Федеральной службой по надзору в сфере связи, информационных технологий и массовых коммуникаций 10 августа 2015 года.
Свидетельство о регистрации Эл № ФС77-62652.

ИНДЕКСИРОВАНИЕ

Scopus, CAS, EBSCO, DOAJ, РИНЦ, ВИНИТИ РАН, Dimensions, BASE, J-Gate, Jisc Library Hub Discover.

OPEN ACCESS Журнал открытого доступа.

УЧРЕДИТЕЛЬ И ИЗДАТЕЛЬ

МИСИС УНИВЕРСИТЕТ НАУКИ И ТЕХНОЛОГИЙ Университет науки и технологий МИСИС

АДРЕС УЧРЕДИТЕЛЯ И ИЗДАТЕЛЯ

119049, г. Москва, Ленинский проспект, д. 4

КОНТАКТЫ РЕДАКЦИИ

Адрес: 119049, г. Москва, Ленинский проспект, д. 4
Телефон: +7 (495) 955-00-77
e-mail: send@misis.ru

MINING SCIENCE AND TECHNOLOGY (Russia)
Горные науки и технологии
SCIENTIFIC AND PRACTICAL E-JOURNAL
eISSN 2500-0632
2024
Vol. 9, no. 4
https://mst.misis.ru/

CONTENTS

ГОРНЫЕ НАУКИ И ТЕХНОЛОГИИ
Mining Science and Technology (Russia)
ЭЛЕКТРОННЫЙ НАУЧНО-ПРАКТИЧЕСКИЙ ЖУРНАЛ
eISSN 2500-0632
2024
Т. 9, № 4
https://mst.misis.ru/

СОДЕРЖАНИЕ

eISSN 2500-0632
https://mst.misis.ru/

GEOLOGY OF MINERAL DEPOSITS

Reviewer paper

https://doi.org/10.17073/2500-0632-2023-08-146
UDC 622.24.051.553.98(567)

New advances in drilling operations in sandstone, shale, and carbonate formations: a case study of five giant fields in the Mesopotamia Basin, Iraq

A. N. Al-Dujaili
Amirkabir University of Technology, Najaf, Iraq
ahmed.noori203@aut.ac.ir

Abstract

Drilling challenges in the Mesopotamian Basin, Southern Iraq, are varied and include such issues as mud loss, bit damage, and differential sticking. This study aims to analyze these problems across the stratigraphic column in the study area. The results show that the MMD65R, EQH16R, and SF74R bits were successfully used for the 16” section, while the MSi616L bit was the most efficient for the 12¼” section. The MMD65R was suitable for the 8½” section, with the EQH12DR bit being used for the remaining parts of this section. The MMD54 bit showed excellent performance, achieving the highest rate of penetration (ROP) of 26.9 m/hr in well horizontal sections. Mud losses were most commonly observed at the base of the Dammam, Rus, Tanuma, Mishrif, Hartha, Shuaiba, and Zubair Formations. An appropriate drilling mud density is 1.28 sg is recommended for Zubair and Mishrif Formations. Additionally, tripping in/out operations must be conducted at controlled speed to prevent surging or swabbing the well. Potassium Chloride concentrations should be maintained between 3 to 5%. A 7” production liner must be run and properly seated to isolate the Mishrif and Zubair Formations, with overlap to prevent potential communication between lower water-bearing zones and shallow loss zones.

Keywords

hydrocarbons, field, reserves, basin, formation, extraction, drilling, well, productivity, solution, accident, mud loss, reservoir, bit, drilling program, torque, control, Mesopotamian Basin, Iraq

For citation

Al-Dujaili A. N. New advances in drilling operations in sandstone, shale, and carbonate formations: a case study of five giant fields in the Mesopotamia Basin, Iraq. *Mining Science and Technology* (*Russia*). 2024;9(4):308–327. https://doi.org/10.17073/2500-0632-2023-08-146

ГЕОЛОГИЯ МЕСТОРОЖДЕНИЙ ПОЛЕЗНЫХ ИСКОПАЕМЫХ

Обзорная статья

Новые достижения в области бурения в песчаниковых, сланцевых и карбонатных формациях на примере исследования пяти крупных месторождений в Месопотамском бассейне Ирака

Ахмед Н. Аль-Дуджайли
Технологический университет имени Амира Кабира, г. Наджаф, Ирак
ahmed.noori203@aut.ac.ir

Аннотация

Проблемы бурения в Месопотамском бассейне (нефтегазоносном бассейне Персидского залива) (южная часть Ирака) разнообразны и касаются таких вопросов, как потери бурового раствора, поломка долота и дифференциальный прихват. Цель настоящего исследования заключается в анализе указанных проблем по всему стратиграфическому разрезу в исследуемом районе. Согласно полученным результатам долота MMD65R, EQH16R и SF74R отлично проявили себя для бурения 16-дюймового профиля, а долото MSi616L показало наибольшую эффективность в 12¼-дюймовом профиле. Для 8½-дюймового профиля было успешно использовано долото MMD65R, а для остальных участков этого профиля применялось EQH12DR. Для долота MMD54 зарегистрированы отличные показатели – наибольшая механическая скорость бурения (ROP) 26,9 м/ч в горизонтальных профилях скважины. Потери бурового раствора чаще всего наблюдались в основании формаций Даммам, Рус, Танума, Мишриф, Харта, Шуайба и Зубейр. Для формаций Зубейр и Мишриф рекомендуется плотность бурового раствора 1,28 г/см^3. Кроме того, во избежание пульсации или свабирования скважины спускоподъемные операции необходимо выполнять с контролируемой скоростью. Концентрация хлористого калия должна поддерживаться в пределах от 3 до 5%. Для изоляции пластов формаций Мишриф и Зубейр следует спустить и правильно установить 7-дюймовую эксплуатационную обсадную колонну с перекрыванием для предотвращения возможного сообщения между нижними водоносными зонами и приповерхностными областями поглощения.

Ключевые слова
углеводороды, месторождение, запасы, бассейн, формация, добыча, бурение, скважина, производительность, раствор, авария, потери бурового раствора, коллектор, долото, план бурения, крутящий момент, управление, Месопотамский бассейн, Ирак

Для цитирования
Al-Dujaili A. N. New advances in drilling operations in sandstone, shale, and carbonate formations: a case study of five giant fields in the Mesopotamia Basin, Iraq. *Mining Science and Technology* (*Russia*). 2024;9(4):308–327. https://doi.org/10.17073/2500-0632-2023-08-146

Acronyms and Abbreviations

API	American Petroleum Institute
BHA	Bottom Hole Assembly
DD	Directional Driller
ECD	Equivalent Circulating Density
GPM	Gallons per Minute
LCM	Lost Circulation Materials
MD	Measured Depth
MJ	Majnoon Field
MW	Mud Weight
NPT	Non-Productive Time
PDC	Polycrystalline Diamond Compacts
POOH	Pull Out of The Hole
PV	Mud Viscosity
RKB	Rotary Kelly Bushing
ROP	Rate of Penetration
RPM	Revolutions per Minute
RSS	Rotary Steerable System
Ru	Rumaila Field
SPM	Strokes per Minute
SSP	Site Safety Plan
TFA	Total Flow Area
WOB	Weight on Bit
WQ	West Qurna Field
YP	Yield Point
Zb	Zubair Field

Nomenclature

HR	Hour
Deg.	Degree
RR	Re-Runnable
In	Inch
Ft	Foot
H_2S	Hydrogen Sulfide
L	Liter
M	Meter/s
Min.	Minute
BBL	Barrel
Avg.	Average
ID	Inside Diameter (in)
PP	Pore Pressure (Psi)
FG	Fracture Gradient
KCl	Potassium Chloride

Introduction

Wells drilling and completion account for over 40% of all investments in the hydrocarbon energy industry. Reducing failures during the drilling process is one of the key prospects for increasing effective drilling time and addressing challenges faced during drilling and their consequences. The main types of complications in the wells drilling process include sticking of the drill string due to deviation, collapsing of unstable rocks, narrowing of the wellbore from crumbling rocks, absorption of drilling mud, gas-oil-water showings, and brine showings [1]. All drill cuttings must be removed from the well during drilling and brought to the surface, a process referred to as hole cleaning [2]. However, some material often remains in the well, leading to issues such as pipe sticking, premature bit wear, slow drilling, formation damage (fracturing), excessive torque and drag, and difficulties in logging and cementing [3].

Complete or partial loss of drilling mud within a formation during the drilling operation, or a situation where the amount of mud recovered from the well does not match the amount injected, is known as drilling fluid loss or retrieval loss [4]. This typically occurs in highly permeable, depleted reservoirs, natural cracks, cavernous formations, and fracture formations [5]. Various techniques are employed to control circulation loss, such as reducing the density of the drilling mud [6], and adding lost circulation materials (LCM) to plug and seal loss zones [7]. Multiple factors may affect drilling fluid loss, including petrophysical properties (porosity, permeability, etc.), characteristics of the drilling mud itself (MW, ECD, YP, PV, etc.), drilling parameters (ROP, WOB, RPM, SPM, SSP, TFA, etc.), and pressure conditions (pore pressure gradient, fracture pressure, etc.) [8]. 54% of stuck pipe incidents examined occurred while tripping and back reaming [9]. The risk of stuck pipe incidents has increased due to the recent expansion of drilling activities, particularly in depleted and higher-risk reservoirs [10]. Several studies suggest using statistical methods to predict stuck pipe events [11].

eISSN 2500-0632
https://mst.misis.ru/

Salih et al. (2018) studied the formations of southern Iraqi oilfields, providing a detailed description from the Upper Fars to the Mishrif formations. The severity of problem in each formation were defined by identifying the causes of issues in the wells or potential risks [12]. Losses are predictable in the Rumaila oilfield at the base of the Dammam Formation, where water ingress occurs during the drilling process. Losses have also been reported in the Hartha Formation, and significant washout have been observed in the Tanuma Formation. The variability of the Mishrif reservoir's architecture and rock types may cause irregular sweep and water breakthrough if higher permeability layers are present. Sloughing formations include the Tanuma, Nahr Umr, and Upper Shale formations. Loses may also occur in the Mishrif and Zubair formations, with potential pipe sticking through the Mishrif, Nahr Umr, and Zubair formations. Bit damage during drilling through anhydrite layers (Lower Fars and Rus Formations) has a lesser effect on the drilling program [13].

1. Geological setting

Iraqi territory is represented by four major tectonic zones. These zones can be classified according to several factors such as rock type, age, thickness, and structural transitions. The zones are [14]:

1. interior settled shelf;
2. exterior unsettled shelf;
3. Shalair territories;
4. Zagros.

The interior and exterior regions of the Arabian Plate are characterized by the absence of metamorphosis and volcanic activities. The Mesopotamia Plain and the Jazira Plain are the main parts of the Mesopotamia Foredeep in Iraq. This foredeep is characterized by being less tectonically problematic and is formed from quaternary alluvial deposits of the Tigris and Euphrates Rivers and their tributaries, which completely cover the central and southeastern parts of the basin. Wrapped with Miocene rocks, the Jazira Plain marks the extension of the Mesopotamia Plain towards the northwest [15]. The Mesopotamia basin generally has a flat topography. Surface structures resulting from tectonic activity are scarce in this basin, but it contains several structures, including faults, folds, and diapiric structures [16].

The stratigraphic column of southern Iraq [17, 18] is characterized by a thick Cretaceous depositional sequence with significant hydrocarbon accumulations in many formations [19] (Fig. 1, *a*).

1.1. Majnoon Field

Majnoon Field comprises a banana-shaped, crested anticline with a general N-S elongation [20]. It represents a compression fold, likely underlain by salt below the Jurassic level. The field consists of four major and seven minor reservoirs from the Lower Cretaceous

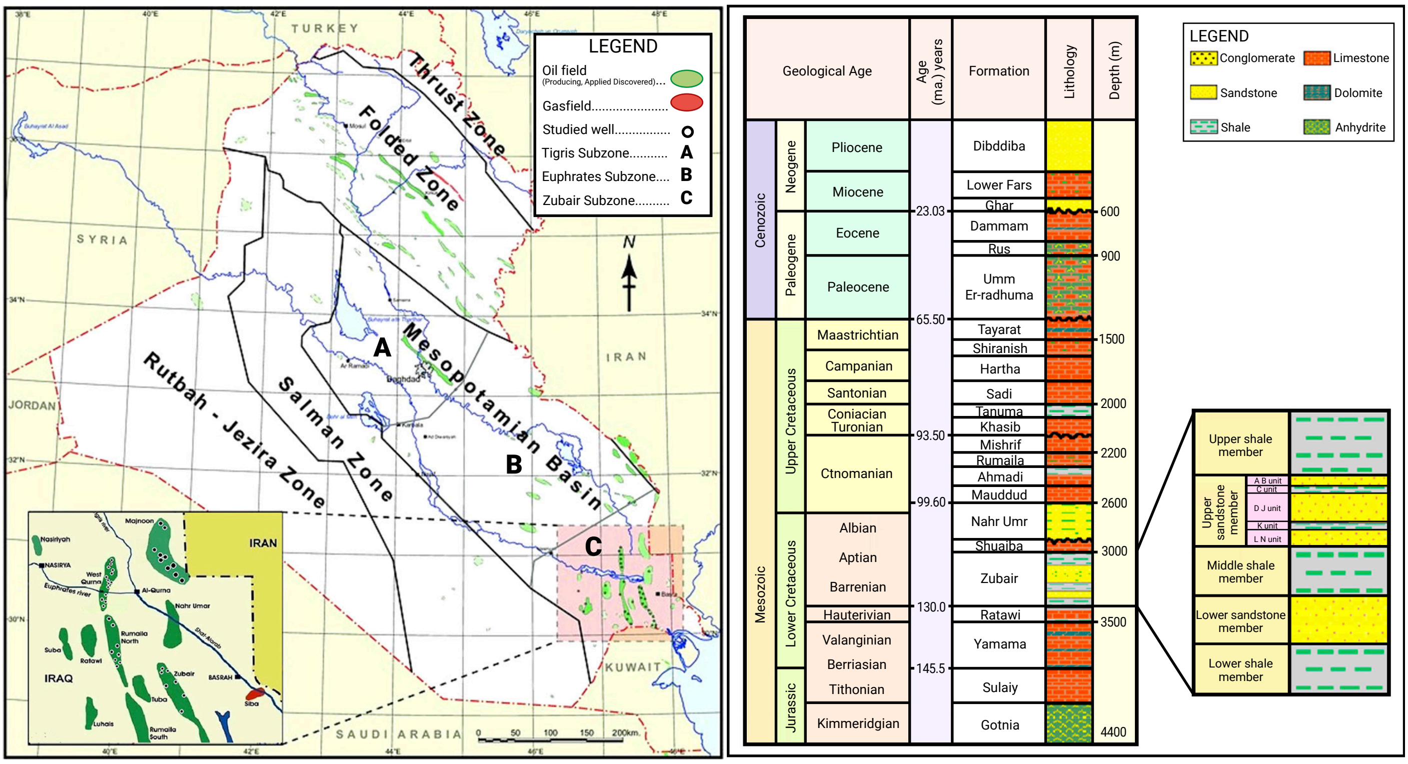

a *b*

Fig. 1. Locations of the wells under study and their drilling dates – *a*; Stratigraphic column in southern Iraq – *b* [17, 18]

to Paleocene age, spanning a vertical interval of about 3000 m [21]. The four main reservoirs, in-depth order, are the Hartha, Mishrif-Ahmadi, Nahr-Umr, and Zubair formations, with the deepest being the high-pressure Yamama carbonate formation. These account for 80% of Majnoon's hydrocarbons. The Yamama and Mishrif formations alone account for 50% of the major reservoir volume. The minor reservoirs may indicate hydrocarbons in the Khasib, Sadi, Tanuma, Ghar, Shiranish, and Shuaiba Formations [22] (see Fig. 1, *a*).

1.2. Rumaila Field

The Rumaila field is a supergiant oilfield located 50 km west of Basrah city in southern Iraq [23]. It has stacked pay in multiple clastic and carbonate reservoirs. The Rumaila field was discovered in 1953 and accounts for 33% of Iraq's total oil production. The Rumaila structure represents a mildly tilted longitudinal anticline, extending approximately 83 km in length and 12 km in width [24]. Two faults, Takadid-Qurna and Al-Batin, extend from the northeast to the southwest. These faults are reactivated Precambrian transverse faults that define the Zubair fault block or subzone of the Mesopotamian basin [25] (see Fig. 1, *a*).

The most significant hydrocarbon system in this stratigraphic column is the Early Cretaceous–Miocene petroleum system. In this system, the Sulaiy and Yamama formations serve as source rocks; the Tanuma, Shranish, and Rus formations act as sealing rocks; and the Yamama, Zubair, Nahr Umr, and Mishrif formations serve as reservoir rocks [26] (Fig. 1, *b*).

1.3. West Qurna (1 and 2) Field

Iraq's supergiant oilfields are mainly located in southern Iraq, and one of these is the West Qurna oilfield [27, 28]. It is located northwest of Basra city, within the Zubair Subzone, and is structurally part of a large isocline to the North. The field is estimated to contain approximately 30 to 40 billion barrels of recoverable reserves [29]. The West Qurna oilfield represents the northern extension of the supergiant Rumaila oilfield [30] (see Fig. 1, *a*).

1.4. Zubair Field

The Zubair Field is located within the Mesopotamian zone, on the unstable sill of the Arabian Platform [31]. Zubair is one of the mature oilfields in southern Iraq, located 20 km southwest of Basra city [32] (see Fig. 1, *a*).

This field was discovered in 1949, consisting of four domes (Al-Hamar, Shuaiba, Rafidyah) in the NW and (Safwan) to the SE, connected through an aquifer that extends beyond the Iraqi and Kuwaiti border [33]. The field structure includes four reservoirs: Mishrif, Upper Shale Membrane, and the Third and Fourth Pay zone [34].

1.5. Productive Formations

The Mishrif Formation is divisible by a prominent unconformity into two large-scale regressive sequences, particularly distinguishable in the east of the Mesopotamian Basin. Multiple reservoir units are present in both sequences. The west of the basin is dominated by the lower sequence, which has relatively few reservoir intervals. The shallow-water reservoir units in the east are thick, reflecting relatively high subsidence rates during the Cenomanian [35]. Subsidence rates in the western side of the basin were lower, resulting in thinner and more limited reservoir units.

The best reservoir conditions in the Mishrif Formation occur in rudist-bearing facies, such as rudstones and rudistid packstone/grainstones [27] (Fig. 2, *a*).

The Mauddud Formation is a shallow-water carbonate, distributed widely in the subsurface of the Persian Gulf. It is recognizable in the Northern Gulf (Iraq and Kuwait), eastern Arabia (Saudi Arabia, Bahrain), and the Southern Gulf (United Arab Emirates and Oman) [36]. In southern Iraq, the formation was described from the Zubair-3 well by Owen and Nasr (1958) (Fig. 2, *b*). The Mauddud Formation consists of organic, detrital, and occasionally pseudo-oolitic limestone with streaks of green or bluish shale [37].

The Zubair Formation, dating from the early Cretaceous (Hauterivian to Early Aptian), is aregionally extensive oil-producing sandstone sequence found in Syria, Iraq, and Iran [38]. The Zubair sandstones are environmentally and genetically similar to the Nahr Umr sandstones of the Kuwaiti fields, consisting of clean, well-sorted quartz arenites, sourced from the Arabian shield and deposited from west to east into the Mesopotamian Basin during the Early Cretaceous. The Zubair sandy deposits comprise numerous depositional cycles composed of shallowing-upward successions of dark grey shale, siltstone, and fine- to medium-grained sandstone [39] (Fig. 2, *c*). These cycles are interpreted as a series of sea-level transgressions and regressions during a longer-term transgression. Typical lithofacies within these cycles include marine shelf, prodelta, delta front, and delta plain [40]. Litho-stratigraphically, the formation is subdivided into five sub-units:

1. Upper Shale Member: contains isolated, massive (10–15 m-thick) oil-bearing sandstones. This unit has been producible from a few wells (e.g. Zb-X7).

2. Upper Sandstone Member (Third Pay): contains stacked pay sands and 32° API gravity oil. This reservoir unit has been producible from about 80 wells.

3. Middle Shale Member.

4. Lower Sandstone Member (Fourth Pay): contains stacked pay sands with 38° API gravity oil. This unit has been producible from eight wells.

5. Lower Shale Member.

Each reservoir unit is isolated by intervening shaly zones. The reservoir drive mechanism is mainly gas expansion, with a weak to moderate water drive [41].

The Yamama Formation is the primary Lower Cretaceous carbonate reservoir in southern Iraq, belonging to the late Berriasian-Aptian cycle. It is described from the shore to the deep basin by the Zubair, Ratawi, Yamama, Shuiaba, and Sulaiy formations [42]. The Ratawi Formation usually conformably overlies The Yamama Formation. In SE Iraq, at the Nasiriya, West Qurna, and Majnoon fields, probable sequence boundaries can be identified within the Yamama Formation of the top of oolite facies. In southern Iraq, the Yamama Formation is recognized by the presence of limestone below the last shale streak at the base of the Ratawi Formation [43]. The Yamama Formation is one of the most important oil-producing reservoirs in the southern Mesopotamian zone (West Qurna, North Rumaila, and Majnoon fields) and extends from the Valanginian to Early Hauterivian within the main retrogressive depositional cycle (Berriasian-Aptian) in the southern Iraq [42] (Fig. 2, *d*).

2. Historical Review of drilling operations

The problems encountered during drilling processes in southern Iraq formations can be summarized in (Fig. 3), based on a previous study that discussed these issues [13], which will be adapted in this research. Losses should be expected at the base of the Dammam Formation and in the Hatha, Mishrif, and Zubair Formations. A significant washout occurred in the Tanuma Formation. The variability of Mishrif reservoir architecture and rock types might lead to irregular sweep and water breakthroughs. Sloughing formations are represented by Tanuma, Nahr Umr,

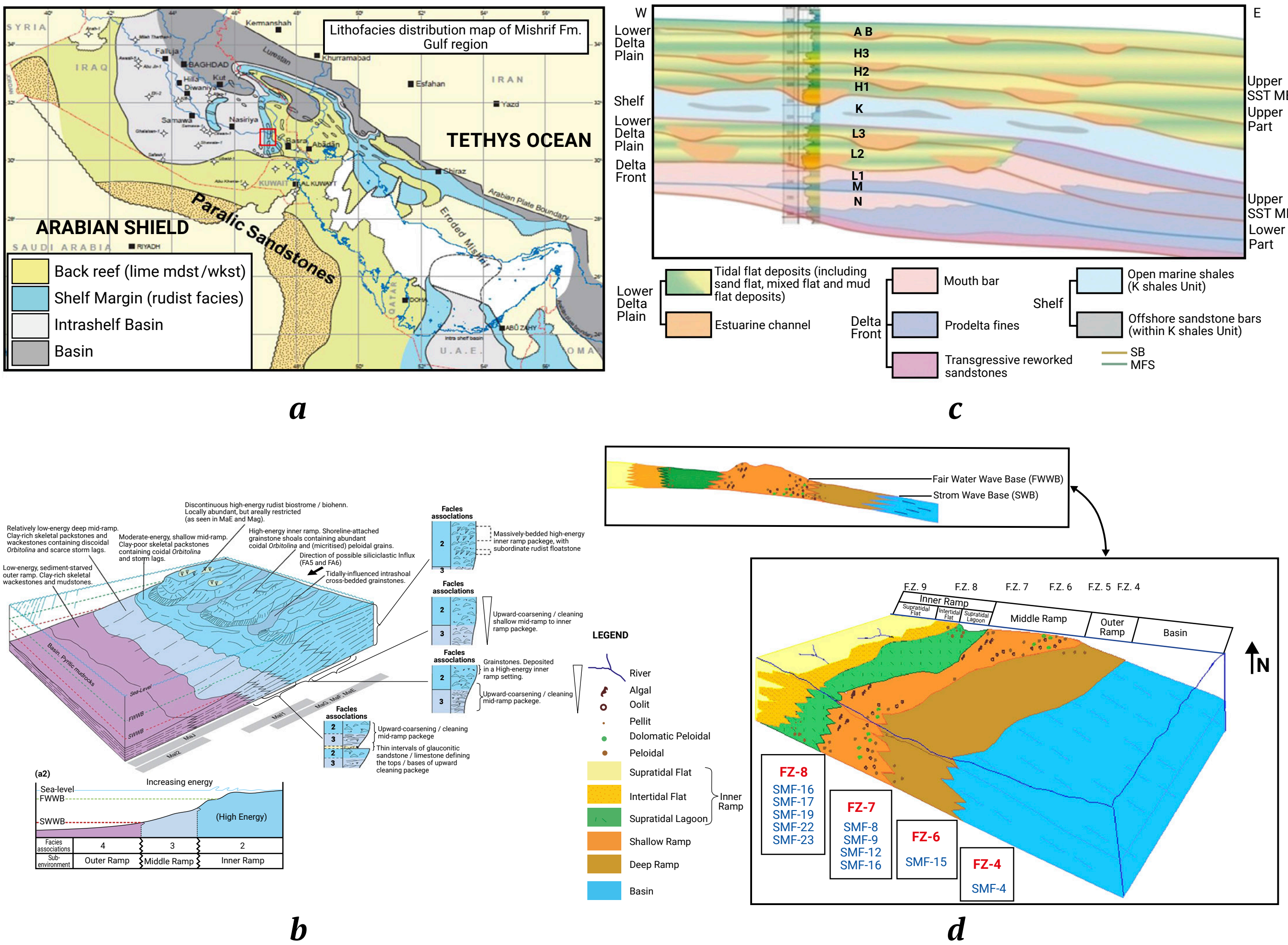

Fig. 2. Lithofacies distribution for the Mishrif Formation in the Gulf Region – *a* [44]; Depositional model for Mauddud – *b* [37]; Zubair – *c* [ZFOD, (Zubair Field Operating Division). Sedimentological and Reservoir Quality Study of the Zubair Formation. 2014. (Unpublished Study)]; Yamama Formations – *c* [45]

MINING SCIENCE AND TECHNOLOGY (RUSSIA)
ГОРНЫЕ НАУКИ И ТЕХНОЛОГИИ
2024;9(4):308–327

eISSN 2500-0632
https://mst.misis.ru/

and Upper Shale. The potential of stuck pipes is noticeable in the Mishrif, Nahr Umr, and Zubair Formations. Bit damage during drilling through entire anhydrite layers in the Lower Fars and Rus Formations was a problem, though with a lower impact on the drilling program. The Dammam Formation faced the most drilling problems, according for 56.4% of all wells drilled (caving and mud loss), while no significant issues were reported in the Dibdibba, Khasib, Rumaila, Ahmedi, Mauddud, and Shuaiba Formations [46]

3. Methodology

The wells, which can be relied upon to achieve the results of this research, can be divided into seven groups according to the date of the drilling process. Fig. 4 shows the locations of the wells under study and the date of the drilling process.

Data were utilized from 10, 8, 12, and 6 wells in the Majnoon, Rumaila, West Qurna (1 and 2), and Zubair Fields, respectively. In addition, data were obtained from the offset wells in these fields (see Fig. 1, *a*).

3.1. Bit performance

The most suitable drilling technique varies with the conditions and equipment, so modifying the recommendations for drilling might be considered to obtain the best results. The effect of such changes on the drilling rate must be carefully examined, especially if these changes do not immediately increase the drilling rate.

3.1.1. For the Rumaila Field

From 2011 to 2013, 22 bits of the MSi616L type design were tested in 24 wells on different drive types in the Rumaila Field before being run in R-X33 to experiment with the best performance.

3.1.2. For the Majnoon Field

The 16” SFD75D bit type was used in 25 directional wells from 2012 to 2016, starting with well MJ-X2. The same bit was used again in wells MJ-X4 and MJ-X5, while the SFD76C bit type was tested in well MJ-X7.

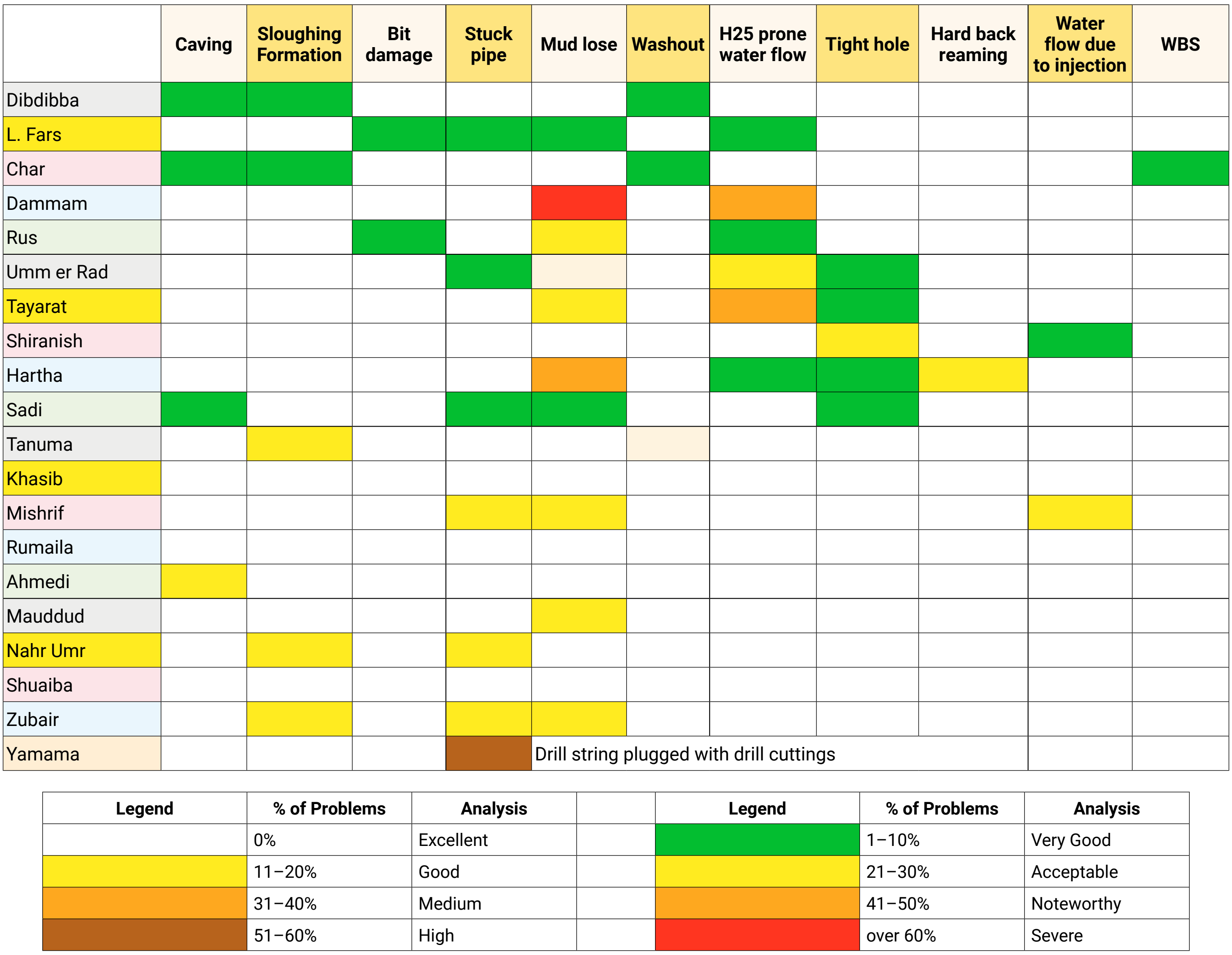

Fig. 3. Analysis of drilling problems for each formation in the Rumaila Field [13]

3.1.3. For the Zubair Field

Four new bits types were tested in 18 wells on different drive types in the Zubair Field from 2012 to 2014, aiming to improve performance based on lessons learned in the previous fields (Table 1).

3.1.4. For the West Qurna 1 and 2 Field

Several well trajectories with different targets were drilled in the WQ Field, including S-Shape, J-Shape, and horizontal wells, during the period from 2015 to 2018. The 12¼” SFE66DH bit type was used with an ROP of 15.81 m/hr through the Dammam, Rus, Umm Er Radhuma, Tayarat, Shiranish, Hartha, and Sadi formations.

The 15.8 is considered the second-best ROP achieved throughout the horizontal wells in this field. The directional plan for the 12¼” section was to hold the inclination angle at 12–15°, then built the inclination to 20°, and finally hold it at 20–22°.

The MME65R bit type was used to drill the 8½” section due to losses encountered in the Mishrif Formation. The same bit was used to drill out the cement plug through this formation.

3.2. Lost Circulation

Lost circulation is a common problem encountered during drilling and cementing operations. It can range from being a minor issue to a major, dangerous, and expensive problem due to loss of mud and rig time. A host of leading-edge technologies was implemented to solve lost circulation problems. Fig. 5 shows the well design for different types of wells and for different productive zones.

Table 1

Bit types used in the Zubair Field

Size	Type	New/Used	Nozzles
26”	VE598	Used	–
26”	CKL	New	–
16”	VGA-T318	New	–
8½”	HC506ZX	New	Without nozzles
8½”	RC216	New	Without nozzles
12¼”	GT-1	Used	Without nozzles
12¼”	Q506FX	Used	6 x 13/32

a

b

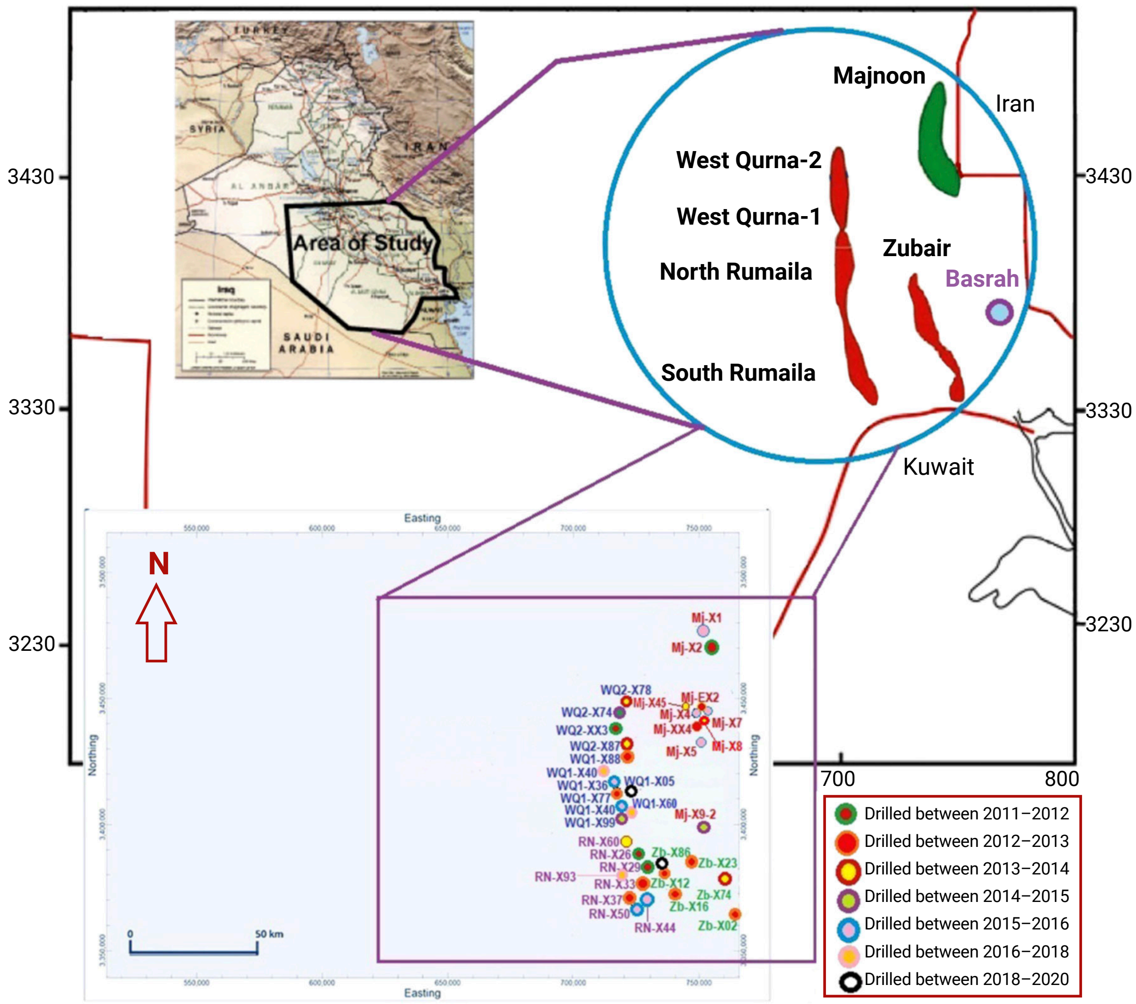

Fig. 4. Well groups categorized by drilling date and their locations in the Mesopotamian basin

eISSN 2500-0632
https://mst.misis.ru/

3.2.1. For Non-Productive Formations

Potential losses in the Dammam, Rus, and Hartha formations can be considered the main challenges during the drilling process. Controlling the ROP or POOH was adopted to overcome losses in these formations. The drilling program for wells in these formations includes using a 12¼" slick BHA with large nozzles and pumping a balanced cement plug through the bit.

3.3. Other Problems

1. Sulfurous water may be present in the Umm-Er-Radhuma and Tayarat Formations.

2. The potential release of H_2S while drilling the Nahr Umr sandy formation poses serious health risks for humans and the environment.

3. Hole instability issues may be observable in the Nahr Umr Formation.

4. The Mishrif is a depleted reservoir prone to mud losses and stuck pipes if not adequately bridged.

5. Swelling shales lead to tight over-pulls and sloughing, with a risk of caving, which can result in stuck pipes in the Nahr Umr Formation.

6. Shale instability and cavings are observed in shale membrane zones for the Zubair Formation.

7. The variability of reservoir architecture and rock types in the Mishrif, Mauddud, Zubair, and Yamama reservoir might lead to irregular sweep and water breakthrough if higher permeability layers are present.

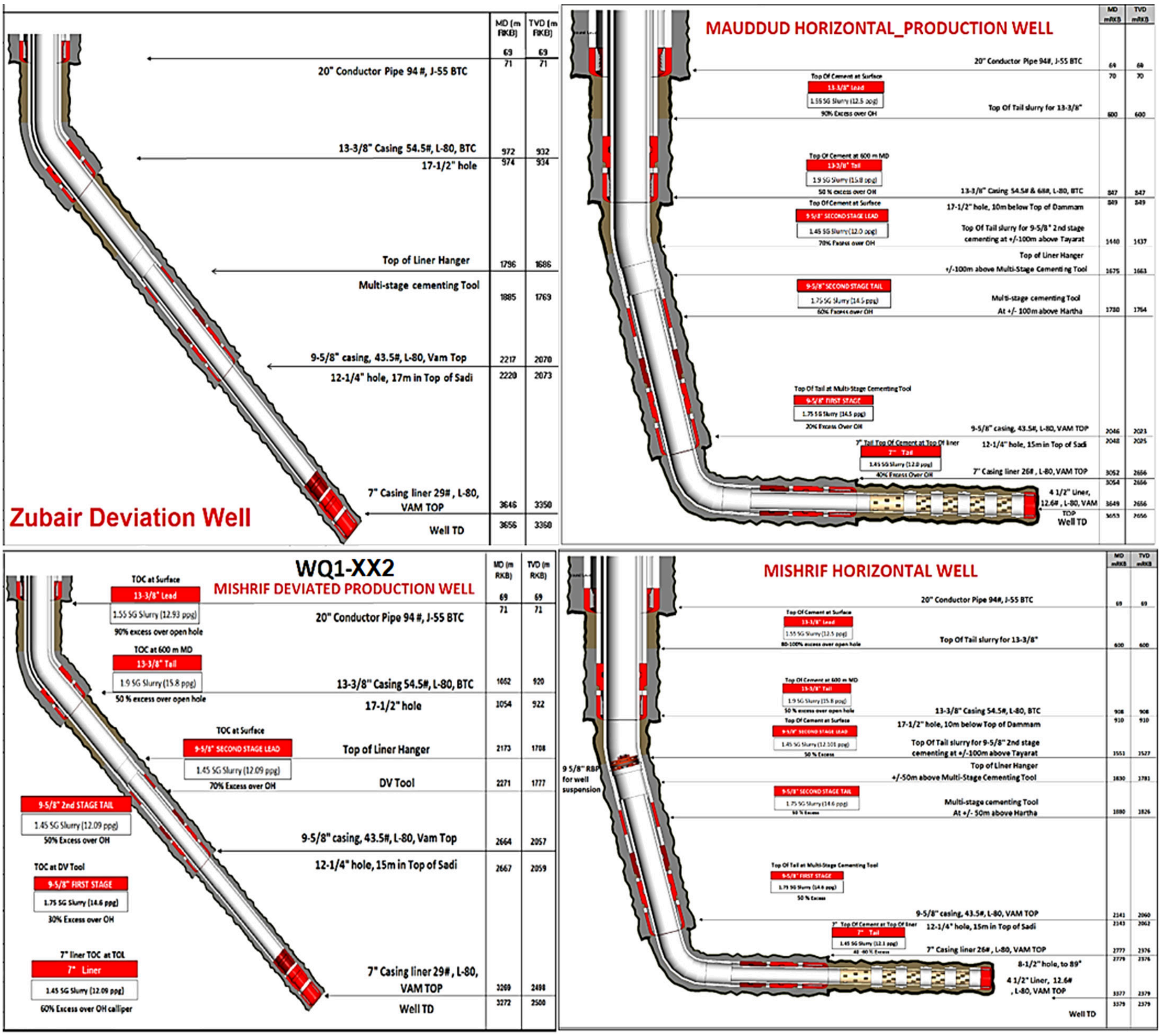

Fig. 5. Well schematic for the wells by Powerdraw™ [46]

4. Results

4.1. Bit Performance

4.1.1. Rumaila Field

Twenty-two bits of the MSi616L type design were used in 24 wells on different drive types in the Rumaila Field before being run in well R-X33. A summary of the MSi616L type bit performance is as follows (Fig. 6).

The bit records for the 12¼” MSi616L type design in offset wells indicate a median drilling distance of 1000 m per bit and a median ROP of 13 m/hr per run. (see Fig. 6).

According to Fig. 7, the majority of the cutting structure on this bit is green. There are a couple of broken cutters, one on the outer cone area of Blade #1 and the other on the nose of Blade #6.

Fig. 8 shows a comparison of drilling parameters between the MSi616L and QD506FX bit for the Shiranish Formation (1642–1835 m) in well R-X33 in the Rumaila Field. The bit records for the 12¼” MSi616L design in offset wells indicate a median drilling distance of 1000m per bit and a median ROP of 13 m/hr per run. Thus, the 12¼” MSi616L is a well-proven design in the Rumaila application.

4.1.2. Majnoon Field

The 16” SFD75D bit was run similarly after being used in well MJ-X2 to drill 1822 m cumulatively in wells MJ-X4 and MJ-X5. The ROP performance in these wells averaged 27 m/hr, and the cutting bit had 7 blades with 19 mm of cutters. Fig. 9 shows a comparison between different kinds of bits used in the Majnoon Field.

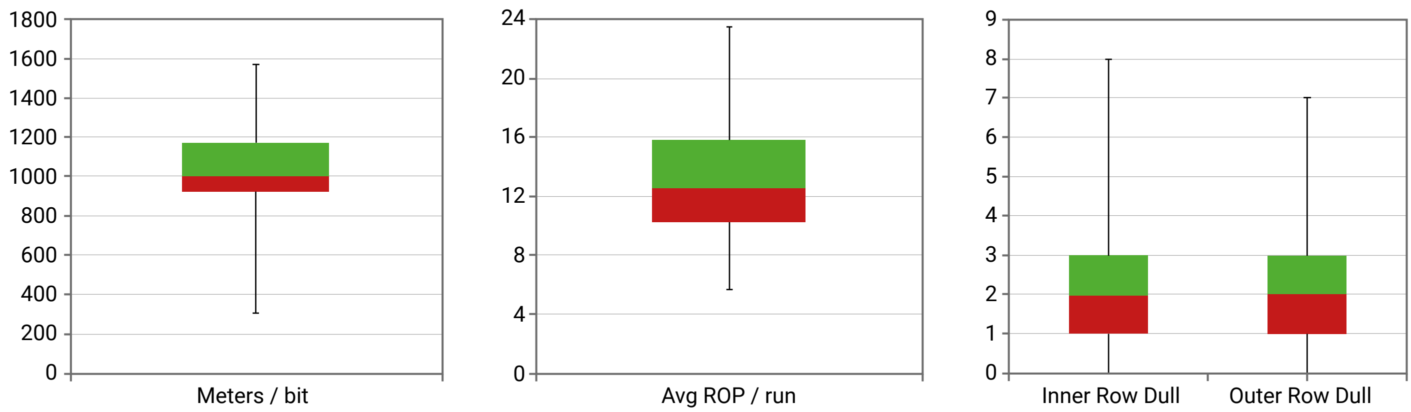

Fig. 6. Performance of MSi616L type bits in the Rumaila Field

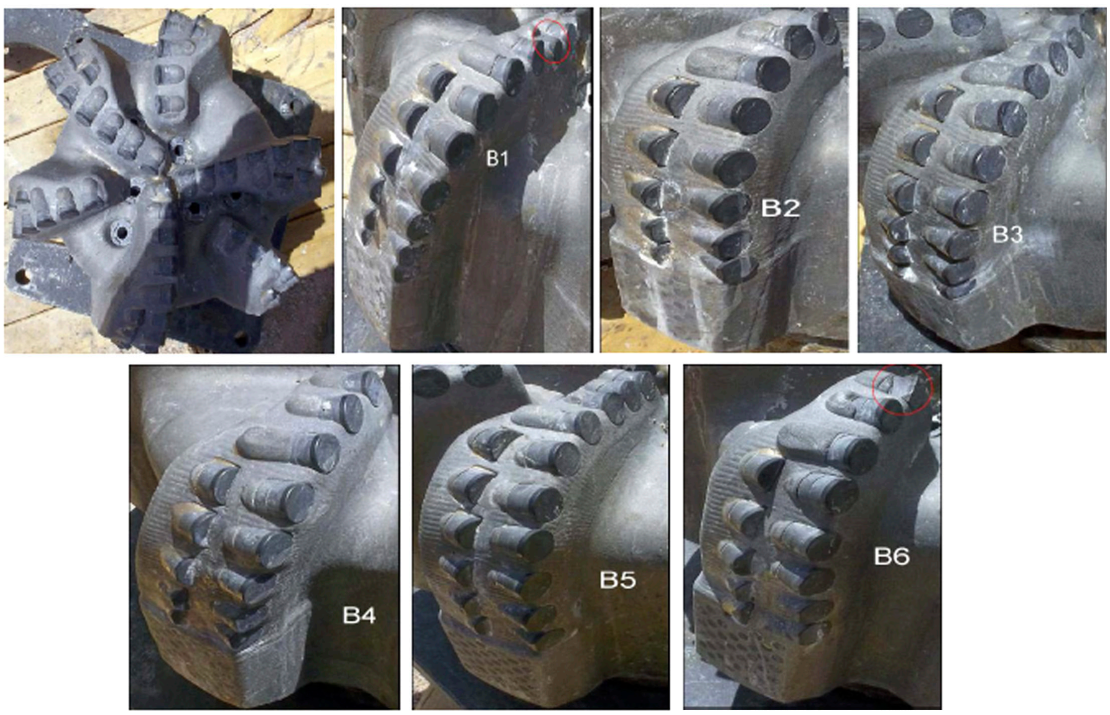

Fig. 7. 12¼” MSi616LPX (JF4376) bits from the wells studied in the Rumaila Field

In well MJ-X3, which achieved the highest ROP and fewer trips, the 8½" MMD65R bit was successfully used on a motor assembly, achieving an ROP of 16.7 m/hr. The drive system was changed from POOH to the RSS, and the 8½" MME74H was used to complete the section, achieving an ROP of 16 m/hr (Fig. 10).

The performance comparison between different types of bits (Majnoon Field as an example) shows that MMD65R, EQH16R, and SF74R are the best bits for drilling the 16" section (Fig. 11).

4.1.3. West Qurna-1 and 2 Field

The horizontal sections drilled show consistent performance in the field in terms of ROP and bit condition. The higher performance was achieved in well WQ1-X54, where 601 m was drilled by the MMD64DR bit (6 blades, 13 mm cutter size) at an ROP of 27.3 m/hr. The MMD54 bit (5 Blades, 13 mm cutter size) also showed excellent performance, achieving the highest ROP of 26.9 m/hr in well WQ1-X55, with an excellent accumulated interval throughout the field. A total of 1340 m was drilled in wells WQ1-X57, WQ1-X59, and WQ1-X60 (2nd run) using the MMD54 bit (Fig. 12).

The Fig. also indicates that bit performance in the Yamama Formation for well WQ1-X38 was better than the well WQ1-X63 in terms of ROP and bit condition.

4.1.4. Zubair Field

No data are available for bit performance in this field.

Some of the wells drilled before 2011 (R-XX3 and XX8) experienced stick-slip levels throughout the two PDC runs. Despite variations in formations, formation strengths, drilling parameters, or bit cuttings structures, there was no considerable difference in stick-slip levels (~2xCRPM during both PDC runs). Collar RPM fluctuations were wide in the UER formation but narrowed in subsequent formations, with no change to stick-slip levels (Fig. 13). No significant stick-slip was observed in the wells under study, either Rumaila or other fields, due to the performance of the MSi616LPX bit, which showed no severe vibration levels at the bit with the given drilling parameters and rock types (Fig. 14).

4.2. Lost Circulation

Losses for cutting displacements/losses in the Dammam and Rus formations can be noticeable. The lost-circulation control materials used are FlexPlug, FlexPlug W, FlexPlug OBM, and FlexPlug R, which can be pumped through most BHAs and react with the drilling mud to create a barrier at the face of the zone in the wellbore rather than penetrating the matrix or fracture. Therefore, this technique is less damaging to potentially productive formations.

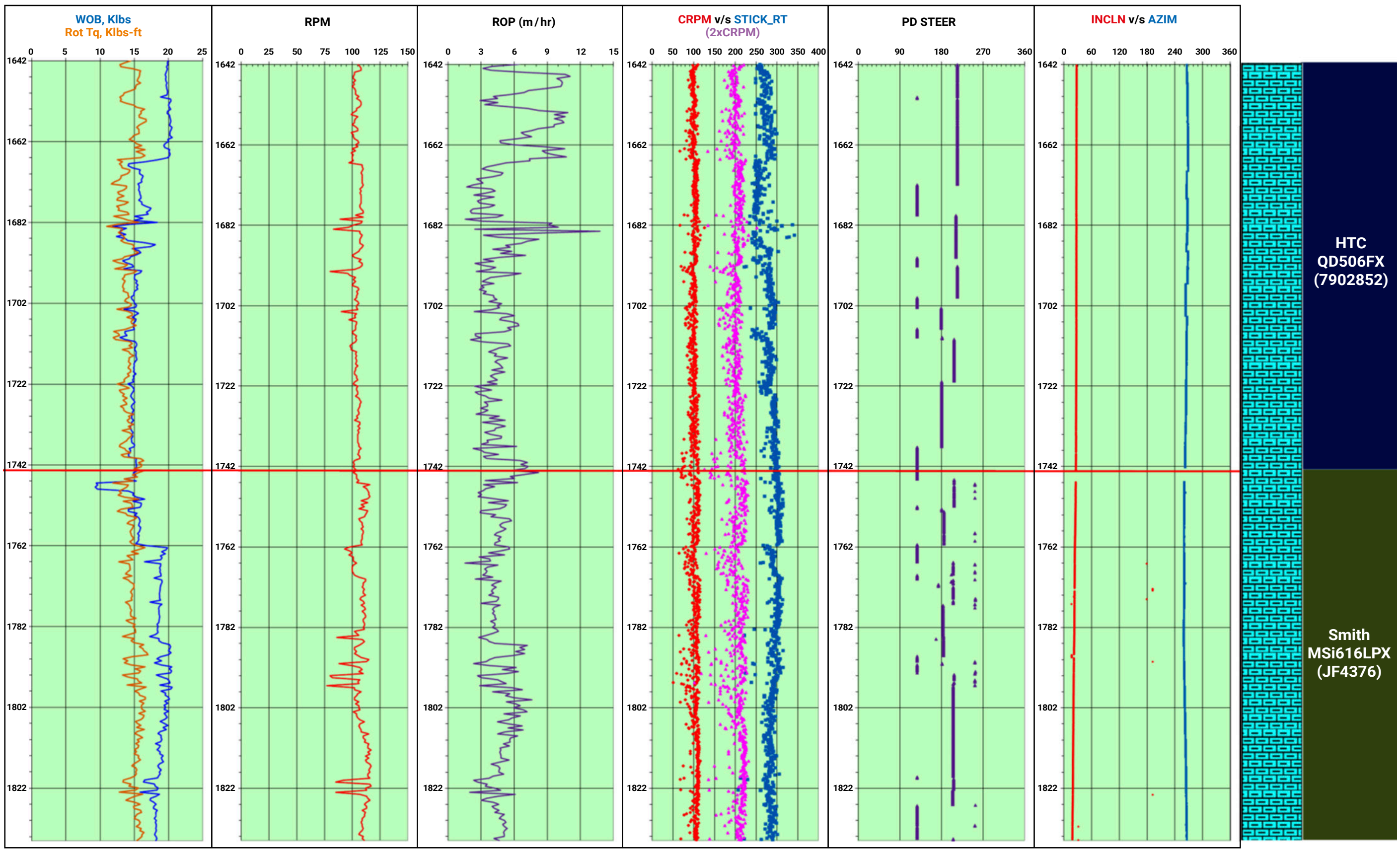

Fig. 8. Section drilled by 12¼" QD506FX & MSi616LPX bits in the Shiranish Formation (1642–1835 m) for well R-X33

The mitigation program includes several possibilities: first; if losses are 1–2 m^3/hr, ROP will be below 10 m^3/hr, and an LCM quantity of 10 m^3 (with a density of 45 lb/bbl) will be pumped. When the losses exceed 2 m^3/hr, the drilling process will be stopped, and a ball will be dropped to open the PBL sub-circulating valve, ollowed by the pumping of 10–20 m^3 of LCM (with a density of 85 lb/bbl). In addition, the annulus around the bit will be opened. In the case of total losses, the PBL sub-circulating valve will be opened, and if no returns are observed, an LCM quantity of 20 m^3 (with a density of 85 lb/bbl) will be pumped (Fig. 15).

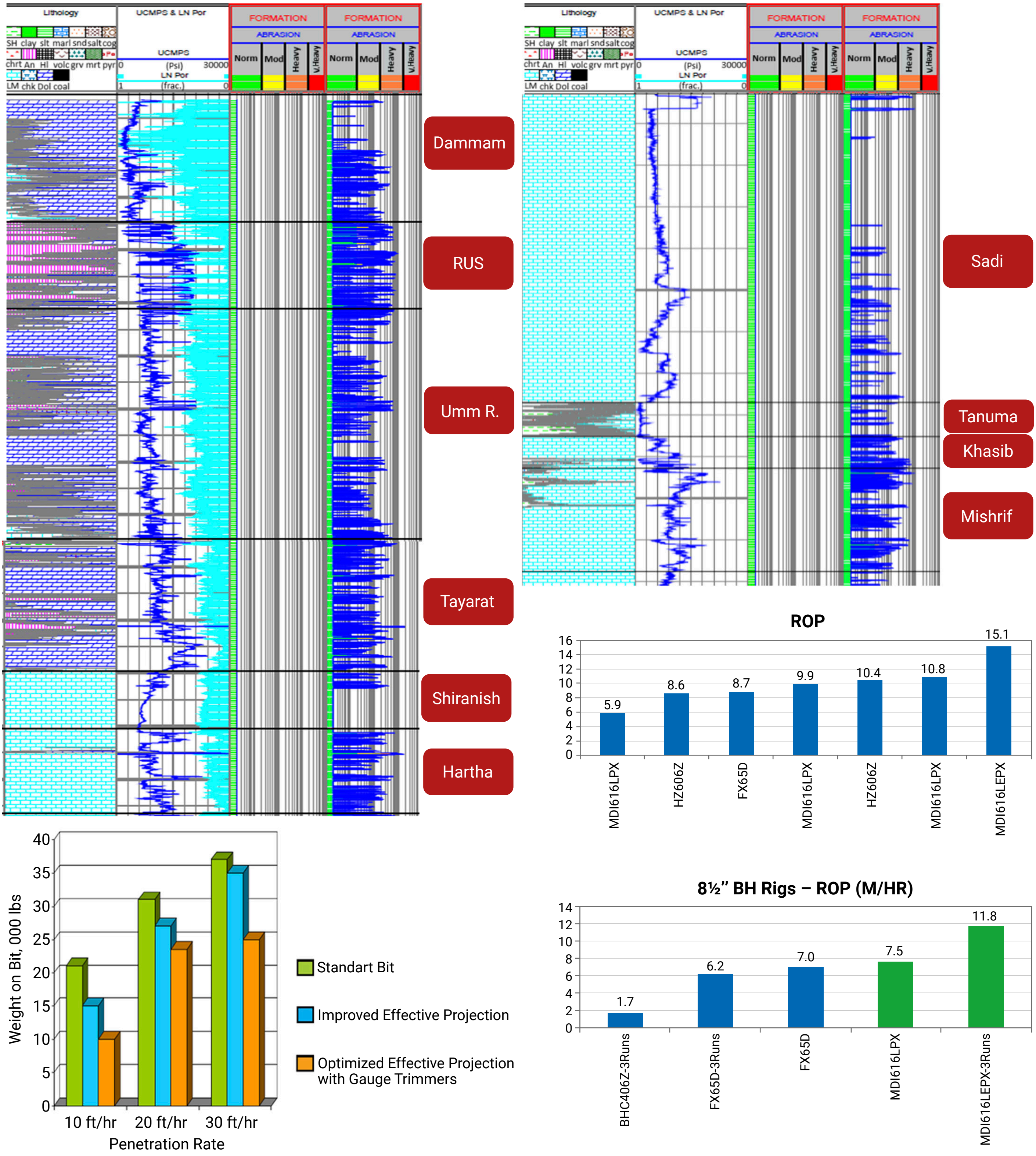

Fig. 9. Comparison of performance for all types of bits used in the Majnoon Field

MINING SCIENCE AND TECHNOLOGY (RUSSIA)
ГОРНЫЕ НАУКИ И ТЕХНОЛОГИИ
2024;9(4):308–327
eISSN 2500-0632
https://mst.misis.ru/

Downward from the Mishrif Formation, another non-productive formation, the Shuaiba Formation, also shows the mud loss phenomena. Fig. 16 indicates mud loss areas, where the red outline encloses the area of severe mud loss, while the black outline indicates partial mud loss. The green outlines arbitrarily mark areas where no mud loss was recorded. It should be noted that the embedded values reflect variable drilling practices and may change in a biased way, either increasing or decreasing.

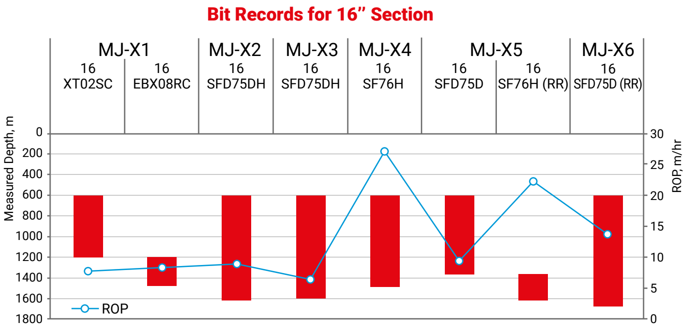

Bit Usage	Size	Bit Type	IADC	Depth In, m	Depth Out, m	Interval, m	Formations
Primary	16”	SFD76C	PDC	600	1639	1039	Lower Fars, Ghar, Part of Dammam
Back up	16”	EBXT08RC	425				

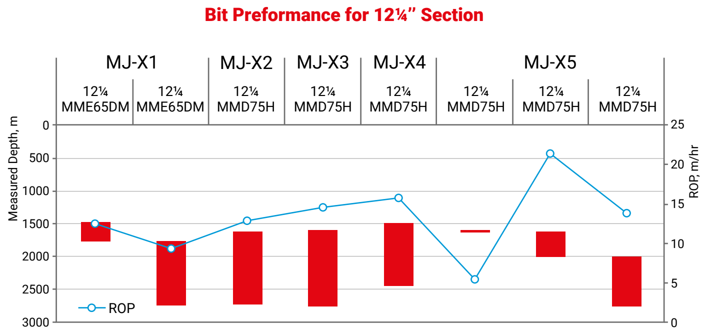

Bit Usage	Size	Bit Type	IADC	Depth In, m	Depth Out, m	Interval, m	Formations
Primary	12¼”	MME75H	PDC	1639	2930	1291	Dammam, UER, Aaliji, Shiranish, Hartha, Sa'adi, Tanuma, Khasib
Back up	12¼”	MMD75H					

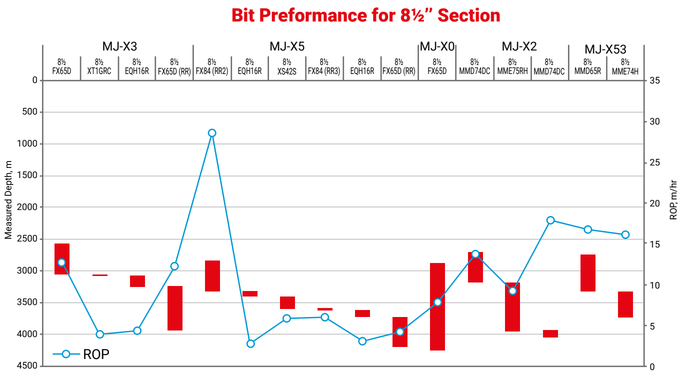

Bit Usage	Size	Bit Type	IADC	Depth In, m	Depth Out, m	Interval, m	Formations
Primary	8½”	MMD65R (RR)	PDC	2930	3326	396	Mishrif, Rumaila, Ahmadi
Back up	8½”	MMD74DC (RR)	PDC				

Fig. 10. Bit performance in the Majnoon Field

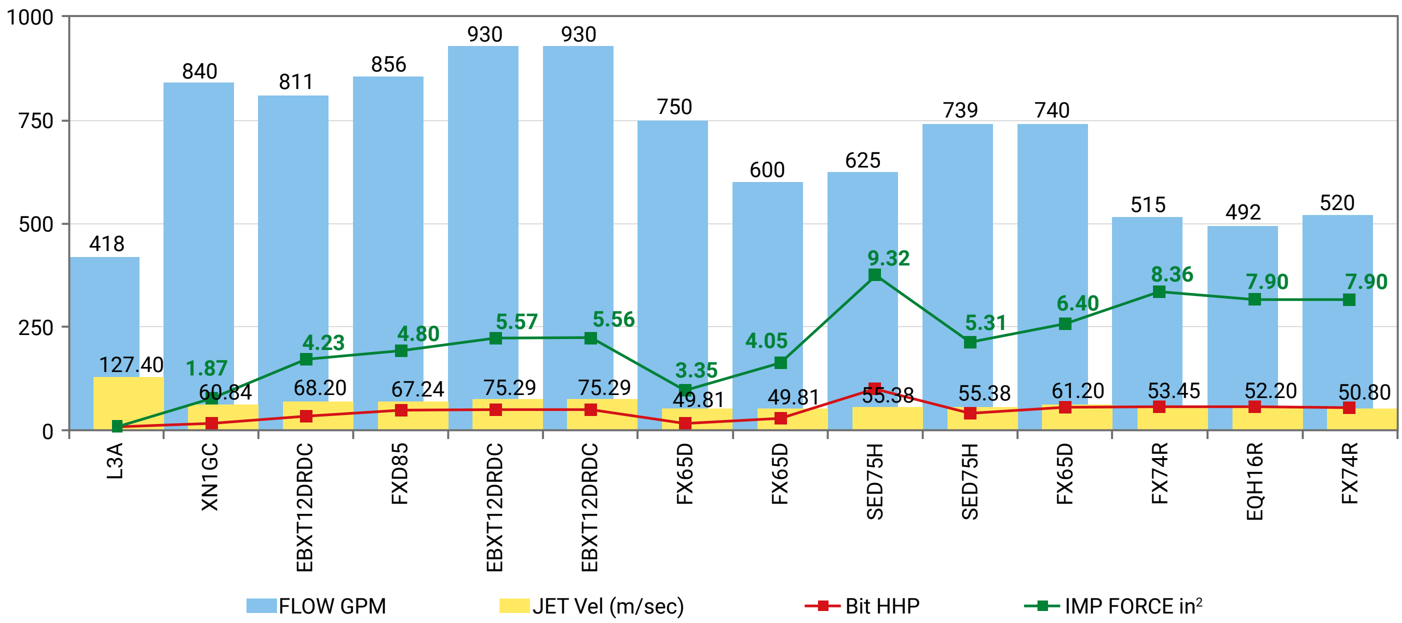

Fig. 11. Comparison of hydraulic performance for 16” bits used in the Majnoon Field

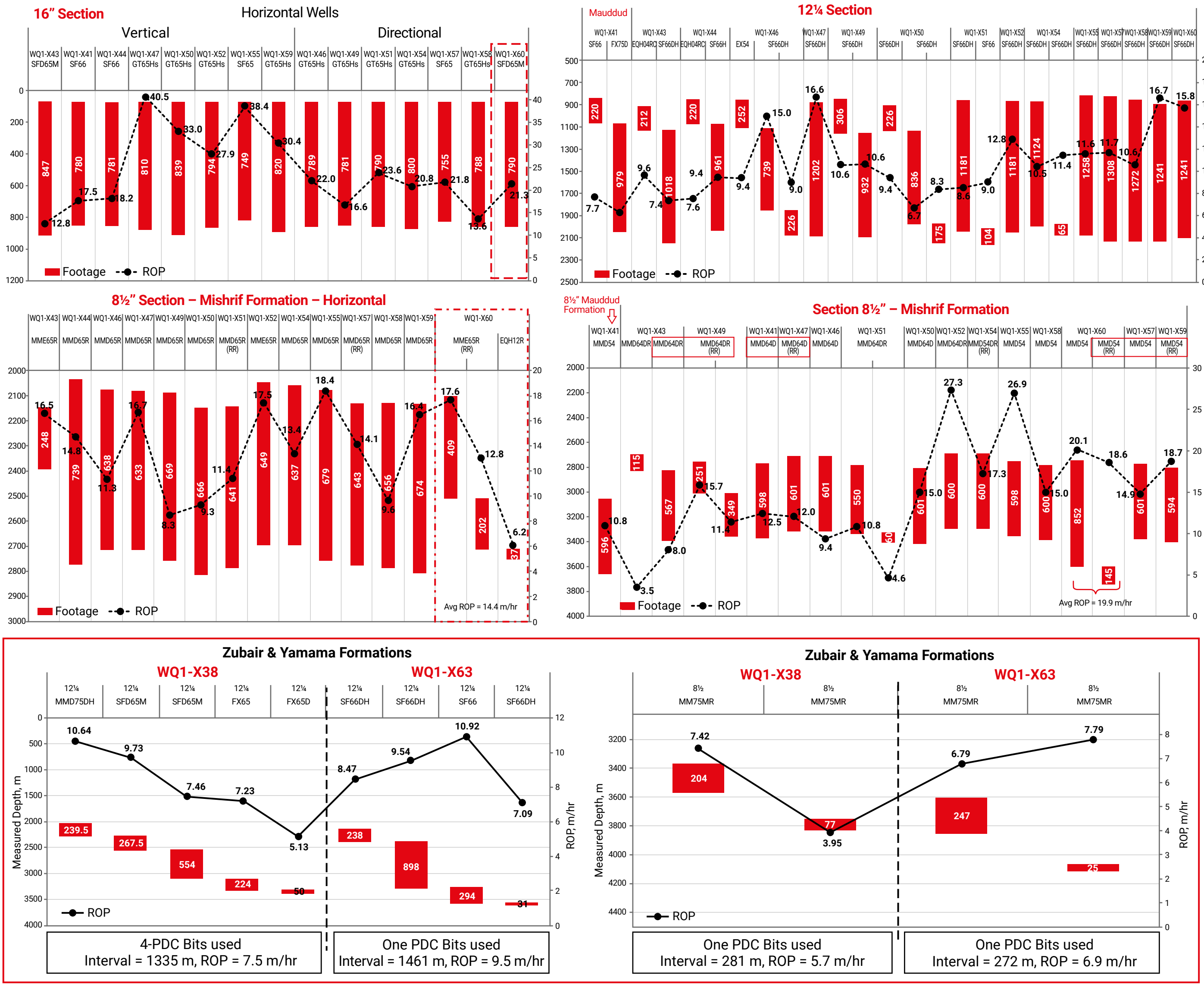

Fig. 12. Bits performance through the non-productive and productive zones (Mishrif, Mauddud, Zubair, and Yamama Formations) in the West Qurna Field

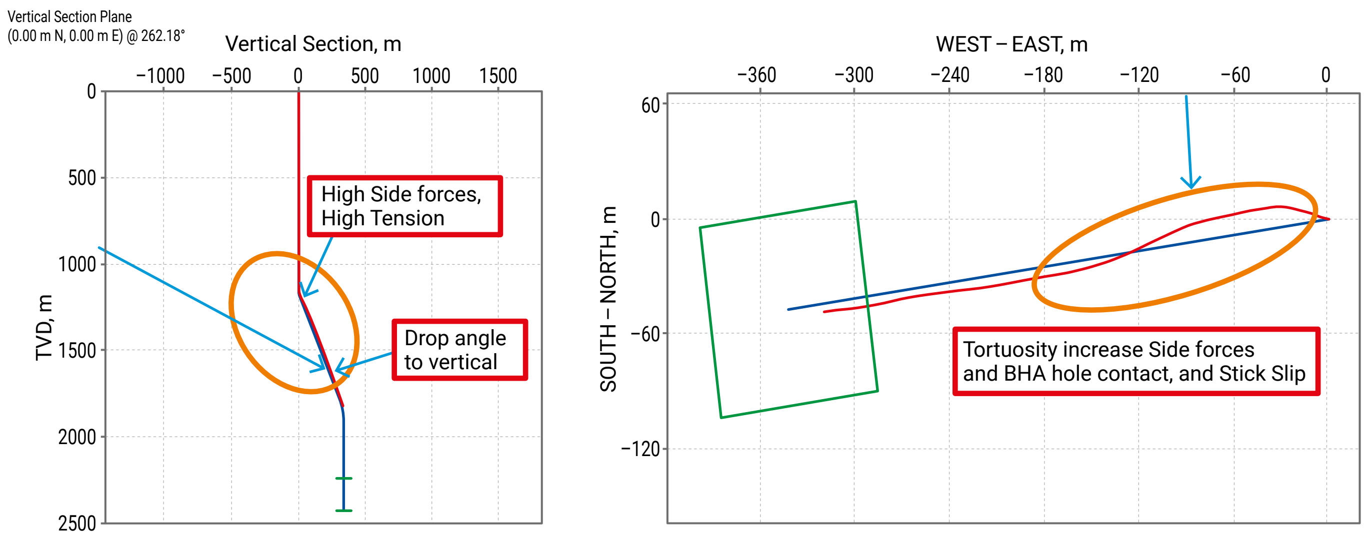

a *b*

Fig. 13. Tortuosity – *a*; Side forces for well R-XX3 – *b*

MINING SCIENCE AND TECHNOLOGY (RUSSIA)
ГОРНЫЕ НАУКИ И ТЕХНОЛОГИИ
2024;9(4):308–327
eISSN 2500-0632
https://mst.misis.ru/

BIT TORQUE				
Axial (g)	Delta, klb-ft	Lateral (g)		
0.2	0.85	5		Excellent
0.4	1.50	10		Good
0.6	2.15	15		Safe
0.8	2.80	20		Moderately Safe
1.0	3.50	25		Unsafe

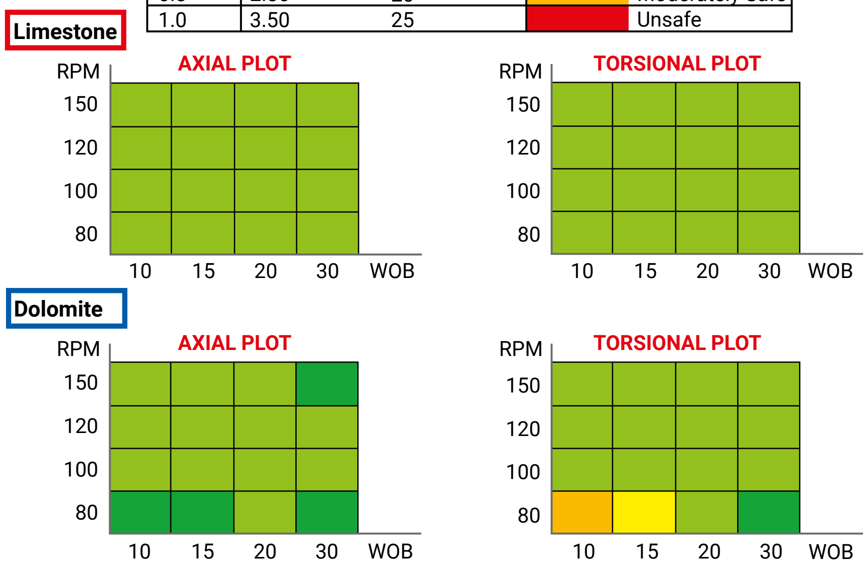

Fig. 14. Sensitivity of axial and torsional torques (RPM vs WOB) for limestone and dolomite formations in the Rumaila Field

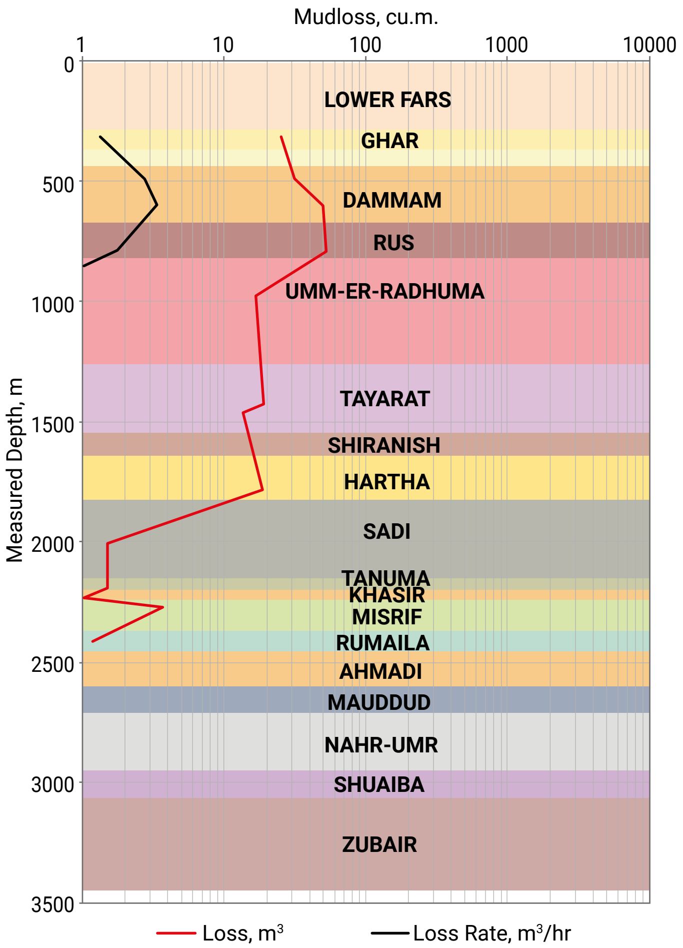

Fig. 15. Mud loss from the surface to the Rumaila Formation

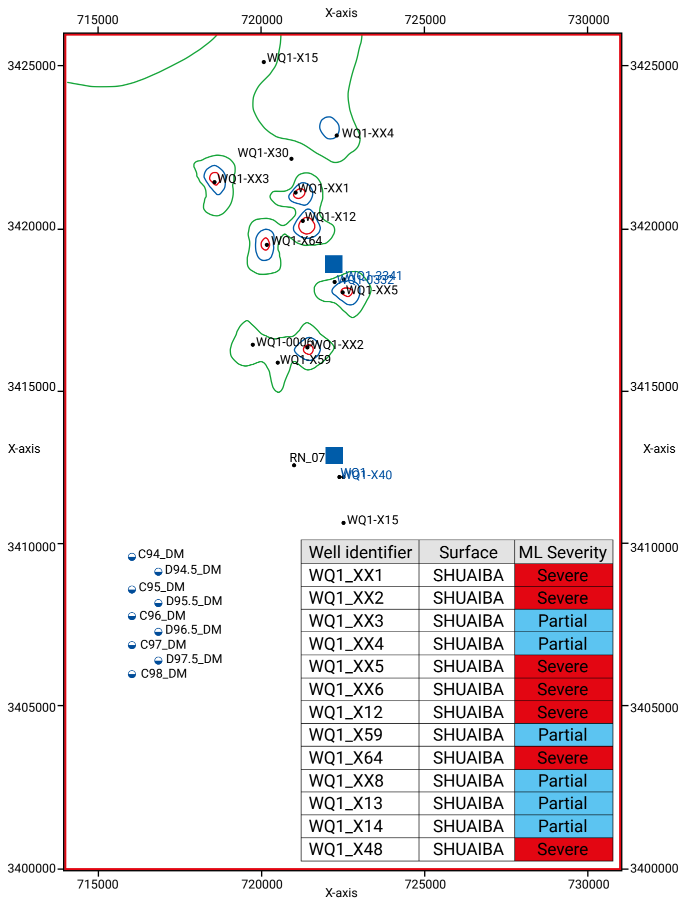

Fig. 16. Mud loss mapping for the Shuaiba Formation in the West Qurna (1 and 2)

4.3. Mitigations for Other Problems

The Mishrif, Mauddud, Zubair, and Yamama Formations must be isolated from the top of the liner to eliminate crossflows and pretend potential communication between the lower water-bearing zones and shallow loss zones during the production phase of the wells.

H_2S detectors must be calibrated and functionally tested before drilling into the Nahr Umr Sandy Formation. The 8½" BHA wipe trip could not pass through the POOH in the Nahr Umr Formation, and re-running with directional BHA was required to clear the obstruction. Surging/swabbing issues were observed in the wells in the Zubair Formation, with the presence of connection gas, background gas, trip gas, and differential sticking.

The 8½" interval in the Zubair Formation will be drilled with an inhibitive KCL/PHPA polymer mud system to provide wellbore hole stability, clay inhibition, and good hole cleaning. Glycol will be used if required, with 3% added in the case of shale problems. CaCO3 will be added to increase mud weight to the desired 1.28 sg.

For the Yamama Formation, the PDC Bit (MMD65R) performed the best. Mud properties should have an MW of 1.60–1.65 sg (as indicated in the last two rows of Table 2). GEM™ GP shale stabilizer and KCl Polymer (5% KCL) must be added, with a flow rate of 1800–2300 LPM, and RPM adjusted as per the DD's recommendations.

5. Discussion

A junk basket must be placed above the bit if the circulating fluid is flowing down the work string. The nozzles must be removable from the bit and from any equipment inside the drill string to ensure they are large enough to allow cuttings to pass when reversing circulation during drilling. Variations in rotary speed and bit weight should be optimized to break metal parts and to re-establish bit penetration. Penetration stoppage because due to "bit tracking" may require lifting the bit off the grilling surface. Rapid bit contact and weight application while continuing rotation will aid in breaking up the bit pattern and help to re-establish bit penetration.

When losses occur in the Nahr Umr, Shuaiba, Upper Shale, Middle Sand, and Middle Shale Formations, or they are accompanied by changes in torque or a drilling break (including bit dropping), they will likely occur at the bottom. However, if losses occur during tripping or while increasing mud weight, they will occur off the bottom. Pipe sticking must be avoided when losses occur, as cuttings may settle around the BHA and stick to the pipe mechanically. The cuttings will act as a packer and exacerbate losses below them. The pipe must be kept moving at all times. Differential sticking must also be considered. For the Mishrif Formation, an advanced drilling strategy was applied to wells WQ1-X52 and subsequent wells drilled between 2017 and 2018, with good performance compared to wells drilled earlier (an average of 30.3 days and NPT of 4.4%). The final drilling program includes adjustments, as shown in Fig. 17. In the Mauddud Formation, there were no encounters with helical or sinusoidal buckling during drilling operations (Fig. 18). The maximum torque at the rotary table (rotating on the bottom – 8300 ft-lbf) remained below the makeup torque for the 3½" DP (Figs. 19 and 20).

Table 2

The Yamama offset wells data and MW selection in the West Qurna Field

Well	Formation	Depth, m TVD	Actual PP, sg	PP, psi	MW (Low), sg	MW (High), sg	Overbalance (Low), psi	Overbalance (High), psi
WQ1-X12 (old well)	Ya – A	3515	1.47	7343	1.50	1.61	150	699
WQ1-X12	Ya – A	3566	1.44	7298	1.50	1.61	304	862
WQ1-X12	Ya – A	3593	1.43	7302	1.50	1.61	357	919
WQ1-X12	Ya – B	3620	1.39	7151	1.50	1.61	566	1132
WQ1-X12	Ya – B	3685	1.37	7175	1.50	1.61	681	1257
WQ1-X38 (2018)	Ya – A	3551	1.46	7368	1.50	1.61	202	757
WQ1-X38	Ya – B	3653	1.39	7216	1.50	1.61	571	1142
WQ1-X63	Ya – A	3836	~1.42	7741	1.55	1.65	709	1254
WQ1-X63 (2019)	Ya – B	3924	~1.42	7919	1.55	1.65	725	1283
WQ1-X63 (~WQ1-X12)	Ya – A	3836	1.47	8014	1.60	1.65	709	981
WQ1-463 (~WQ1-X12)	Ya – A	3836	1.44	7850	1.60	1.65	872	1145

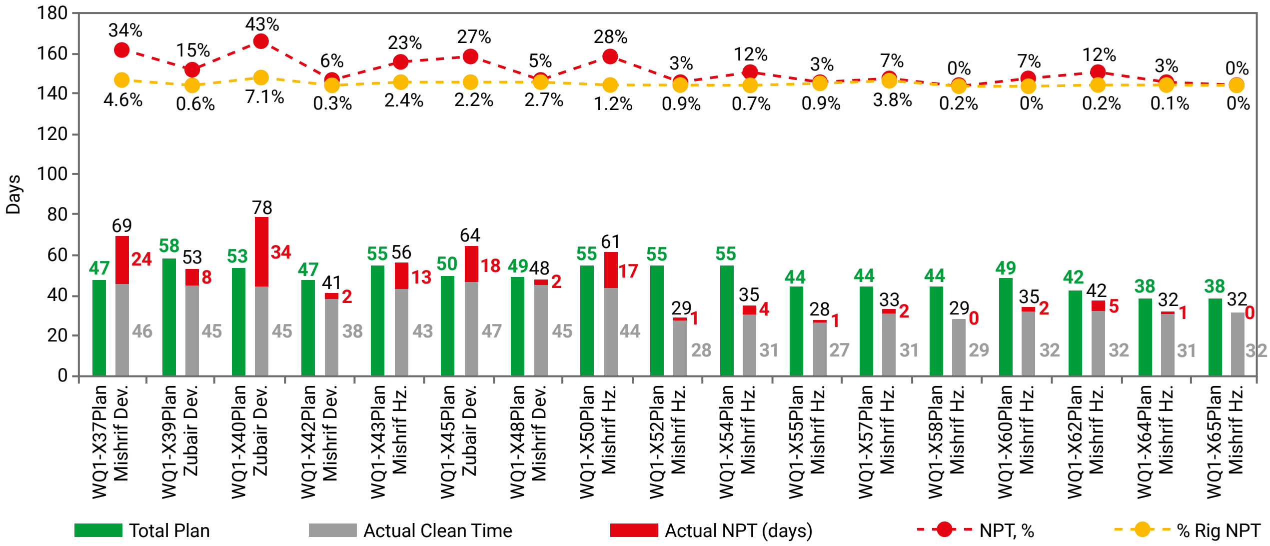

Fig. 17. Wells performance in the West Qurna-1 Field from 2017 to 2018

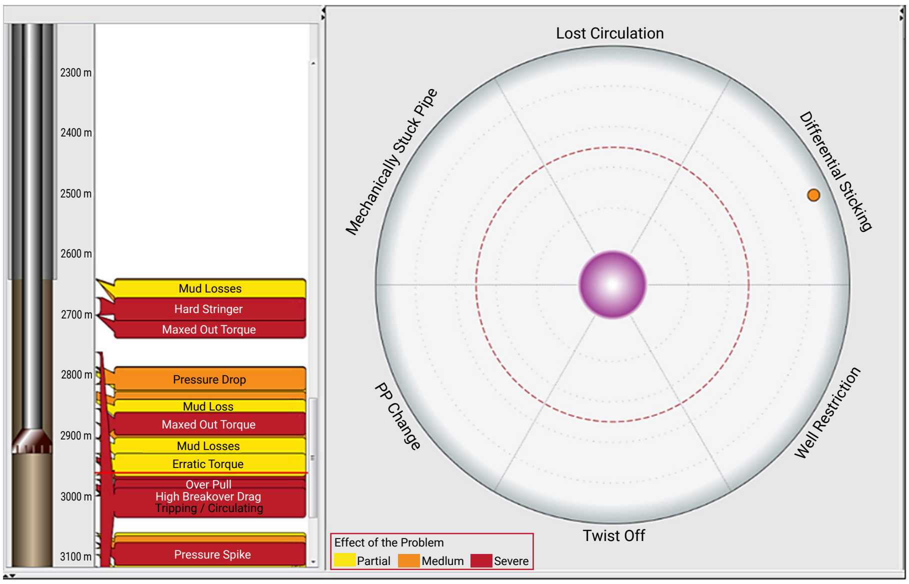

Fig. 18. Drilling optimization through real-time monitoring of drilling problems from the Mishrif to Mauddud Formations

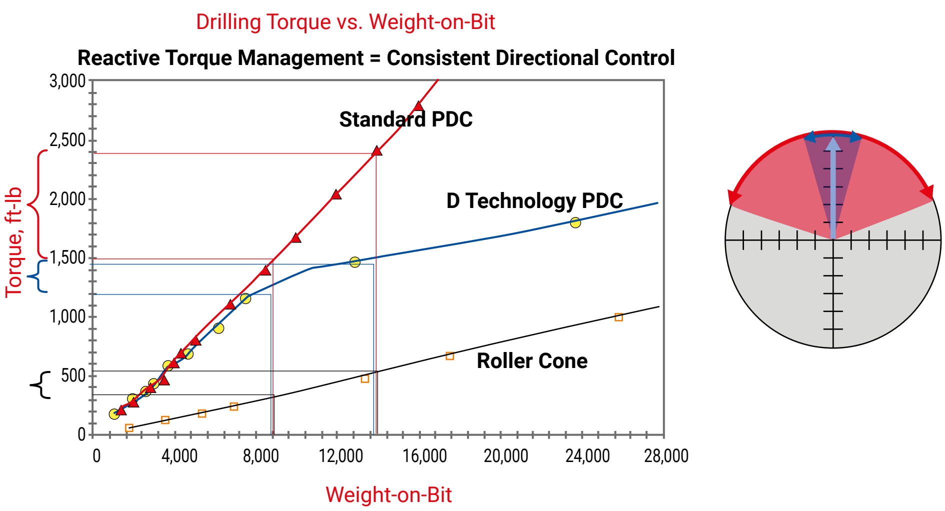

Fig. 19. Reactive torque management with weight on bit

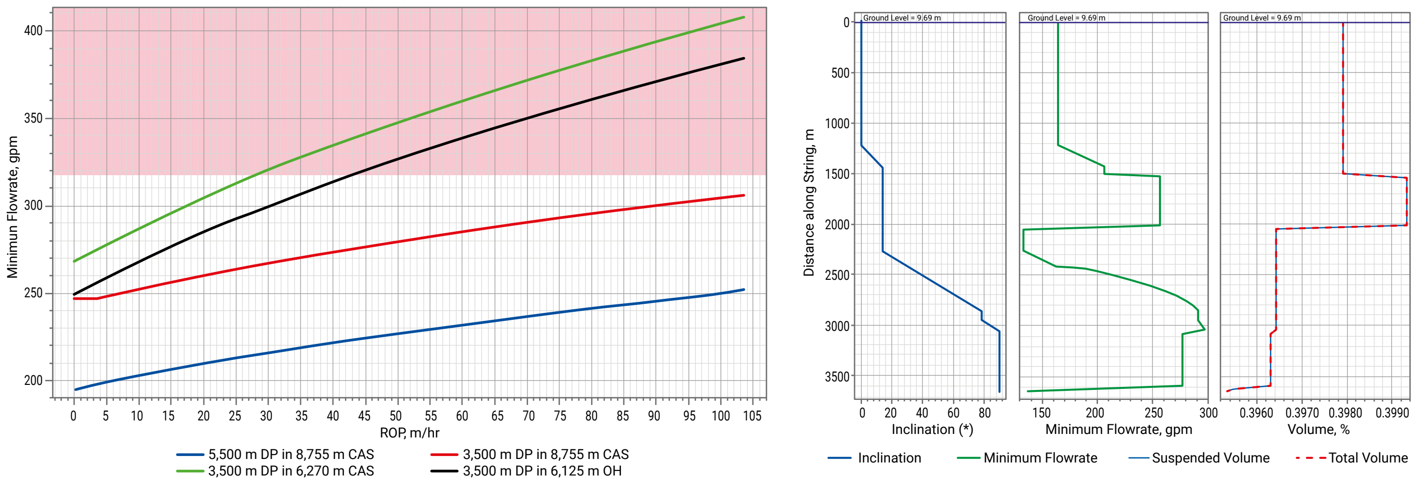

a *b*

Fig. 20. Hole cleaning performance: Minimum flow rate vs ROP – *a*, and Inclination, flow rate, and volume % for the Mauddud Formation in the West Qurna Field – *b*

Conclusion(s)

1. The use of the 16” SFD75D bit in directional wells proved to be the preferred bit for this section. Toward improving performance, the 16” MMD65R, EQH16R, and SF74R bits can also be successfully useable. It is recommended to use the MME65R PDC bit as a primary or backup in upcoming Mishrif horizontal wells in southern Iraq. The MSi616L bit type is a well-proven design for drilling 12¼” section applications in southern Iraq, while the EQH12DR bit type was used in recent drilling operations to complete the remaining parts of the 8½” section and came out in excellent condition. For horizontal sections, the MMD54 bit (5 blades, 13 mm cutter size) showed excellent performance and accumulated intervals, achieving the highest ROP (26.9 m /hr).

2. Changes in the drilling program include running a 12¼” rotary slick BHA with large nozzles and pumping a balanced cement plug through the bit to drill up to 2000 m. In the case of Dammam Formation losses, LCM will be pumped, and a cement plug will be pumped if needed. Then POOH and run an open-ended drill pipe to set the cement plug. Finally, POOH and directional BHA were run to drill to TD. ECD must be controlled, and MW must be optimized before penetrating the Hartha Formation. To minimize losses, high overbalance must be avoided while drilling Hartha, and losses with LCM can be cured.

3. Several successful FlexPlug applications have been completed in southern Iraq fields, providing valuable experience in treating serious lost circulation situations.

4. Only 10 m is required to drill below the top of the Sadi Formation, after which losses must be checked before continuing drilling. PP/FG data must be optimized and updated from the top section as a guide and trend for the bottom interval. The hole must be cleaned, and flow and POOH must be checked. The 12¼” section in the Hartha Formation must be drilled with directional BHA in rotary mode with controlled parameters.

5. Sudden losses in the Tanuma Formation must be managed, and the hole must keep full at all times to prevent the collapse of weak zones. Shale inhibition must be added to the bridging material to control effective shale formations.

6. In the Mauddud Formation, good hole cleaning can be achieved with 250–317 gpm in the horizontal section at a rotary speed of 40 RPM, a settling velocity at 10.2 ft/min, and a Yield point of 3.933 lft/100 ft^2.

7. The suggested parameters before starting to drill the Nahr Umr Formation are a flow rate of 2500–3500 l/min, WOB of 12–15 tons, RPM of 100–160, and MW of 1.25 sg to avoid potential sticking of the pipes and hole sloughing.

8. The mud loss problem will be noticeable in the north of the West Qurna-1 and south of the West Qurna-2 Field, while it will be partial toward the south due to the mud loss in the Shuaiba Formation.

9. The 7” production liner must be run and seated with proper isolation across the Mishrif and Zubair Formations. The liner must be overlapped to prevent potential communication between the lower water-bearing zones and shallow loss zones during well production.

10. The drilling fluid density is 1.28 sg from the top to the bottom of the Zubair and Mishrif Formations, with full holes at all times. Tripping in/out

must be done at controlled speeds to prevent surging/swabbing the well. Frequent flow checks must be performed during drilling breaks, and gas from connections, background, and trips must be monitored. Potassium chloride must be added and maintained at 3–5% as per the program while drilling all sections of the Zubair Formation.

11. For the Yamama Formation, the PDC bit (MMD65R) performed the best. Mud properties should have an MW of 1.60–1. 65 sg, GEM™ GP shale stabilizer/KCl Polymer (5% KCL) must be added, with a flow rate of 1800–2300 LPM, and RPM as per DD's recommendations. An H_2S Scavenger is recommended.

12. The injector(s) should remain shut in until the Mishrif, Mauddud, Zubair, and Yamama Formations are cased off to prevent potential flow.

13. The Dammam Formation faced the most drilling problems, while no significant problems occurred in the Dibdibba, Khasib, Rumaila, Ahmedi, and Mauddud Formations.

References

1. Aldamzharov N. Prevention of accidents and complications during drilling of branched horizontal boreholes. *News of Science of Kazakhstan*. 2017;(3):78–90. (In Russ.) URL: https://vestnik.nauka.kz/storage/docs/2017/2017_NNK_%E2%84%963_End.pdf
2. Nazari T., Hareland G., Azar J. Review of cuttings transport in directional well drilling: systematic approach. In: *SPE Western Regional Meeting*. May 27–29, 2010, Anaheim, California, USA. https://doi.org/10.2118/132372-MS
3. Hashim J., Abdulkadir U., Alkali M., Kumar A. Basic drilling problems and optimization by general intensive knowledge. *International Journal for Advance Research and Development*. 2017;2(5):90–101. URL: https://www.ijarnd.com/manuscripts/v2i5/V2I5-1173.pdf
4. Salih A., Hussein H. Artificial intelligent models for detection and prediction of lost circulation events: a review. *Iraqi Journal of Chemical and Petroleum Engineering*. 2022;23(4):81–90. https://doi.org/10.31699/IJCPE.2022.4.10
5. Miranda C., Oliveira J., Cavalcante G. et al. Materials for controlling severe lost circulation-laboratory evaluation. In: *SPE Latin America and Caribbean Petroleum Engineering Conference*. May 17–19, 2017, Buenos Aires, Argentina. https://doi.org/10.2118/185582-MS
6. Caughron D., Renfrow D., Bruton J. et al. Unique crosslinking pill in tandem with fracture prediction model cures circulation losses in deepwater Gulf of Mexico. In: *IADC/SPE Drilling Conference*. February 26–28, 2002, Dallas, Texas. https://doi.org/10.2118/74518-MS
7. Toreifi H., Rostami H., Manshad A. New method for prediction and solving the problem of drilling fluid loss using modular neural network and particle swarm optimization algorithm. *Journal of Petroleum Exploration and Production Technology*. 2014;4:371–379. https://doi.org/10.1007/s13202-014-0102-5
8. Bloys B., Davis N., Smolen B. et al. Designing and managing drilling fluid. *Oilfield Review*. 1994;6(2):33–43.
9. Yarim G., Uchytil R., May R. et al. Stuck pipe prevention – a proactive solution to an old problem. In: *SPE Annual Technical Conference and Exhibition*. November 11–14, 2007, Anaheim, California, USA. https://doi.org/10.2118/109914-MS
10. Muqeem M., Weekse A., Al-Hajji A. Stuck pipe best practices – a challenging approach to reducing stuck pipe costs. In: *SPE Saudi Arabia Section Technical Symposium and Exhibition*. April 8–11, 2012, Al-Khobar, Saudi Arabia. https://doi.org/10.2118/160845-MS
11. Salminen K., Cheatham C., Smith M., Valiullin K. Stuck-pipe prediction by use of automated real-time modeling and data analysis. *SPE Drilling & Completion*. 2017;32(03):184–193. https://doi.org/10.2118/178888-PA
12. Saleh I., Khalaf A., Al-Jawad M. Southern Iraqi Oil fields drilling problems identification, analysis, and treatment. In: *Offshore Technology Conference Asia*. March 20–23, 2018, Kuala Lumpur, Malaysia. https://doi.org/10.4043/28597-MS
13. Al-Dujaili A. N., Sundos H. A Statistical survey for drilling problems at North Rumaila field, Southern Iraq. A review enhanced with well logs analyses. *Jordan Journal of Earth and Environmental Sciences*. 2023. (In press.)
14. Sissakian V. Geological evolution of the Iraqi Mesopotamia Foredeep, inner platform and near surroundings of the Arabian Plate. *Journal of Asian Earth Sciences*. 2013;72:152–163. https://doi.org/10.1016/j.jseaes.2012.09.032
15. Fouad S., Wafa'a A. Tectonic and structural evolution of Al-Jazira Area. *Iraqi Bulletin of Geology and Mining*. 2009;(3):33–48.

16. Fouad S. Tectonic and structural evolution of the Mesopotamia Foredeep, Iraq. Iraqi Bulletin of Geology and Mining. 2010;6(2):41–53.
17. Handhal A., Jawad S., Al-Abadi A. GIS-based machine learning models for mapping tar mat zones in upper part (DJ unit) of Zubair Formation in North Rumaila supergiant oil field, Southern Iraq. *Journal of Petroleum Science and Engineering*. 2019;178:559–574. https://doi.org/10.1016/j.petrol.2019.03.071
18. Al-Khafaji A., Yonis S., Ibrahim R. et al. Geochemical characterization and origin of the Cretaceous Sa'di, Khasib, Mishrif, and Nahr Umr Crude Oils in Halfaya Oilfield, Southern Mesopotamian Basin, Iraq. *Petroleum Science and Technology*. 2021;39(21–22):993–1007. https://doi.org/10.1080/10916466.2021.1980587
19. Abeed Q., Leythaeuser D., Littke R. Geochemistry, origin and correlation of crude oils in Lower Cretaceous sedimentary sequences of the southern Mesopotamian Basin, southern Iraq. *Organic Geochemistry*. 2012;46:113–126. https://doi.org/10.1016/j.orggeochem.2012.02.007
20. Mehenni M., Guit F. Majnoon Field, SE Iraq: A giant unique among other giants? In: *First EAGE Workshop on Iraq-Hydrocarbon Exploration and Field Development*. 2012. https://doi.org/10.3997/2214-4609.20143558
21. Abbas M., Watheq J. Lithofacies classification of carbonate reservoirs using advanced machine learning: a case study from a Southern Iraqi oil field. In: *Offshore Technology Conference*. August 16–19, 2021, Virtual and Houston, Texas; 2021. https://doi.org/10.4043/31114-MS
22. Al-Ameri T., Jafar M., Janet P. Hydrocarbon generation modeling of the Basrah oil fields, Southern Iraq. In: *AAPG Annual Convention and Exhibition*. April 10-13, 2011, Houston, Texas. 2011;20116.
23. Salih T., Sahi S., AL-Dujaili A. Using different surfactants to increase oil recovery of Rumaila field (experimental work). *Iraqi Journal of Chemical and Petroleum Engineering*. 2016;17(3):11–31. https://doi.org/10.31699/IJCPE.2016.3.2
24. Al-Ansari R. The petroleum geology of the upper sandstone member of the Zubair Formation in the Rumaila South. *Geological Study, Ministry of Oil, Baghdad, Iraq*. 1993.
25. Jassim S., Goff J. *Geology of Iraq*. Geological Society of London; 2006. 341 p.
26. Al-Ameri T., Jafar M., Pitman J. Hydrocarbon generation modeling of the Basrah oil fields, Southern Iraq. In: *AAPG Annual Convention and Exhibition*. March, 2012, Houston, Texas. 2012;20116:2011. https://doi.org/10.3997/2214-4609-pdb.287.1176781
27. Al-Dujaili A., Shabani M., Al-Jawad M. Characterization of flow units, rock and pore types for Mishrif Reservoir in West Qurna oilfield, Southern Iraq by using lithofacies data. *Journal of Petroleum Exploration and Production Technology*. 2021; 11, 4005–4018. https://doi.org/10.1007/s13202-021-01298-9
28. Al-Dujaili A., Shabani M., Al-Jawad M. Lithofacies and electrofacies models for Mishrif Formation in West Qurna Oilfield, Southern Iraq by deterministic and stochastic methods (comparison and analyzing). *Petroleum Science and Technology*. 2024;42(13):1656–1684. https://doi.org/10.1080/10916466.2023.2168282
29. Al-Dujaili A., Shabani M., Al-Jawad M. Lithofacies, deposition, and clinoforms characterization using detailed core data, nuclear magnetic resonance logs, and modular formation dynamics tests for Mishrif formation intervals in West Qurna/1 Oil Field, Iraq. *SPE Reservoir Evaluation & Engineering*. 2023;1–13. https://doi.org/10.2118/214689-PA
30. Al-Dujaili A., Shabani M., AL-Jawad M. Effect of heterogeneity on capillary pressure and relative permeability curves in carbonate reservoirs. A case study for Mishrif Formation in West Qurna/1 Oilfield, Iraq. *Iraqi Journal of Chemical and Petroleum Engineering*. 2023;24(1):13–26. https://doi.org/10.31699/IJCPE.2023.1.3
31. Lazim A., Maki M., Tariq S. Detect faults of Zubair and Mishrif Formations–Zubair Oilfield by Integrate Structural Geology and Pressure Transient Analyses (PTA) to Selected Wells. *IOSR Journal of Applied Geology and Geophysics.* 2020;8(5):67–72. https://doi.org/10.9790/0990-0805016772
32. Al-Jaberi M., A-Jafar M. Elements distribution for the upper sandstone member of the Zubair Formation in Zubair oil field, southern Iraq. *Iraqi Geological Journal*. 2020;53(1E):55–74. https://doi.org/10.46717/igj.53.1E.5Ry-2020-07-05
33. Hussein M., Eren T., Rahman A. et al. Case Study for Curing Circulation Losses during Primary Cementing Operations Using Fiber Cement in Zubair Field/Iraq. In: *SPE/IADC Middle East Drilling Technology Conference and Exhibition*. 29–31 January 2018, Abu Dhabi, UAE. 2018. https://doi.org/10.2118/189339-MS
34. Zainab M., Almallah I., Al-Najm F. Petrophysical properties evaluation using well logging of the upper sand member of Zubair Formation in Zubair oil Field, Southern Iraq. *Basrah Journal of Science*. 2019;37(3):456–480. URL: https://www.basjsci.net/index.php/bsj/article/view/108

35. Al-Dujaili A., Shabani M., AL-Jawad M. Identification of the best correlations of permeability anisotropy for Mishrif reservoir in West Qurna/1 oil Field, Southern Iraq. *Egyptian Journal of Petroleum*. 2021;30(3):27–33. https://doi.org/10.1016/j.ejpe.2021.06.001

36. Sadooni F., Alsharhan A. Stratigraphy, microfacies, and petroleum potential of the Mauddud Formation (Albian–Cenomanian) in the Arabian Gulf basin. *AAPG bulletin*. 2003;87(10):1653–1680. https://doi.org/10.1306/04220301111

37. Cross N., Goodall I., Hollis C. et al. Reservoir description of a mid-Cretaceous siliciclastic-carbonate ramp reservoir: Mauddud Formation in the Raudhatain and Sabiriyah fields, North Kuwait. *GeoArabia*. 2010;15(2):17–50. https://doi.org/10.2113/geoarabia150217

38. Beydoun Z. Productive Middle East clastic oil and gas reservoirs: their depositional settings and origins of their hydrocarbons. In: *Sedimentary Facies Analysis: a Tribute to the Research and Teaching of Harold G. Reading*. Wiley; 1995. Pp. 329–354. https://doi.org/10.1002/9781444304091.ch14

39. Ibrahim M.W. Lithostratigraphy and subsurface geology of the Albian rocks of south Iraq. *Journal of Petroleum Geology*. 1981;4(2):147–162. https://doi.org/10.1111/j.1747-5457.1981.tb00530.x

40. Al-Zaidy A., Al-Mafraji T. Geohistory analysis and basin development of the Late Berriasian-Aptian Succession, Southern Iraq. *Iraqi Geological Journal*. 2019;52(2):36–52. https://doi.org/10.46717/igj.52.2.3Ms-2019-12-26

41. Idan R., Faisal R., Nasser M. et al. Hydrocarbon potential of Zubair Formation in the south of Iraq. *Arabian Journal of Geosciences*. 2015;8:4805–4817. https://doi.org/10.1007/s12517-014-1569-6

42. Al-Ghuribawi M., Rasha F. An Integrated Microfacies and Well Logs-Based Reservoir Characterization of Yamama Formation, Southern Iraq. *Iraqi Journal of Science*. 2021;62(10):3570–3586. https://doi.org/10.24996/ijs.2021.62.10.16

43. Chafeet H. Yamama reservoir characterization in the West Qurna oil field, Southern Iraq. *Iraqi Journal of Science*. 2016;57(2A):938-947.

44. Aqrawi A., Mahdi T., Sherwani G., Horbury A. Characterization of the Mid-Cretaceous Mishrif Reservoir of the southern Mesopotamian Basin, Iraq. In: *American Association of Petroleum Geologists Conference and Exhibition*. 7–10 March 2010; Manama, Bahrain. Pp. 7–10. https://doi.org/10.3997/2214-4609-pdb.248.104

45. Al-Iessa I., Zhang W. Facies evaluation and sedimentary environments of the Yamama Formation in the Ratawi oil field, South Iraq. Scientific Reports. 2023;13(1):5305. https://doi.org/10.1038/s41598-023-32342-9

46. Al-Dujaili A.N., Shabani M., Al-Jawad M.S. The efficient and economical application of a cement slurry programme for sandstone and carbonate reservoirs. A case study of the Zubair, Mauddud, and Mishrif formations in a supergiant oilfield, in southern Iraq. *Bulletin of Geophysics & Oceanography*. 2024;65(3):439–460. https://doi.org/10.4430/bgo00450

Information about the author

Ahmed N. Al-Dujaili – PhD, Doctor, Petroleum Engineering Department, Amirkabir University of Technology, Najaf, Iraq; ORCID 0000-0003-0509-4504, Scopus ID 57224971849, ResearcherID GOH-1398-2022; e-mail ahmed.noori203@aut.ac.ir

Received 26.08.2023
Revised 27.03.2024
Accepted 02.05.2024

MINING SCIENCE AND TECHNOLOGY (RUSSIA)
ГОРНЫЕ НАУКИ И ТЕХНОЛОГИИ
2024;9(4):328–340
eISSN 2500-0632
https://mst.misis.ru/

GEOLOGY OF MINERAL DEPOSITS

Research paper

https://doi.org/10.17073/2500-0632-2024-03-230
UDC 553.048:004.942(043.3)(476.7)

GIS modeling of a Cenozoic strata structure in Brest region for forecasting and evaluation of non-metallic deposits

M.A. Bogdasarov[1], **A.N. Mayevskaya**[1], **D.O. Petrov**[2], **N.N. Sheshko**[2]
[1] *Brest State A.S. Pushkin University, Brest, Republic of Belarus*
[2] *Brest State Technical University, Brest, Republic of Belarus*
✉ *bahdasarau@gmail.com*

Abstract
To date, considerable experience has been accumulated in solving the problems of forecasting and evaluation of minerals, primarily fossil fuels and ore minerals. Virtually any such forecast requires the use of computer modeling methods, which today have become an integral part of geological industry, operating with large data sets. But despite such significant successes in solving the problem of natural (mineral) resources forecasting using up-to-date information technologies, scientific and methodological approaches to modeling the subsoil of territories where commonly occurring mineral resources (COMR) are concentrated are still insufficiently developed. Due to insufficient funding, this type of resources is often overlooked, despite its important socio-economic significance for the development of local industry of various ranks in regions. COMR are also important for the territory of the Brest region of Belarus. The development of the mineral resource base of this region due to the peculiarities of its geological structure (the territory is formed by a thick strata of Cenozoic sediments) is associated with commonly occurring types of raw materials. Therefore, scientific research aimed at modeling the geological structure of Cenozoic sediments in the Brest region to assess the prospects for dicovering new deposits of non-metallic minerals in the region is very relevant. The *purpose* of this work is to create a digital geological model of the Cenozoic sediments of the Brest region as a basis for forecasting the new COMR deposits, being most accessible for development in the region, and assessing the prospects for their development. *Objectives:* to systematize data on the geological structure of the Brest region; to create a digital geological model of the Cenozoic strata in the Brest region; to develop an approach to the grouping of the region's lands according to their acceptability for the development of COMR deposits; to develop a scheme of involvement of the predicted COMR deposits of the Brest region in development. *Study subject:* Cenozoic sediments in the Brest region. *Methods:* computer modeling, geoinformation, approximation, cartographic, classification, expert review. *Results:* a new, targeted scientific and methodological approach to the geological modeling of the subsoil and non-metallic mineral deposits in the Brest region was proposed. The regional-level digital geological model created on its basis makes it possible to perform primary forecasting of COMR deposits confined to the Cenozoic sediments, as well as to assess the acceptability of involvement of the identified deposits in development.

Keywords
geology, geological model, Cenozoic, Cenozoic sediments, commonly occurring mineral resources, mineral resource base, raw material, forecast, GIS, ArcGIS, evaluation, schematic map, Brest region

For citation
Bogdasarov M.A., Mayevskaya A.N., Petrov D.O., Sheshko N.N. GIS modeling of a Cenozoic strata structure in Brest region for forecasting and evaluation of non-metallic deposits. *Mining Science and Technology* (*Russia*). 2024;9(4):328–340. https://doi.org/10.17073/2500-0632-2024-03-230

ГЕОЛОГИЯ МЕСТОРОЖДЕНИЙ ПОЛЕЗНЫХ ИСКОПАЕМЫХ

Научная статья

ГИС-моделирование строения кайнозойской толщи Брестской области для прогноза и оценки залежей нерудного сырья

М.А. Богдасаров[1], **А.Н. Маевская**[1], **Д.О. Петров**[2], **Н.Н. Шешко**[2]
[1] *Брестский государственный университет имени А.С. Пушкина, г. Брест, Республика Беларусь*
[2] *Брестский государственный технический университет, г. Брест, Республика Беларусь*
✉ *bahdasarau@gmail.com*

Аннотация
К настоящему времени накоплен значительный опыт в решении задач прогноза и оценки полезных ископаемых, прежде всего горючих и рудных. Практически любой подобный прогноз не обходится без использования методов компьютерного моделирования, которые сегодня стали неотъемлемой

составляющей геологической отрасли, оперирующей большими массивами данных. Но несмотря на столь значительные успехи в решении проблемы прогнозирования полезных ископаемых с использованием современных информационных технологий, научно-методические подходы к моделированию недр территорий, в которых сконцентрированы общераспространенные полезные ископаемые (ОПИ), все еще разработаны недостаточно. Ввиду незначительного финансирования данный вид ресурсов часто оставляют без внимания, несмотря на их важное социально-экономическое значение для развития местной промышленности регионов разного ранга. Важное значение ОПИ имеют и для территории Брестской области Беларуси. Развитие минерально-сырьевой базы данного региона в связи с особенностями его геологического строения (территория сложена мощной толщей кайнозойских отложений) связано именно с общераспространенными видами сырья. Поэтому научные исследования, направленные на моделирование геологического строения кайнозойских отложений территории Брестской области для оценки перспектив выявления новых залежей нерудных видов минерального сырья в регионе, являются весьма актуальными. *Цель* настоящей работы заключается в создании цифровой геологической модели кайнозойских отложений территории Брестской области как основы для прогноза новых наиболее доступных для освоения залежей ОПИ в регионе и оценки перспектив их освоения. *Задачи:* систематизировать сведения о геологическом строении Брестской области; создать цифровую геологическую модель кайнозойской толщи территории Брестской области; разработать подход к группировке земель региона по приемлемости к освоению залежей ОПИ; разработать схему вовлечения прогнозных залежей ОПИ территории Брестской области в разработку. *Объект:* кайнозойские отложения территории Брестской области. *Методы:* компьютерного моделирования, геоинформационный, аппроксимации, картографический, классификации, экспертных оценок. *Результаты:* предложен новый, адресный научно-методический подход к геологическому моделированию недр территории Брестской области и находящихся в них залежей нерудных полезных ископаемых. Созданная на его основе цифровая геологическая модель регионального уровня позволяет выполнить первичный прогноз на залежи ОПИ, приуроченных к толще кайнозойских отложений, а также провести оценку приемлемости вовлечения выявленных залежей в разработку.

Ключевые слова
геология, геологическая модель, кайнозой, кайнозойские отложения, общераспространенные полезные ископаемые, минерально-сырьевая база, сырье, прогноз, ГИС, ArcGIS, оценка, картосхема, Брестская область

Для цитирования
Bogdasarov M.A., Mayevskaya A.N., Petrov D.O., Sheshko N.N. GIS modeling of a Cenozoic strata structure in Brest region for forecasting and evaluation of non-metallic deposits. *Mining Science and Technology* (*Russia*). 2024;9(4):328–340. https://doi.org/10.17073/2500-0632-2024-03-230

Introduction

To date, a huge amount of research has been carried out to solve the problems of forecasting and evaluation of oil and gas deposits. The growing interest in these raw materials is determined by the permanent growth of demand and prices for them. In addition, such studies are characterized by large amounts of both governmental and private investments. At the same time, commonly occurring mineral resources (COMR)[1], which are of great socio-economic importance for the development of local industry in regions, are quite often undeservedly neglected.

COMR should to solve one of the most important problems for regions of different ranks – to meet the needs of the construction industry with local raw materials. That is why the systematic geological study of such resources is seen as a very relevant area of research at the present stage. Geological studies of the raw materials base of COMR are also important for the territory of the Brest region (the Republic of Belarus), which (its subsoil) is geologically composed of a thick sedimentary strata, mainly Cenozoic. The most accessible for development deposits of COMR in the region and in the country as a whole are genetically connected with this strata.

Detailed studies of Cenozoic sediments in the Brest region, first of all the Quaternary strata, were carried out since the middle of the XIX century and were connected with the construction of railroads and industrial enterprises, which created a demand for construction raw materials [1]. Today, numerous deposits of construction materials (clays, loams, sands and sand-and-gravel rocks, etc.) have already been explored in the region. A significant portion of such deposits are being developed. The rest serve as reserve bases for businesses in the region.

Despite the achieved successes in the creation and development of the raw material base of COMR in the Brest region, the problem of forecasting and assessment of such resources continues to be an ur-

[1] The Interparliamentary Assembly of CIS Member States: The Model Code for Subsoil Management and Subsoil Usage for CIS Member States. URL: https://base.spinform.ru/show_doc.fwx?rgn=29299 [Accessed February 29, 2024].

eISSN 2500-0632
https://mst.misis.ru/

gent problem here. This is primarily due to the need to update the results accumulated by the predecessors using the latest (most complete) geological drilling data. At the present stage, this problem can be solved most effectively with the use of computer modeling methods. Updating of data on COMR reserves/resources in the region will allow geologists to plan further study of subsoil for the development of mineral resource base (MRB) of Brest region and create a qualitative basis for providing interested organizations with information on promising deposits of construction raw materials.

Based on the above, the aim and objectives of the present study can be formulated.

The *purpose of the study* is to create a digital geological model of the Cenozoic sediments of the Brest region as a basis for forecasting the new most accessible for development COMR deposits in the region and assessing the prospects for their development.

Research objectives:

– to systematize the accumulated data on the geological structure of the Brest region;

– to create a digital geological model of the Cenozoic strata in the Brest region;

– to develop an approach to grouping the lands of the Brest region according to their acceptability for the development of COMR deposits;

– to develop a reasonable scheme of involvement of predicted COMR deposits in the Brest region in development.

The *study subject* is Cenozoic sediments in the Brest region.

Source materials

The database of drilling exploration maturity of the Brest region, compiled by the authors on the basis of materials provided by the State Enterprise "Scientific and Production Center for Geology" and the State Scientific Institution "Institute of Nature Management of the National Academy of Sciences of Belarus" served as the source data for the present study implementation.

The described database contains information on more than 5500 wells that were drilled at different times in the region. For each horizon penetrated by a particular well, more than 20 characteristics are given here. Among them the most significant for the purpose of the present research are the following: location, depth of occurrence, stratigraphic description, lithological description, absolute elevations of the upper and lower contacts, thickness of rocks.

A characteristic feature of the described well network is the unevenness of its distribution over the territory of the Brest region. As can be seen in Fig. 1, the concentration of wells in the western part of the region is very high, while in the eastern part, on the contrary, it is extremely low. This feature has had a significant impact on the development of a digital geologic model of the Cenozoic sediments of the region.

Research techniques

Currently, there are a wide variety of techniques devoted to solving the problem of geologic computer modeling for mineral deposit prediction. At the same time, most of these approaches, which have

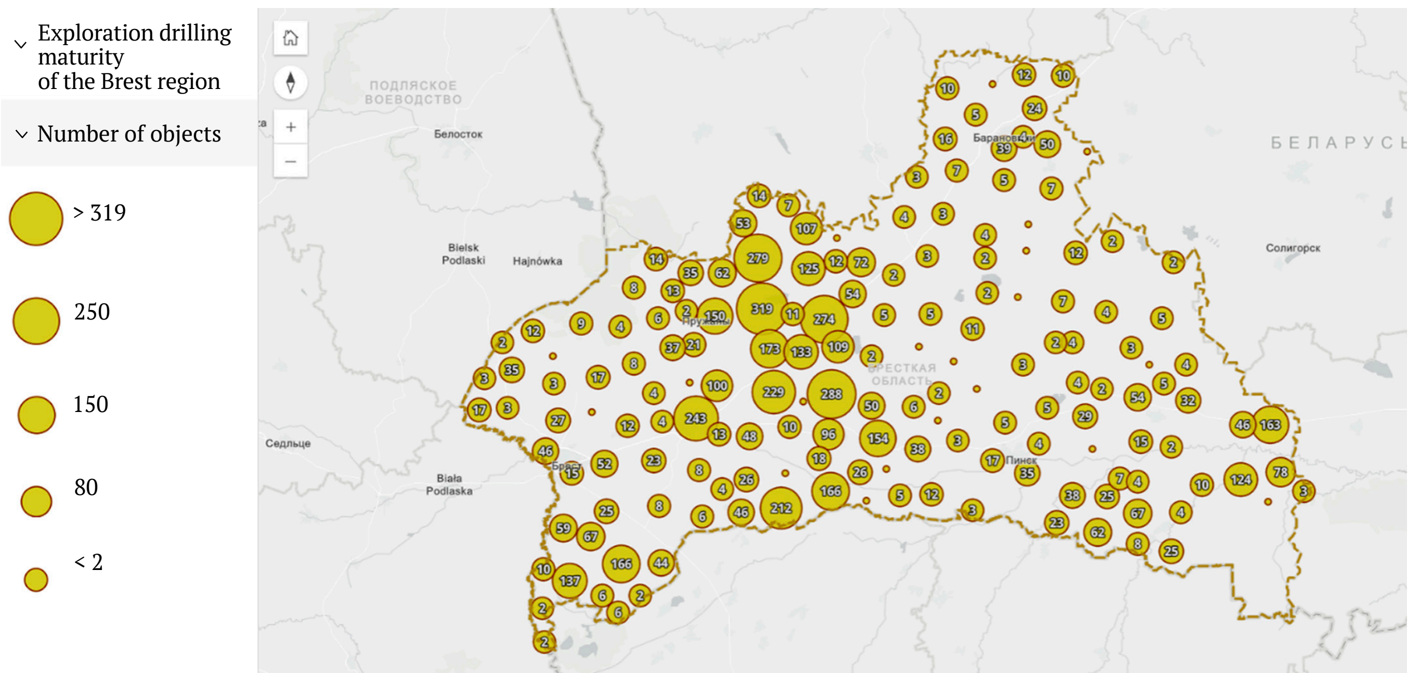

Fig. 1. Distribution of drilling wells over the territory of the Brest region

proven their practical effectiveness, are focused on the creation of models with respect to the forecast of ore and fossil fuels deposits. To a lesser extent, these approaches are focused on building subsoil models for COMR forecasting. This is due not only to the smaller amount of funding for research in the field of forecasting of commonly occurring raw materials, but also to the specificity of specialized GIS programs. A large number of tools presented in such GIS were developed in the context of oil exploration tasks, where the data network is dense and uniform. Applying them to a heterogeneous and sparse network of data (most inherent in COMR) is often infeasible. That is why the creation of models of subsoil structure for forecasting non-metallic minerals quite often requires the use of specially developed algorithms, methods, and technologies.

Taking into account the above-mentioned, as well as the experience accumulated in domestic and foreign practice in the field of geological modeling [2–4], to achieve the purpose of this study, the author's method of forecasting and evaluation of COMR deposits occurring in Cenozoic sediments of the Brest region [5] is proposed. The scheme assumes realization of forecasting and evaluation on the basis of digital geological model of the given strata. The main blocks of the proposed methodology are shown in Fig. 2. In the following, we will elaborate on each of these blocks in more detail.

Block 1. Systematization and updating of data on the geological structure of the Brest region. In view of the fact that the main objective of the study is to forecast new COMR deposits in the region, the first stage of the study, according to the authors, should be the systematization of the accumulated extensive material on the geological structure of the Brest region. After all, it is the geological structure that is the key factor determining the regularities of the region's mineral raw material base location and its specificity. In addition, it is impossible to build a correct geologic model without understanding the specifics of the geologic structure.

The direct implementation of this block included: *1* – collection and generalization of numerous materials on the geological structure of this territory; *2* – clarification of data obtained in the historical researches of this territory on the basis of the author's set of horizon-by-horizon isopachyte schematic maps.

Block 2. Selection of software products for creating a digital geological model. In view of the fact that the goal set in the paper can be achieved most effectively with the use of information products, this block became a significant part of the study.

As practice shows, a variety of GIS packages are used as a software basis for geological modeling, which can be combined into two groups [6]: subsoil use GIS (Rock-works, GMS, Surfer, Petrel, etc.) and general geographic GIS (ArcGIS, MapInfo, QGIS, etc.).

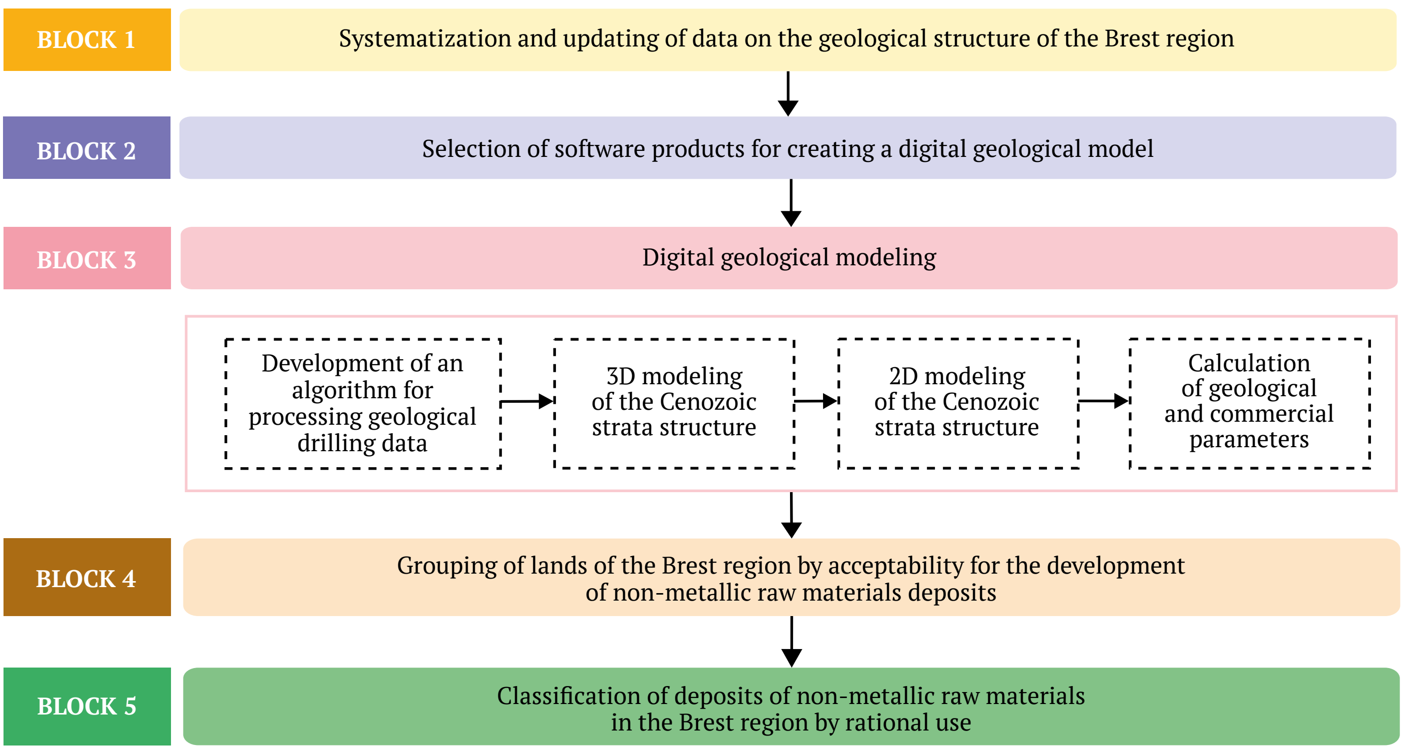

Fig. 2. Structural and logical scheme of the methodology of forecasting and evaluation of COMR deposits in the Brest region

The use of such programs as GIS Petrel and GIS ArcGIS 10.5 was considered for creation of digital geological model of the studied region. However, since Petrel package was developed for the use in oil exploration and production sector, where drilling data network is very dense and uniform, it was not possible to apply it to model creation for the purpose of COMR deposit prediction. Therefore, preference was given to the ArcGIS 10.5 general geographic system.

In addition to the selection of GIS as the main modeling platform, this stage included the selection of additional software tools that extend the basic functionality of the selected GIS package. The use of the following means was justified: MS Access DBMS,Microsoft Excel, Blender 3D computer graphics software, Wolfram Mathematica computer algebra system.

Block 3. Digital geological modeling. The block under consideration is the key block of the study and the longest in terms of implementation time. It included the following steps:

– development of an algorithm for processing the materials presented in the exploration drilling database in order to identify erroneous data present in them;

– creation of a three-dimensional digital geologic model of the region [7];

– converting the three-dimensional model into a two-dimensional format;

– calculation of the most significant geological and commercial parameters(vertical thickness of sediments, overburden thickness, overburden ratio);

– construction of a set of prognostic-mineralogenic schematic maps reflecting data on the patterns of distribution and promising areas of the most significant types of non-metallic raw materials in the investigated territory in terms of thickness.

Block 4. Grouping of lands of the Brest region by acceptability for the development of non-metallic raw materials deposits. Inclusion of a block allowing to take into account the type of land of the deposit location area in the evaluation scheme is connected with the specifics of COMR mining. The development of these types of raw materials is usually carried out by open-pit mining, which leads to negative impact on environmental components. This, in turn, increases the cost of developing such resources due to the need for subsequent compensation for damage, primarily related to the degradation of different types of land.

In the Brest region, the use of such a block is also significant due to the fact that here the extraction of construction raw materials is often carried out through the development of on-farm quarries, that makes commercialization of the disturbed lands extremely problematic.

The final result produced by the block under consideration was the authors' proposed approach to grouping of the Brest region lands in terms of the feasibility of open-pit mining [8].

Block 5. Classification of deposits of non-metallic raw materials in the Brest region by rational use. The final block of the proposed methodology was the classification of COMR deposits of the Brest region identified during the modeling by their acceptability for development. The classification procedure was carried out on the basis of complexing raster coverages, reflecting geological and commercial parameters for each deposit, and calculated weighting coefficients, characterizing the acceptability of the groups of lands of the Brest region selected at stage 4 for COMR development. The algorithm of deposit classification is described in more detail in [9].

Results and their discussion

A complex analysis of the geological structure of the Brest region territory as a key factor determining the regularities of formation of the region raw-materials base and its specificity was carried out. A brief characterization of the main features of the region territory geological structure is given below.

The territory of the Brest region is located in the western part of East European paleoplatform. Taking into account the depth the crystalline basement top, the following tectonic elements were distinguished within the basement: Podlyassko-Brestsky Depression (eastern part), Polesskaya Anticline, Pripyatsky Trough (western part), Mikashevichsko-Zhitkovichsky nose of the crystalline basement, Ivatsevichsky buried nose of the Belarusian Anticlise, Lukovsko-Ratnovsky gorst, Volynskaya monocline of the Volyno-Azovsky plate. The sedimentary cover sediments are ubiquitous and united into structural complexes, successively alternating in the section of the formation series and separated by nondepositional hiatuses. These complexes correspond to the main tectonic stages of the territory's development: Gothic, Lower Baikaskyl, Upper Baikalsky, Caledonian, Hercynian, Cimmerian-Alpine.

The most widespread among the rocks of the platform cover of the studied region are Cenozoic sediments, primarily Quaternary ones. The accumulation of the Cenozoic sediments occurred during three geologic periods with different paleogeographic conditions that influenced the nature of sedimentation and the present-day structure of the sedimentary cover of the region.

The Paleogene system sediments occupy significant areas within the region. Absolute elevations of their base vary from 30–40 m in the north and northwest to 150 m in the south and southwest. The sediments thickness in most of the region is 20–30 m.

The Neogene system sediments within the Brest region occupy extensive areas, overlying the Paleogene and underlying Quaternary. They occur at absolute elevations of 30–150 m, reaching maximum elevations in the southwest. Their average thickness is 15–20 m.

The Quaternary sediments are widespread in the study area and superpose the formations of older geological systems. Their thickness varies from a few tens to 240 m.

Since the greatest prospects for the development of raw-materials base in the region are associated with the Cenozoic sediments, a set of horizon-to-horizon isopachyte schematic maps was produced to clarify the specifics of their structure. One of them is shown as an example in Fig. 3.

A digital geological model of Cenozoic sediments in the Brest region was developed. It represents a concentrated system of data on structural, lithologic, and mining and geological features of the structure of the Cenozoic strata in the region [7].

Due to the multi-layered structure of the data used for modeling, the model was initially generated in a volumetric form. The three-dimensional model was realized on the basis of the author's algorithm executed with the use of an independently developed module in the C++ programming language. This algorithm is based on constructions based on Voronoi diagram. As can be seen in Fig. 4, the volumetric model consists of a set of convex polyhedra in three-dimensional space. The adjacent groups of these polyhedrons represent sedimentary rock deposit bodies that may be considered as potential for development of COMR in the region.

Since the construction of the three-dimensional model was based in some parts on a sparse network of wells, it differs to a great extent from the classical volumetric models, which are presented in the scientific literature devoted to modeling of oil reservoirs. This led to the necessity to carry out the procedure of its approximation and formation of a two-dimensional model, which is also the most familiar from the viewpoint of analysis for profile specialists. The algorithm for transforming a three-dimensional model into a two-dimensional format is described in detail in [7].

On the whole, the created two-dimensional model represents data sets structured as an ArcGIS geodatabase files: *1* – vector point layers obtained

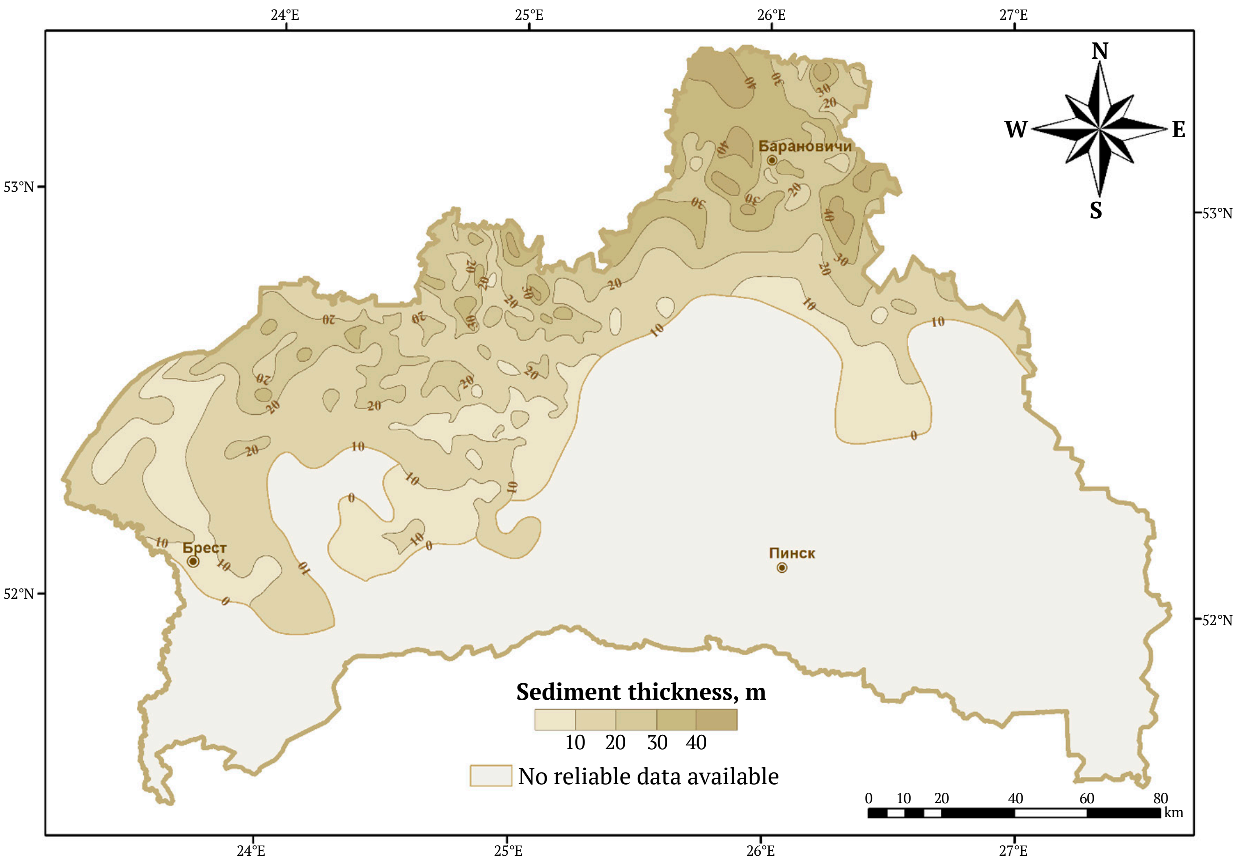

Fig. 3. Isopachyte schematic map of the Sozh subhorizon of the Pripyatsky horizon (Q_2pr_1 sz) of the Quaternary system in the territory of the Brest region

during numerical processing of the volumetric model “sliced” into layers; *2* – raster covers for each of the 19 rock types; *3* – classes of polygonal objects reflecting preliminary boundaries of COMR deposits, their thicknesses, thicknesses of overlying sediments, and occurrence elevations.

The two-dimensional model served as a basis for creating a basic set of digital prognostic-mineralogenic schematic maps of the region, which was performed for such rock types as sands, rubbly-gravel-sandy rocks (sand-gravel-rubbly rocks), clays, clay loams and sandy loams, and peat. It is these rocks that are the most significant in terms of thickness and areal representation within the study territory. An example of the map from the described set is shown in Fig. 5.

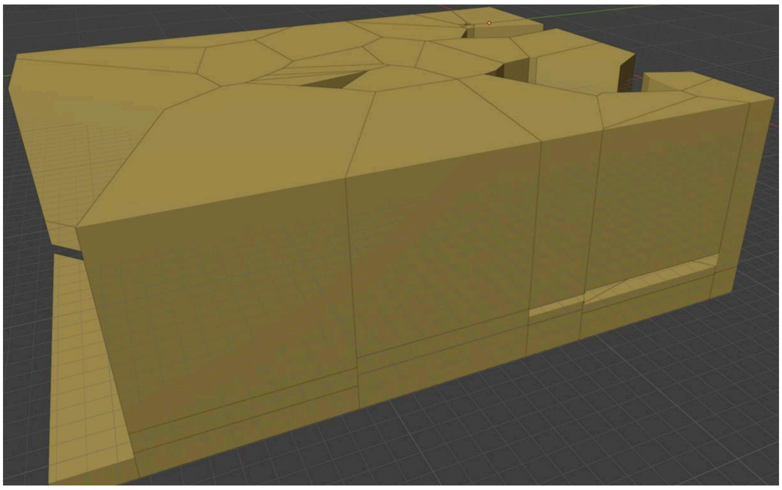

Fig. 4. Example of the generated volumetric model reflecting the distribution of sand deposits in the Quaternary sediments in the territory of Zhabinka district of the Brest region, author's algorithm

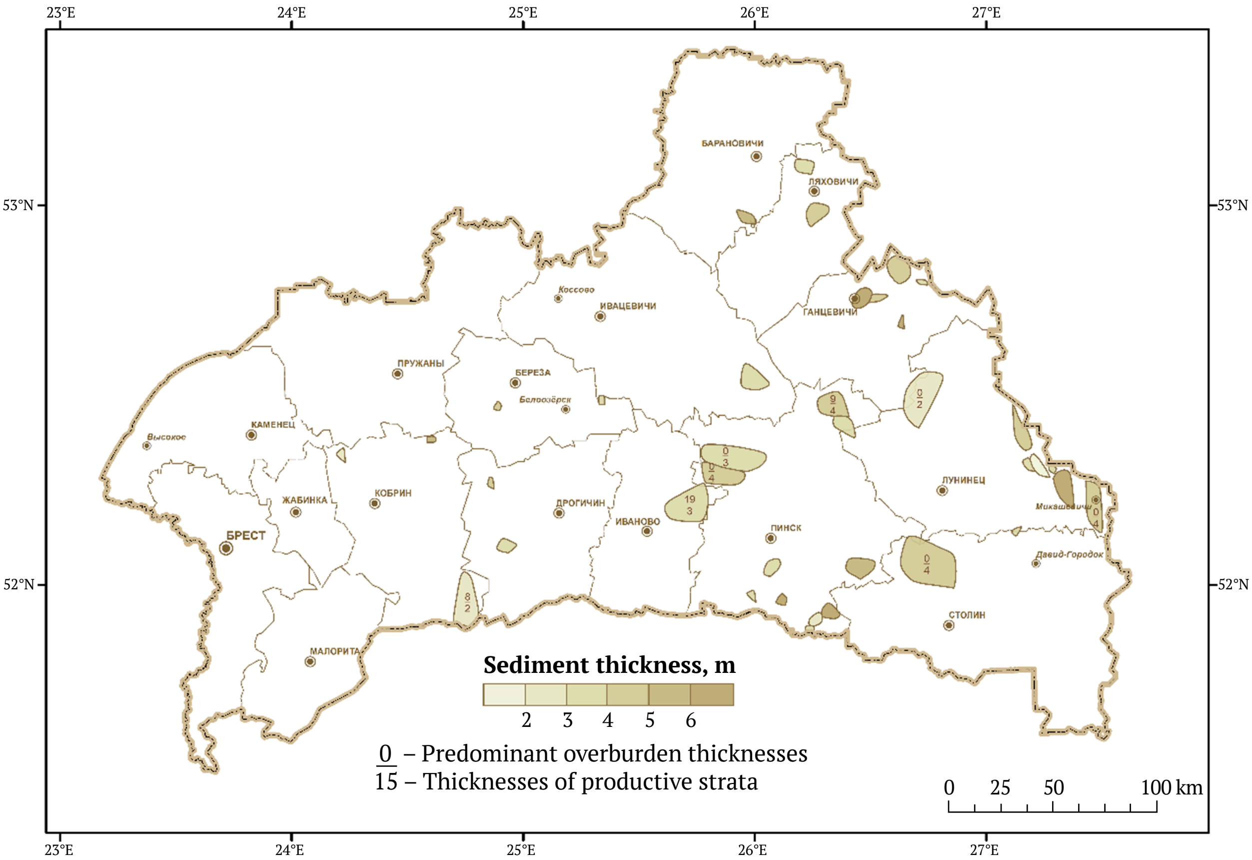

Fig. 5. Schematic map of regularities of location and forecasting of peat deposits in Cenozoic sediments in the Brest region

eISSN 2500-0632
https://mst.misis.ru/

The approach to grouping of the Brest region lands according to their acceptability for development of COMR deposits is proposed. When classifying the lands, consideration was given to: *1* – legal norms regulating the possibility of using lands of different types in the Republic of Belarus for quarrying[2]; *2* – approaches to grouping of lands according to their acceptability for development of COMR deposits, used in the works of other researchers[3] [10, 11]; *3* – the approach to grouping of lands according to the degree of anthropogenic impact on natural landscapes, used in the work of B.I. Kochurov [12].

The land groups are the result of systematization of a set of land subtypes[4] [13] in the Brest region land information system database. A total of six land groups were identified due to the grouping (Table 1).

To ensure the possibility of using the developed classification when assessing the acceptability of the development of COMR deposits in the Brest region, weighting coefficients were calculated for each group of lands based on the method of hierarchy analysis T. Saati [13, 14].

Based on the land grouping and the calculation of weighting coefficients , a digital raster model was created (Fig. 6), reflecting the acceptability of the distinguished groups of lands in the region for the development of deposits of construction raw materials.

The scheme of involvement of predicted COMR deposits in the Brest region into development was developed. As a result of creating a raster model reflecting the acceptability of different groups of land in the Brest region to the development of COMR deposits, it became possible to substantiate the rational sequence of involving the construction raw materials

[2] National Legal Internet Portal of the Republic of Belarus. Land Code of the Republic of Belarus. URL: https://pravo.by/document/?guid=12551&p0=H12200195 [Accessed February 29, 2024]; National Legal Internet Portal of the Republic of Belarus. Subsoil Code of the Republic of Belarus. URL: https://pravo.by/document/?guid=3871&p0=Hk0800406 [Accessed February 29, 2024]; Belarus Legal Forum. Draft Resolution of the Council of Ministers of the Republic of Belarus “On the procedure of location, development, reclamation and accounting of on-farm quarries”. URL: https://forumpravo.by/publichnoe-obsuzhdenie-proektov-npa/forum15/16239 [Accessed February 29, 2024].

[3] Lyutyagin D.V. Geological and economic substantiation of involvement in development of deposits of commonly occurring mineral resources [Ph.D. thesis in Economics]. Moscow; 2006. 28 p. (In Russ.).

[4] National Legal Internet Portal of the Republic of Belarus. Land Information System of the Republic of Belarus. Procedures for creating, maintaining (operating and updating). URL: https://pravo.by/document/?guid=12551&p0=W22137315&p1=1&p5=0 [Accessed February 29, 2024].

Table 1

Grouping of the Brest region lands in terms of acceptability for the development of construction raw materials deposits

Code	Land group	Land subtype
1	Land most acceptable for the development of COMR	Other unused land; sands devoid of vegetation; ravines and scour holes; bars; pits
2	Land acceptable for the development of COMR	Derelict land; meadow; meadow (bushy); meadow (waterlogged); meadow (waterlogged, bushy); improved meadow; unforested
3	Land allowable for the development of COMR	Arable; greenhouses, hot houses; orchards; berry fields; plantations; fruit crop nurseries; forests; plantings; forest belts; field, forest roads; clearings
4	Land restricted for the development of COMR	Lands disturbed during mining and extraction of minerals; lands disturbed during peat and sapropel extraction; lands disturbed during construction works; burnt-out peatlands; former agricultural lands contaminated with radionuclides; lands under reclamation construction; lands in the stage of fertility restoration; dumps and spoil heaps; pits/quarries and other facilities at the stage of mineral extraction; lands at the stage of peat and sapropel extraction; active construction sites and other sites at the stage of construction; lands used for waste storage; animal burial sites.
5	Land extremely restricted for the development of COMR	Country roads; improved roads – right-of-way (carriageway); improved roads – slopes; cattle runs; railroads – right-of-way; railroads – slopes; railroads – platforms; other transportation lanes; lands under pipelines; bridges, overpasses, trestles; squares; streets and passages; carriageways of streets; parks, squares, boulevards, other green areas; lawns and flowerbeds; mounds; cemeteries; lands provided to citizens for collective gardening; homestead lands; yards (without division into industrial and residential buildings; open warehouses; pens; residential buildings; non-residential buildings; light-type buildings; other buildings and structures; silage pits
6	Land prohibited for the development of COMR	Rivers; canals and ditches; lakes; reservoirs and ponds; dams; weirs; under-edges; swamps

deposits of the studied region in development. For this purpose, a procedure of complexing several types of raster surfaces was carried out in ArcGIS 10.5 software package: 1 – rasters of thicknesses of the identified promising areas of local raw materials; 2 – rasters of overburden thicknesses over the identified deposits; 3 – raster showing the availability of the Brest region lands for COMR development [9].

Two types of schematic map sets were generated based on the complexing results:

1) schematic maps providing a general concept of the acceptability of development of the identified non-metallic raw materials in the region. An example of such a map is shown in Fig. 7;

2) schematic maps providing a detailed concept of the acceptability of development of each individual deposit. An example of such a map is shown in Fig. 8.

As can be clearly seen in both figures, all the deposits are grouped into five classes on the schematic maps:

1) the most acceptable for development deposits, which occur close the surface, have significant thicknesses of productive strata, and are confined to unused or poorly used agricultural and forest lands;

2) acceptable for development deposits, the stripping ratio of which is predominantly equal to one, confined to agricultural and forest lands with high intensity of use;

3) Deposits, development of which is allowed when there is an acute demand for a raw material, mainly occurring under disturbed lands, with stripping ratio equal to or exceeding 1;

4) Deposits, development of which is highly undesirable, occurring under developed lands with stripping ratio exceeding 1;

5) Deposits, development of which is impossible, occurring under water bodies and swamps, with the overburden thickness significantly (two or more times) exceeding the productive strata thickness.

At the same time, it should be noted that the presented approach to justification of the feasibility of a deposit development taking into account the status of lands should be considered as preliminary. The final decision on the acceptability of developing a particular deposit should be made only after a detailed study of the area where it is located. This will allow a more objective assessment of the impact of the planned works on the natural environment components.

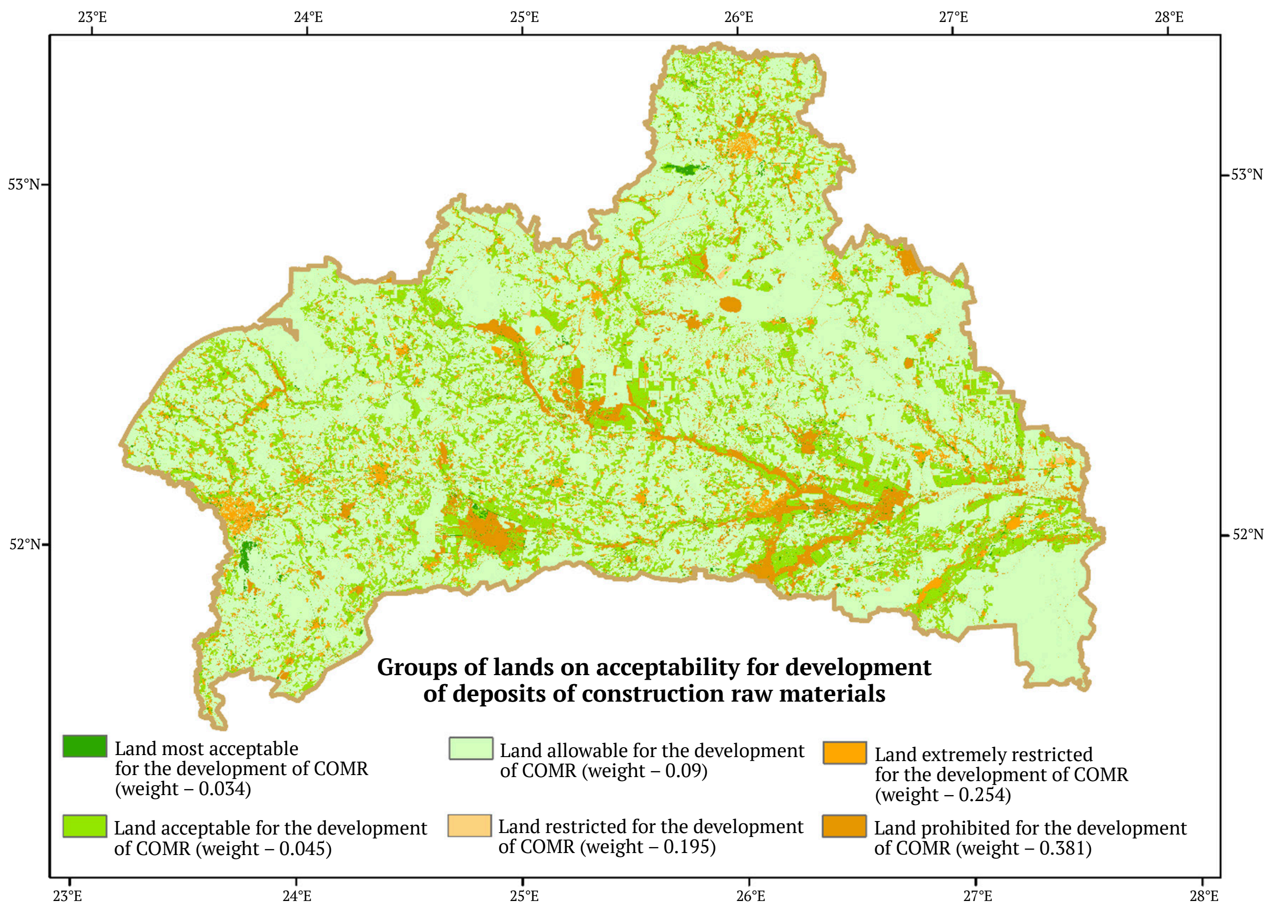

Fig. 6. Raster model reflecting the acceptability of different groups of lands in the Brest region for the development of deposits of construction raw materials

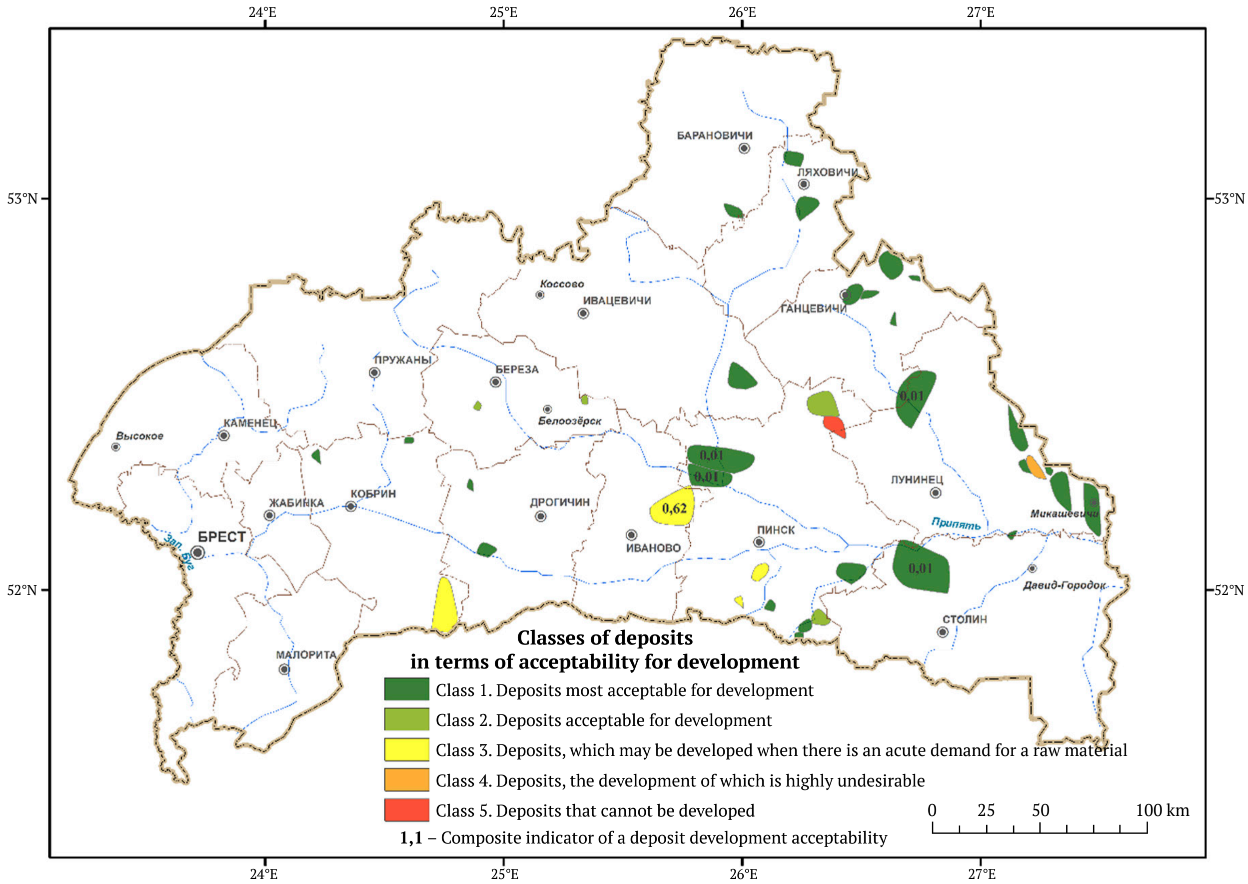

Fig. 7. Schematic map of peat deposits in the Brest region classified in terms of development prospects

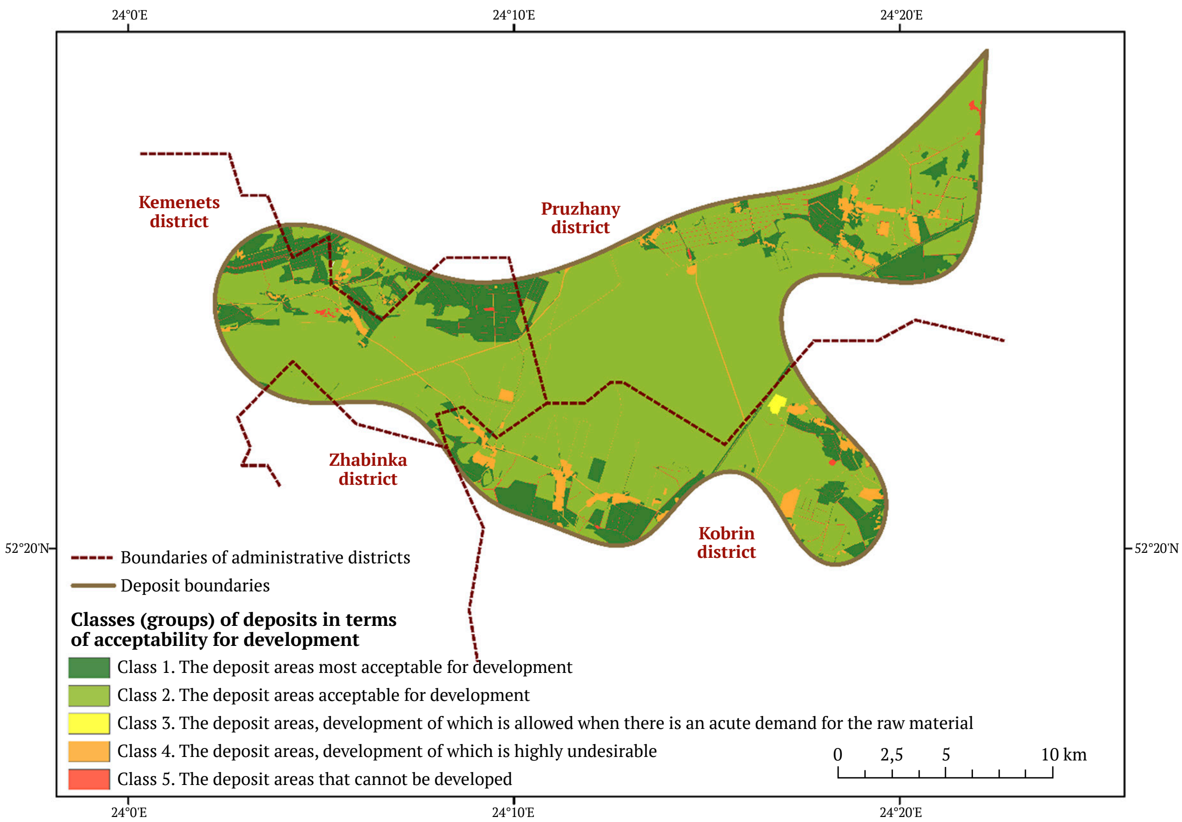

Fig. 8. Schematic map reflecting the acceptability of development of an individual sand and gravel deposit within the Brest region

Practical application of the research results

The results obtained during the implementation of the research described in this paper have already found their application both in the educational and production process. In particular, the developed algorithm of geological survey data processing and a set of tools designed to automate its work are used in the educational process and research work by the students of the Department of Urban and Regional Development of the Faculty of Natural Science of the Brest State University named after A.S. Pushkin, as well as by the students of the Department of Environmental Management of the Faculty of Engineering Systems and Ecology of the Brest State Technical University. This is confirmed by the relevant adoption deeds.

The created sets of isopachite schematic maps, prognostic-mineralogenic schematic maps, schematic maps of acceptability of involvement of non-metallic raw materials deposits in the Brest region into development are introduced and used in the study of Cenozoic sediments of the region in the laboratory of recent geodynamics and paleogeography of the Institute of Nature Management of the National Academy of Sciences of Belarus, as well as in the Quaternary geology department of the branch Institute of Geology of the Republican Unitary Enterprise “Scientific and Production Center for Geology”.

The economic significance of the obtained results can be assessed in the case of making appropriate management decisions on the development of the region mineral resources base and consists in the availability of relevant and verifiable information on the geological structure of the territory, significantly facilitating both solving the problems of further prospecting for new mineral deposits and the subsoil use for the purposes unrelated to development of mineral resources.

Areas of further research

The authors see the prospects for further research on the forecast and assessment of COMR deposits in the Brest region in supplementing the proposed methodology with a block for assessment of deposit accessibility. In this paper we propose to understand accessibility as the proximity / remoteness of deposits in relation to raw material consumption clusters and in relation to the available transportation infrastructure. The authors suggest assessing accessibility using the following criteria:

– remoteness of deposits in relation to transportation lanes;

– remoteness of deposits in relation to consumption clusters [5].

The last criterion can be analyzed in two ways:

– assessment of remoteness relative to settlements as areas of potential construction, expansion or repair of various construction facilities, as well as areas acting as places of labor force concentration;

– assessment of remoteness relative to specialized industrial enterprises, taking into account their demand for certain types of construction raw materials.

Conclusion

The study for the first time presents the results of the forecast and assessment of deposits of mineral construction raw materials concentrated in the Cenozoic sediments of the Brest region with the use of computer modeling methods. The main results of the conducted work can be summarized in the following conclusions:

1. On the basis of the materials accumulated by predecessors and a series of the author's digital horizon-by-horizon isopachite maps, the analysis of the geological structure of the studied region was performed. The data obtained during the analysis provided the possibility of visual assessment of the correctness of the results obtained at different stages of creating a digital geological model of the Cenozoic sediments in the Brest region.

2. A three-dimensional digital geological model of the Cenozoic sediments in the Brest region was developed. An author's algorithm based on the application of the Voronoi diagram has been developed for its creation. Due to the fact that the created volumetric model differs significantly from classical two-dimensional models, the algorithm includes the possibility of approximating it by switching to a two-dimensional model. The obtained two-dimensional model gives a holistic view of the geological structure of the Cenozoic sediments in the region and serves as a basis for the creation of a series of digital schematic maps reflecting the features of spatial tracking of the COMR deposits in the region identified in the course of modeling.

3. An approach to land grouping in the Brest region was developed. On its basis, all lands in the region were grouped into six groups (classes) in terms of their acceptability for COMR extraction. For each group of lands weight coefficients were calculated and a digital raster model was created, which served as a basis for the classification of COMR deposits in the Brest region according to the “rational sequence” of development.

4. The approach to classification of COMR deposits in the Brest region identified in the course of modeling in terms of their acceptability for develop-

ment is proposed. It is based on taking into account such characteristics as the thickness of a deposit, the overburden thickness above the deposit, and the weight value of the land groups under which the deposit is located. As a result of the classification, a set of schematic maps reflecting the acceptability of the region's COMR deposits for development was created. Attributive information is attached to each deposit on the generated digital schematic maps. The obtained sets of the schematic maps and the associated databases of the attributive information may be of interest to local territorial authorities in the development of a regional action plan for the study, development, and rational use of deposits of local raw materials.

Список литературы / References

1. Lukashev K.I. et al. *History of geological sciences in the Byelorussian SSR*. Minsk: Nauka i Tekhnika Publ.; 1978. 272 p. (In Russ.)
2. Zakrevsky K.E. *Geological 3D modeling*. Moscow: IPTs Maska LLC Publ.; 2009. 376 p. (In Russ.)
3. Poklonov V.I., Semyonov F.V., Ivanov S.K. Creation of forecasting mathematical model of regularities of quartz sands placement for construction works in the territory of the Republic of Mari El. *Prospect and Protection of Mineral Resources*. 2015;(7):23–26 (In Russ.)
4. Boissonnat J-D., Nullans S. Reconstruction of Geological Structures from Heterogeneous and Sparse Data. *The 4th ACM international workshop on Advances in geographic information systems*. 1996;3069:3–24. URL: https://inria.hal.science/inria-00073623
5. Bogdasarov M.A., Maevskaya A.N., Sheshko N.N. Methodical specifics of forecasting and evaluating commonly occurring mineral resources. *Prospect and Protection of Mineral Resources*. 2023;(3):45–52. https://doi.org/10.53085/0034-026X_2023_03_45
6. Petin A.N., Vasiliev P.V. *Geoinformatics in rational subsoil use*. Belgorod: BelSU Publ.; 2011. 268 p. (In Russ.)
7. Mayeuskaya H.M., Bahdasarau M.A., Piatrou D.A., Sheshka M.M. Geological and genetic modelling of the Cenozoic deposits of the Brest region using information technologies. *Journal of the Belarusian State University. Geography and Geology*. 2023;(1):107–118. (In Russ.) URL: https://elib.bsu.by/handle/123456789/298810
8. Mayevskaya A.N., Bogdasarov M.A., Sheshko N.N. Ranking of the land fund of the administrative districts of the Brest Region according to the acceptability to the development of deposits of construction raw materials. *Natural Resources*. 2022;(2):45-56. (In Russ.) URL: https://priroda.belnauka.by/jour/article/view/140
9. Mayevskaya A.N., Bogdasarov M.A., Sheshko N.N. Justification of schemes of rational use of deposits of non-metallic raw materials in Brest region. *Prirodopol'zovanie*. 2023;(1):135–150 (In Russ.)
10. Peshkova G.Yu. Express-evaluation of clay deposits mining effectiveness on the base of economic-geological criteria (using Leningrad region as an example). *Corporate governance and innovative economic development of the North: Bulletin of the Research Center of Corporate Law, Management and Venture Capital of Syktyvkar State University*. 2016;(1):121–128.
11. Cheremisina E.N., Nikitin A.A. Applying geoinformation systems in nature use. *Geoinformatika*. 2006;(3):5–20. (In Russ.)
12. Kochurov B.I. *Ecodiagnosis and sustainable development*. Moscow: INFRA-M Publ.; 2016. 362 p. (In Russ.)
13. Saati T. *Analytical Planning. Systems Organization*. Moscow: Radio i Svyaz' Publ.; 1991. 224 p. (In Russ.)
14. Saaty T. *Decision Making. Hierarchy Analysis Method*. Moscow: Radio i Svyaz' Publ.; 1993. 278 p. (In Russ.)

Information about the authors

Maksim A. Bogdasarov – Corresponding Member of the National Academy of Sciences of Belarus, Professor, Dr.Sci. (Geol. and Mineral.), Vice-Rector for Science, Professor of the Department of Urban and Regional Development, Professor of the Department of Biological and Chemical Technologies, Brest State A.S. Pushkin University, Brest, Republic of Belarus; ORCID 0000-0002-2039-679X, Scopus ID 57191968270, ResearcherID HPG-0293-2023; e-mail bahdasarau@gmail.com

Anna N. Mayevskaya – Cand. Sci. (Geol. and Mineral.), Senior Lecturer at the Department of urban and regional development, Brest State A.S. Pushkin University, Brest, Republic of Belarus; ORCID 0009-0006-0448-450X; e-mail maevskaya.anna@inbox.ru

Dmitry O. Petrov – Cand. Sci. (Eng.), Associate Professor of the Department of Electronic Computing Machines and Systems, Faculty of Electronic Information Systems, Brest State Technical University, Brest, Republic of Belarus; ORCID 0000-0001-6164-9936; e-mail polegdo@gmail.com

Nikolay N. Sheshko – Cand. Sci. (Eng.), Associate Professor, Head of the Research Department, Associate Professor of the Department of Environmental Management, Faculty of Engineering Systems and Ecology; Brest State Technical University, Brest, Republic of Belarus; ORCID 0000-0001-6373-8166, Scopus ID 57214638269; e-mail optimum@tut.by

Received 12.03.2024
Revised 12.04.2024
Accepted 20.05.2024

GEOLOGY OF MINERAL DEPOSITS

Research paper

https://doi.org/10.17073/2500-0632-2024-02-217
UDC 622.243.2:622.143:553.98(26)(575.4)

Directional drilling of an exploratory well in the shallow waters of the Caspian Sea

A.R. Deryaev
Natural Gas Research Institute, Turkmengaz State Concern, Ashgabat, Turkmenistan
annagulyderyayew@gmail.com

Abstract
In the rapidly evolving energy landscape, achieving not only economic benefits but also ensuring energy stability for the region and the global energy resource market has become a key objective. This study aims to optimize the processes of directional and inclined drilling of exploratory wells in the Caspian Sea offshore area in Turkmenistan, focusing on enhancing efficiency and reducing environmental impact. Among the methods used, the analytical method, classification method, functional method, statistical method, synthesis method, and others should be noted. The study involved an analysis of directional drilling processes in exploratory wells in the Caspian Sea offshore area of Turkmenistan. Innovative technologies were developed and successfully implemented to streamline production processes with an emphasis on environmental considerations. This comprehensive approach not only improves the technical readiness of energy projects in the region but also supports adherence to high standards of environmental sustainability, which is a critical component of modern energy management. Thus, the exploration of these processes is inherently connected with the formation of a sustainable and efficient energy strategy for the Caspian region. The study's focus centers on the need for effective analysis and refinement of directional drilling processes for exploratory wells in the Caspian Sea offshore area in Turkmenistan. Key considerations include not only the goal of enhancing hydrocarbon extraction but also maintaining a balanced focus on the environmental aspects of production. The research results confirmed the effectiveness of new methods that support increased hydrocarbon production, reduce time costs, and minimize adverse environmental impacts. This study highlights not only the importance of modern technological solutions in the energy sector but also their substantial contribution to the region's sustainable development and energy security. The practical significance of this study lies in providing innovative solutions to improve directional drilling processes for exploratory wells in the Caspian Sea offshore area of Turkmenistan.

Keywords
energy security, drilling, efficiency, exploration, innovative technology, well, marine environment, Caspian Sea

For citation
Deryaev A.R. Directional drilling of an exploratory well in the shallow waters of the Caspian Sea. *Mining Science and Technology* (*Russia*). 2024;9(4):341–351. https://doi.org/10.17073/2500-0632-2024-02-217

ГЕОЛОГИЯ МЕСТОРОЖДЕНИЙ ПОЛЕЗНЫХ ИСКОПАЕМЫХ

Научная статья

Бурение направленной разведочной скважины в мелководье Каспия

А.Р. Деряев
Научно-исследовательский институт природного газа ГК «Туркменгаз», г. Ашгабат, Туркменистан
annagulyderyayew@gmail.com

Аннотация
В условиях быстро меняющейся энергетической ситуации важной задачей становится не только достижение экономической выгоды, но и обеспечение энергетической стабильности в регионе и на мировом рынке энергоресурсов. Целью проведенного исследования являлось совершенствование процессов наклонно-направленного бурения разведочных скважин в акватории Каспийского моря в Туркменистане для повышения эффективности и снижения негативного воздействия на окружающую среду. Среди использованных методов следует отметить аналитический метод, метод классификации, функциональный метод, статистический метод, метод синтеза и другие. В рамках исследования был проведен анализ процессов наклонно-направленного бурения разведочных скважин в акватории Каспийского моря в Туркменистане. Были разработаны и успешно внедрены инновационные технологии, направленные на рационализацию производственных процессов с учетом экологических аспектов. Такой комплексный подход не только повышает техническую готовность энергетических проектов в регионе, но также содействует соблюдению высоких стандартов экологической устойчивости, что является важным эле-

ментом в современном энергетическом управлении. Таким образом, изучение этих процессов неотъемлемо связано с формированием устойчивой и эффективной энергетической стратегии для Каспийского региона. Проблематика данного исследования сосредоточена на необходимости эффективного изучения и совершенствования процессов наклонно-направленного бурения разведочных скважин в акватории Каспийского моря в Туркменистане. Основные аспекты включают в себя не только стремление к повышению добычи углеводородов, но и сбалансированное внимание к экологическим аспектам производства. Результаты исследования подтвердили эффективность новых методов, способствующих увеличению добычи углеводородов, сокращению временных затрат и снижению негативного воздействия на природную среду. Это исследование подчеркивает не только важность современных технологических решений в энергетической отрасли, но и их существенный вклад в устойчивое развитие региона и обеспечение энергетической безопасности. Практическое значение данного исследования заключается в предоставлении инновационных решений для совершенствования процессов наклонно-направленного бурения разведочных скважин в акватории Каспийского моря в Туркменистане.

Ключевые слова
энергетическая безопасность, бурение, эффективность, разведка, инновационная технология, скважина, морская среда, Каспий

Для цитирования
Deryaev A.R. Directional drilling of an exploratory well in the shallow waters of the Caspian Sea. *Mining Science and Technology* (*Russia*). 2024;9(4):341–351. https://doi.org/10.17073/2500-0632-2024-02-217

Introduction

The study of directional and inclined drilling processes for exploratory wells in the Caspian Sea offshore area of Turkmenistan is an essential component of strategic planning in the energy sector. This research gains critical importance in light of the constant changes within the energy industry and the need to ensure stable supply of energy resources. The development of innovative technologies and streamlining of drilling processes contributes to increased hydrocarbon extraction efficiency and reduced environmental impact. Understanding these processes provides economic benefits and plays a key role in ensuring the region's energy security and stability in the global energy market amid a constantly shifting energy paradigm. This comprehensive approach enhances the technical readiness of energy projects in the region and supports compliance with high standards of environmental sustainability, which is a vital element of modern energy management. Consequently, the study of these processes is inherently linked to shaping a sustainable and effective energy strategy for the Caspian region.

In [1], the application of innovative methods in directional and inclined drilling to improve hydrocarbon extraction efficiency in the Caspian Sea offshore area is emphasized. However, this study does not address the development of integrated management systems that could ensure long-term sustainability in oil and gas operations.

The research in [2] considers the development of sustainable directional drilling methods with an emphasis on environmental aspects; however, the work does not give due attention to the environmental considerations and possible impacts of these methods on the marine environment.

Study [3] highlights the of using analytical methods to assess the impact of drilling on marine biodiversity but does not consider classification methods that could help adapt to geological changes and reduce risks.

In [4], the author points out the progressive nature of synthesis methods in directional drilling (DD), which enhances hydrocarbon extraction. However, the calculations for directional well drilling with dual completion are not presented in detail.

Study [5] emphasizes the need for classification methods for effective management of directional drilling processes but does not consider the long-term effects of synthetic approaches and their impact on the marine ecosystem.

Article [6] raises a key question about the effectiveness of statistical methods in analyzing the performance of directional drilling conducted within the analytical approach framework. The study does not delve into issues regarding the social acceptability of statistical methods and their influence on public opinion.

Materials and methods

The analytical method provided a deeper understanding of the complex interconnections and dynamics in the directional and inclined drilling processes for exploratory wells in the Caspian Sea offshore area. This method helped identify the factors affecting drilling efficiency and facilitated a systematic review of data, significantly enriching knowledge about the physical and geological parameters influencing the success of hydrocarbon extraction operations.

The statistical method was employed to identify key patterns and trends characterizing the directional drilling processes in exploratory wells in the Caspian

Sea offshore area. This method allowed for the analysis of large volumes of data gathered during well operations and highlighted statistically significant parameters affecting drilling efficiency. The statistical method also enabled an assessment of the reliability and predictability of drilling results, a critical factor in decision-making within the energy industry. The statistical data obtained on overall drilling efficiency, time expenditures, and other parameters served as a fundamental basis for further refining strategies and tactics used in the drilling processes in this offshore area.

The functional method helped establish the primary functional relationships between various parameters and processes associated with directional drilling of exploratory wells in the Caspian Sea offshore area. This method revealed the influence of different variables on overall drilling efficiency, identified optimal parameter values, and determined key factors affecting the success of hydrocarbon extraction operations.

The deductive method allowed for logical conclusions regarding the directional drilling processes for exploratory wells in the Caspian Sea offshore area. By applying this method, it was possible to uncover causal relationships among various drilling aspects, define the main principles and laws underlying effective technologies. Thus, using the deductive method enriched the understanding of the principles governing and managing directional drilling processes.

The application of the synthesis method led to the development of innovative solutions and technologies aimed at streamlining the directional drilling processes for exploratory wells in the Caspian Sea offshore area. This method facilitated the systematic integration of various components and variables to create effective strategies that combined technical efficiency with environmental considerations. The synthetic method enabled the incorporation of advanced technologies while accounting for numerous variables influencing drilling processes. The innovations developed through synthesis contribute not only to increased productivity but also to reduced environmental impact on the marine ecosystem. The resulting solutions represent a comprehensive set of measures, including technical enhancements, risk management, and adherence to high standards of environmental sustainability. Consequently, the synthesis method proved to be an essential tool for creating comprehensive and innovative approaches to optimizing drilling in this offshore area.

The classification method facilitated the organization of various geological formations and conditions that affect directional drilling processes for exploratory wells in the Caspian Sea offshore area. Applying this method enabled the identification of characteristics and features of different drilling zones, significantly simplifying the adaptation of drilling strategies to diverse geological conditions. The classification method also contributed to establishing a system for determining effective drilling parameters based on specific geological characteristics. This allowed for improved precision and efficiency in drilling processes, reduced potential risks, and enhanced overall efficiency. The classification results serve as a foundation for developing more precise and adaptive strategies for directional drilling in the Caspian Sea offshore area in Turkmenistan.

Results

In recent decades, global exploration and production activity in the oil and gas sector has been steadily increasing, with countries located near resource-rich regions playing a key role in this process. Turkmenistan, strategically positioned along the shores of the Caspian Sea, is one such country. Directional drilling of exploratory wells in the waters of this unique inland sea presents complex engineering and environmental challenges but also opens up broad energy prospects for the country [7].

One of the key aspects of drilling in the Caspian Sea is the use of directional well technology. This innovative approach enables drillers to extract hydrocarbons from multiple points within an underwater field, maximizing efficiency and increasing production volumes. With its vast natural resources, Turkmenistan aims to leverage advanced technology to efficiently exploit and maximize the potential of its fields.

However, despite the opportunities associated with directional exploratory drilling in the Caspian Sea, challenges also exist. Environmental concerns are paramount, as even the most advanced technologies can pose risks to the marine ecosystem. Discharges of drilling fluids, vapor emissions, and potential accidents may have serious consequences for the environment and the health of local communities [8].

Therefore, countries conducting drilling activities in the Caspian Sea must strictly adhere to international safety and environmental standards. The development and implementation of integrated control systems, continuous environmental monitoring, and active collaboration with research institutions are essential components of sustainable development in this sector [9].

A primary objective for Turkmenistan's oil and gas industry is to increase hydrocarbon reserves. President of Turkmenistan Serdar Berdymukhamedov underscores the importance of boosting hydrocarbon production in the oil and gas sector, considering it a vital factor for ensuring the country's stability and economic independence. At the current stage of oil industry development, with advancements in drilling technology, new drilling equipment, and chemical agents, previously unknown methods and types of well construction are now feasible [10].

Traditionally, all exploratory wells were drilled vertically, but there is now justification for altering this standard practice. Experience gained from constructing the H1 horizontal directional well at the Northern Goturdepe field in collaboration with Schlumberger demonstrates the feasibility of exploratory drilling with horizontal directional wells in the shallow waters of the Caspian Sea. Drilling wells in various directions from existing artificial islands significantly reduces field exploration costs, as noted in the study [11]. At Turkmenistan's Goturdepe Drilling Operations Department, the first successful experience with horizontal directional drilling has been achieved. Specialists from Goturdepe and Schlumberger drilled the inclined directional well H2 at the Northern Goturdepe field, deviated from the vertical at a depth exceeding 1000 m. Drilling reached 3000 m using local resources, with the directional segment drilled with Schlumberger's specialized equipment.

The well successfully reached the planned depth of 4850 m (measured depth). The drilling process to a depth of 3000 m conformed to the technical project and was similar to methods used in other wells in the country. The kick-off point for directional drilling was set at 3000 m to achieve a zenith angle with an azimuth of 270°. The planned parameters included a zenith angle of 45°, a maximum build rate of 3.5° per 30 m, and a well deviation of 1046.58 m.

Before beginning the directional section at 3000 m, the previous water-based mud was replaced with a hydrocarbon-based mud system called Versadrill. This hydrocarbon-based formulation, developed with specialized chemical additives, contains up to 80% hydrocarbons and 20% water. The primary advantage of such muds is their high resistance to water, which results in the formation of thin and flexible mud cakes [12]. This also preserves the natural reservoir properties of the productive section, significantly reducing clay dispersion in the mud, along with other beneficial characteristics.

The use of hydrocarbon-based muds can present challenges for well cementing with cement slurries [13]. This issue arises when cement mixes with hydrocarbon-based muds, leading to coagulation, which increases the mixture's fluidity and compaction. To prevent such issues, the Nebitgazylmytaslama Institute developed a special hydrocarbon-based spacer fluid successfully used in drilling the H2 well at Northern Goturdepe.

During the drilling of this well, systematic geological and technical testing was conducted using the new GTL Station, "Geotest-5". The "Geotest-5" device automatically collects, processes, and visualizes geological, geochemical, and technical data related to the drilling process [14]. This tool monitors drilling parameters, assesses overall drilling conditions, identifies reservoir sections, and determines their saturation levels, helping to prevent potential complications and accidents.

The station comprises three main modules: technological, gas logging, and geological [15]. The technological module manages the drilling process in real time, ensuring efficient and accurate control over drilling operations. The gas logging module records overall gas content and analyzes the gas mixture composition, playing a critical role in assessing the safety and efficiency of the process. The geological module conducts real-time analysis of core samples, drill cuttings, mud, and formation fluids, providing valuable information to assess geological characteristics and well material composition [16].

Fig. 1 shows a segment of a chart reflecting the technological parameters during the curvature build-up phase in the drilling process, while Fig. 2 presents a fragment of the straight interval of the inclined section of the well.

Drilling at a depth of 3000 m was conducted using the following equipment: a downhole motor with a diameter of 295.3 mm, model A800M 4553 HR-8.92 m; followed by a 269 mm non-magnetic spiral-blade stabilizer (SBS); then a crossover sub with a check valve, 206 mm in diameter, and a 204 mm weighted drill pipe (WDP) measuring 8.93 m. Next, the "Telescope-825NF" telemetry system was installed at 8.06 m, followed by another weighted drill pipe with a diameter of 203 mm and a length of 37.15 m, a hydraulic jar measuring 10.07 m, another weighted drill pipe with a diameter of 203 mm and a length of 9.19 m, a crossover sub, an additional crossover sub, and a weighted drill pipe with a diameter of 172 mm measuring 9.34 m. This assembly was completed with drill pipes running to the wellhead.

To maintain the specified build rate of the zenith angle during angle build-up, the following method was applied: drilling was conducted to a depth of 4–5 m at a specific azimuth with the rotary locked to achieve angle build-up, followed by drilling an additional 4–5 m with rotary motion and a bottom-hole assembly (BHA) configuration to stabilize the zenith angle. This process is illustrated in Column 3 of Fig. 1 by curves showing the rotary speed and the position of the hoisting block.

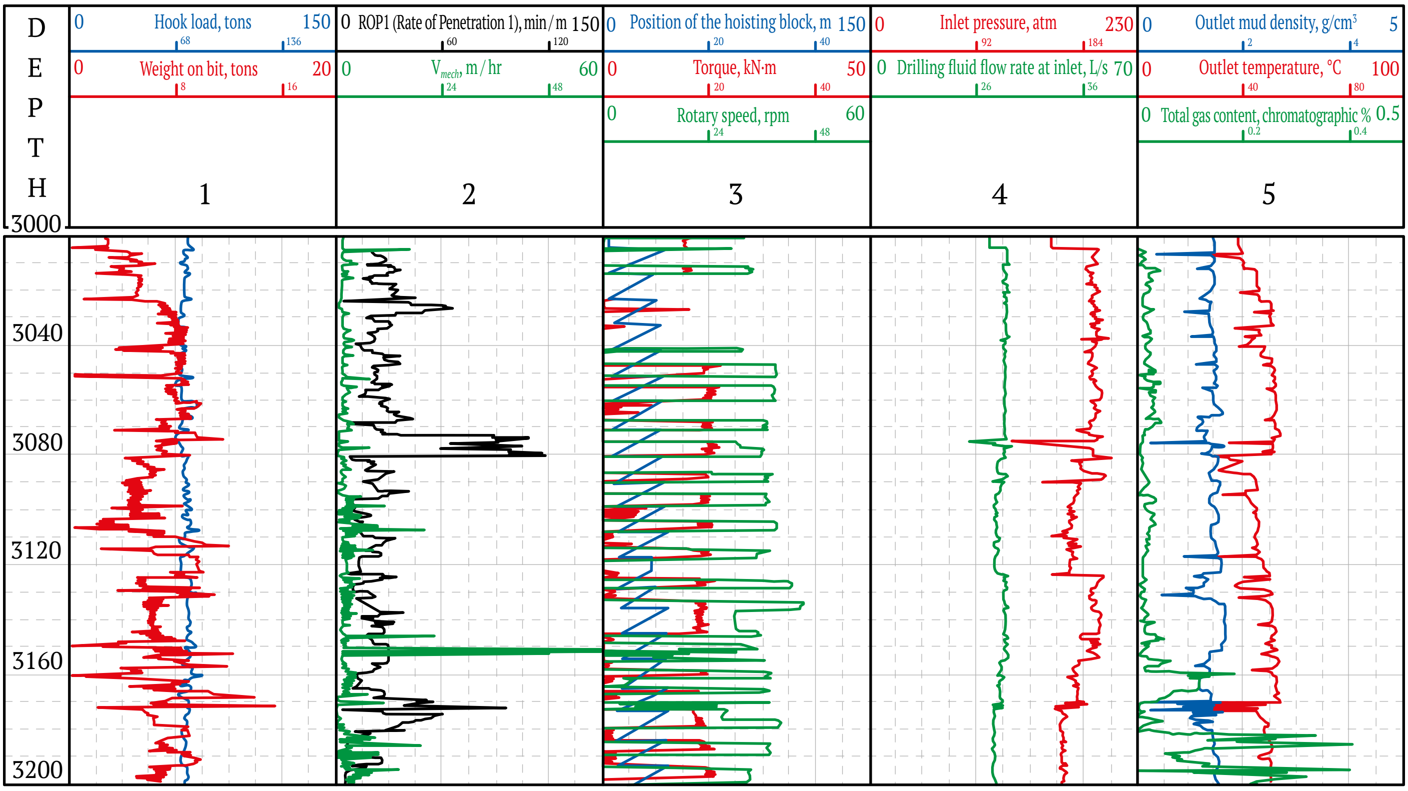

Fig. 1. Well deepening parameters during curvature build-up [compiled by the author]

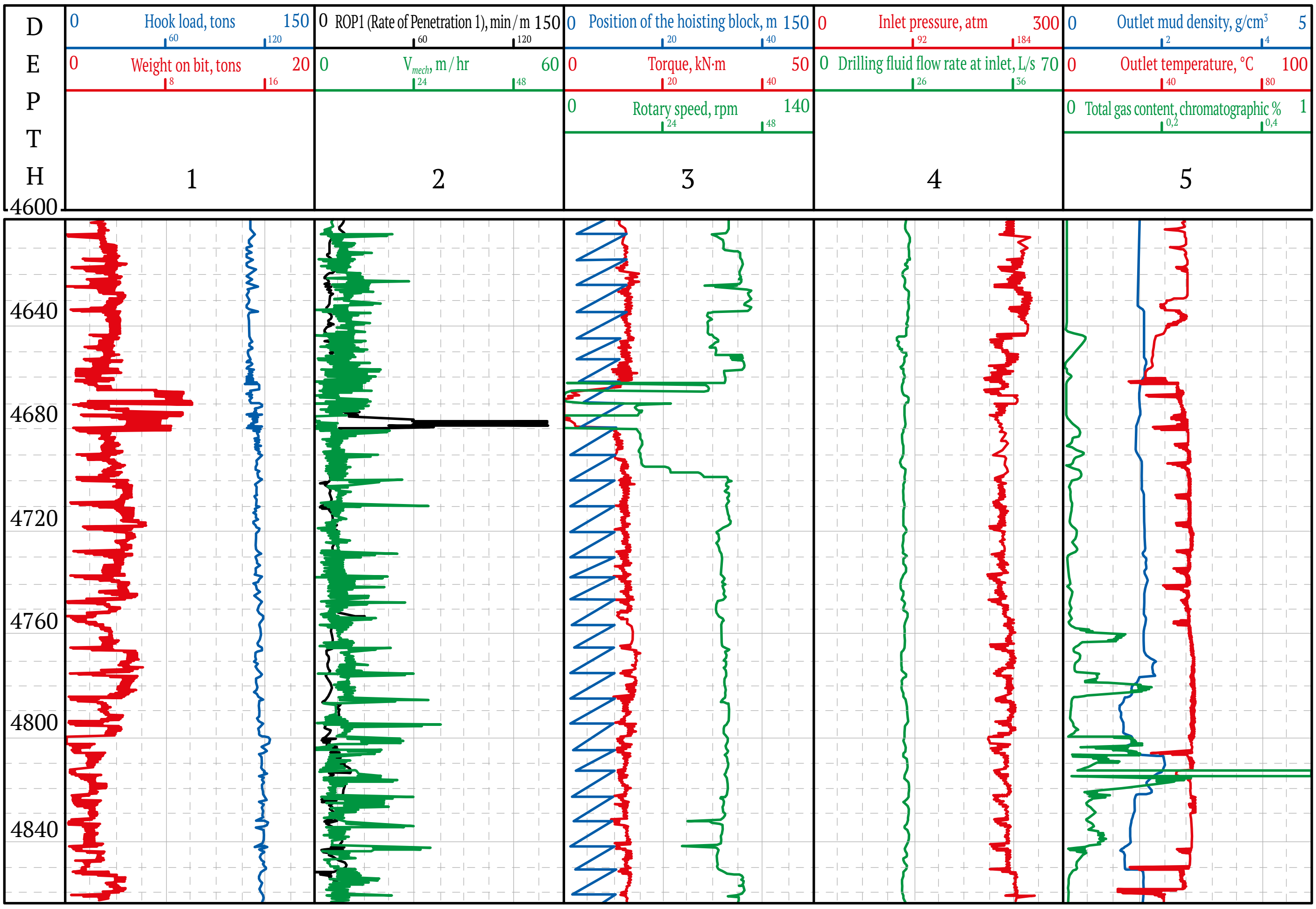

Fig. 2. Well deepening parameters in the straight inclined section [compiled by the author]

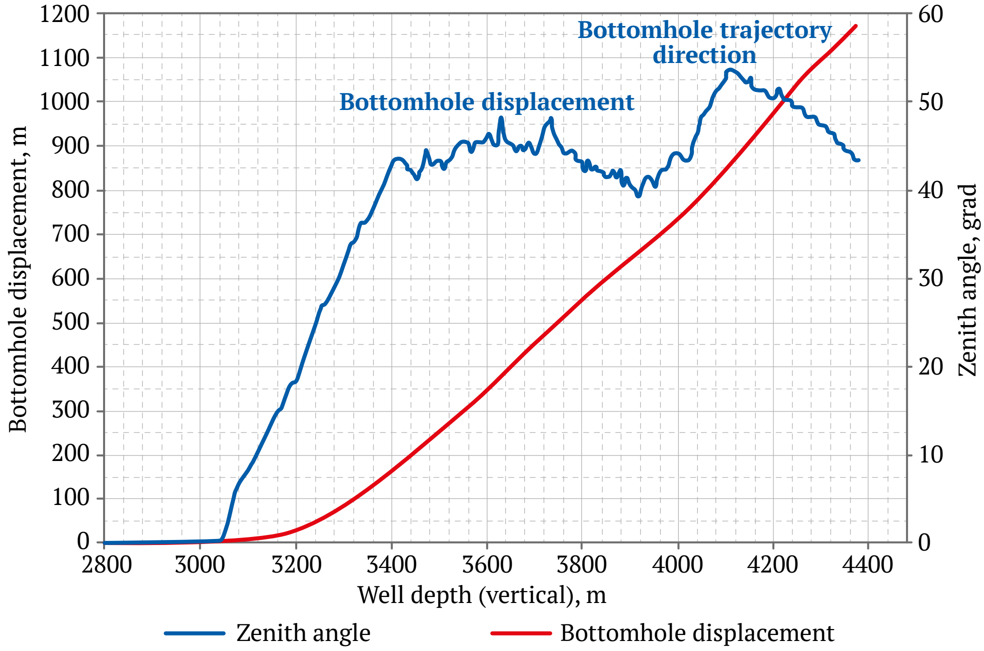

Fig. 3. Inclination angle change and bottomhole displacement in Well X2 at the Northern Goturdepe field [compiled by the author]

The technological parameters of well deepening in the straight inclined section were optimized using continuous rotary motion and an appropriate configuration of the bottom-hole assembly (see Fig. 2). The stability of the wellbore trajectory was maintained by adjusting the stabilizer positions in the drill string and alternating between PDC bits and roller-cone bits in the straight section of the well.

At a measured depth of 4450 m, a 244.5 mm casing was successfully run and secured in the well. This process was conducted in two stages. Later, when the well reached the planned depth, a decision was made to continue deepening it for a more detailed study of the productive NK3 horizon layers. The well depth was extended to 4865 m, after which a 139.7 mm production casing was installed.

During the drilling of Well X2 at the Northern Goturdepe field, the maximum bottomhole deviation reached 1167.48 m at a magnetic azimuth of 266.15°, and the maximum zenith angle at a depth of 4440 m was 53.46°. The changes in the vertical profile and zenith angle of the well are illustrated in Fig. 3. Production from the first reservoir (NK3) yielded a maximum flow rate of 80 tons per day. The results of the analysis of this product, conducted in the oil, gas, and rock geochemistry laboratory at the Nebitgazylmytaslama Institute, are presented in Table 1.

The well construction chart shown in Fig. 4 highlights opportunities to increase drilling speed for this type of well. One of the key factors impacting drilling efficiency and productivity is the reduction of preparation time for drilling the inclined section [17]. In the current chart context, it is evident that the time spent preparing for inclined drilling can be minimized. This is a critical observation, as more efficient and faster preparation for drilling the inclined section will reduce delays and improve overall drilling productivity.

This aspect holds strategic significance, as increasing drilling speed leads to faster hydrocarbon extraction, which, in turn, enhances economic efficiency and provides a quicker return on investment. Such prospects reflect the industry's commitment to continuously advancing technologies and processes to optimize production and ensure long-term sustainability.

Table 1

Oil analysis from well X2 at the Northern Goturdepe field [compiled by the author]

Interval (measured depth), m		4820–4830	4832–4844
Horizon		NK	
Water content, %		47.0	30.5
Oil density, g/cm^3		0.8545	0.8560
Pour point, °C		+4	+4
Viscosity, Pa·s	20 °C	11,4	11,5
	50 °C	5,0	5,1
Conclusion		Liquid hydrocarbon fluid – light oil	

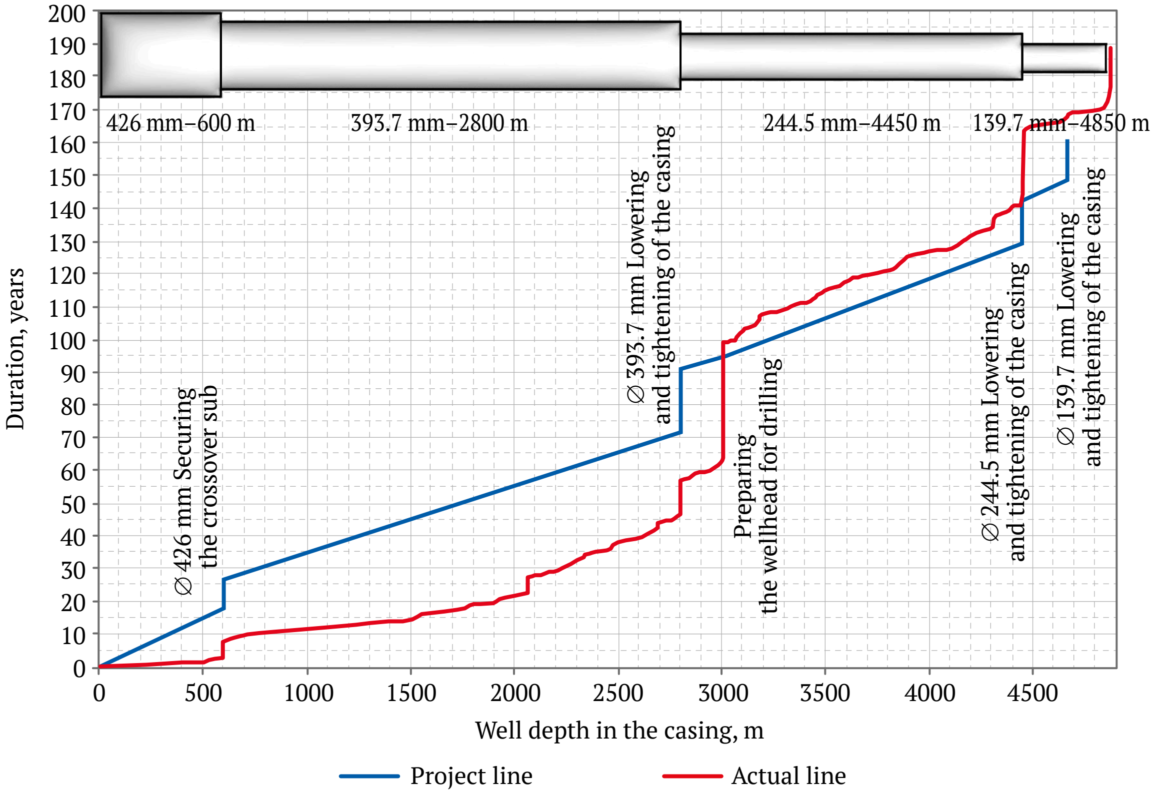

Fig. 4. Timeline diagram of well X2 construction at Northern Goturdepe [compiled by the author]

The commercial productivity of the well is defined by an average drilling speed of 817 m per month, with fully effective drilling time at 100%. The time distribution among main operations is as follows: 27.3% allocated to drilling, 17.2% to tripping operations, 18.06% to casing processes, and 35% to auxiliary tasks. These metrics are crucial for assessing the overall efficiency of the drilling process and provide insights into the time expenditures for each stage of operation.

In conclusion, directional drilling of exploratory wells in the Caspian Sea offshore area represents a complex yet promising path for a country aiming to utilize its natural resources with maximum efficiency. It is essential to strike a balance between economic gains and responsible environmental stewardship to ensure sustainable development and preserve the unique natural environment of this region.

Discussion of the results

Directional drilling of exploratory wells in the Caspian Sea offshore area in Turkmenistan presents both opportunities and challenges. This process holds significant strategic importance for Turkmenistan, which aims to maximize its hydrocarbon extraction potential.

Turkmenistan has substantial oil and gas reserves in the Caspian Sea offshore area. Directional drilling offers a unique opportunity for efficient extraction of these resources. This technology allows for hydrocarbon production from various points within fields, thereby increasing overall output and strengthening the country's energy security.

The use of directional exploratory wells requires advanced technologies and engineering solutions. Implementing modern drilling and geological exploration methods can significantly improve extraction efficiency and precision. Such innovations not only increase production volumes but also help to reduce the environmental impact.

Serious attention must be given to the environmental and social aspects of offshore drilling in the Caspian Sea. Discharges and emissions can adversely affect the marine ecosystem as well as the health of local communities. Therefore, strict adherence to international standards, the development and deployment of environmentally friendly technologies, and public engagement are key elements of a sustainable approach to hydrocarbon exploration and production.

The success of drilling in the Caspian Sea offshore area also depends on geopolitical factors.

Turkmenistan must engage in dialogue and cooperation with neighboring countries that have vested interests in the region. Effective resource management and the resolution of boundary issues contribute to stability and increased investment in the energy sector.

Overall, directional drilling of exploratory wells in the Caspian Sea offshore area in Turkmenistan represents a complex task that requires an integrated approach, balancing interests and considering environmental and social factors. Project implementation that takes these aspects into account can become a key component of sustainable development in the country's energy sector

According to recent studies by T. Eren, directional drilling positioning calculations play a crucial role in ensuring the accuracy and efficiency of this technological process. The primary goal of these calculations is to precisely determine the well's coordinates at various depths, allowing engineers and drilling specialists to effectively adjust the drilling direction and angle to meet specific objectives. In directional drilling, tools such as gyroscopes and accelerometers are used to determine the position and angle of the well relative to the vertical axis. This data is then subjected to complex mathematical calculations involving trigonometry and geometry to determine the precise well coordinates at each stage of drilling. Accurate positioning calculations not only enhance hydrocarbon recovery but also reduce the risk of potential issues, such as cross-drilling into neighboring wells or deviating from the target formation. This is especially important in complex geological structures or offshore environments [18].

These findings align with the points discussed in the previous section. Positioning calculations in directional drilling are an integral part of the technology, ensuring process accuracy and efficiency. Modern methods and technologies in this field contribute to the rationalization of hydrocarbon extraction and support sustainable exploration and field development.

According to Fang Peng, the study of key technologies for intelligent directional drilling equipment is a critical aspect in the development of the oil and gas industry. These technologies aim to improve drilling processes, increase accuracy and efficiency, and reduce the risks associated with hydrocarbon extraction. One of the key elements is the use of advanced navigation and control systems, including integrated gyroscopes, accelerometers, and geomagnetic sensors. Intelligent equipment enables real-time monitoring of drilling parameters such as inclination angle, direction, and well depth. Data processing algorithms based on artificial intelligence (AI) allow for the prediction and prevention of potential issues, significantly enhancing drilling safety and productivity. The application of AI technologies also involves automating decision-making processes based on collected data. This enables operators to quickly respond to changing conditions and adjust drilling parameters in real-time, improving performance. Such systems also minimize human involvement in the drilling process, which reduces the risk of accidents and errors [19].

It is worth noting that research on these technologies is directed toward creating sustainable, intelligent drilling systems capable of adapting to various geological conditions. These innovations open up new prospects in hydrocarbon exploration and production, enhancing efficiency and reducing environmental impact.

Researcher H. Li identified that the modified Boltzmann annealing differential evolution algorithm represents an innovative approach to the inversion of directional logging measurements for resistivity during drilling. Log data inversion is a key tool in geophysical research, providing information on rock properties, well characteristics, and the surrounding environment. The differential evolution algorithm combined with the Boltzmann annealing method offers an efficient rationalization method, allowing researchers to determine preferred rock resistivity values in real-time. The algorithm modification is designed to improve its convergence and stability under complex drilling conditions, making it especially useful in oil and gas exploration [20].

This perspective aligns with the view that applying the algorithm to directional logging data enables a more accurate reconstruction of rock resistivity at various well depths. This is crucial for determining rock composition, identifying economically viable zones, and optimizing hydrocarbon production processes. Such innovative inversion methods significantly enhance the accuracy and informativeness of data obtained in real-time during drilling.

Research conducted by D. Cao has demonstrated that the development and application of real-time deep learning models represent significant progress in enhancing the efficiency of directional drilling. This innovative technology relies on neural networks to analyze data collected during drilling and to make decisions based on that analysis. Deep learning enables the creation of complex models capable of automatically extracting high-level features from multidimensional data, such as drilling parameters, geological characteristics, and other factors. These models can predict changes in well geology and prevent potential issues in real-time. The application of real-time deep learning models in directional drilling allows for more precise control and adjustment of drilling direction and angle. This leads to increased productivity, reduced drilling time, and decreased risks of possible failures [21]. These findings support the previous research, as the development and application of real-time deep learning models in directional drilling present the oil and gas sector with opportunities to improve processes, reduce costs, and enhance overall efficiency.

As noted by B. Harris, numerical research on the use of directional wells to extract geothermal energy from abandoned oil and gas wells represents a promising approach that combines high efficiency and sustainability in the renewable energy sector. Abandoned oil and gas wells provide a unique infrastructure that can be repurposed to extract geothermal energy, giving these resources a second life. Numerical modeling allows for the assessment of geothermal energy potential at various depths of abandoned wells, taking into account the geothermal gradient and other geological parameters. The use of directional wells further enhances this process, allowing for more efficient extraction of thermal energy from rock formations. This approach not only enables the reuse of outdated infrastructure but also supports a sustainable and environmentally friendly method of energy production. Energy derived from geothermal sources can serve local power systems and reduce dependency on traditional energy sources [22]. The analysis of the results shows the importance of such studies, as they help to identify effective technologies and geological parameters for utilizing abandoned wells to extract geothermal energy. This direction could contribute to diversifying the energy mix, enhancing its sustainability, and reducing environmental impact.

Researcher A. Ihnatov determined that the development of optimized bottom-hole assemblies (BHAs) for directional drilling is a crucial area in drilling engineering, aimed at streamlining processes and increasing hydrocarbon production efficiency. This task requires a comprehensive approach, including the study of geological features, consideration of well requirements, and the application of advanced engineering solutions. Rational BHAs for directional wells incorporate enhanced drill bits, rotors, and other tools designed specifically for the drilling conditions. Innovative geometries and materials can improve wear resistance, extend equipment life, and reduce maintenance costs. An effective BHA configuration also enables more precise control of drilling direction, which is critical for achieving target objectives in challenging geological conditions. Integrating advanced technologies for drilling process automation and real-time monitoring of wellbore parameters allows for immediate responses to changes, enhancing accuracy and predictability [23].

Thus, the development of optimized BHAs for directional drilling not only contributes to streamlining technological processes but also enhances productivity, reduces risks, and supports the sustainable development of the oil and gas industry.

Conclusions

1. The H1 and H2 wells at Northern Goturdepe successfully fulfilled their role in exploration and prospecting activities, confirming the presence of hydrocarbon reserves in this part of the field without the need for additional expenses or time to construct a specialized artificial drilling pad. The experience of drilling a directional well with a curved borehole at the Northern Goturdepe field in Turkmenistan enables the simplification and acceleration of exploration and prospecting activities in the Caspian Sea offshore area. Effective use of existing artificial pads has significantly reduced the financial costs of geological exploration at the Northern Goturdepe field.

2. The drilling of directional wells in a field lacking seismic exploration has expanded a significant portion of the field within exploration and prospecting operations. From an ecosystem protection perspective in the Caspian Sea, the use of cluster drilling of directional wells, with minimal creation of new islands, is particularly important.

3. Directional drilling in the Caspian Sea enables the efficient extraction of hydrocarbons from various points within fields, which is essential given the complex geology. Streamlining drilling processes with consideration for well orientation helps improve overall productivity and reduce delays. This approach not only increases energy resource production but also supports operational sustainability and enhances economic efficiency. The development of technologies, such as modern navigation and control systems, complements the drilling process, ensuring accuracy and safety.

4. Drilling in the Caspian Sea offshore area in Turkmenistan is becoming an essential component of the country's energy strategy, and the effective use of directional exploratory wells reflects a continuous commitment to innovation and technological improvement in the oil and gas industry.

5. It is necessary to further study the environmental impact and ecosystem effects of directional drilling processes in the Caspian Sea offshore area in

Turkmenistan to develop more ecologically sustainable and socially responsible approaches to energy resource extraction.

6. The conclusions drawn from directional exploratory drilling in the Caspian Sea offshore area in Turkmenistan highlight the strategic importance of this approach for hydrocarbon production in the region. Turkmenistan, with its vast oil and gas reserves, is actively implementing innovative drilling methods to maximize production efficiency.

Список литературы / References

1. Geldimyradov A.G. Determination of formation parameters based on studies of pressure change curve under conditions of gas wells of Turkmenistan. *In: Science, Society, Technology: Problems and Prospects for Interaction in the Modern World.* Collection of articles of the International Scientific and Practical Conference. Petrozavodsk, February 17, 2022. Petrozavodsk: International Center for Scientific Partnership "Novaya Nauka"; 2022. Pp. 150-163. (In Russ.) https://doi.org/10.46916/21022022-1-978-5-00174-478-8
2. Pulatov B.R. Technological aspects and emerging complications when drilling wells in rapiferous zones. *Innovation in the Oil and Gas Industry.* 2021;2(3):103–114. (In Russ.) URL: https://tadqiqot.uz/index.php/petroleum/article/view/4232/4015
3. Kholbaev B.M., & Muhammadiev Sh.Sh. (2023). Selection of the type of drilling fluid for drilling wells. *Innovative Development in Educational Activities.* 2023;2(8):684–686. (In Russ.)
4. Deryaev A. Features of the construction of directional deep wells in Turkmenistan. *Neftyanoe Khozyaystvo* 2024;(2):43–47. (In Russ.) https://doi.org/10.24887/0028-2448-2024-2-43-47
5. Amanniyazov Y., Nurlyev B., Akmukhammedov M. Drilling fluids. Their role in the drilling process. In: *Modern Tasks and Promising Directions for Innovative Development in Science.* Collection of articles based on the results of an international scientific and practical conference. Irkutsk, February 09, 2023. Sterlitamak: AMI; 2023. Pp. 87–88. (In Russ.) URL: https://ami.im/sbornik/MNPK-458.pdf#page=87
6. Geldiev Sh., Ovezmammedov B. Analysis and identification of factors of the impact of the development of the fuel and energy complex on the development of Turkmenistan. In: *Science Innovations – 2022.* Collection of articles of the international scientific and practical conference. Petrozavodsk, October 31, 2022. Petrozavodsk: International Center for Scientific Partnership "Novaya Nauka"; 2022. (In Russ.)
7. Bashir B., Piaskowy M., Alusta G. Overview on directional drilling wells. *ARPN Journal of Engineering and Applied Sciences.* 2021;16(22):2305–2316.
8. Njuguna J., Siddique S., Kwroffie L.B. et al. The fate of waste drilling fluids from oil & gas industry activities in the exploration and production operations. *Waste Management*. 2022;139:362–380. https://doi.org/10.1016/j.wasman.2021.12.025
9. Magana-Mora A., Affleck M., Ibrahim M. et al. Well control space out: A deep-learning approach for the optimization of drilling safety operations. *IEEE Access*. 2021;9:76479–76492. https://doi.org/10.1109/ACCESS.2021.3082661
10. Deryaev A.R. Drilling horizontal wells in Western Turkmenistan. *SOCAR Proceedings Special.* 2023;(2):32–40. (In Russ.) https://doi.org/10.5510/OGP2023SI200877
11. Deryaev A.R. Development of well design for multi-layer fields for the purpose of simultaneous separate operation of one well. *SOCAR Proceedings.* 2022;(1):94–102. https://doi.org/10.5510/OGP20220100635
12. Mohamed A., Salehi S., Ahmed R. Significance and complications of drilling fluid rheology in geothermal drilling: A review. *Geothermics*. 2021;93:102066. https://doi.org/10.1016/j.geothermics.2021.102066
13. Tewari S., Dwivedi U.D., Biswas S. Intelligent drilling of oil and gas wells using response surface methodology and artificial bee colony. *Sustainability*. 2021;13(4):1664. https://doi.org/10.3390/su13041664
14. Li Y., She L., Wen L., Zhang Q. Sensitivity analysis of drilling parameters in rock rotary drilling process based on orthogonal test method. *Engineering Geology*. 2020;270:105576. https://doi.org/10.1016/j.enggeo.2020.105576
15. Sun J., Chen M., Li Q., et al. A new method for predicting formation lithology while drilling at horizontal well bit. *Journal of Petroleum Science and Engineering*. 2021;196:107955. https://doi.org/10.1016/j.petrol.2020.107955
16. Fabre C. Advances in Laser-Induced Breakdown Spectroscopy analysis for geology: A critical review. *Spectrochimica Acta Part B: Atomic Spectroscopy*. 2020:166:105799. https://doi.org/10.1016/j.sab.2020.105799
17. Huque M.M., Rahman M.A., Zendehboudi S. et al. Experimental and numerical study of cuttings transport in inclined drilling operations. *Journal of Petroleum Science and Engineering*. 2022;208:109394. https://doi.org/10.1016/j.petrol.2021.109394

18. Eren T., Suicmez V.S. Directional drilling positioning calculations. *Journal of Natural Gas Science and Engineering*. 2020;73:103081. https://doi.org/10.1016/j.jngse.2019.103081
19. Fang P., Yao K., Wang L. et al. Research on key technologies of the ZDY25000LDK intelligent directional drilling equipment. *Coal Geology & Exploration*. 2022;50(1):2. https://doi.org/10.12363/issn.1001-1986.21.10.0597
20. Li H., Wang H., Wang L., Zhou X. A modified Boltzmann Annealing Differential Evolution algorithm for inversion of directional resistivity logging-while-drilling measurements. *Journal of Petroleum Science and Engineering*. 2020;188:106916. https://doi.org/10.1016/j.petrol.2020.106916
21. Cao D., Hender D., Ariabod S. et al. The development and application of real-time deep learning models to drive directional drilling efficiency. In: *IADC/SPE International Drilling Conference and Exhibition*. Galveston, Texas, USA, March 3–5, 2020. https://doi.org/10.2118/199584-MS
22. Harris B.E., Lightstone M.F., Reitsma S. A numerical investigation into the use of directionally drilled wells for the extraction of geothermal energy from abandoned oil and gas wells. *Geothermics*. 2021;90:101994. https://doi.org/10.1016/j.geothermics.2020.101994
23. Ihnatov A., Koroviaka Y., Rastsvietaiev V., Tokar L. Development of the rational bottomhole assemblies of the directed well drilling. In: *E3S Web of Conferences. IV International Scientific and Technical Conference "Gas Hydrate Technologies: Global Trends, Challenges and Horizons" (GHT 2020)*. 2021;230:01016. https://doi.org/10.1051/e3sconf/202123001016

Information about the author

Annaguly R. Deryaev – Dr. Sci. (Eng.), Principal Researcher, Natural Gas Research Institute, Turkmengaz State Concern, Ashgabat, Turkmenistan; ORCID 0009-0004-8569-6277, Scopus ID 57929694600, ResearcherID HPB-6027-2023; e-mail annagulyderyayew@gmail.com

Received 11.02.2024
Revised 15.05.2024
Accepted 20.05.2024

MINING SCIENCE AND TECHNOLOGY (RUSSIA)
ГОРНЫЕ НАУКИ И ТЕХНОЛОГИИ
2024;9(4):352–386
eISSN 2500-0632
https://mst.misis.ru/

GEOLOGY OF MINERAL DEPOSITS

Review paper

https://doi.org/10.17073/2500-0632-2024-05-248
UDC 553.04:553.43

Mineral resource base of Russia's copper: current state and development prospects

G.Y. Boyarko[1] ✉, **A.M. Lapteva**[2], **L.M. Bolsunovskaya**[1]
[1] *National Research Tomsk Polytechnic University, Tomsk, Russian Federation*
[2] *Russian Scientific Research Institute of Mineral Raw Materials, Moscow, Russian Federation*
✉ *gub@tpu.ru*

Abstract
This study addresses the need for a comprehensive understanding of current state of Russia's cupper mineral resource base. *Its objective* is to assess Russia's copper reserves (balance reserves and forecast resources), analyze the spatial distribution of copper deposits by ore formation types and across ore provinces, and evaluate prospects for sustaining national copper production. Methods: The study employs statistical, graphical, and logical analysis methods. *Results:* The research presents a consolidated map of Russia, highlighting 25 copper provinces and 150 significant copper deposits across various ore formations, as well as prospective sites and areas. Key characteristics of Russia's main ore formations, copper ore provinces, and outlying copper deposits are detailed. Copper production in Russia is currently concentrated in sulfide copper-nickel and copper-pyrite deposits, with emerging mining operations in copper-porphyry and copper-skarn formations. In 2021, copper production in Russia reached 1,147 Kt. Upcoming projects to develop copper deposits could increase annual production by 635–1,053 Kt, equivalent to a 55–91% rise over 2021 levels. The total estimated balance reserves and forecast resources amount to 102.7 million tons, with conditional reserves accounting for 16.1 million tons. The largest copper reserves are found in copper-nickel formations (34.4%), copper-porphyry formations (23.9%), copper sandstones formation (19.6%), and copper-pyrite formation (14.5%), with all other formations contributing 7.6%. Key provinces include Norilsk-Kharayelakh (30.9% Russian reserves), Kodar-Udokan (20.3%), and the Urals (18.9). The share of reserves is growing in newer provinces: Primorsky (8.29%), Okhotsk-Chukotka (6.23%), and East Tuvinian (3.7%). Remaining copper mining provinces account for 11.68% of reserves. Current reserves are estimated to suffice for at least 47 years of optimal extraction. The most substantial reserves are associated with copper-nickel, copper-porphyry, and copper sandstone formations, whereas balance ore reserves in copper-pyrite and copper-skarn formations are nearly exhausted. Sufficient reserve security is available in the Norilsk-Kharayelakh, Kola, and Rudny Altai provinces. However, significant reserve is observed in the traditional Ural and emerging East Trans-Baikal provinces. In the North Caucasus province, a high security results in low production levels and underutilized reserve deposits. The copper-nickel formation's reserve availability remains low, though new rich ore deposits may exist at greater depths within the Kharaelakh and Tangaralakh ore-bearing intrusions. Copper-pyrite formation reserves may expand with further exploration of deep horizons and the periphery of known deposits in the Ural province, alongside new deposits discoveries in the Circumpolar and Polar Urals. For copper-polymetallic formation, extensive deposits exist in old Ore-Altai, Salair, and North Caucasian provinces, with promising potential in the new East Tuvinian and Okhotsk-Chukotka provinces. Exploration for porphyry copper has intensified in the East Tuvinian, Primorsky, and Okhotsk-Chukotka provinces, indicating strong potential for discovering new large porphyry copper deposits. Additional reserves of copper sandstone formation may be developed within the Kodar-Udokanskaya, Igarskaya, Bilyakchan-Kolyma, and Shoria-Khakass provinces. New technology for underground copper leaching opens opportunities for exploring and utilizing smaller copper sandstone deposits in the Pre-Ural and Donetsk provinces. The recorded cooper balance reserves in Russia do not yet account for native copper deposits in basaltoid formations within the Shoria-Khakass, Norilsk-Kharayelakhskaya, and Bilyakchan-Kolyma provinces.

Keywords
copper, ore, strategic raw materials, ore formations, deposit, province, region, reserves, resurce, mining, forecasting, national projects, Russia

For citation
Boyarko G.Y., Lapteva A.M., Bolsunovskaya L.M. Mineral resource base of Russia's copper: current state and development prospects. *Mining Science and Technology* (*Russia*). 2024;9(4):352–386. https://doi.org/10.17073/2500-0632-2024-05-248

MINING SCIENCE AND TECHNOLOGY (RUSSIA)
ГОРНЫЕ НАУКИ И ТЕХНОЛОГИИ
eISSN 2500-0632
https://mst.misis.ru/
2024;9(4):352–386

ГЕОЛОГИЯ МЕСТОРОЖДЕНИЙ ПОЛЕЗНЫХ ИСКОПАЕМЫХ

Обзорная статья

Минерально-сырьевая база меди России: состояние, возможности развития

Г.Ю. Боярко[1] ✉, **А.М. Лаптева**[2], **Л.М. Болсуновская**[1]

[1] *Национальный исследовательский Томский политехнический университет, г. Томск, Российская Федерация*

[2] *Всероссийский научно-исследовательский институт минерального сырья им. Н.М. Федоровского, г. Москва, Российская Федерация*

✉ *gub@tpu.ru*

Аннотация

Актуальность работы обусловлена необходимостью получения максимально полной картины состояния минерально-сырьевой базы меди по Российской Федерации. *Цель*: изучение состояния минерально-сырьевой базы меди России (балансовых запасов, прогнозных ресурсов), пространственного размещения месторождений меди по типам рудных формаций и в пределах рудных провинций, перспектив национального производства добычи меди. *Методы*: статистический, графический, логический. *Результаты*: Представлена сводная карта-схема России, включающая 25 меднорудных провинций и выборку из 150 наиболее значимых месторождений меди различных рудных формаций, перспективных объектов и площадей. Даны характеристики основных рудных формаций, месторождения меди которых имеются в России, а также меднорудных провинций и медных месторождений вне провинций. В России основная добыча сконцентрирована на сульфидных медно-никелевых и медно-колчеданных месторождениях, а также начата добыча на медно-порфировых и медно-скарновых месторождениях. В 2021 г. уровень добычи меди в Российской Федерации составил 1147 тыс. т. Реализация новых подготавливаемых проектов разработки медных месторождений может увеличить уровень годовой добычи России на 635–1053 тыс. т (на 55–91 % от уровня добычи 2021 г.). В России по состоянию на 01.01.2022 г. учтено 102,7 млн т балансовых запасов и прогнозных ресурсов в пересчете на условные запасы – 16,1 млн т. Наибольшие объемы запасов меди приходятся на медно-никелевую (34,4 % от российских запасов), меднопорфировую (23,9 %) формации, формацию медистых песчаников (19,6 %) и медно-колчеданную формацию (14,5 %) и 7,6 % на все остальные рудные формации. По провинциям на Норильско-Хараелахскую приходится 30,9 % от российских запасов, на Кодаро-Удоканскую – 20,3 % на Уральскую – 18,9 %. Отмечается увеличение показателей долей запасов меди для новых провинций: Приморской – 8,29 %, Охотско-Чукотской – 6,23 % и Восточно-Тувинской – 3,7 %. На остальные меднорудные провинции приходится 11,68 % российских запасов меди. В целом имеющихся запасов меди Российской Федерации хватит минимум на 47 лет оптимальной эксплуатации. Наиболее обеспечены запасами разрабатываемые месторождения медно-никелевой и медно-порфировой формаций, а также формации медистых песчаников. Для месторождений медно-колчеданной и медно-скарновой формаций имеет место срабатывание имеющихся запасов балансовых руд. По эксплуатационным регионам достаточная обеспеченность имеется лишь для Норильско-Хараелахской, Кольской и Рудно-Алтайской провинций. В старой горнопромышленной Уральской и новой Восточно-Забайкальской провинциях отмечается серьезное срабатывание запасов балансовых руд. В старой горнопромышленной Северо-Кавказской провинции имеет место высокий уровень обеспеченности, что является следствием малого уровня добычи и наличия невостребованных запасов резервных медных месторождений. Обеспеченность запасов прогнозными ресурсами медно-никелевой формации невысокое, но возможны открытия новых месторождений богатых сливных руд на глубине в пределах Хараелахского и Тангаралахского рудоносных интрузивов. Для медно-колчеданной формации прирост запасов возможен за счет оценки глубоких горизонтов и периферии известных месторождений Уральской провинции, а также поиска новых месторождений на территории Приполярного и Полярного Урала. Для медно-полиметаллической формации известно множество месторождений в старых горнопромысловых Рудно-Алтайской, Салаирской и Северо-Кавказской провинциях, а также при исследовании новых Восточно-Тувинской и Охотско-Чукотской провинций. Для медно-порфировой формации увеличились масштабы геологоразведочных работ в Восточно-Тувинской, Приморской и Охотско-Чукотской провинциях, где имеются все предпосылки к обнаружению новых, в том числе крупных медно-порфировых месторождений. Для формации медистых песчаников возможен прирост запасов в пределах Кодаро-Удоканской, Игарской, Билякчанско-Приколымской и Шорско-Хакасской провинциях. В условиях развития новых технологий подземного выщелачивания меди становятся привлекательными поиски, разведка и вовлечение в эксплуатацию небольших месторождениий медистых песчаников в Приуральской и Донецкой провинциях. В учтенных балансовых запасах меди России отсутствуют объекты месторождений формации самородной меди в базальтоидах, известные в пределах Шорско-Хакасской, Норильско-Хараелахской и Билякчанско-Приколымской провинций.

Ключевые слова
медь, руда, стратегическое сырье, рудные формации, месторождение, провинция, регион, запасы, ресурсы, добыча, прогнозирование, национальные проекты, Россия

Для цитирования
Boyarko G.Y., Lapteva A.M., Bolsunovskaya L.M. Mineral resource base of Russia's copper: current state and development prospects. *Mining Science and Technology* (*Russia*). 2024;9(4):352–386. https://doi.org/10.17073/2500-0632-2024-05-248

Introduction

Copper ranks third in global production and consumption among base industrial metals, following iron and aluminum [1]. It is widely used in electrical applications as a conductor, in various alloys (such as brass, bronze, and nickel silver), in copper compounds for producing antiseptics, micronutrients, and catalysts for oxidative processes, among other applications [2]. Copper is designated as a strategic mineral in Russia's national list of essencial raw materials (Decree of the Russian Federation Government, 30.08.2022 No. 2473-r). It is also classified in the first group of minerals in Russia's Mineral and Raw Material Base Development Strategy, with reserves that are expected to meet national demand under any economic scenario through 2035 and beyond (Decree of the RF Government, 22.12.2018 No. 2914-r) [3]. Copper holds a similar strategic status in the USA, the European Union, Canada, China, and India [4]; in some countries (e.g., Japan, South Korea, and Australia), it is even included in the list of critical, import-dependent commodities [5, 6].

Global consumption – and, accordingly, the supply – of primary copper increased by 60% from 2000 to 2021, while global reserves grew by a factor of 2.6. This growth primarily reflects the rapid expansion of the Chinese economy and the shift toward a global "green" economy, marked by a greater reliance on renewable energy sources and efforts to reduce carbon dioxide emissions from industrial and human activities [1, 2, 7]. Copper is essential in low-carbon energy technologies, including wind turbines and electric vehicle engines. The growth in copper consumption remains robust, even amid global economic downturn and political uncertainties, while supply has shown signs of lagging due to delays in commissioning new large-scale extraction operations [8].

Russia possesses a substantial copper resource base, ranking 2nd worldwide in terms of reserves, 6th in production, and 3rd-4th in exports[1]. In the 1990s, with the transition economy leading to reduced domestic consumption, Russian copper production declined from 800 Kt in 1991 to 500–580 Kt/year between 1995 and 2012. However, following the rise in global prices starting in 2013, production began to increase, reaching 1,028 Kt in 2019[2]. This growth in extraction and production of refined copper was accompanied by a significant rise in exports shares from 20–30% in 2011–2013 to 60–70% in 2015–2020. Russia's cooper mineral resource base and production facilities fully cover domestic needs and hold considerable export potential. Given global trends toward increasing copper consumption in the near future, expanding national production to boost Russia's share in the global copper market appears highly promising.

Methods

To analyze Russia's copper mineral resource, data on Russian copper production for the period 2002–2021, as well as reserves and forecast resources of copper deposits as of 01.01.2021, were collected. The data sources include state reports from the Ministry of Natural Resources and Ecology of Russia[3], certificates on the state and prospects of mineral resource use across Russian regions[4], state cadastral passports of deposits and mineral occurrences in Russia[5] and publications on copper resources available in the public domain. Copper reserves and production are measured in metric tons of 100% Cu. The volumes of forecasted copper resources are given by category in the stated absolute values, and, when aggregated, in terms of conditional reserves of category C_2, accounting for correction factors for different

[1] Ministry of Natural Resources and Environment of the Russian Federation. URL: https://www.mnr.gov.ru/docs/gosudarstvennye_doklady/o_sostoyanii_i_ispolzovanii_mineralno_syrevykh_resursov_rossiyskoy_federatsii/

[2] I bid.

[3] I bid.

[4] Information on the state and prospects of using the mineral resource base of the regions of the Russian Federation (as of 01.01.2022). St. Petersburg: VSEGEI, State Assignment No. 049-00018-22-01, 2022 dated 14.01.2022. URL: http://atlaspacket.vsegei.ru/?v=msb2021#91474d2e700eb6c90

[5] Passports of copper deposits. Russian Federal Geological Fund. The unified fund of geological information about the subsurface. The register of primary and interpreted information. 2023. URL: https://efgi.ru/

categories. A consolidated schematic map of Russia is presented, summarizing significant copper deposits across various ore formations, promising sites for copper exploration, previously designated copper ore provinces, and proposed new copper ore provinces. The paper identifies environmental restrictions on new copper deposit development. The authors also examine opportunities for advancing the copper mining industry by implementing innovative technologies for copper ores extraction and processing. Additionally, the paper provides an analysis of the state of balance reserves and forecast resources across ore formations and copper provinces.

State of the Russian mineral resource base of copper

Russia ranks 2nd globally in cooper reserves (after Chile), 6th in mining (following Chile, Peru, China, Congo, and the USA), 5th in refined copper production (after China, Chile, Japan, and DR Congo), and 3rd–4th in terms of exports (alongside Japan) after Chile and DR Congo[6] [9]. The foundation of Russia's copper resource base consists of deposits in sulfide copper-nickel, copper-porphyry, copper-pyrite, and stratiform geological-industrial types. Major mining operations are concentrated in sulfide copper-nickel and copper-pyrite deposits, with increasing production volumes at copper-porphyry sites[7].

Based on the collected data, the following was compiled:

– An overview map of Russia's copper ore provinces and primary copper deposits (see Fig. 1);

– Charts of copper production volumes and shares from 2002 to 2021 by types of ore formations (Fig. 2) and copper provinces (Fig. 7);

– Charts showing the shares of copper reserves and production (2021) by ore formation type (Fig. 3) and copper provinces (Fig. 6);

– A chart on the volume of balance reserves and forecast resources by ore formation type (Fig. 4);

– Charts on the volume of copper reserves and production by province (Fig. 6).

The paper also provides descriptions of the copper ore formations found within the Russian Federation and details on copper deposits both within and outside the designated copper ore provinces.

[6] U.S. Geological Survey (USGS). URL: http://minerals.usgs.gov/minerals/pubs/commodity/

[7] Ministry of Natural Resources and Environment of the Russian Federation. URL: https://www.mnr.gov.ru/docs/gosudarstvennye_doklady/o_sostoyanii_i_ispolzovanii_mineralno_syrevykh_resursov_rossiyskoy_federatsii/

Formations of copper deposits

The development of copper deposits has been known since the Bronze Age, and throughout the history of copper mining, geological copper ore formations have been studied in terms of their attractiveness and relevance for the copper mining industry.

Initially, copper ore exploration focused on near-surface, copper-rich ores in copper-skarn, copper-pyrite formations, and of copper sandstone formations. It also possible to identify a significant *formation of the secondary enrichment zone with supergene copper*, with rich ores formed in near-surface conditions in deposits of almost all copper ore formations, often evolving from low-grade and ordinary ores. Previously, these secondary, copper-rich ores were the primary targets for development; however, they are now rare, and this ore formation has, in fact, become exotic. Due to the initial predominance of small-scale, near-surface artisanal mining, numerous small deposits were mined for copper, while medium and large copper deposits were locally damaged by mining operations that selectively extracted the available, most copper-rich fragments.

With growing copper demand, larger deposits of copper-pyrite and copper-nickel formations began to be put into operation. A notable unique and exotic deposit of native copper in basaltoids (Lake Superior deposit, USA) was entirely mined out.

The development of flotation enrichment technologies for sulfide ores has enabled the exploitation of deposits with disseminated copper mineralization, even those with relatively low-grade copper ores, provided they have a significant ore mass. Production has included deposits from the porphyry copper formation, which currently leads in supplying copper to the market. Flotation technologies have also enabled the to extraction of copper concentrate from deposits in other ore formations with associated copper mineralization (polymetallic, low-sulfide platinum-metal, quartz-sulfide, carbonatite, etc.). New enrichment technologies (flotation, hydrometallurgy) have also made it possible to mine porphyry copper from formations where previously only rich ores (copper-nickel, copper-pyrite, copper sandstones) were developed.

Hydrometallurgical technologies, such as heap and in-situ leaching, enable the development of fundamentally new formations, including technogenic deposits (e.g., dumps, drainage waters of mine workings), as well as previously unattractive small copper deposits and copper-bearing formations.

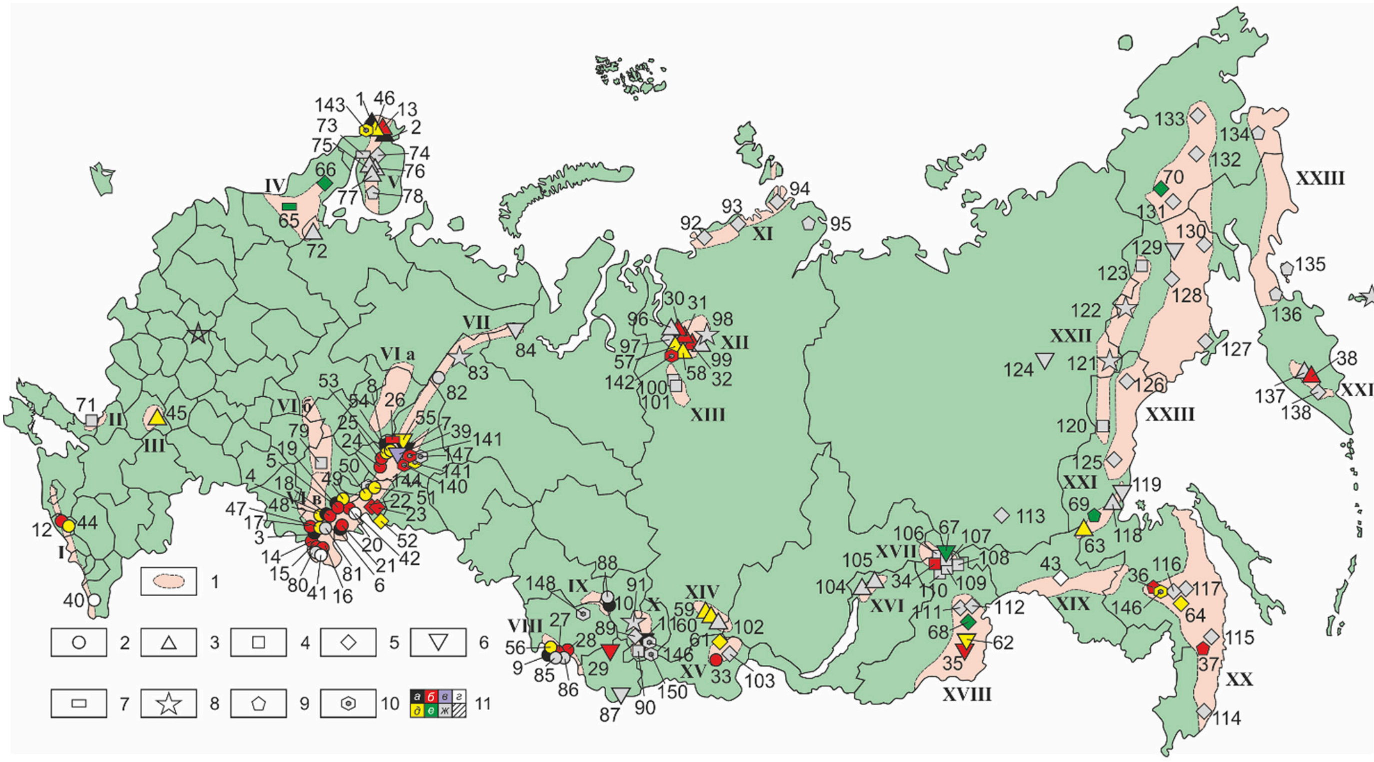

Fig. 1. Copper ore provinces, copper deposits by geological and technological types, and their status in production: 1 – copper ore provinces; 2–10 – geological and technological types of copper deposits (2 – copper-pyrite and pyrite-polymetallic, 3 – copper-nickel, 4 – copper sandstones, 5 – copper-porphyry, 6 – copper-skarn, 7 – copper-iron, 8 – native copper, 9 – with associated copper mineralization; 10 – technogenic); 11 – the status of copper deposit involvement in production: a – exhausted and suspended/shutdown mines (mothballed), b – developed by open-pit and underground methods, c – geotechnological development, d – unallocated subsoil fund, e – prepared for development, g – at the geological exploration stage, h – at the prospecting evaluation stage for sites and areas. Copper provinces: I – North Caucasus, II – Donetsk, III – Voronezh, IV – Karelian, V – Kola, VI – Pre-Ural (VIa – Ufa Stage, VIb – Kazan Stage, VIc – Tatar Stage), VII – Ural, VIII – Rudny Altai, IX – Salair, X – Shoria-Khakass (Mrassu-Batenev), XI – Central Arctic, XII – Norilsk-Kharayelakh, XIII – Igarka, XIV – Sayan, XV – East Tuvan, XVI – North Baikal, XVII – Kodar-Udokan, XVIII – East Trans-Baikal, XIX – Umlekan-Ogoja, XX – Primorsky, XXI – Jugjur, XXII – Bilyakchan-Kolyma; XXIII – Okhotsk-Chukotka, XIV – Koryak, XV – Kamchatka. Copper deposits: 1–11 – exhausted and suspended: 1 – Kotselvaara-Kammikivi, Semiletka, 2 – Tundra, Zapolyarnoye, 3 – Dergamyshskoye, 4 – Sibayskoye, 5 – Uchalinskoye, 6 – Aleksandrinskoe, 7 – Mednorudyanskoye, Turyinsky group, 8 – Tarnyerskoe, 9 – Zmeinogorskoye, 10 – Kamenushinskoye, 11 – Keyalykh-Uzen, Glafirinskoye, Julia; 12–38 – deposits under development: 12 – Urupskoye, 13 – Zhdanovskoye, 14 – Gayskoye, 15 – Osennee, 16 – Vesenne-Aralchinskoye, Dzhusinskoye, 17 – Yubileynoye, 18 – Kamagan, 19 – Ozernoye, Zapadno-Ozernoye, 20 – Talganskoye, Uzelginskoye, Molodezhnoye, 21 – Chebachye, 22 – Tominskoye, 23 – Mikheevskoye, 24 – Safyanovskoye, 25 – Novo-Shemurskoye, 26 – Volkovsky, 27 – Karbalikhinskoye, Zarechenskoye, 28 – Stepnoye, 29 – Sinyukhinskoye, 30 – Oktyabrskoye, 31 – Talnakhskoye, 32 – Norilsk-I, 33 – Kyzyl-Tashtyg, 34 – Udokan, 35 – Bystrinskoye [Cu–Fe], 36 – Pravourminskoye, Festivalnoye, Sobolinoye, Perevalnoye, 37 – Vostok-2, 38 – Shanuch; 39 – geotechnological development (Gumeshevskoye); 40–43 – undistributed reserve deposits: 40 – Kizil-Dere, 41 – Komsomolskoye, 42 – Novoye, Yuzhnoye, 43 – Ikanskoye; 44–64 – deposits prepared for development: 44 – Khudesskoye, Skalistoye, Pervomayskoye, 45 – Elanskoye, Elkinskoye, 46 – Bystrinskoye [Cu–Ni], Verkhneye, Sputnik, 47 – Podolskoye, Severo-Podolskoye, 48 – Vishnevskoye, 49 – Novo-Uchalinskoye, 50 – Sultanovskoye, 51 – Maukskoye, 52 – Tarutinskoye, 53 – Saumskoye, 54 – Severo-Kaluginskoye, 55 – Severnoye-3, 56 – Talovskoye, 57 – Maslovskoye, 58 – Chernogorskoye, 59 – Kingashskoye, 60 – Verkhnekingashskoye, 61 – Ak-Sugskoye, 62 – Kultuminskoye, 63 – Kun-Manye, 64 – Malmyzh; 65–70 –deposits at the exploration stage: 65 – Viksha, 66 – Lobash-1, 67 – Chineyskoye (Rudny site), 68 – Lukagonskoye, 69 – Konder-Rudny, 70 – Peschanka; 71–136 – promising areas, prospecting and evaluation sites: 71 – Bakhmutskaya, 72 – Voloshovskoye, 73 – Kolvitskoye, 74 – Pellapakhk, 75 – Poaz, Nyud, 76 – Nittis-Kumuzhya-Travyanaya, Sopcha (ore horizon 330), 77 – Arvarench, Moroshkovoye-Ozero, 78 – Fedorovo-Pan Tundra 79 – Belebeevskaya (Karsak mines), 80 – Blyavinskaya, 81 – Membetovskaya-Karagayskaya, Novopetrovskaya, 82 – Volinskaya, Grubeinsko-Tykotlovskaya, 83 – Khultymyinskaya, 84 – Novogodnee-Monto, 85 – Novonikolskaya, 86 – Kholodnaya, 87 – Ulandryk, 88 – Uskandinskoye, 89 – Bazinskoye, 90 – Taymetskoye, 91 – Malo-Labyshskoye, 92 – Uboininskoye, 93 – Verkhnetareyskoye, 94 – Porfyrovaya, 95 – Nadezhda, Pavlovsky, Koshka, 96 – Morongovskaya, 97 – Bolgokhtokhskoye, 98 – Arylakhskoye, 99 – Samoyedovskaya, 100 – Graviyskoye, 101 – Sukharikhinskoye, 102 – Kakhtarminskaya, 103 – Kyzyk-Chadrskoye, 104 – Yoko-Dovyrenskoye, 105 – Chayskoye, 106 – Unkurskoe, 107 – Krasnoe, 108 – Burpalinskoye, 109 – Sakinskoye, 110 – Pravoingamakitskoye, 111 – Zapadno-Mostovskaya, 112 – Borovaya, 113 – Ryabinovoe, Yllymakhskoye, Morozkinskoye, 114 – Lazurnoe, 115 – Malakhitovoe, 116 – Central Anajak, 117 – Ponyskaya, 118 – Nyandominskaya, 119 – Malokomuyskoye, 120 – Bilyakchanskoye, Severny-Uy, Borong, 121 – Rosomakha, Jalkan, Kharat, 122 – Batko, 123 – Oroek, Luchistoye, Vesnovka, 124 – Agylkinskoye, 125 – Chelasinskaya, 126 – Darpirchanskaya, 127 – Shkhiperskaya, 128 – Bebekan, 129 – Med-Gora, 130 – Mechiveemskaya, 131 – Nakhodka, 132 – Kavralyanskaya, 133 – Tanyurerskaya, 134 – Mainitskaya, 135 – Valaginsko-Karaginskaya, 136 – Snezhnoye, 137 – Kvinum, Kuvalorog, 138 – Kirganik, 139 – Beregovoe; 140–149 – technogenic deposits: 140 – slag dump of the Sredneuralsky Copper Smelter (CS), 141 – Cheremshansk sludge storage of the Vysokogorsky mine, 142 – tailings storage of the Norilsk Processing Plant (PP), 143 – dumps of the Allarechensk deposit, 144 – escorial of the Karabash CS, 145 – waste dump of the Kirovgrad CS, 146 – dumps of the Solnechniy PP, 147 – tailings dump of the Krasnouralsky concentrating plant (CP), 148 – slag dump of the Loktevskiy Silver Smelter, 149 – dumps of the Tuim CP, 150 – dumps of the Mainsky CP

The copper-nickel formation is a specific mafic-ultramafic magmatic formation in which, during magma intrusion, melt differentiation and segregation occurred, producing silicate and sulfide liquids, with the sulfide melt concentrating in the lower parts of magmatic intrusions [10, 11, 12]. This process forms stratum-, plate-, and lens-shaped deposits of rich ores and horizons (reefs) of copper-nickel mineralization nodules. Melt differentiation and crystallization may occur repeatedly, but the largest deposits of predominantly rich copper-nickel ores form during a prolonged cycle in structures long platform margins (Norilsk type) and cratons (Pechenga type) [13]. Under conditions of multiple cycles of melt differentiation and segregation, beds and horizons are formed, predominantly with disseminated copper-nickel mineralization, as well as platinum-metal mineralization with associated copper-nickel ore [14]. Such copper-nickel deposits are found in platform margin structures on craton (Monchegorsk type in ultramafic rocks) and are primarily located in metallogenic orogenic zones of mobile belts within mafic complexes [13]. It should be noted that in deposits with predominantly disseminated copper ores, the nickel-to-copper ratio can increase from 0.5–1.0 to much higher values (up to 6.5 at the Shanuch deposit), reducing the economic significance of copper while increasing the concentration and economic importance of platinum group metals. Copper-nickel mineralization also appears as an associated component in deposits of the *low-sulfide platinum-metal formation*.

Interest in the copper-nickel formation was initially driven by the significance of its nickel content, with copper often a secondary or by-product. However, following the development of large Norilsk deposits of rich ores in the 1960s and 1970s, the copper-nickel formation became the leading source of national copper production, accounting for 60–65% of Russian output in the 2000s. However, due to a slight decline in copper-nickel ore production (from 500 Kt/year to 430 Kt in 2021) and the commissioning of new copper deposits from the porphyry copper and skarn copper formations, the of the copper-nickel formation's share of Russian production declined to 36.5% by 2021 (see Fig. 2, 3). Nevertheless, based on the recorded reserves and resources, the copper-nickel formation accounts for 34.4% of balance reserves and 15.8% of forecasted resources, reduced to conditional reserves [9]. Thus, this formation retains a leading position in reserves (see Fig. 3, 4).

Deposits of rich copper-nickel ores are located in the Norilsk-Kharayelakh and Kolskaya provinces, deposits of mainly disseminated copper-nickel ores are in the Voronezh, Kola, Sayan, North Baikal, and Jugjur provinces, and deposits of the low-sulfide platinum-metal formation with associated copper-nickel mineralization are found in the Karelian, Karyak, and Kamchatka provinces.

The copper-pyrite formation is a diverse group of deposits characterized by volcanogenic hydrothermal-sedimentary and hydrothermal-metasomatic origins, consisting of sulfide ores with pyrite and copper sulfides playing a dominant role [15, 16].

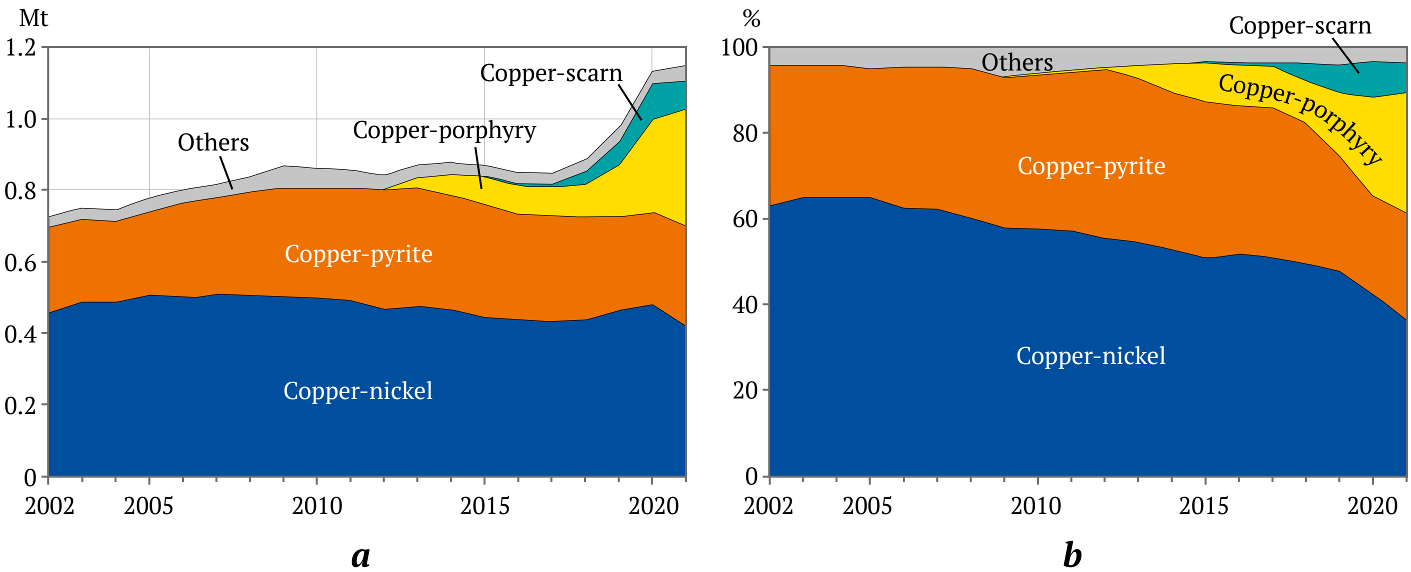

Fig. 2. Dynamics of copper production in Russia (2002–2021) by copper ore formation types:
a – production volumes, million tons; *b* – shares of total production in the Russian Federation, %
Source: Ministry of Natural Resources and Environment of the Russian Federation. URL: https://www.mnr.gov.ru/docs/gosudarstvennye_doklady/o_sostoyanii_i_ispolzovanii_mineralno_syrevykh_resursov_rossiyskoy_federatsii/

Morphologically, these deposits appear as plate- and lens-shaped formations of massive sulfide ores, often accompanied by halos of disseminated sulfide mineralization. Distinguished within this formation are the copper-pyrite deposits in basaltoid formations of eugeosynclines, the copper-zinc-pyrite deposits in rhyolite-basalt formations of eugeosynclines, and the unique Cypriot type of cobalt-bearing copper-pyrite deposits [17]. It is notable that there is both a similarity and a paragenetic relationship between the copper-pyrite and copper-nickel formations [18].

From the 19th century until the 1950s, products from copper-pyrite deposits formation led Russian copper mining, before yielding leadership to the copper-nickel formation. In the 2000s and 2020s, production from copper-pyrite deposits has ranged from 230–330 Kt/year (23–38% of Russian production), reaching 285 Kt (24.8%) in 2021 (see Fig. 2, 3). According to recorded copper reserves and resources, the copper-pyrite formation accounts for 14.5% of balance reserves and 36.3% of forecasted resources (reduced to conditional reserves) [9] (see Fig. 3, 4). This distribution indicates both the utilization of high-grade massive ores and the potential for additional reserves in the form of previously undeveloped disseminated copper-pyrite ores. Due to the depletion of many near-surface copper-pyrite ores, there has been a shift toward developing deep horizons of massive ores and utilizing disseminated ores on the flanks of established deposits.

The majority of copper-pyrite deposits are located in the Ural province, which accounts for over 90% of the ore production of this formation; deposits are also found in the North Caucasus, Karelia, Rudny Altai, Salair, and Eastern Tuva provinces.

The copper-polymetallic formation is essentially a genetic counterpart of the volcanogenic copper-pyrite formation, where the main components are zinc and lead, with copper mineralization as a secondary element [19, 20]. The volume of associated copper production at Russian polymetallic deposits is small, amounting to 12–30 Kt/year (1.1–3.5% of Russian production) and, in 2021, reaching 12.3 Kt (1.1%) (see Fig. 2, 3). According to recorded reserves and resources of copper, the copper-polymetallic formation accounts for 0.9% of balance reserves and 8.3% of forecasted resources, reduced to conditional reserves [9] (see Fig. 3, 4). This imbalance between reserves and resources arises from a critical view of copper as an associated component, which often complicates the enrichment process and may not always be efficient or cost-effective. Consequently, at the geological assessment stage, associated components are accounted for as fully as possible; however, during the exploration and planning of a mining enterprise, these components are often transferred

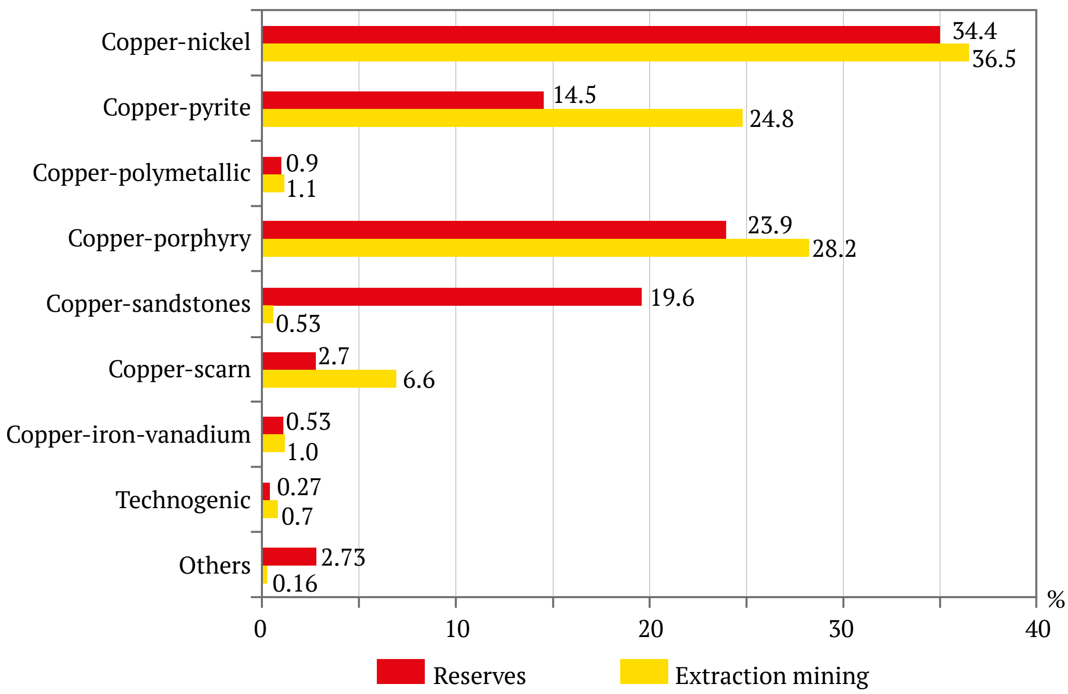

Fig. 3. Shares of copper reserves and production (2021) by copper ore formation types as a percentage of total indicators for the Russian Federation, %

Source: State Reports of the Ministry of Natural Resources (https://www.mnr.gov.ru/docs/gosudarstvennye_doklady/o_sostoyanii_i_ispolzovanii_mineralno_syrevykh_resursov_rossiyskoy_federatsii/), Information on the state and prospects of mineral resource base in the regions of the Russian Federation (http://atlaspacket.vsegei.ru/?v=msb2021#91474d2e700eb6c90) and Y.V. Alekseev [9]

to off-balance reserves. Copper-polymetallic deposits dominate in the Salair and Rudno-Altai provinces and are also present in the North Caucasus, Karelia, Eastern Tuva, and Okhotsk-Chukotka provinces.

The porphyry copper formation is the undisputed global leader in copper and molybdenum production, as well as in their reserves and forecast resources. Porphyry-type deposits are large-volume bodies of veined- disseminated sulfide copper-molybdenum formations associated with intrusive bodies, often displaying a porphyry texture (the origin of the formation's name) which acts as a substrate for mineralization [21, 22]. Interest in these relatively low-grade, but resource-abundant deposits grew with advancements in enrichment technologies – initially gravity-based, followed by highly effective flotation enrichment of sulfides. As a result, porphyry deposits of copper and molybdenum have become the primary source for the extraction of these metals [23]. In addition to copper and molybdenum, significant volumes of associated components, including Au, Ag, and Re, are extracted from mined ores in deposits of this type. The porphyry copper formation is often interpreted as the Mo–Cu–Au formation [24]. Within the porphyry formation, several ore-forming types are identified: gold-copper-porphyry in basaltoid volcanogenic-plutonic belts (island-arc and riftogenic) and molybdenum-copper-porphyry in andesite volcanogenic-plutonic belts, formed through activation on a substrate of various composition and age [25, 26].

In the Soviet-era joint economy, Russia did not developed its porphyry copper deposits due to sufficient production from the Kounrad (Kazakhstan) and Almalyk (Uzbekistan) GOKs. Nonetheless, porphyry deposits were known in Russia and, where possible, exploited, with ongoing exploration, evaluation, and development of new porphyry copper deposits. According to the recorded reserves and resources, the porphyry copper formation accounts for 23.9% of balance reserves and 32.3% of forecasted resources, reduced to conditional reserves [9] (see Fig. 3, 4). Since 2013, the exploitation of porphyry copper deposits in the Ural province has begun, and by 2021 production from these deposits reached 323 Kt (28.2% of Russian production) (see Fig. 2, 3). A cross-border porphyry copper deposit in the Chelyabinsk Region (bordering Kazakhstan), as well as deposits in the Eastern Tuva and Primorsky provinces, are being prepared for operation. Geological exploration is underway in East Trans-Baikal and northern Okhotsk-Chukotka provinces. Additionally, many areas and within these and other provinces – Kola, Central Arctic, Umlekan-Ogoja, and Kamchatka– show promise for further prospecting and evaluation.

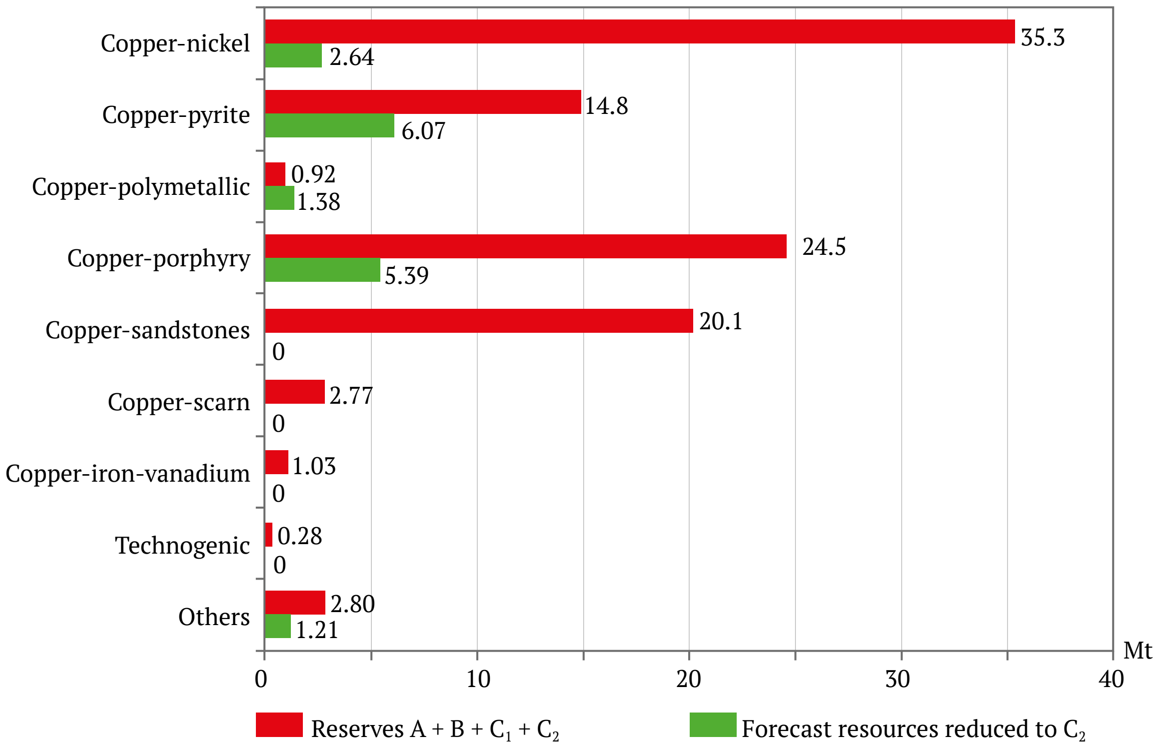

Fig. 4. Volumes of balance reserves and forecast resources of copper by ore formation types as of 2021, million tons

Source: State Reports of the Ministry of Natural Resources (https://www.mnr.gov.ru/docs/gosudarstvennye_doklady/o_sostoyanii_i_ispolzovanii_mineralno_syrevykh_resursov_rossiyskoy_federatsii/), Information on the state and prospects of mineral resource base in the regions of the Russian Federation (http://atlaspacket.vsegei.ru/?v=msb2021#91474d2e700eb6c90) and Y.V. Alekseev [9]

The copper sandstone formation includes stratiform deposits in sedimentary rocks with copper sulfide formations occurring on geochemical barriers with sources of exhaled copper in seawater or released through leaching of copper-bearing rocks by infiltrated reservoir waters [27, 28, 29, 30]. In terms of production volumes and reserves, the copper sandstone formation ranks second globally after the porphyry copper formation.

In Russia, small copper sandstone deposits were mined in the Pre-Ural province until the mid-19th century. During the USSRs collaborative economy, with the large Dzhezkazgan copper sandstone deposit in Kazakhstan already in operation, exploration in Russia focusede only prospecting and exploration of deposits within this formation. The ultra-large Udokan copper sandstone deposit in the Kadaro-Udokan province, discovered in 1949, was initially located far from well-developed infrastructure in mountainous tundra (before the construction of the Baikal-Amur Mainline). The deposit was not put into operation until 2023, and geological exploration is ongoing in nearby prospective areas. Copper production at the Udokan deposit reached 6.1 Kt in 2021 (0.5% of Russian production), with plans to increase output to 65 Kt (6–7%) by 2027 and, in the future, up to 175 Kt/year (up to 15–17%). According to copper inventory, the copper sandstone formation represents 19.6% of balance reserves, but no officially approved forecast resources are listed for this formation [9]. In addition to the aforementioned provinces, deposits and indications of copper sandstones are also known in the Donetsk, Igarka, Shoria-Khakass, and Bilyakchan-Kolyma provinces.

The copper-skarn formation consists of metasomatic (skarn) deposits at the contact between intrusive rocks (ranging from basic to acidic in composition) with calcareous sedimentary rocks, where newly formed skarns serve as the substrate for overlapping copper mineralization [31, 32]. Copper skarn deposits are typically high in grade but limited in reserves (primarily in the Ural and Shoria-Khakass provinces), and nearly all have been exhausted. Some skarn deposits with associated copper mineralization are still being mined, but their contribution to copper production remains minor (1–2 Kt/year). The copper-iron skarn type has the highest potential, with vein-disseminated cooper mineralization superimposed on on the substrate of iron ore bodies [33]. Exploitation of copper-iron skarn deposits in the East Trans-Baikal province began in 2013, with annual production at these deposits rising from 3 to 94 Kt by 2020, accounting for 8.3% of Russian output (see Fig. 2, 3). New copper-skarn deposits are being prepared for exploitation in the Ural and East Trans-Baikal provinces, while exploration is underway, and new areas are being explored in the Ural, Kadaro-Udokan, and Okhotsk-Chukotka provinces, as well as in regions the established provinces. Based on recorded copper reserves, the copper-skarn formation accounts for 2.7% of balance reserves, though no approved forecast resources are available for this formation [9] (see Fig. 3, 4).

The copper-iron-vanadium magmatic formation in Russia is represented by the unique Volkovsky deposit, which contains complex apatite- and vanadium-bearing titanomagnetite and copper sulfide ores, along with associated gold-palladium mineralization formed during the differentiation and crystallization of the Volkovsky gabbroid massif. This process resulted in lenses of dessiminated sulfide and titanomagnetite mineralization [34]. Copper production at the Volkovskoye deposit ranges from 4–12 Kt/year (0.5–1.1% of Russian production), reaching 12.6 Kt (1.1%) in 2021 (see Fig. 2, 3). Cu–Fe–V magmatic formations are relatively rare, but the Veksha deposit and the Pudozhgorskoye manifestation in the Karelian province, the Kolvitskiy deposit on the Kola Peninsula, and the Pogorelovskoye manifestation in the Chelyabinsk region are similar to the Volkov-type of iron-copper ores. The Cu–Fe–V formation reserves in Russia are small, totaling 1.03 million tons (0.53% of Russian reserves) (see Fig. 3, 4), and there are no forecasted resources of this formation.

The formation of native copper is of interest due the historical significance of the Lake Superior deposit in the USA, a unique, large, and high-grade native copper deposit in amygdaloidal diabases of blanket effusions, which was mined out in the 19th century, producing over 4.5 million tons of copper [35]. The discovery of such high-grade copper deposits has been a goal in many countries, including Russia, though with limited success [36]. Nevertheless, deposits and occurrences of native copper in volcanogenic settings are known in Russia, located of the Ural, Shoria-Khakass, Norilsk-Kharayelakh, and Bilyakchan-Kolyma provinces, with some sizeable deposits such as Taymetskoye (Gornaya Shoria, Kemerovo region) and Arylakhskoye (North of the Krasnoyarsk Territory).

Ore formations with associated copper mineralization include several different types of ore formations, where copper is only a secondary associated component.

The most economically significant among them is *the formation of low-sulfide platinum-metal ores with associated copper-nickel mineralization* in the form of disseminated mineralization within mafic and ultramafic magmatic rocks in orogenic zones, ranging from Archean to Neogene age [13, 37, 38, 39]. Deposits and occurrences of this type are mainly targeted for platinum exploration and are found in the Voronezh, Karelian, Kola, Norilsk-Kharayelakh, Sayan, North Baikal, Jugjur, Okhotsk-Chukotka, Koryak, and Kamchatka provinces. Currently, the balance reserves and forecast resources of the low-sulfide deposits are included within traditional copper-nickel formations.

The quartz-sulfide formation with associated copper mineralization includes genetically diverse ore formations of non-ferrous (tin, tungsten) and precious metals (gold, silver). Copper concentrate is extracted as a by-product at tin [40] and tungsten [41] deposits in the Primorsky Province, as well as at numerous gold deposits [41] outside the known copper provinces.

Copper mineralization may also occur within carbonatite formations, such as the Palabora copper-zirconium-phosphate carbonatite deposit currently under development in South Africa [42]. In Russia, occurrences of carbonatite formations with disseminated copper-sulfide mineralization are known on the Taimyr Peninsula and in the carbonatite massifs of the Maymech-Kotui province.

The technogenic formation results from anthropogenic impact on the subsurface, creating new deposits of technogenic raw materials (e.g., dumps of overburden and substandard ores, tailings and intermediate products storage from processing plants, slag heaps, residues from metallurgical ore conversion, and mineralized mine waters) [43, 44]. Copper extraction from slag is underway at the dumps of the Sredneuralsky copper smelter {No. 140} and the sludge storage at the Cheremshansky facility of the Vysokogorsky mine {No. 141} in Sverdlovsk region (up to 16 Kt/year), as well as from the tailings of the Norilsk processing plant (PP) {No. 142} (up to 1.5 Kt/year)[8], (for the numbering of sites, see Fig. 1). Sabstandard ore dumps of the Allarechensk deposit {No. 143} in Murmansk region [45], slag heaps at the Karabash Copper smelter (CS) {No. 144} in Chelyabinsk region, and residues at the Kirovgrad CS {No. 145} in Sverdlovsk Region [43], and dumps at the Solnechniy PP {No. 146} in Khabarovsk Territory are being prepared for operation[9]. The potential for dump mining is also being evaluated for the Krasnouralsky concentrating plant (CP) {No. 147} in Sverdlovsk region, the dumps of the Loktevskiy Silver Smelting Plant {No. 148} in Altai Territory, as well as dumps of the Tuim CP {No. 149} and Mainsky CP {No. 150} in Khakassia. Estimated copper reserves in technogenic deposits in Russia total 270 Kt, with an annual production of 8–16 Kt/year (0.7–1.9% of Russian production), reaching 8.5 Kt (0.7%) in 2021 (see Fig. 3, 4). Resources of technogenic deposits are undervalued due to limited exploration at tailings dumps of processing plants (only 4 out of 36 operating and closed PP) and limited surveys at individual substandard ore dumps in developed and mothballed deposits [46].

[8] Ministry of Natural Resources and Environment of the Russian Federation. URL: https://www.mnr.gov.ru/docs/gosudarstvennye_doklady/o_sostoyanii_i_ispolzovanii_mineralno_syrevykh_resursov_rossiyskoy_federatsii/

[9] I bid.

Copper provinces

The North Caucasian province includes volcanogenic-sedimentary structures of the Peredovoy Ridge and Privodorazdelnaya Area along the border of the Scythian Platform and folded rock of the Great Caucasus. Numerous *copper-pyrite deposits* found here. Since the 1950s, the Urupskoye deposit {No. 12} [47] has been mined, though now significantly depleted, with production in 2021 reached 5.4 Kt. The Khudesskoye, Skalistoye, and Pervomaiskoye deposits {No. 44} are being prepared for exploitation, with over 100 ore occurrences recorded. The Kizil-Dere deposit {No. 40}, with copper reserves of 1.17 Mt of 100% at an average grade of 2.14% Cu, has been explored and is held in reserve [48]. Altogether, the North Caucasus province accounts for 2.23 million tons of balance copper reserves (2.17% of Russian reserves), with an annual production of 5.4 Kt (0.47% of Russian production) in 2021 (see Fig. 5, 6).

The Donetsk province contains copper sandstone deposits of the Kartamyshinsky formation from the Lower Permian within the Dnieper-Donetsk trough on the East European platform. Copper mining in this area dates back to the Bronze Age (e.g., Kartamyshskoye, Vyskrivka, Pilipchatino) and continued into the 19th century [49]. promising areas for the discovery of significant copper sandstone deposits include the Bakhmutskaya ({No. 71}, with 28 occurrences) and Kalmius-Toretskaya (with 3 occurrences) [50]. In the 1960s, the «Artemgeologia» searched for mineralized zones in the Kartamyshinsky syncline, identificating copper-rich layers (e.g., Berestyanskoye, Sour Hill), along with indications of copper, lead, and zinc mineralization (e.g., Serebryanskoye, Sukhodolskoye, Odnobokovskoye) [51]. The Donetsk province represents only a portion of copper sandstone distribution along the periphery of the Ukrainian shield, extending to the Pridobrudzhsky trough in the west [52].

The Voronezh province includes the well-known Voronezh Crystalline Massif (VCM), where deposits and occurrences of *sulfide platinum-copper-nickel ores of the Elan type* (e.g., Elan and Elkinskoye deposits, as well as over 20 ore occurrences) are found. These are genetically related to norites of the subvolcanic orthopyroxenite-norite-diorite formation, and the *Mamon type* (e.g., Nizhnemamonskoye, Podkolodnovskoye deposits, Jubilee, with numerous occurrences in the Nizhnemamonsky and Anninsky ore districts), associated with ultramafic dunite-peridotite-pyroxenite-gabbronorite formations [53]. The Elan and Elkinskoye PGE-copper-nickel deposits {No. 45} are the most prepared for exploitation, with copper reserves of 58.8 and 17.3 Kt, respectively. However, despite favorable conditions, a significant obstacle to their development is the potential alienation of fertile lands and the proximity of protected areas. Balance copper reserves in the Voronezh Province are recorded at 0.08 Mt (0.08% of Russian reserves) (see Fig. 5, 6).

The Karelian province is situated in the eastern part of the Fennoscandian Shield. Copper mining in this region dates back to the 18th century, when small copper-pyrite deposits were mined (Voitskoe, Voronovoborskoe, Pyalozerskoe mines, etc.), with further development continuing into the 19th century. Geological studies, have since identified deposits of various ore formations. Known deposits *of the copper-pyrite ore formation include those* in the Central Karelian (Vedlozerskoe, Hautavaarskoye, Chalkinskoye, etc.), Sumozersko-Vygozerskaya (Parandovskoye), and West Karelian (Yalonvaarskoye) mineragenic zones. The province also hosts *copper-nickel sulfide ultramafic-mafic formation*, including the Vostochno-Vozhminskoye deposit (associated with theVozhminskoye ultrabasite massif) and the Lebyazhin deposit (within the Kumbuksin ultramafic massif), as well as komatiite formations (Zolotoporozhskoye, Leshchevskoye, Rybozerskoye occurrences in the basalt and komatiite sequences of the Sumozero-Kenozero greenstone belt). Additionally, deposits of *the copper-molybdenum-porphyry formation* (Lobash, Pyayavaara, Yalonvara), *the low-sulfide platinum-metal-titanium-vanadium formation* in the Koikar-Svyatnavolok mineragenic zone (Viksha deposit in the Koikar gabbro-dolerite sill), and the copper sandstone formation (the mined-out Voronov Bor deposit and other occurrences) are present [54]. Exploration work has been conducted at the Viksha {No. 65} [55] and Lobash-1 {No. 66} [56] deposits, with cooper reserves of 125 and 56.4 Kt, respectively. Additionally, over 50 copper-nickel occurrences were recorded in the southeastern part of

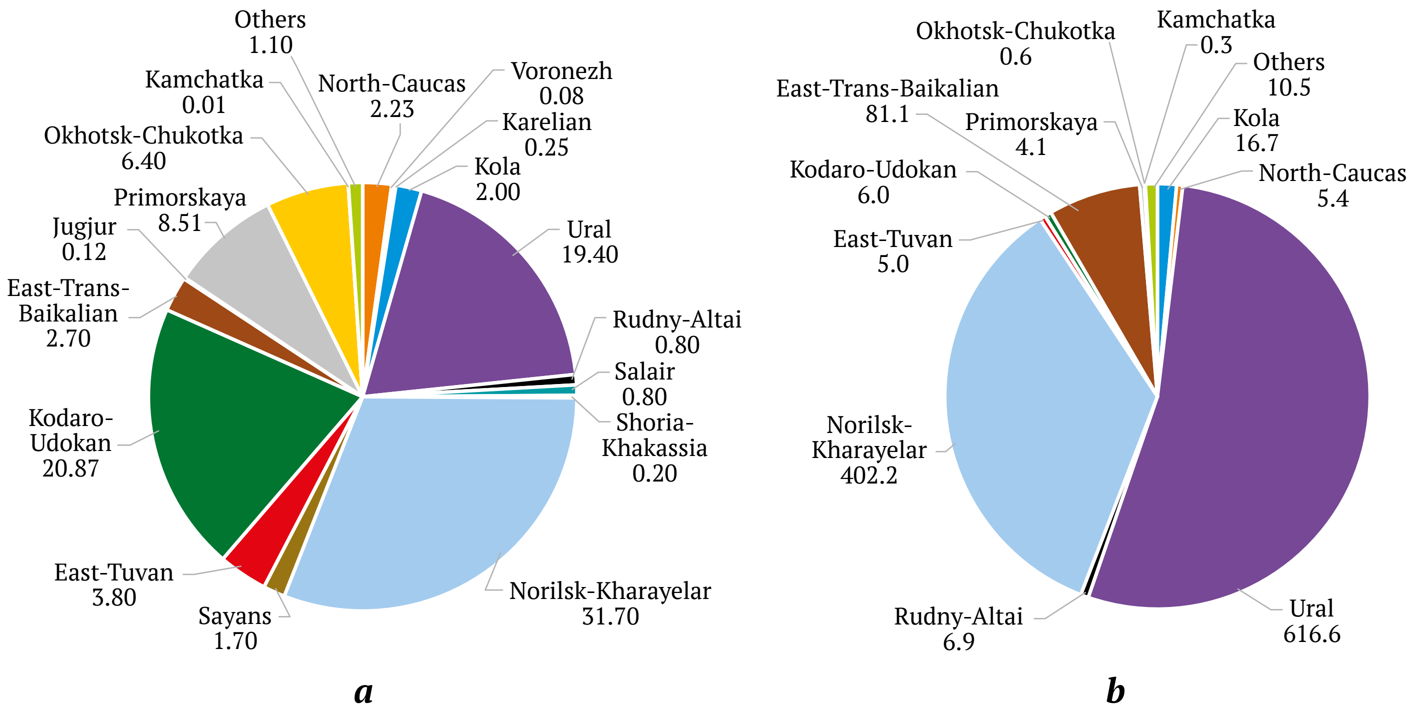

Fig. 5. Cooper reserves, million tons – *a*, and annual production, Kt – *b* by province as of 2021

Source: State Reports of the Ministry of Natural Resources (https://www.mnr.gov.ru/docs/gosudarstvennye_doklady/o_sostoyanii_i_ispolzovanii_mineralno_syrevykh_resursov_rossiyskoy_federatsii/), Information on the state and prospects of mineral resource base in the regions of the Russian Federation (http://atlaspacket.vsegei.ru/?v=msb2021#91474d2e700eb6c90) and Y.V. Alekseev [9]

the province, specifically in the Astrakhan region. However, prospecting efforts have primarily focused on two massifs within the Kamennoozersky kamatiite complex, associated with the Voloshovskoye copper-nickel deposit {No. 72}, where drilling evealed disseminated sulfide mineralization was uncovered, resources of 277 Kt of copper were calculated with an average content of 0.15% Cu [57]. 0.25 Mt of balance reserves of copper (0.24% of Russian reserves) were calculated for the Karelian province, see Fig. 5, 6.

The Kola province is situated in the northern part of the Fennoscandian Shield. Within the riftogenic Pechenga-Imandra-Varzug greenstone belt, numerous Paleoproterozoic stratified intrusions are present, including several ore-bearing (PGE–Cu–Ni) intrusions that are part of the Pechenga, Monchegorsk, and Fedorovo-Panskiy ore districts. These areas contain deposits of *copper-nickel sulfide ore formations* and *low-sulfide platinum-metal ores with associated copper-nickel mineralization* [58].

In *the Pechenga ore district*, two main ore nodes are recognized, featuring deposits of the stratified sulfide copper-nickel formation of mafic and ultramafic rocks [59]: the Western Node (Kotselvaara-Kammikivi and Semiletka deposits) and the Eastern Node (Zhdanovskoye, Zapolyarnoye, Bystrinskoye [Cu–Ni],

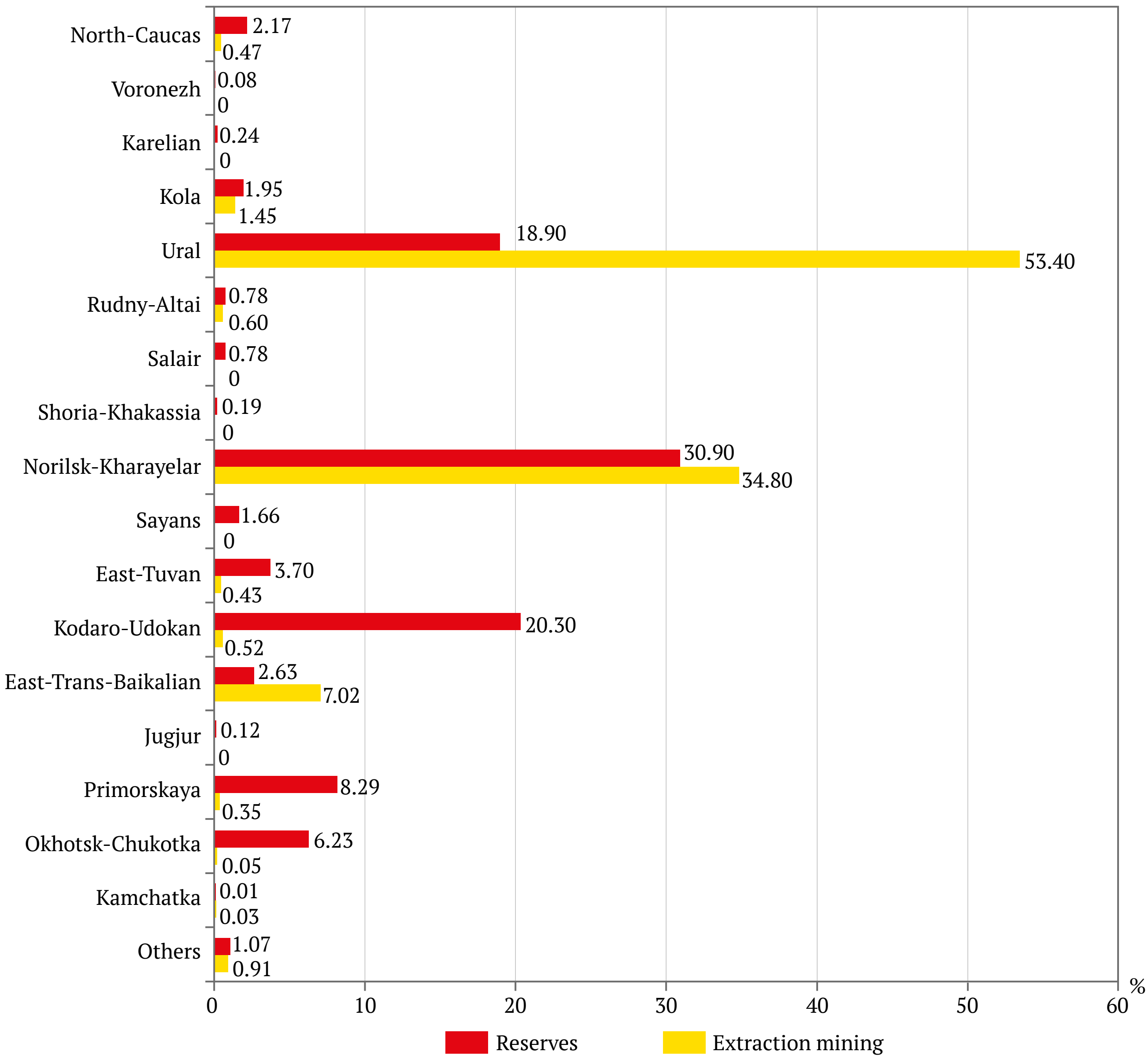

Fig. 6. Share of copper reserves and production by provinces (as of 2021) from total figures for the Russian Federation. No reserves and production recorded in Donetsk, Pre-Ural, Central Arctic, and Bilyakchan-Kolyma provinces

Source: State Reports of the Ministry of Natural Resources (https://www.mnr.gov.ru/docs/gosudarstvennye_doklady/o_sostoyanii_i_ispolzovanii_mineralno_syrevykh_resursov_rossiyskoy_federatsii/), Information on the state and prospects of mineral resource base in the regions of the Russian Federation (http://atlaspacket.vsegei.ru/?v=msb2021#91474d2e700eb6c90)

Tundra, Sputnik, and Verkhnoye). Mining of the Western Node deposits began in the 1930s, with the Eastern Node following in the 1960s. Nowdays, richest copper-nickel ores reserves at Kotselvaara-Kammikivi, Semiletka, Tundra, and Zapolyarnoye have been depleted and preserved. Currently, the Zhdanovskoye deposit, containing disseminated copper-nickel ores with reserves of 840.5 Kt at an average grade of 0.31% Cu, is under active development, while the Bystrinskoye, Sputnik, and Verkhneye deposits are being prepared for exploitation.

The Monchegorsk ore district, with deposits and occurrences known since the 1930s, contains both sulfide cooper-nickel ores and low-sulfide platinum-metal ores (PGM) with minor copper-nickel mineralization [60]. Major sulfide copper-nickel deposits here include Poaz (443 Kt, average grade of 0.13% Cu), Nyud (188 Kt, 0.24% Cu) {No. 75}, Nittis-Kumuzhya-Travyanaya (229 Kt, 0.16% Cu), Sopcha (ore horizon 330) (109 Kt, 0.23% Cu) {No. 76}, Arvarench (246 Kt, 0.26% Cu), and Moroshkovoye-Ozero (172 Kt, 0.20% Cu) {No. 77}. Notable low-sulfide platinum-metal deposits with minor copper-nickel mineralization include Loypishnyun [61], Yuzhnaya Sopcha, and Wuruchuaiwench, each containing 30–50 Kt of copper resources.

The Fedorovo-Panskiy ore district {No. 78} is primarily known for low-sulfide platinum-metal ores with minor copper-nickel mineralization. Deposits in this district, such as Fedorovotundra and Kievey [62] and Eastern Chuavry [63], were initially evaluated for platinum group metals, with copper and nickel as secondary components. These deposits represent reef horizons in stratified mafic rocks.

Among other copper ore formations in the Kola province, the Pellapakhk deposit {No. 74} contains *copper-molybdenum-porphyry ores* of 203 Kt at 0.15% Cu and has been deemed economically viable [64]. Additionally, the Kolvitskoye deposit {No. 73} represents the *copper-iron-vanadium magmatic formation* [65].

Altogether, the Kola province holds 2.0 million tons of copper reserves (1.95% of Russia's reserves), with an annual production in 2021 of 16.7 Kt (1.48% of Russian production) (see Fig. 5, 6).

The Pre-Ural province lies within the Pre-Ural foreland basin of the East European Platform, where numerous deposits and occurrences of *copper sandstones formations are present within* the Upper Permian strata of the Ufa, Kazan, and Tatar Stages [66]. These formations have been mined since the Bronze Age until the mid-19th century. Archaeological data indicate that over 500 sites with copper sandstone deposits were under development in this region [67]. Due to their small size and limited reserves, these copper sandstone occurrences are not attractive for traditional open-pit mining methods but hold significant potential for geotechnological methods of underground copper leaching [68].

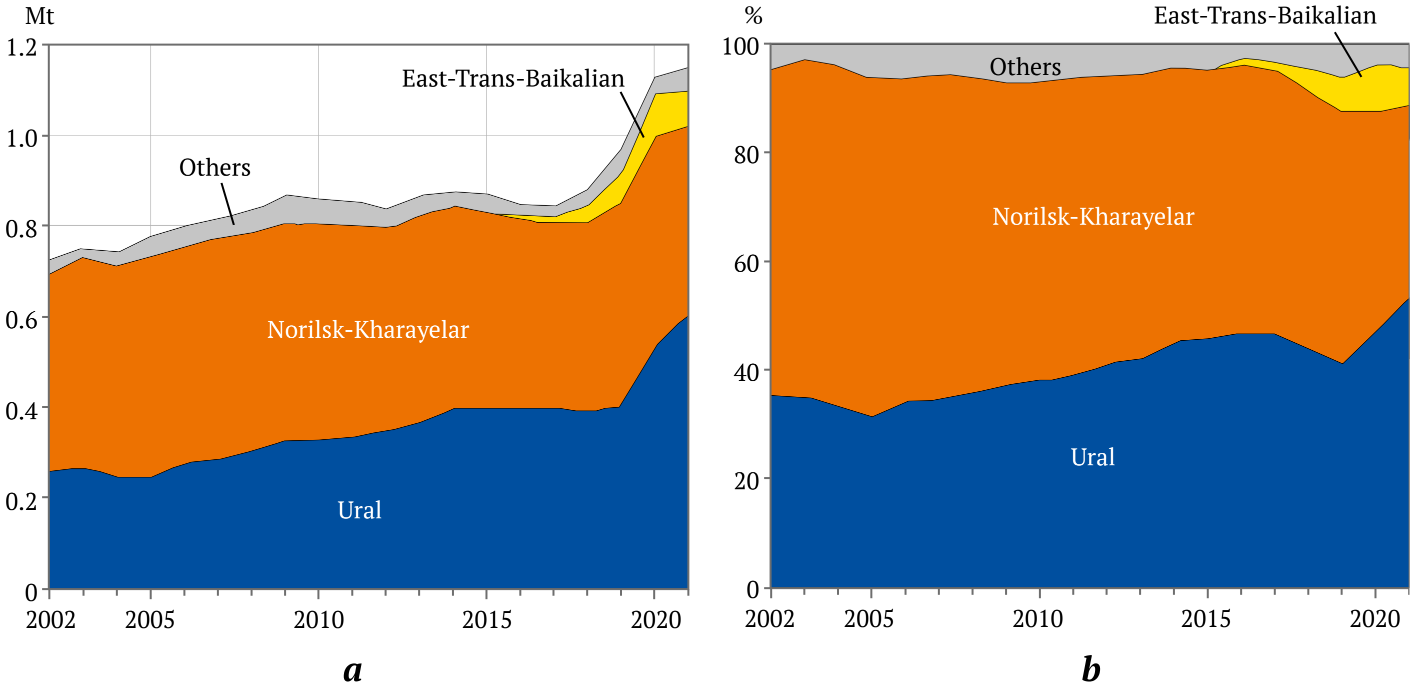

Fig. 7. Dynamics of copper production in Russia (2002-2021) by ore provinces: *a* – production volumes, million tons; *b* – percentage shares of total production in the Russian Federation, %

Source: Ministry of Natural Resources and Environment of the Russian Federation. URL: https://www.mnr.gov.ru/docs/gosudarstvennye_doklady/o_sostoyanii_i_ispolzovanii_mineralno_syrevykh_resursov_rossiyskoy_federatsii/

The Ural province is located within the Ural Orogenic System and contains hundreds of deposits and occurrences of copper-pyrite, copper-porphyry, copper-skarn, vanadium-bearing copper-iron magmatic formations, as well as formations of copper sandstone and native copper [69]. The Ural province holds 19.4 million tons of prepared copper reserves (18.9% of Russian reserves), with 707 Kt of copper extracted, or 52.5% of national production (see Fig. 5, 6). There is a trend toward toward increasing production over time, raising the Ural province's share in Russia's cooper output (see Fig. 7). In addition, Ural plants process up to 490 Kt/year of copper concentrate imported from Kazakhstan[10].

Copper-skarn deposits were among the earliest targets of development Ural mining region, including those of the Turyinsky group, which are now depleted [70], as well as the Gumeshevskoye [71] and Mednorudnyanskoye deposits [72] {No. 7}. These deposits, though small in size and reserves, were highly attractive due to rich ore and the secondary enrichment zones developed along them. Currently, new copper-skarn deposits are being prepared for development, including the Severnoye-3 deposit {No. 55}. The Novogodnee-Monto gold-iron skarn deposit {No. 84} in the Polar Urals is also being evaluated for its copper mineralization [73]. At the Gumeshevskiy copper-skarn deposit {No. 39}, redeposited oxidized copper ores in loose karst sediments, known as "copper clays", have been identified as a separate industrial type [74]. Since 2004, these ores have been extracted via underground copper leaching, with annual production of 1.0–3.5 Kt/year [75] and with estimated resources of 455 Kt [9].

Copper-pyrite deposits are widespread in the Paleozoic paleovolcanic belts (Shchuchinsko-Tagilskiy, Sakmarskiy or Krakinsko-Mednogorskiy, West and East Magnitogorsk, Kamenskiy, Kateninskiy, Oktyabrsko-Denisovskiy, and Irgizskiy) and zones (Bolshakovsko-Reftinskaya, Birgildinsko-Polyanovskaya, Kolpakovskaya, Elenovsko-Kumakskaya, Buryktalsko-Kundybaevskaya) of the Southern and Middle Urals [69]. Copper-pyrite deposits have been a traditional cooper source for mining enterprises in these regions for many decades [76]. Many deposits are now decommissioned or mothballed, including Dergamyshskoye {No. 3}, Sibayskoye {No. 4}, Uchalinskoye {No. 5}, Aleksandrinskoye {No. 6}, and Tarnyerskoye {No. 8}. Active development continues at the Gayskoye deposit {No. 14} I4.37 Mt of reserves at 1.32% Cu, producting 93 Kt of Cu in 2021) [77], as well as Osennee {No. 15}, Vesenne-Aralchinskoye, Dzhusinskoye {No. 16}, Novo-Sibayskoye, and Yubileynoye {No. 17} (1.24 Mt at 1.65% Cu, 22 Kt in 2021) [78]. Other active deposits include Kamaganskoye, Ozernoye, and Zapadno-Ozernoye {No. 19} (373 Kt, producing 11 Kt in 2021) [79], Talganskoye, Uzelginskoye, Molodezhnoye, Chebachye, and Novo-Shemurskoye[11]. The Podolskoye and Severo-Podolskoye copper-pyrite deposits are being prepared for development {No. 47}, along with Vishnevskoye {No. 48}, Novo-Uchalinskoye {No. 49} (1.09 Mt at 0.98% Cu) [80], Sultanovskoye {No. 50} (67 Kt at 3.25% Cu), Maukskoye {No. 51} (47 Kt at 1.58% Cu), Tarutinskoye {No. 52} (64 Kt at 1.33% Cu), Saumskoye {No. 53} (21 Kt at 2.78% Cu), and Severo-Kaluginskoye[12]. The Komsomolskoye copper-pyrite deposit {No. 41}, with reserves of 504 Kt at 1.78% Cu), is held in the Reserve Fund. Prospecting for copper-pyrite deposits is ongoing in the promising Blyavinskaya {No. 80}, Membetovskaya-Karagayskaya (520 Kt of resources), and Novopetrovskaya {No. 81} areas of the Southern and Middle Urals[13], as well as in the Circumpolar Urals (Volinskiy and Grubeinsko-Tykotlovskiy ore districts) {No. 82} [81].

The second most significant *formation* in the Ural province is *the porphyry copper formation*, represented by deposits within the North Sosvinskiy, Volinskiy, and Grubeinsko-Tykotlovskiy volcanic belts of the Southern Urals, prinarily in its eastern part [82]. Key copper-porphyry deposits include Tominskoye {No. 22} with reserves of 3.85 Mt at an average grade of 0.34% Cu, producting 212 Kt of Cu in 2021, and Mikheevskoye {No. 23} with reserves of 1.8 Mt at 0.37% Cu, producing103 Kt in 2021) copper-porphyry deposits [83]. Appraisal work is ongoing at the Birgildinsky, Zapadny, and Tarutinsky sites near the Tominskiy deposit. Copper-porphyry occurrences within the North Irendyk, Verkhneuralskaya, Dombarovsko-Aschebutakskaya [84], and Alapaevsko-Sukholozhskaya [85] metallogenic zones of the Middle Urals also require further assessment.

The unique Volkovsky deposit {No. 26}, an igneous *copper-iron ore formation containing* vanadium [86], is also located in the Ural province, with reserves of 805 Kt at an average grade of 0.63% Cu, producting 13 Kt of Cu in 2021. Many occurrences of the igneous copper-iron ore vanadium formation exhibit transitional characteristics toward copper-skarn formations of similar composition.

[10] Ministry of Natural Resources and Environment of the Russian Federation. URL: https://www.mnr.gov.ru/docs/gosudarstvennye_doklady/o_sostoyanii_i_ispolzovanii_mineralno_syrevykh_resursov_rossiyskoy_federatsii/

[11] I bid.

[12] I bid.

[13] I bid.

In the Circumpolar region of the Ural province, within the Lyapinskiy mineragenic zone, there are *occurrences of copper sandstone formations*, including stratiform hydrosluidic copper sandstones (Musyurskoye, Kosyunskoye, and Tesninoye) and polymetallic sandstones (Kozhimskoye) [87].

In the Northern Urals, occurrences of *native copper formation* are known in the Khultymya mineralized zone, associated with amygdaloidal olivine basalts and their ash tuffs in the Tournaisian Stage volcanics of the Lower Carbonierous [88].

The Rudny Altai province within the Russian Federation is part of a larger polymetallic province of the same name, with the main and most significant deposits located in Kazakhstan (Kolba-Narym metallogenic region). However, numerous deposits and occurrences of the *polymetallic pyrite formation*, including copper components, are found within the Russian part of the Rudny Altai province. Like the Ural province, Rudny Altai is an orogenic structure formed by arc magmatism, characterized by basaltoid formatons in the Urals and rhyolite formations in the Altai, resulting in distinct metallogenic specialization – copper-zinc in the Urals and copper-polymetallic in the Altai [20].

Polymetallic deposits in the Zmeinogorsk ore district have been exploited since the Bronze Age, with industrial development starting at the Zmeinogorskiy deposit in the 18th century. While the Zmeinogorskoye deposit is now depleted, the Karabalikhinskoye pyrite-polymetallic deposit {No. 27}, with cooper reserves of 316 Kt at an average grade of of 1.5% Cu, remains active, producting 6.3 Kt in 2021. Other polymetallic deposits with associated copper mineralization, such as Zarechenskoye (Cu 3.1 Kt, 0.17% Cu) {No. 27} and Stepnoye {No. 28} (25 Kt, 1.18% Cu), are also in operation. The Talovskoye copper-polymetallic deposit {No. 56} is being prepared for exploitation, while exploration continues in the Ural province at the promising Novonikolskaya (resources of 91 Kt) {No. 85} and Kholodnaya (resources of 82 Kt) {No. 86} sites with potential to expand search areas within the Altai Republic. The Rudny Altai province has 0.8 million tons of balance copper reserves (0.78% of Russian reserves), with annual production in 2021 totaling 6.9 Kt (0.6% of Russian production) (see Fig. 5, 6).

The Salair province corresponds to the Salair mineragenic zone, an orogenic arc structure with basalt-andesite-rhyolite magmatism from the Salair phase of folding, featuring numerous pyrite-polymetallic deposits [89]. This historical mining area has been exploited since the early 19th century, though active mining has since ceased. The Kamenushinskiy copper-polymetallic deposit is preserved, and the province still contains various *copper-pyrite polymetallic occurrences* (Uskandinskoye, Prichumyshskaya group), including those overlain by the sedimentory cover of the West Siberian Plate. Copper reserves in the Salair province amount to 0.8 million tons (0.78% of Russian reserves)[14] (see Figs. 5, 6).

The Shoria-Khakass province is located in the southern part of the Kuznetsk Alatau orogenic within the Mrassko-Batenev anticlinorium structural-formational zone. This area features thick deposits of Riphean-Cambrian-Ordovician age enriched with volcanic rocks of the basalt-andesite-trachyte-liparite group, formed during Early Paleozoic diorite and plagiogranite magmatism of the Salair or Early Caledonian tectogenesis cycle [90]. Deposits and occurrences of copper-skarn, copper-porphyry formations, and formations of native copper and copper sandstones are present here. *Copper-molybdenum-skarn* deposits are associated with Early Paleozoic granitoids, the largest of which – Kiyalykh-Uzen, Glafirinskoye [91], and Julia [92] {No. 11} – have now been mined out. The Malo-Labyshskoye deposit {No. 91} belongs to the *copper-molybdenum-porphyry formation*, with cooper resources 264 Kt at 0.12% Cu [93]. Mauntain Shoria is home Russia's largest *native copper deposit*, Taymetskoye {No. 90}, with copper resources totaling 1.57 million tons at an average grade of 0.76% Cu [94]. In Khakassia, occurrences of *copper sandstone formations*, such as Bazinskoye and Kharajulskoye, are also recorded. The Shoria-Khakass province contains 0.2 million tons of cooper reserves[15].

The Central Arctic province encompasses the relatively unexplored areas of the Taimyr Peninsula and the Severnaya Zemlya islands. This province was identified through geological surveys, which recorded occurrences and deposits of the *copper-porphyry formation* within the Central Arctic gold-bearing Late Paleozoic-Early Mesozoic copper-molybdenum-porphyry belt [95]. Numerous copper-molybdenum occurrences have been documented here, with the most promising being Uboininskoye {No. 92}, Verkhnetareyskoye {No. 93}, and Porphyrovoye {No. 94}, with the province's potential copper resources estimated at 2.5 million tons [95].

[14] Ministry of Natural Resources and Environment of the Russian Federation. URL: https://www.mnr.gov.ru/docs/gosudarstvennye_doklady/o_sostoyanii_i_ispolzovanii_mineralno_syrevykh_resursov_rossiyskoy_federatsii/

[15] I bid.

The Norilsk-Kharaelakh province, located in the far northwest of the Dorifeian Siberian Platform near the pericratonal Yenisei-Khatanga Trough [96], host unique copper-nickel deposits with substantial reserves and high quality. The province also contains copper-porphyry and native copper deposits. This area holds 30.9% of Russia's copper reserves (31.7 million tons) and accounts for 34.8% of Russian copper production (402 Kt), (see Fig. 5, 6). However, due to increasing production in the Ural and East Trans-Baikal province, the share of copper production in the Norilsk-Kharayelakh province within Russia's overall production balance is gradually decreasing (see Fig. 7).

The unique Norilsk *copper-nickel* deposits are products of Mesozoic trappean activity in the pericratonic cover of the Siberian Platform [13]. Key deposits include Oktyabrskoye {No. 30}, with reserves of 18.34 Mt of Cu at an average grade of 1.61% Cu, producting 273 Kt in 2021; Talnakhskoye {No. 31}, with reserves of 9.90 Mt at 1.09% Cu, producing 121 Kt in 2021); and Norilsk-1 {No. 32} with reserves of 2.57 Mt at 0.47% Cu, producing 9 Kt in 2021. Additional deposits, Maslovskoye {No. 57} with reserves of 1.10 Mt at 0.53% Cu [97] and Chernogorskoye {No. 58} with 400 Kt, at 0.29% Cu [98], are being prepared for development. Exploration is underway in the promising Morongovskaya {No. 96} and Samoyedovskaya {No. 99} areas[16], and further discoveries of copper-nickel deposits in the Kharaelakh depression, where some deposits may be concealed at depth [99, 100].

In the 1960s, the Bolgokhtokhskoe deposit, a porphyry copper formation with cooper resources of 462 Kt at 0.27% Cu, was discovered on the western flank of the Norilsk-Kharayelakh province [101].

In the 1970s, *native copper deposits* were identified in the North Kharayelakh ore zone, with prospecting conducted at the Arylakhskoye deposit {No. 98} with cooper resources of 600 Kt at 0.41% Cu [102].

The Igarka province is notable for *copper sandstone formations found* in the sediments of the Gravian Vendian formation and the Sukharikhinskaya Vendian – Lower Cambrian formation, located in the horst of the Igarka baykalid uplift in the northwest of the Siberian Platform [103]. In the 1970s, Graviyskoye {No. 100} deposit, with cooper resources of 359 Kt at 2.42% Cu, and Sukharikhinskoye {No. 101}, with 120 Kt at 1.08% Cu, discovered and preliminarily assessed within this cratonic area [104].

The Sayan province lies in the southwestern part of the Siberian Platform, where serpentinized ultrabasic rocks of the gabbro-peridotite-dunite magmatic formation, bearing disseminated platinum-copper-nickel mineralization, are found within Early Proterozoic metamorphites of the Karagan series along the western periphery of the Kansk block [13]. The Kingashskoye {No. 59}, with cooper reserves of 1.1 Mt at 0.17% Cu [105], and Verkhnekingashskoye {No. 60}, with 632 Kt at 0.24% Cu [106], are being prepared for development. Further copper-nickel deposits may be found in the adjacent areas surrounding the Kingash massif, including the promising Kakhtarminskaya {No. 102}, Berezovskaya, Erminskaya, and Agulskaya sites [107]. The Sayan province has recorded copper reserves of 1.7 million tons, or 1.66% of Russian reserves[17] (see Fig. 5, 6).

The Eastern Tuvan province encompasses early Caledonian (Salair) and Baikalian rocks of the Tuvan-Mongolian massif and East Sayan rigid block. Within these areas, metal-bearing volcanic-plutonic complexes from the Cambrian-Devonian period host numerous copper occurrences across the Aksug-Kandat, Khamsarin, Ozhinsko-Derzyg, Balyktyghem-Bilinsky, East Tannuol, Central Sayan, Khemchik, and Mongun-Taiga metallogenic zones [108]. The Ak-Sugskoye deposit {No. 61}, a *copper-porphyry formation* with cooper reserves of 3.63 Mt at 0.67% Cu, is being prepared for operation [109]. Other copper-porphyry sites include Kyzyk-Chadrskoye deposit {No. 103} with reserves of 2.35 Mt at 0.29% Cu) [110], and the Kyzyl-Tashtyg deposit {No. 33}, *pyrite-polymetallic formation with associated copper mineralization*, which is already operational with reserves of 37 Kt at 0.65% Cu [111]. The Eastern Tuva province has recorded cooper reserves of 3.8 million tons, accounting for 3.7% of Russian reserves[18] (see Fig. 5, 6).

The North Baikal province is situated in the southeastern folded margin of the Siberian Platform, where rift-related dunite-troktolite-gabbro intrusions (Yoko-Dovyrenskiy, Avkitskiy, Chayskiy, Hasan-Dyakitskiy, and Nyurundukan) with platinum-copper-nickel mineralization formed within the Riphean Baikal-Muya island arc [112]. Since the 1980s, studies have been conducted on the *PGE-copper-nickel* deposits and occurrences within this

[16] Ministry of Natural Resources and Environment of the Russian Federation. URL: https://www.mnr.gov.ru/docs/gosudarstvennye_doklady/o_sostoyanii_i_ispolzovanii_mineralno_syrevykh_resursov_rossiyskoy_federatsii/

[17] I bid.

[18] I bid.

province. The most researched sites are Yoko-Dovyrenskoye {No. 104}, with 51 Kt of copper resources, and Chayskoye {No. 105}, with resources of 260 Kt at 0.18% Cu [112, 113, 114].

The Kodar-Udokan province is located in the marginal Udokan trough in the southern Siberian Platform, comprising Early Proterozoic carbonate-terrigenous deposits of the Udokan series, which include *copper sandston formations* [115]. The largest deposit in Russia, the Urdocan copper sandstone deposit {No. 34}, was commissioned in 2023 with reserves of 20.09 Mt at an average grade of 1.44% Cu, and produced 6 Kt of cooper inpilot operations in 2021. Additional promising sites in the Udokan basin include Burpalinskoye {No. 108} with 739 Kt at 1.17% Cu, Pravoingamakitskoye {No. 110} with 608 Kt at 0.88% Cu [117], Sakinskoye {No. 109} with 404 Kt at 0.98% Cu [118], Unkurskoe {No. 106} with 320 Kt at 0.57% Cu) [119], and Krasnoe {No. 107} with 933 Kt at 1.81% Cu [120]. On the northeastern flank of the Kodar-Udokan province is the Chinaian gabbro-norite massif of Late Proterozoic age, which intrudes the Early Proterozoic carbonate-terrigenous deposits of the Udokan series. In its middle stratified part, it includes mineralization of the *copper-skar formation* (noble metal-copper-sulfide) within the Rudny area of the Chineyskoye deposit {No. 67}, with cooper reserves of 775 Kt at an average grade of 0.52% Cu [121]. The resource potential of this formation could be further expanded by copper ore occurrences in the adjacentLuktursky and Mailava massifs of the Chiney complex [118].

In total, in the Kodar-Udokan province has recorded balance copper reserves of 20.87 million tons (20.3% of Russian reserves), with annual pilot production in 2021 amounted to 6.0 Kt, or 0.52% of Russian output (see Fig. 5, 6).

The East Trans-Baikal province is rich in multimetal deposits and occurrences of Mo, W, Sn, Au, Cu, Bi, Pb, Zn, As, Sb, Hg, U, rare, and rare earth elements, located within the stagnant oceanic slab of the Dalainor-Gazimuro-Olekminsky mineragenic zone, formed from the Aalenian (J2) to Cenomanian (K2) [122]. Copper deposits in this province are represented by copper-iron ore-skarn and copper-porphyry formations. The Bystrinskoye [Cu-Fe] deposit {No. 35}, of the *copper-iron-skarn formation*, is currently under development with cooper reserves of 2.04 Mt at an average grade of 0.74% Cu, producing 79 Kt in 2021 [123]. Another deposit in this formation, the Kultuminskoye site {No. 62}, is being prepared for operation with reserve of 587 Kt at 0.91% Cu [124]. Geological exploration is ongoing on the periphery of this site, specifically at the Ochunogdinsky, Preobrazhensky, and Engineering sites, with cooper resources of 487 Kt. The explored Lukagonskoye deposit {No. 68} is a complex structure, where the upper section shows classical copper-skarn mineralization [125], which transitions at depth to typical *copper-porphyry formation* mineralization [126], with cooper reserves of 604 Kt at 0.40% Cu [127]. To expand the resource base of the Bystrinsky GOK, exploration is also underway at the Zapadno-Mostovskaya {No. 111} and Borovaya {No. 112} promising sites for copper-porphyry formations. There are also favorable conditions for identifying copper-porphyry deposits within the Uronai ore node and in the Gazimuro-Zavodsky, Mogochinsky, and Verkhne-Olekminsky ore regions of the East Trans-Baikal province. The recorded copper reserves in this province total 2.7 million tons (2.63% of Russian reserves), with production in 2021 reaching 81.1 Kt (7.0% of Russian production)[19] (see Fig. 5, 6).

The Umlekan-Ogoja province encompasses the volcanic-plutonic belt of the same name in the Amur region [128], featuring Late Mesozoic basalt-andesite volcanic rocks and gabbro-diorite plagiogranitic plutonic formations with copper-porphyry mineralization [129]. In the central part of this province, the Ikanskoye deposit {No. 43} is in reserve as a *porphyry-copper formation* with cooper reserves of 459 Kt at an average grade of 0.21% Cu, along with nearby occurrences at Borgulikan and Eastern Double [130]. The Umlekan-Ogoja province has a recorded total of 0.8 million tons of copper reserves[20].

The Primorsky Province, like the Trans-Baikal province, contains abundant multimetal deposits and occurrences of Sn, W, Au, Mo, Cu, Pb, Zn, rare elements, and other minerals, spanning a wide geological timeframe from the Paleozoic to the Meso-Cenozoic. This province is part of the Pacific Ore Belt [131]. Copper deposits are here represented by the porphyry-copper formation and deposits with associated copper mineralization. Sites under development *include* Pravourmiyskoye (Cu reserves of 37.2 Kt), Festivalnoye (124.5 Kt), Sable (53.6 Kt), and Perevalnoye (25.1 Kt) tin ore deposits {No. 36}, which produced 916 t of cooper in 2021 [132], and the Vostok-2 tungsten deposit {No. 37} with 7.3 Kt of cooper [133]. The Malmyzh deposit {No. 64}, a *copper-molybdenum-porphyry formation* with coper

[19] Ministry of Natural Resources and Environment of the Russian Federation. URL: https://www.mnr.gov.ru/docs/gosudarstvennye_doklady/o_sostoyanii_i_ispolzovanii_mineralno_syrevykh_resursov_rossiyskoy_federatsii/

[20] I bid.

reserves of 8.31 Mt at an average grade of 0.35% Cu, located in the northern part of the Zhuravlevo-Amur terrane of the Early Cretaceous Sikhote-Alinsky orogenic belt, is being prepared for operation [134]. There is potential for identifying copper-porphyry deposits within the Central Anajak {No. 116} area, with cooper resources of 800 Kt, and the Ponyskaya {No. 117} area, with 714 Kt) of cooper, both adjacent to the Malmyzh field [135]. Additionally, the Lazurnoe {No. 114} deposit, with187 Kt at 0.48% Cu [136, 137], and the Malakhitovoe {No. 115} deposit, with 1.94 Mt at 0.30% Cu [138], are located in the southern part of the Zhuravlevo-Amur terrane [139]. The recorded copper reserves in the Primorsky Province total 8.51 million tons (8.29% of Russian reserves), with production in 2021 reaching 4.1 Kt (0.35% of Russian output)[21] (see Fig. 5, 6).

The Jugjur province is located on the eastern flank of the Dzhugdzhur-Stanovy mobile belt, formed through Proterozoic and Mesozoic tectonic activities [140]. This belt contains deposits of copper-nickel, copper-skarn and low-sulfide formation with associated copper mineralization.

The Kuhn-Manye deposit {No. 63} of the *PGE-copper-nickel formation* is the most advanced for development, with reserves of 31.5 Kt at an average grade of 0.21% Cu [141]. At the eastern end of the province lies the Nyandominskaya perspective area {No. 118} within the Early Archean gabbro-anartosite of the Lanthar section of the Dzhugdzhur anorthosite massif [142], where PGE–Cu–Ni occurrences such as Batomg and Nyandomi, as well as PGE–Cu occurrences like Skeletal and Mukdakindya, have been recorded. The Nyandoninsky area is estimated to hold cooper resources totaling 235 Kt.

The Konder magmatic massif, located in the western part of the Jugjur province, is a complex, multi-age structure with a Proterozoic dunite core surrounded by a Mesozoic syenite ring intrusion. The dunites hosts known schlieren PGE-chromite mineralization, along with fields of Late Cretaceous alkaline pegmatites, where sulfide copper mineralization enriched with platinoids (*low-sulfide formation with associated copper mineralization*) is spatially confined [143]. This mineralization is the focus of geological exploration at the Konder-Rudny deposit {No. 69}, with estimated copper reserves of 61 Kt.

In the easten part of the Jugjur province, the Malokomuyskoye deposit {No. 119} contains copper-lead-zinc ores within the Late Cretaceous granodiorites of the Jugjur complex. in the structure of [144]. Copper reserves at this *copper-skarn deposit* are estimated at 33 Kt, with additional forecast resources of 100 Kt.

Overall, the recorded copper reserves in the Jugjur province total 0.12 million tons (0.12% of Russian reserves)[22] (see Fig. 5, 6).

The Bilyakchan-Kolyma province is a Proterozoic metallogenic belt rich in copper-bearing sedimentary rocks and native copper in basalts, stretching from the Bilyakchansk seam zone in the Khabarovsk Territory to the Oriek ore zone within the Prikolymsky terrane in the Magadan region. This belt hosts known occurrences and deposits of Proterozoic age *copper sandstone formations, such as* Bilyakchanskoe [145], Severny-Uy [146], and Borong [147] {No. 120}, as well as Oroekskoye [148] and Luchistoye [149] {No. 123}, with additional occurrences from the Early Paleozoic era, like Vesnyanka {No. 123} [147]. Occurrences and deposits of the of the Middle Proterozoic *native copper formation* age found in the Sette-Daban ore zone, including Jalkan, Rosomakha, and Hurat [150] {No. 121} and the Urultinsky ore zone – the Batko ore mineralization point {No. 122} [147].

The Okhotsk-Chukotka province aligns with the Late Jurassic-Early Cretaceous Okhotsk-Chukotka volcanic belt, a segment of the global Pacific ore belt [131]. This region contains deposits and occurrences of both copper-porphyry and copper-skarn formations. Noteworthy among the *copper-porphyry deposits* is a group of ore bodies in the Baim ore zone [151], including the largest explored deposit, Peschanka {No. 70}, with reserves of 6.4 Mt at an average grade of 0.53% Cu) [151, 152], and its satellite, Nakhodka {No. 131}, with reserves of 3.1 Mt at 0.34% Cu [151, 153], both dated to the Late Jurassic-Early Cretaceous. Northward, exploration is active in promising areas such as Kavralyanskaya {No. 132} [154] and Tanyurerskaya {No. 133} [155] for potential copper-porphyry mineralization. In the southern part of the Okhotsk volcanic belt, within the Khabarovsk Territory, lies the Late Cretaceous Chelasinskoye copper-(Au)-porphyry deposit {No. 125}, with cooper reserves of 2.0 Mt [156], as well as the promising Darpirchanskaya area {No. 126},

[21] Ministry of Natural Resources and Environment of the Russian Federation. URL: https://www.mnr.gov.ru/docs/gosudarstvennye_doklady/o_sostoyanii_i_ispolzovanii_mineralno_syrevykh_resursov_rossiyskoy_federatsii/

[22] I bid.

containing resources of 324 Kt. Within the Magadan region, exploration is ongoing for copper-porphyry deposits in the promising areas like Shkhiperskaya {No. 127}, which hosts Early Cretaceous deposits and occurrences such as Nakhatanjinskoye, Lora, Osennoye, Etanja, and Muromets, totaling 1.0 Mt in resources [157], and Mechiveemskaya {No. 130}, with Late Cretaceous deposits such as Dvoustnaya, resources also totaling 1.0 Mt in resources [158]. The Bebekan molybdenum-copper deposit {No. 128}, from the Early Cretaceous and located in the Levo-Omolon ore zone [158], is also within this province. Additionally, this zone includes the Early Cretaceous *copper-skarn deposit*, Med-Gora {No. 129} [159]. Overall, the Okhotsk-Chukotka province contains an estimated 6.4 million tons of copper reserves (6.23% of Russian reserves), though this figure is likely conservative (see Fig. 5, 6).

The Koryak province is located in the northern part of the Koryak-Kamchatka Mesozoic-Cenozoic volcanic belt [160]. Known deposits and occurrences of *low-sulfide platinoid formations with associated copper mineralization* are found in alpine-type mafic-ultramafic complexes here. Prospecting and evaluation are also underway in the Mainitskaya {No. 134} [161] and Valaginsko-Karaginskaya {No. 135} [162] promising areas for low-sulfide-PGE formations with associated copper mineralization. In the southern part of the province, the Late Cretaceous Snezhnoye low-sulfide PGE-chromite deposit, also with associated copper mineralization, is identified {No. 136} [163].

The Kamchatka Province is situated in the southern part of the Koryak-Kamchatka Mesozoic-Cenozoic volcanic belt. Here deposits of the *copper-nickel formation* are associated with hornblende peridotites and gabbroids in the Late Cretaceous-Paleocene Kvinum-Kuvalorog ore zone. This includes the substantially developed Shanuch nickel deposit with associated copper mineralization {No. 38}, holding reserves of 7.4 Kt of cooper at an average grade of 0.3% Cu) [139, 164], with its copper-nickel ores designated fro export. The Kvinum and Kuvalorog copper-nickel deposits {No. 137} [165, 166] are also found under this ore zone. The southern part of the province hosts the Kirganik *copper-porphyry deposit* {No. 138} from the Late Cretaceous [167]. Altogether, the Kamchatka province holds 0.01 Mt of copper reserves, with an annual production of 0.3 Kt in 2021 (see Fig. 5, 6).

In regions without defined provinces, copper deposits are found in poorly explored territories, where the classification of certain deposits by ore formation type remains unclear.

Noteworthy among these is the associated copper mineralization at the Sinyukhinskoye *gold-skarn deposit* {No. 29}, currently under development, with recorded copper reserves of 28 Kt [168, 169] and annual output reaching up to 1 Kt of extracted copper concentrate from the Vesely mine.

The Ulandryk iron-copper-rare earth deposit {No. 87}, an IOCG-type (iron-oxide-copper-gold) deposit, lies in the southern Altai Mountains, containing 1.2 Mt of cooper at an average grade of 0.70% Cu [170]. This deposit exhibits copper-gold and rare earth mineralization overlaying iron ore within Silurian-Devonian rhyolitic volcanic rocks and their tuffs in contact, in contact with Devonian subvolcanic leucogranites of the Ulandryk massif. This unique deposit may be part of a larger copper province extending into the Xinjiang Altai region in China, where the Chacha iron-copper and Minke copper deposits are located [171].

Potential analogs to the Palabora copper-zirconium-phosphate carbonatite deposit [42] include occurrences copper-sulfide mineralization occurrences within the Dumtaley carbonatite massif [172 and the Nadezhda, Pavlovsky, and Koshka massifs [173] {No. 95} in Eastern Taimyr. Notable sulfide mineralization in these carbonatite complexes suggests a rare opportunity for industrial copper mining and warrants further assessment.

Uncommon occurrences of copper-sulfide mineralization have also been found in potassium-rich alkaline intrusions in the Central Aldan region, an area activated in the Late Mesozoic on the Aldan shield [174]. During geological exploration for gold, zones of copper and molybdenum sulfide mineralization were identified, with Au, Cu, and Mo mineralization zones independently distributed in space. This led to the development of the concept of a *molybdenum-copper-gold porphyry formation, characterized by a potassium* rather than sodium *profile of igneous rocks* [175]. The Ryabinovoe copper-gold-porphyry deposit {No. 113} is located on the igneous massif of the same name [175, 176], as is the Yllymakhskoye deposit {No. 113} [177]. Copper mineralization is also recorded in the central type massifs of Yakokutsky and Tommotsky. Additionally, copper mineralization has been identified in previously considered oreless syenite porphyry laccoliths, including the Morozkinskoye deposit within the Gora-Rudnaya laccolith [178] {No. 113} and the syenite porphyry of the Gloomy laccolith.

The Agylkinskoe *copper-tungsten skarn deposit* {No. 124} is unique, being the only large occurrence of copper and tungsten within the Verkhoyansk gold-dominant metallogenic province [179]. The deposit is a contact body in the zone of a yet undiscovered Late Mesozoic granitoid pluton, with registered copper reserves of 206 Kt at an average grade of 2.7% Cu and estimated resources of 84 Kt of Cu.

Among the copper occurrences in lesser-known provinces, the Beregovoye deposit {No. 139} on the northwestern tip of Cape Sulkovsky, Medny Island, in the Commander Islands archipelago, is noteworthy. Discovered by Russian industrialist E.S. Basov, who gathered substantial quantities of copper nuggets, it has since been the subject of geological studies. Research conducted in 1903 by I.A. Morozevich and L. Konyushevsky and in1958 byYu.V. Zhegalov and V.P. Vdovenko identified fine inclusions of native copper in the dikes of Cenozoic augite andesites (*native copper formations*). However, the residual bench placer of native copper has been depleted, and both I.A. Morozevich and Yu.V. Zhegalov classified this deposit as non-industrial [180]. Due to the limited land areas of the Commander Islands, it has not been possible to define a distinct province for native copper mineralization on Copper Island.

Reserves and forecast resources of copper in the Russian Federation

Accounting reserves and resources. As of January 1, 2022, the Russian Federation accounted for 102.7 million tons of balance reserves of categories A, B, C_1, and C_2, and 79.9 million tons of forecast resources of categories P_1, P_2, and P_3[23]. Forecast resources are additionally evaluated by conversion to conditional reserves. According to MPR Methodology (MPR Order No. 68250, April 18, 2022), the conditional reserves calculated by converting to C_2 as follows: $C_2 = 0.5P_1 + 0.25P_2 + 0.125P_3$, amount to 16.7 million tons. Another approach to copper resources, developed by Ya.V. By Alekseev, calculates C_2 conversion as $1.0P_1 + 0.6P_2$, yielding 16.1 million tons [9] – comparable to the MPR method's recalculations. The results from this latest method are used in assessing the resources of copper ore formations.

Mining reserve sufficiency. The existing balance of copper reserves in the Russian Federation is projected to support the current national production rate – including upcoming capacity expansions – sufficiently for at least 47 years of operation. Additionally, the Oktyabrskoye, Talnakhskoye, Norilsk-I, and Gaiskoe deposits have sustained copper production levels for over 100 years. Meanwhile, some deposits with limited remaining reserves and set for decommissioning, including Osennee, Dzhusinskoye, Vesenne-Aralchinskoye, Talganskoye and others.

Copper formations. In terms of the production-to-reserve ratio within Russia's total copper output, only the copper-nickel (1.06) and copper-porphyry (1.18) formations show a balance between production and reserves (see Fig. 3). Reserves supply concerns and potential depletion issues for these formations therefore not significant. In contrast, the copper-pyrite (1.96) and copper-carbonate (2.44) formations have a high production-to – reserve ratio, indicating an increased activation of ore reserves of these types. For copper sandstones, the production-to-reserves ratio stands as just 0.03, reflecting the early stage of exploitation for this type, as seen with Udokan.

Copper mining provinces. In terms of the production-to-reserves within Russia's copper mining regions, only the Norilsk-Kharayelakh (1.13), Kola (0.74), and Rudny Altai (0.77) provinces show a balanced relationship between production and reserves (see Fig. 3). In the well-established mining region of the Urals, this ratio is 2.85, indicating significant reserve activation in this area. A similar pattern is observed in the newer Eastern Trans-Baikal Province (2.67). Conversely, in the older North Caucasus province mining region, the production-to-reserves ratio is only 0.21, suggesting untapped copper reserves, including deposits like Kizil-Dere. In the newly developed regions, such as Primorsky (0.04), Okhotsk-Chukotka (0.01), and Eastern Tuva (0.12), the ratios remain low, as copper deposits are still in the initial stages of development.

Development plans for new copper deposits. In 2023, the Udokan copper sandstone deposit in the Kodar-Udokan province was put into operation, with an initial production capacity of 136 Kt annually, projected to increase to 542 Kt in the second stage. In the Ural province, two copper-pyrite deposits are in the final preparation stage: Podolskoye, with an expected production level of 85 Kt/year, and Novo-Uchalinskoye, with initial production in the first stage at16 Kt/year, reaching 28 Kt/year in the second stage. The Ak-Sugskoye porphyry-copper deposit is under prepared in the Eastern Tuva province, with an output of 151 Kt/year. Preparations for the Malmyzh porphyry-copper deposit in the Primorsky province also nearing completion, with an anticipated annual production level of 300 Kt. Of the explored depos-

[23] Ministry of Natural Resources and Environment of the Russian Federation. URL: https://www.mnr.gov.ru/docs/gosudarstvennye_doklady/o_sostoyanii_i_ispolzovanii_mineralno_syrevykh_resursov_rossiyskoy_federatsii/

its, the most advanced preparation is underway for the Peschanka porphyry-copper deposit in the Okhotsk-Chukotka province, with production projected to reach up to 350 Kt /year.

The implementation of these projects could increase annual cooper production in Russia by 635–1053 Kt, or 55–91% of the 2021 production level. With the commissioning of the Peschanka deposit, Russian copper production may rise by as much as118% compared to the 2021 level.

The state of forecast copper resource base. The prospects for developing the mineral resource best evaluated through the resources (converted to C_2) and reserves volumes. For the *copper-nickel formation*, the ratio is 0.46, reflecting a high exploration level for known deposits in the Norilsk-Kharayelakh and Kola provinces, primarily of drained ores, with relatively lower expectations for reserve growth from projected resources of disseminated copper-nickel ores. However, new deposits of rich drained ores could potentially be discovered at depths within the Kharaelakh and Tangaralakh ore-bearing intrusions [99, 100]. For the *copper-pyrite formation*, the resour-to-reserve ratio is very high at 2.5, due to significant exploration efforts in the Ural province for both drained and disseminated ores. Reserve growth for copper-pyrite ores remains possible through assessing deep horizons and the peripheries of known deposits, as well as by identifyng new deposits in the Circumpolar and Polar Urals regions [73, 81]. The *copper-polymetallic formation* has an even higher resources / reserves ratio of 9.2 as it includes numerous deposits and occurrences, most of which are medium or small and have not previously been prioritized for exploration. As demand for copper increases, these deposits are becoming attractive, especially in the traditional mining areas of Rudny Altai, Salair, and the North Caucasian provinces [19, 89], as well as in the newly studied regions of Eastern Tuva and Okhotsk-Chukotka. For the *porphyry-copper formation*, the resources-to-reserves ratio of stands at 1.35. With rapid engagement of deposits of this type (such as Tominskoye, Mikheevskoye, Malmyzh, and Peschanka), exploration and prospecting have intensified in the Eastern Tuva, Primorsky, and Okhotsk-Chukotka provinces, which offer favorable conditions for discovering new, potentially large, copper-porphyry deposits [151, 154, 155, 156, 157]. Other copper ore formations show low forecasted resources relative to balance reserves. For the *copper-skarn formation*, this is primarily because most of these objects are accounted for within the copper-polymetallic formation. In contrast, the low level of forecast resources form *copper sandstone formations stems* from the limited interest in the technologically complex ores they contain. Geological exploration has been limited primarily to the Udokan deposit, which is unique in its mineralization. Only low level assessments have been performed on nearby deposits and occurrences in the Kodar-Udokan province (Unkurskoye, Krasnoe, Burpalinskoye, Sakinskoye, Pravoingamakitskoye), as well as in the Igarka province (Graviyskoye, Sukharikhinskoye). Beyond these, exploration of these deposits in the newly identified Bilyakchan-Kolyma [148] and Shoria-Khakass provinces is also feasible. With new technologies for underground copper leaching, known and previously developed copper sandstone deposits in the Pre-Ural [68], Igarka [102], and Donetsk [51] provinces may become viable for exploration and exploitation. Currently, no *native copper deposits* in basaltoids formations are included in Russia's balance of recorded copper reserves. However, such deposits are known within the Shoria-Khakass, Norilsk-Kharayelakh, and Bilyakchan-Kolyma copper ore provinces. Unfortunately, the largest and most studied of their deposits (Taymetskoye [94] and Arylakhskoye [102]) lie within protected areas and are unlikely to be available for commercial exploitation.

Conclusions

1. A summary map of Russia has been compiled, including 25 copper ore provinces and the 150 most significant copper deposits of various ore formations, as well as promising sites and areas. Some copper-ore provinces contain only one type of ore formations: copper sandstones in the Pre-Ural, Igarka, and Donetsk provinces; others are dominated by a single primary formation, such as copper-nickel in the Norilsk-Kharayelakh and Kola provinces, copper sandstones in the Kadaro-Udokan provinces, and copper-polymetallic in the Rudny Altai and Salair provinces. In the Ural province, deposits of two formations – copper-pyrite and copper-porphyry – predominate. Many provinces contain deposits of various formations and ages, indicating a shared geochemical specialization within each province's territory, often irrespective of the geological features of ore-bearing complexes.

2. In contrast to the global distribution of copper ore formations, where the copper-porphyry formation leads in both reserves and production, Russia ranks the copper-nickel technological type of ores first in reserves and production. The main production focuses on copper-nickel sulfide depos-

its (419–508 Kt/year, or 36-65% of Russian production) and pyrite copper deposits (227-334 Kt/year, or 23–40%). Production is also expanding for copper-porphyry deposits (reaching up to 323 Kt/year, or 25%, since 2013) and copper-skarn deposits (since 2018, reaching up to 94 Kt/year, or 8.3%). In 2021, copper production in the Russian Federation totaled 1,147 Kt. In 2023, the ultra-large Udokan copper sandstone deposit, with a maximum production potential of 175 Kt/year, was put into operation. The comp letionof new cooper projects currently in preparation could further raise Russia's annual production by 635–1053 Kt, a 55–91% increase over the 2021production level.

3. As of January 2022, Russia's copper reserves include102.7 million tons of balance reserves and 79.9 million tons of forecast resources accross categories P_1 + P_2 + P_3, equivalent to 16.1 million tons in terms of conditional reserves in category C_2. The largest share of copper reserves are concentrated in copper-nickel formations (34.4% of Russian reserves), copper-porphyry formations (23.9%), copper sandstones (19.6%), and copper-pyrite formation (14.5%), with the remaining 7.6% distributed among other ore formations. By region, the Norilsk-Kharayelakh area holds 30.9% of Russia's cooper reserves, followed by the Kodar-Udokan region with 20.3%, and the Ural region with 18.9%. Newer provinces are also showing increases in their copper reserves: Primorsky (8.29%), Okhotsk-Chukotka (6.23%), and Eastern Tuva (3.7%). All other copper-producing provinces combined hold 11.68% of Russia's copper reserves. Overall, Russia's current copper reserves re projected to sustain 47 years of operation at current production levels.

4. In comparing the shares of copper reserves and production acroos ore formations, the copper-nickel (1.06) and copper-porphyry (1.18) formations show the most balanced and favorable security ratios. The production-to-reserves ratio is even more favorable for copper sandstones, reflecting the early stages of exploitation of deposits like Udokan. However, high production shares in copper-pyrite (1.96) and copper-skarn (2.44) formations indicate an intensive drawdown of reserves for these ore types. By region, only the Norilsk-Kharaelakh (1.13), Kola (0.74), and Rudny Altai (0.77) provinces maintain favorable ratios of production to reserves. In contrast, older mining provinces like the Ural (2.85) and newer ones like East Trans-Baikal (2.67) exhibit significant depletion of ore reserves. In the North Caucasus, an established mining region, the ratio of production to reserves is low at 0.21, indicating untapped copper potential, particularly at sites like Kizil-Dere.

5. Each ore formation has distinct prospects for expanding the copper mineral resource base. The copper-nickel formation shows a resource-to-reserve ratio of 0.46, indicating a high exploration density within the Norilsk-Kharayelakh and Kola provinces. However, additional reserves of high-grade ores could potentially be uncovered at depths within the Kharaelakh and Tangaralakh ore-bearing intrusions. The copper-pyrite formation (2.5) presents opportunities for reserve expansion through assessment of deeper horizons and periphery areas of known deposits within the Ural province, along with exploration in the Circumpolar and Polar Urals. Copper-polymetallic formation reserves (9.2) offer numerous known deposits, but most are medium and small, interest in this formation is growing, especially in the mature Rudny Altai, Salair, and North Caucasus provinces, as well as in the emerging Eastern Tuva and Okhotsk-Chukotka provinces. For copper-porphyry formation (1.35), and with the rapid operational engagement of deposits of this type, the scale of geological exploration for this mineralization has expanded in the Eastern Tuva, Primorsky, and Okhotsk-Chukotka provinces, where all conditions are favorable for discovering new, including large, copper-porphyry deposits. Copper sandstone formations, with relatively low forecast resources, have seen limited exploration due to the complex processing requirements for these ores. The Kodar-Udokan province hosts several underexplored deposits, such as Unkurskoe, Krasnoe, Burpalinskoye, Sakinskoye, and Pravoingamakitskoye, as does the Igarka provinc with Graviyskoye and Sukharikhinskoye deposits. In addition, the Bilyakchan-Kolyma and Shoria-Khakass provinces provinces present new prospects for this formation. New underground copper leaching technologies may also support development of smaller copper sandstone deposits within the Pre-Ural and Donetsk provinces. Although deposits of native copper in basaltoids are not currently included in Russia's recorded balance reserves, they are present within the Shoria-Khakass, Norilsk-Kharayelakh, and Bilyakchan-Kolyma copper ore provinces. Unfortunately, the largest and most studied deposits of this type, Taymetskoye and Arylakhskoye, are situated within protected areas, unlikely preventing their commercial exploitation.

References

1. Kondratyev V.B., Popov V.V., Kedrova G.V. Global copper market. *Russian Mining Industry*. 2019;(3):80–87. https://doi.org/10.30686/1609-9192-2019-3-145-80-87; *Russian Mining Industry*. 2019;(4):100–104. https://doi.org/10.30686/1609-9192-2019-4-100-101 (In Russ.)
2. *The World Copper Factbook 2021*. Lisbon: International Copper Study Group; 2022. Pp. 61–68. URL: https://dev.icsg.org/wp-content/uploads/2021/11/ICSG-Factbook-2021.pdf
3. Vikentiev I.V. Critical and strategic minerals in the Russian Federation. *Geologiya Rudnyh Mestorozdenij*. 2023;65(5):463–475. (In Russ.) https://doi.org/10.31857/S0016777023050106
4. Coulomb R., Dietz S., Godunova M., Nielsen Th.B. *Critical minerals today and in 2030: an analysis of OECD countries*. OECD Environment working papers. London, UK. 2015;91:1–51. https://doi.org/10.1787/5jrtknwm5hr5-en
5. Skirrow R.G., Huston D.L., Mernagh T.P. et al. *Critical commodities for a hightech world: Australia's potential to supply global demand*. Canberra: Geoscience Australia; 2013. Pp. 1–118.
6. Bortnikov N.S., Volkov A.V., Galyamov A.L. et al. Mineral resources of high-tech metals in Russia: state of the art and outlook. *Geologiya Rudnyh Mestorozhdenij*. 2016;58(2):97–119. (In Russ.) https://doi.org/10.7868/S0016777016020027
7. *The Growing Role of Minerals and Metals for a Low Carbon Future*. Washington: The World Bank; 2017. Pp. 1–88. https://doi.org/10.1596/28312
8. Petrov I.M. Russia's export position in the global non-ferrous metal market. *Mineral Recourses of Russia. Economics and Management*. 2020;(3):73–75. (In Russ.)
9. Alexeev Ya.V., Korchagina D.A. Mineral base of copper in Russia: the state and development prospects for up to 2040. *Otechestvennaya Geologiya*. 2023;(1):3–19. (In Russ.) https://doi.org/10.47765/0869-7175-2023-10001
10. Distler V.V., Genkin A.D., Dyuzhikov O.A. Sulfide petrology and genesis of copper-nickel ore deposits. In: *Geology and Metallogeny of Copper Deposits. Proceedings of the Copper Symposium 27th International Geological Congress*. Moscow, 1984. (Special Publication of the Society for Geology Applied to Mineral Deposits). 2024:111–123. URL: https://link.springer.com/book/10.1007/978-3-642-70902-9
11. Marakushev A.A., Paneyakh N.A., Zotov I.A. Specific features of the formation of copper-nickel sulfide deposits in trap rocks: evidence from the Pechenga and Noril'sk regions. *Doklady Earth Sciences*. 2002;383(2):129–133. (Orig. ver.: Marakushev A.A., Paneyakh N.A., Zotov I.A. Specific features of the formation of copper-nickel sulfide deposits in trap rocks: evidence from the Pechenga and Noril'sk regions. *Doklady Akademii Nauk*. 2002;382(5):668–673. (In Russ.))
12. Naldrett A.J. *Magmatic sulfide deposits: Geology, Geochemistry and Exploration*. Berlin, Heidelberg: Springer, Verlag; 2004. 727 p.
13. Zaskind E.S., Konkina O.M. Sulfide Cu-Ni and PGM deposit typification for forecasting and prospecting. *Otechestvennaya Geologiya*. 2019;(2):3–15. (In Russ.) https://doi.org/10.24411/0869-7175-2019-10010
14. Likhachev A.P. Platinum-copper-nickel and platinum deposits: the birth, intrusion and becoming ore- bearing mafic-ultramafic magmas. *Ores and Metalls*. 2012;(6):9–23. (In Russ.)
15. Borodaevskaya M.B., Gorzhevsky D.I., Krivtsov A.I. et al. *Pyrite deposits of the world*. Moscow: Nedra Publ. House; 1979. 284 p. (In Russ.)

16. Robb L.J. *Introduction to ore-forming processes*. Library of Congress Cataloging-in-Publication Data. Malden, Oxford, Carlton: Blackwell Publ.; 2005. 386 p.
17. Vikentyev I.V. *Conditions of formation and metamorphism of pyrite ores*. Moscow: Nauchny Mir, 2004. 344 p. (In Russ.)
18. Marakushev A.A., Rusinov V.L., Paneyakh N.A. et al. The intermediate member in the genetic chain between Cu-Ni sulfide and Cu-Zn massive sulfide deposits. *Doklady Earth Sciences*. 2001;381:932–934. (Orig. ver.: Marakushev A.A., Rusinov V.L., Paneyakh N.A. et al. The intermediate member in the genetic chain between Cu-Ni sulfide and Cu-Zn massive sulfide deposits. *Doklady Akademii Nauk*. 2001;380(5):667–670. (In Russ.))
19. Marakushev A.A., Paneyakh N.A., Zotov I.A. Petrogenetic types of massive sulfide (VMS) and polymetalic deposits. *Lithosphere* (*Russia*). 2011;(3):84–103. (In Russ.)
20. Seravkin I.B., Kosarev A.M. South Urals and Rudny Altai: a comparative paleovolcanic and metallogenic analysis. *Geologiya Rudnyh Mestorozdenij*. 2019;61(2):3–22. (In Russ.) https://doi.org/10.31857/S0016-77706123-22
21. Sotnikov V.I. Porphyry copper-molybdenum ore association: genesis, dimensions, and boundaries. *Geologiya i Geofizika*. 2006;47(3):355–363. (In Russ.)
22. Sun W., Zhang C.-C., Li H. et al. The formation of porphyry copper deposits. *Acta Geochimica*. 2017;36(1):9–15. https://doi.org/10.1007/s11631-016-0132-4
23. Zvezdov V.S. Major and giant porphyry copper deposit formation environments. *Otechestvennaya Geologiya*. 2019;(5):16–35. (In Russ.)
24. Heinrich C.A., Halter W., Landtwing M.R., Pettke T. The formation of economic porphyry copper (-gold) deposits: constraints from microanalysis of fluid and melt inclusions. *Geological Society Special Publication*. 2005;248:247–263. https://doi.org/10.1144/gsl.sp.2005.248.01.13
25. Lee C.-T. A., Tang M. How to make porphyry copper deposits. *Earth and Planetary Science Letters*. 2020;529:115868. https://doi.org/10.1016/J.EPSL.2019.115868
26. Migachev I.F., Zvezdov V.S., Minina O.V. Formational types of porphyry copper deposits and their ore-magmatic systems. *Otechestvennaya Geologiya*. 2022;(1):26–48. (In Russ.)
27. Lur'ye A.M. Formation conditions of copper-sandstone and copper-shale deposits. In: *Geology and Metallogeny of Copper Deposits*. *Proceedings of the Copper Symposium 27th International Geological Congress*. Moscow, 1984. Springer Link; 1986. Pp. 477–491.
28. Lur'ye A.M. Genesis of copper sandstones and shales. Moscow: Nauka Publ. House; 1988. 180 p. (In Russ.)
29. Boyle R.W., Brown A.C., Jefferson C.W. et al. *Sediment-hosted stratiform copper deposits*. Ottawa: Geological Association of Canada; 1989. 710 p.
30. Gablina I.F. Role of geochemical barriers in forming sulfide ores in various geological environments. *Otechestvennaya Geologiya*. 2021;(2):63–73. (In Russ.)
31. Sinyakov V.I. *Genetic types of scarn ore-forming systems. Proceedings of the institute of geology and geophysics.* Novosibirsk: Nauka, SB of the USSR Academy of Sciences. 1990;774:1–71. (In Russ.)
32. Meinert L.D., Hedenquist J.W., Satoh H., Matsuhisa Y. Formation of anhydrous and hydrous skarn in Cu-Au ore deposits by magmatic fluids. *Economic Geology*. 2003;98:147–156. https://doi.org/10.2113/GSECONGEO.98.1.147
33. Grabezhev A.I., Shardakova G.Yu. Ore-bearing granitoids of uralian copper-skarn deposits: pertrogeochemistry in connection with ore-metasomatic zonality features. *Lithosphere* (*Russia*). 2006;(4):68–78. (In Russ.)
34. Poltavets Y.A., Poltavets Z.I., Nechkin G.S. Volkovsky deposit of titanomagnetite and copper-titanomagnetite ores with accompanying noble-metal mineralization, the Cen-

tral Urals, Russia. *Geology of Ore Deposits*. 2011:53(2):126–139. https://doi.org/10.1134/S1075701511020061

35. Bornhorst T.J., Barron R.J. Copper deposits of the western Upper Peninsula of Michigan. *The Geological Society of America. Field Guide*. 2011;24:83–99. https://doi.org/10.1130/2011.0024(05)
36. Novgorodova M.I. *Native metals in hydrothermal ores*. Moscow: Nauka Publ. House; 1983. 288 p. (In Russ.)
37. Burrows D.R., Lesher C.M. Copper-rich magmatic Ni-Cu-PGE deposits. In: Hedenquist J.W., Harris M., Camus F. *Geology and genesis of major copper deposits and districts of the world*: *A tribute to Richard H. Sillitoe*. Society of Economic Geologists; 2012. Pp. 515–552. https://doi.org/10.5382/SP.16
38. Peck D.C., Huminicki M.A.E. Value of mineral deposits associated with mafic and ultramafic magmatism: Implications for exploration strategies. *Ore Geology Reviews*. 2016;72(P1):269–298. https://doi.org/10.1016/j.oregeorev.2015.06.004
39. Turchenko S.I., Turchenko F.A. Cu-Ni-PGE resources of the precambrian sulphide deposits: analytic review. *Regional Geology and Metallogeny*. https://doi.org/10.52349/0869-7892_2021_89_93-106
40. Sillitoe R.H., Lehmann B. Copper-rich tin deposits. *Mineralium Deposita*. 2022;57(1):1–11. https://doi.org/10.1007/s00126-021-01078-9
41. Seltmann R., Soloviev S., Pirajno F. et al. Metallogeny of Siberia: tectonic, geologic and metallogenic settings of selected significant deposits. *Australian Journal of Earth Sciences*. 2010;57(6):655–706. https://doi.org/10.1080/08120099.2010.505277
42. Vielreicher N.M., Groves D.I., Vielreicher R.M. The Phalaborwa (Palabora) deposit and its potential connection to iron-oxide cooper-gold deposits of olympic dam type. In: Porter T.M. (Ed.) *Hydrothermal Iron Oxide Copper-Gold & Related Deposits: A Global Perspective*. Adelaide: PGC Publ. 2000;1:321–329.
43. Makarov A.B., Khasanova G.G., Talalay A.G. Technogenic deposits: research features. *News of the Ural State Mining University*. 2019;(3):58–62. https://doi.org/10.21440/2307-2091-2019-3-58-62
44. Potravny I., Novoselov A., Novoselova I. et al. The technogenic deposits' development as a factor of overcoming resource limitations and ensuring sustainability. *Preprints*. 2023:1–16. https://doi.org/10.20944/preprints202309.1430.v1
45. Seleznev S.G., Stepanov N.A. Dumps of allarechensky sulphide copper-nickel deposit as a new type of geological and industrial man-made deposits. *Izvestiya Vysshikh Uchebnykh Zavedenii. Gornyi Zhurnal*. 2011;(5):32–40. (In Russ.)
46. Ukraintsev I.V., Trubilov V.S., Klepikov A.S. Poor, ill-conditioned and technogenic raw materials as a prospective source of copper obtaining. *Tsvetnye Metally*. 2016;(10):36–42. (In Russ.) https://doi.org/10.17580/tsm.2016.10.05
47. Bobomurotov B.B. Cu and Zn spatial distribution in the main ore body of the urup massive sulfide deposit, northern Caucasus. *Metallogeniya Drevnikh i Sovremennykh Okeanov*. 2022;28:226–229. (In Russ.)
48. Kurbanov M.M., Bogush I.A., Krylov V.G. *The pyrite deposit of Kizil-Dere in Mountainous Dagestan*. Moscow: Nauchnyy Mir; 2014. 244 p. (In Russ.)
49. Tatarinov S.I. About the mining and metallurgical center of the Bronze Age in Donbass. *Sovetskaya Arkheologiya*. 1977;(4):192–207. (In Russ.)
50. Shevyrev L.T., Savko A.D., Chereshinskii A.V. Evolution of geodynamic circumstances of east european platform and its framing in phanerozoic and associated mineragenic transgressions. *Proceedings of Voronezh State University. Series: Geology*. 2016;(2):13–21. (In Russ.)

51. Shubin Yu.P. Features of the material composition, genesis and control of copperore mineralization of the Donbass Bakhmut Basin. *Collection of Scientific Papers of Donbass State Technical Institute*. 2020;(20):23–30. (In Russ.)
52. Kompanetz G.S., Kovalchuk M.S., Konstantinenko L.I. et al. Copper-bearing of the upper-jurassic red-colour-terrigenios subformation ofthe near-dobrudgian depression. *Collection of Scientific Works of the IGS NAS of Ukraine*. 2012;(5):99–105. (In Ukranian)
53. Chernyshov N.M. Sulfide platinoid-copper-cobalt-nickel deposits of Novokhopersk Ore District and the problems of their integrated development under strict environmental constraints and preservation of the unique ecosystem. *Ores and Metalls.* 2013;(6):5–13. (In Russ.)
54. Golubev A.I., Shchiptsov V.V., Mikhailov V.P. Glushanin L.V. Republic of Karelia's mineral resources. In: *Geology of Karelia from the Archean to the Present Day*. Petrozavodsk: Institute of Geology KarSC RAS; 2011. Pp. 123–134. (In Russ.)
55. Korneev A.V., Vikhko A.S., Fatov N.V., Ivashenko V.I. Viksha deposit – The first large industrially promising PGM locality in Karelia. *Gornyi Zhurnal*. 2019;(3):31–34. (In Russ.) https://doi.org/10.17580/gzh.2019.03.06
56. Tytyk V.M., Frolov P.V. Lobash Molybdenum Deposit: a big promising economic deposit in the republic of karelia. *Proceedings of the Karelian Scientific Center of the Russian Academy of Sciences*. 2014;(1):56–62. (In Russ.)
57. Ivanova N.V., Gusev A.V., Matrenichev A.V. et al. The state geological map of the Russian Federation on a scale of 1 : 200 000. The second edition. The Karelian series. P-37-XV. An explanatory note. The Ministry of Natural Resources of Russia, Rosnedra, the All-Russian Scientific Research Geological Institute named after A. P. Karpinsky (VSEGEI), North-Western PGO JSC. St. Petersburg: VSEGEI; 2023. 136 p. (In Russ.)
58. Turchenko S.I. Platinum-metal and sulfide-nickel metallogeny in the Paleoproterozoic rifting on the Baltic Shield. *Geologiya Rudnyh Mestorozhdenij*. 2017;59(2):83–92. (In Russ.) https://doi.org/10.7868/S0016777017020058
59. Barnes S.J., Melezhik V.A., Sokolov S.V. The composition and mode of formation of the Pechenga nickel deposits, Kola Peninsula, Northwestern Russia. *The Canadian Mineralogist*. 2001;39(2):447–471. https://doi.org/10.2113/gscanmin.39.2.447
60. Chashchin V.V., Ivanchenko V.N. Sulfide pge-cu-ni and low-sulfide pt-pd ores of the monchegorsk ore district (Arctic Western Sector): geology, mineralogy, geochemistry, and genesis. *Geologiya i Geofizika*. 2022:63(4):622–650. (In Russ.) https://doi.org/10.15372/gig2021184
61. Chashchin V.V., Petrov S.V., Drogobuzhskaya S.V. Loypishnyun low-sulfide Pt–Pd deposit of the Monchetundra basic massif, Kola peninsula, Russia. *Geology of Ore Deposits*. 2018;60(5):418–448. https://doi.org/10.1134/S1075701518050021
62. Subbotin V.V., Korchagin A.U., Savchenko E.E. Platinum-metal mineralization in the Fedorovo-Pan ore node: types of mineralization, mineral composition and features of genesis. *Bulletin of the Kola Scientific Center of the Russian Academy of Sciences*. 2012;(1):54–65. (In Russ.)
63. Groshev N.Yu., Pripachkin P.V., Rundkvist T.V. et al. Geological structure, geochemistry and copper-nickel-platinum-metal mineralization of the East Pana layered intrusion (Kola region, Russia). *Proceedings of the Fersman Scientific Session of the Mining Institute of KSC RAS*. 2023;20:57–67. (In Russ.) https://doi.org/10.31241/FNS.2023.20.006
64. Kalinin A.A., Galkin N.N. Precambrian copper-molybdenum porphyry deposit of Pellapakh (Kolmozero-Voronya greenstone belt). *Bulletin of the Kola Scientific Center of the Russian Academy of Sciences*. 2012;(1):79–91. (In Russ.)
65. Voytekhovsky Yu.L., Neradovsky Yu.N., Grishin N.N. et al. Kolvitsa field (geology, material composition of ores). *Vestnik of MSTU*. 2014;17(2):271–278. (In Russ.)

66. Naugolnykh S.V., Ivanov A.V., Uliakhin A.V., Novikov I.V. Paleoecological and depositional environment of permian copper-bearing sandstone fossil plants and tetrapod localities: Records from Bashkortostan and Kargalka river basin, Orenburg region, Russia. *Paleontological Journal*. 2022;56(11):1538–1555. https://doi.org/10.1134/S0031030122110120

67. Kharitonov T.V. *Perm copper: A review of the literature*. Perm: Perm State University; 2016. 1098 p. (In Russ.)

68. Khalezov A.B. Perspectives and problems of the industrial exploitation of copper deposits of the upper permian red-coloured formation of the west preduralye (by methods of the bore hole and glomeroplasmatic leaching). *Ores and Metalls*. 2011;(5):5–14. (In Russ.)

69. Kontar E.S. *The geological-industrial types of the* cu, *zn, pb deposits in the urals (geological conditions of setting, history of the formation, the prospects)*. Yekaterinburg: UGSU; 2013. 203 p.

70. Grabezhev A.I., Ronkin Y.L., Rovnushkin M.Y. et al. Krasnotur'insk skarn copper ore field, northern urals: the U-Pb age of ore-controlling diorites and their place in the regional metallogeny. *Doklady Earth Sciences*. 2014;456(2):641–645. https://doi.org/10.1134/S1028334X14060117 (Orig. ver.: Grabezhev A.I., Ronkin Y.L., Rovnushkin M.Y. et al. Krasnotur'insk skarn copper ore field, northern urals: the U-Pb age of ore-controlling diorites and their place in the regional metallogeny. *Doklady Akademii Nauk*. 2014;456(4):443–447. (In Russ.) https://doi.org/10.7868/S0869565214160191)

71. Grabezhev A.I., Sotnikov V.I., Borovikov A.A., Azovskova O.B. Genetic typification of the gumeshevsk skarn copper deposit, middle urals. *Doklady Earth Sciences*. 2001;380:830–832. (Orig. ver.: Grabezhev A.I., Sotnikov V.I., Borovikov A.A., Azovskova O.B. Genetic typification of the gumeshevsk skarn copper deposit, middle urals. *Doklady Akademii Nauk*. 2001;380(2):242–244. (In Russ.))

72. Chudinova N.D. History of the mednorudyanskoe mine: the beginning. *Mineralogy*. 2015;(1):81–85. (In Russ.)

73. Soloviev S.G., Kryazhev S.G., Dvurechenskaya S.S. Geology, mineralization, stable isotope geochemistry, and fluid inclusion characteristics of the Novogodnee-Monto oxidized Au-(Cu) skarn and porphyry deposit, Polar Ural, Russia. *Mineralium Deposita*. 2013;48(5):603–627. https://doi.org/10.1007/s00126-012-0449-9

74. Barannikov A.G., Savelyeva K.P. The composition and structure of copper containing clays of Gumeshevski copper-scarn field. *Bulletin of Perm University. Geology*. 2011;(3):60–69. (In Russ.)

75. Altushkin I.A., Levin V.V., Korol Yu.A., Karev B.V. The practice of in-situ leaching of copper from the Gumeshevskoe deposit ores. Tsvetnye Metally. 2019;(5):17–32. (In Russ.) https://doi.org/10.17580/tsm.2019.05.03

76. Tuchina M.V., Ermakova Yu.V. Reserve sufficiency of South and Middle Urals copper mines, their mineral base status and prospects. *Ores and Metalls*. 2019;(3):12–21. (In Russ.) https://doi.org/10.24411/0869-5997-2019-10019

77. Borodaevskaya M.B., Vakhrushev M.I., Kontar E.S. *The geological structure of the Gaisky ore region and the conditions of localization of copper-crusted mineralization in it* (*Southern Urals*). Moscow: TSNIGRI; 1968. 214 p. (In Russ.)

78. Miniyarova D.V. Jubilee copper-pyrite deposit. *Ustoychivoye Razvitiye Nauki i Obrazovaniya*. 2019;(1):253–255. (In Russ.)

79. Petrova O.V., Bainazarova G.R., Yanturina Yu.D. Justification of design solutions for the development of the Ozernoye and Zapadno-Ozernoye fields, taking into account the prevented environmental damage. *Aktual'nyye Problemy Sovremennoy Nauki, Tekhniki i Obrazovaniya*. 2012;70(1):51–54. (In Russ.)

80. Galiullin I.B. Features of the geological structure and material composition of ores of the Novo-Uchalinsky copper-crusted deposit, Southern Urals. *Metallogeniya Drevnikh i Sovremennykh Okeanov*. 2011;(1):294–295. (In Russ.)

81. Kantemirov V.D., Titov R.S., Yakovlev A.M. Assessment of the potential and technologies of development of deposits of copper-pyrite ores in the zone of the Subpolar Urals. *Izvestija Tulskogo Gosudarstvennogo Universiteta. Nauki o Zemle*. 2018;(4):190–203. (In Russ.)

82. Minina O.V., Migachev I.F. Porphyry Copper Provinces and Zones of the Southern Urals (Forecasting- Metallogenic Zoning). *Otechestvennaya Geologiya*. 2018;(4):26–41. (In Russ.)

83. Altushkin I.A., Levin V.V., Gordeev A.I., Pikalov V.A. Development of the Tominsk and Mikheevsk copper ore deposits of the Southern Urals. *Tsvetnye Metally*. 2019;(7):21–28. (In Russ.) https://doi.org/10.17580/tsm.2019.07.02

84. Andreev A.V., Girfanov M.M., Kulikov D.A. Ore districts with porphyry copper mineralization – prospective mineral base in the Southern Urals. *Otechestvennaya Geologiya*. 2018;(4):3–17. (In Russ.)

85. Grabezhev A.I., Korovko A.V., Azovskova O.B., Pribavkin S.V. Potentially commercial Alapayevsk-Sukhoy Log porphyry copper zone (the Middle Urals). *Lithosphere* (*Russia*). 2015;(3):79–92. (In Russ.)

86. Poltavets Yu.A., Poltavets Z.I., Nechkin G.S. Volkovskoye deposit of titanium-magnetite and copper-titanium-magnetite ores, with concomitant noble metal mineralization in the Middle Urals of Russia. *Geologiya Rudnyh Mestorozdenij*. 2011;53(2):143–157. (In Russ.)

87. Dushin V.A. Metallogeny of the Lyapinsky megablock (Subpolar Urals). *News of the Ural State Mining University*. 2021;(2):88–105. https://doi.org/10.21440/2307-2091-2021-2-88-105

88. Savchuk Y.S., Volkov A.V., Aristov V.V. Cupriferous basalts of the Northern Urals. *Lithosphere* (*Russia*). 2017;17(3):133–144. (In Russ.)

89. Seravina T.V. The position of pyrite-polymetallic deposits of Siberia in the volcanogenic section (on the example of the Rudnoaltai, Salair, Kyzyl-Tashtyg and Priargun mineragenic zones). *Metallogeniya Drevnikh i Sovremennykh Okeanov*. 2018;(1):104–108. (In Russ.)

90. Alabin L.V. Structural-formational and metallogenic zonality of the Kuznetsk Alatau. *Proceedings of the institute of geology and geophysics*. Novosibirsk: Nauka, SB of the USSR Academy of Sciences. 1983;527:1–111. (In Russ.)

91. Soloviev S.G., Voskresensky K.I., Sidorova N.V. et al. The Glafirinskoe and related skarn Cu-Au-W-Mo deposits in the Northern Altai, SW Siberia, Russia: geology, igneous geochemistry, zircon U-Pb geochronology, mineralization, and fluid inclusion characteristics. *Ore Geology Reviews*. 2021;138:104382. https://doi.org/10.1016/j.oregeorev.2021.104382

92. Soloviev S.G., Sidorova N.V., Kryazhev S.G. et al. Geology, mineralization, igneous geochemistry, and zircon U-Pb geochronology of the early paleozoic shoshonite-related Julia skarn deposit, SW Siberia, Russia: toward a diversity of Cu-Au-Mo skarn to porphyry mineralization in the Altai-Sayan orogenic system. *Ore Geology Reviews*. 2022;142:104706. https://doi.org/10.1016/j.oregeorev.2022.104706

93. Rudyuk A.K., Metalnikova E.S. Minerals of Kuzbass. Molybdenum. In: *Proceedings of the VI International Youth Environmental Forum*. Kemerovo, November 16–17, 2022 Kemerovo: Kuzbass State Technical University; 2023. Pp. 322.1–322.4. (In Russ.)

94. Kozlovsky E.A. (Ed.) *Geology of the USSR. Volume XIV. Western Siberia* (*Kemerovo, Novosibirsk, Omsk, Tomsk regions, Altai Territory*). *Minerals*. In 2 books. Moscow: Nedra Publ. House. 1982;2:1–319. (In Russ.)

95. Proskurnin V.F., Petrov O.V., Romanov A.P. et al. Central Arctic gold-bearing copper-molybdenum-porphyric belt. *Regional Geology and Metallogeny*. 2021;85:31–49. (In Russ.)

96. Strunin B.M., Dyuzhikov O.A., Barmina O.A., Komarov V.V. *Geological map of the Norilsk ore region scale 1:200000. Explanatory note*. Moscow: Geoinformmark; 1994. 122 p. (In Russ.)

97. Erykalov S.P., Kovalchuk K.K., Snisar S.G. Geology and structure of Maslovskii platinum-copper-nickel deposit. *Prospect and Protection of Mineral Resources*. 2010;(9):31–34. (In Russ.)

98. Malitch K.N. Forecasting criteria for sulphide PGE-copper-nickel deposits of the Noril'sk province. *Lithosphere* (*Russia*). 2021;21(5):660–682. https://doi.org/10.24930/1681-9004-2021-21-5-660-682

99. Staroseltsev V.S. On the possibility of discovering rich copper-nickel-platinum mineralization in the north of the Kharaelakh Mountains. *Geology and Mineral Resources of Siberia*. 2016;(4):84–86. (In Russ.)

100. Miroshnikova L.K., Mezentsev A.Yu., Semenyakina N.V., Kotel'nikova E.M. Geological and geochemical signs and criteria of potential mineralization in the Tangaralakh intrusion. *Mining Informational and Analytical Bulletin*. 2020;(6):115–130. (In Russ.) https://doi.org/10.25018/0236-1493-2020-6-0-115-130

101. Komarova M.Z. Copper-molybdenum ores in Taimyr. *Ores and Metalls*. 2012;(6):74–78. (In Russ.)

102. Bragin V.I., Matsko N.A., Kharitonova M.J. Estimation of efficiency of development of copper and gold deposits of Krasnoyarsk North. *Arctic and North*. 2017;26:5–13. (In Russ.) https://doi.org/10.17238/issn2221-2698.2017.26.5

103. Gablina I.F. Genetic types of copper mineralization in the Igarka area, west of the Siberian platform. *Geology and metallogeny of copper deposits. Proceedings of the copper symposium 27th International Geological Congress.* Moscow, 1984. Springer Link; 1986. Pp. 524–539.

104. Rzhevsky V.F., Gablina I.F., Vasilovskaya L.V., Lurie A.M. Genetic features of the Arabian copper deposit. *Lithology and Minerals*. 1988;(2):86–97. (In Russ.)

105. Lomaeva G.R., Tarasov A.V. The Kingash Sulfide, precious metal and nickel-copper deposit, the first discovered in the Eastern Sayan. *Prospect and Protection of Mineral Resources.* 2010;(9):28–31. (In Russ.)

106. Kravtsova O.A., Motorin Y.M., Kozyrev S.M. et al. Promising copper-nickel raw materials of the Kingash ore region on the example of the Verkhnekingash ore occurrence. *Prospect and Protection of Mineral Resources.* 2006;(8):32–37. (In Russ.)

107. Smagin A.N., Parnachev V.P. About the new Kakhtarma potentially ore-bearing area of the East Sayan nickel-platinum province. *Tomsk State University Journal*. 2012;363:214–218. (In Russ.)

108. Burdin N.V., Lebedev V.I., Lebedev N.I. Gold-copper-molybdenum-porphyry ores. *Advances in Current Natural Sciences*. 2009;(5):15–22. (In Russ.)

109. Mongush Ai.D., Lebedev V. Ak-Sug copper-molibdenum-porphyry deposit: mineral composition of rocks and ores. *Proceedings of the Siberian Department of the Section of Earth Sciences, Russian Academy of Natural Sciences. Geology, Prospecting and Exploration of Ore Deposits*. 2013;(1):22–29. (In Russ.)

110. Andreev A.V., Girfanov M.M., Starostin I.A. et al. Geological structure, ore-metasomatic and mineralogical geochemical zoning of Au-Mo-Cu porphyry Kyzyk-Chadr deposit, Tyva republic. *Ores and Metals*. 2021;(1):57–76. (In Russ.) https://doi.org/10.47765/0869-5997-2021-10004

111. Kuzhuget R.V., Ankusheva N.N., Kalinin Y.A. et al. Mineralogical and geochemical peculiarities and Pt conditions of ores from the Kyzyl-Tashtyg VMS polymetallic

deposit, Eastern Tuva: fluid inclusion and S, O, C isotopic data. *Ore Geology Reviews*. 2022;142:104717. https://doi.org/10.1016/j.oregeorev.2022.104717

112. Kislov E.V. The North Baikal PGE-Ni-Cu province: geodynamics, petrology, ore genesis. In: *Metallogeny of Ancient and Modern Oceans – 2023. Mineralogy and geochemistry of ore deposits: from theory to practice Proceedings of the Professor V.V. Zaykov XXIXth Scientific Youth School*. Miass; 2023. Pp. 40–44. (In Russ.)
113. Rudashevsky N.S., Kretser Yu.L., Orsoev D.A., Kislov E.V. Palladium-platinum mineralization in copper-nickel vein ores in the ioko-dovyren layered massif. *Doklady Earth Sciences*. 2003;391(6):858–861. (Orig. ver.: Rudashevsky N.S., Kretser Yu.L., Orsoev D.A., Kislov E.V. Palladium-platinum mineralization in copper-nickel vein ores in the ioko-dovyren layered massif. *Doklady Akademii Nauk*. 2003;391(4):519–522. (In Russ.))
114. Konnikov E.G., Tsygankov A.A., Orsoev D.A. Chayskoye copper-nickel deposit. *Deposits of Transbaikalia*. 1995;1(1):39–47. (In Russ.)
115. Gongalsky B., Krivolutskaya N. *World-class mineral deposits of Northeastern Transbaikalia, Siberia, Russia*. Cham, Switzerland: Springer; 2019. 323 p. https://doi.org/10.1007/978-3-030-03559-4
116. Chechetkin V.S., Volodin R.N., Narkelyun L.F. et al. Udokan deposit of copper sandstones. *Deposits of Transbaikalia*. 1995;1(1):10–19. (In Russ.)
117. Trubachev A.I., Chechetkin V.S., Sekisov A.G. et al. Stratiform deposits of the bam zone and problems of their development. *Transbaikal State University Journal*. 2014;(12):51–64. (In Russ.)
118. Gongal'sky B.I. Potential resources of the Udokan-Chinei ore cluster, Transbaikalia. *Ores and Metals*. 2011;(3–4):45. (In Russ.)
119. Yakubchuk A.S., Bachulya L.I., Adyrkhayev V.V., Shmatov S.A. What else is hidden near Udokan? *Ratsionalnoe Osvoenie Nedr*. 2020;(1):58–61. (In Russ.) https://doi.org/10.26121/RON.2020.61.32.005
120. Gongalskiy B.I. Copper and uranium deposits of the Kodaro-Udokan district. *Prospect and Protection of Mineral Resources.* 2023;(2):12–21. (In Russ.) https://doi.org/10.53085/0034-026X_2023_02_12
121. Tsymbalist S.I., Ryabkin V.K., Litvintsev E.G. et al. Rational technology pre-sky radiometriche enrichment copper sulphide platinum metal ore area ore deposits chineyskoye. *Prospect and Protection of Mineral Resources*. 2017;(2):37–40. (In Russ.)
122. Khomich V.G., Boriskina N.G. Advancement of mineragenic regionalization of eastern transbaikalia based on geophysical studies. *Russian Geology and Geophysics*. 2017;58(7):822–835. https://doi.org/10.1016/j.rgg.2017.06.005 (Orig. ver.: Khomich V.G., Boriskina N.G. Advancement of mineragenic regionalization of eastern transbaikalia based on geophysical studies. *Geologiya i Geofizika*. 2017;58(7):1029–1046. (In Russ.) https://doi.org/10.15372/GiG20170706)
123. Kovalenker V.A., Abramov S.S., Kiseleva G.D. et al. The large bystrinskoe Cu–Au–Fe deposit (Eastern Trans-Baikal region): Russia's first example of a skarn–porphyry ore-forming system related to adakite. *Doklady Earth Sciences*. 2016;468(2):566–570. https://doi.org/10.1134/S1028334X1606012X (Orig. ver.: Kovalenker V.A., Abramov S.S., Kiseleva G.D. et al. The large bystrinskoe Cu–Au–Fe deposit (Eastern Trans-Baikal region): Russia's first example of a skarn–porphyry ore-forming system related to adakite. *Doklady Akademii Nauk*. 2016;468(5):547–552. (In Russ.) https://doi.org/10.7868/S0869565216170205)
124. Kovalev K.R., Kalinin Yu.A., Turkina O.M. et al. Kultuminskoe gold-copper-iron-skarn deposit (Eastern Transbaikalia, Russia): petrogeochemical features of magmatism and ore-forming processes. *Russian Geology and Geophysics*. 2019;60(6):749–771. (In Russ.) https://doi.org/10.15372/GiG2019078

125. Redin Yu. O., Redina A. A., Prokopiev I. R. et al. The lugokanskoe Au–Cu skarn deposit (Eastern Transbaikalia): mineral composition, age, and formation conditions. *Russian Geology and Geophysics*. 2020;61(2):216–242. (In Russ.) https://doi.org/10.15372/GiG2019085

126. Salikhov V. S., Ignatiev A. A. Structural and dynamic features of the lugokan ore node and its prospects (South-Eastern Transbaikalia). *Transbaikal State University Journal*. 2023;29(3):16–25. (In Russ.) https://doi.org/10.2109/2227-9245-2023-29-3-16-25

127. Redin Yu. O., Kalinin Yu. A., Nevolko P. A. et al. Mineral assemblages and zonation of the Lugokanskiy ore cluster mineralization (Eastern Transbaikalia). *Geology and mineral resources of Siberia*. 2014;(2):83–92. (In Russ.)

128. Derbeko I. M., Agafonenko S. A., Kozyrev S. K., Vyunov D. L. The Umlekan-Ogodzha volcanic belt (the problem bodily separation). *Lithosphere* (*Russia*). 2010;(3):70–77. (In Russ.)

129. Perestoronin A. E., Vyunov D. L., Stepanov V. A. Deposits of gold-copper-molybdenum-porphyry formation Priamurskaya gold-bearing province. *Regional Geology and Metallogeny*. 2017;70:78–85. (In Russ.)

130. Melnikov A. V., Stepanov V. A., Ostapenko . S., Moiseenko V. G. Blagorodnometallny mineralization of deposits and ore occurrence copper molybdenum – a porphyritic formation upper priamurye (Far East, Russia). *Prospect and Protection of Mineral Resources*. 2020;(7):20–26. (In Russ.)

131. Smirnov S. S. Pacific ore belt within the USSR. *Priroda*. 1946;(2):52–60. (In Russ.)

132. Arkhipov G. I. The state and prospects of subsoil use in the Khabarovsk Territory. *Izvestiya Vysshikh Uchebnykh Zavedenii. Gornyi Zhurnal*. 2010;(1):10–19. (In Russ.)

133. Soloviev S. G., Kryazhev S. G., Dvurechenskaya S.S. Geology, mineralization, stable isotope, and fluid inclusion characteristics of the Vostok-2 reduced W-Cu skarn and Au-W-Bi-As stockwork deposit, Sikhote-Alin, Russia. *Ore Geology Reviews*. 2017;86:338–365. https://doi.org/10.1016/j.oregeorev.2017.02.029

134. Soloviev S. G., Voskresensky K. I., Kryazhev S. G. et al. The superlarge Malmyzh porphyry Cu-Au deposit, Sikhote-Alin, Eastern Russia: igneous geochemistry, hydrothermal alteration, mineralization, and fluid inclusion characteristics. *Ore Geology Reviews*. 2019;113:103–112. https://doi.org/10.1016/j.oregeorev.2019.103112

135. Prilukova V. A., Dorzhiev B. B., Melkiy V. A., Verkhoturov A. A. Geology aspects and type of mineralization of the Central Anadzhakan area (Khabarovsk territory). In: *Oil and Gas Complex: Problems and Solutions*. *Technological Solutions, Geological Structure, Seismicity, Aerospace Monitoring, Geodetic Support Materials. The Third National Scientific and Practical Conference with International Participation*. Yuzhno-Sakhalinsk, Russia, 2–4 December 2020. Yuzhno-Sakhalinsk: Institute of Marine Geology and Geophysics FEB RAS; 2021. Pp. 25–30. (In Russ.)

136. Yushmanov Yu. P. Structure and zonality of Au-Cu mineralization, the Lazurny deposit, Central Sikhote-Alin. *Tikhookeanskaya Geologiya*. 2002;21(2):85–90. (In Russ.)

137. Soloviev S. G., Kryazhev S. G., Avilova O. V. et al. The Lazurnoe deposit in the Central Sikhote-Alin, Eastern Russia: combined shoshonite-related porphyry Cu-Au-Mo and reduced intrusion-related au mineralization in a post-subduction setting. *Ore Geology Reviews*. 2019;112:103063. https://doi.org/10.1016/j.oregeorev.2019.103063

138. Khanchuk A. I., Ratkin V. V., Ryazantseva M. D. et al. *Geology and minerals of the Primorsky Territory: An essay*. Vladivostok: Dalnauka; 1995. 81 p. (In Russ.)

139. Khanchuk A. I., Arkhipov G. I., Ivanov V. V. Copper resources of the Russian Far East: situation, problems and prospects of development. *Vestnik of the Far East Branch of the Russian Academy of Sciences*. 2019;(2):12–24. (In Russ.) https://doi.org/10.25808/08697698.2019.204.2.002

140. Prikhod'ko V.S., Perestoronin A.N., Gur'yanov V.A. et al. Dzhugdzhur-Stanovoy belt of small bodies of mafic-ultramafic and related Cu-Ni sulphide mineralization. *Vestnik Otdeleniya nauk Zemle RAS*. 2010;(2):NZ10005. (In Russ.) https://doi.org/10.2205/2010NZ000054

141. Guryanov V.A., Petukhova L.L., Abrazhevich A.V. et al. The geological position, minerals of rare and noble metals in the ores of the Kun-Manie copper-nickel deposit (southeastern fringe of the Siberian Platform). *Russian Journal of Pacific Geology*. 2022;16(6):525–543. https://doi.org/10.1134/s1819714022060057 (Orig. ver.: Guryanov V.A., Petukhova L.L., Abrazhevich A.V. et al. Geological position, minerals of rare and noble metals in the ores of the Kun-Manie copper-nickel deposit (southeastern fringe of the Siberian Platform). *Tikhookeanskaya Geologiya*. 2022;41(6):3–23. (In Russ.) https://doi.org/10.30911/0207-4028-2022-41-6-3-23)

142. Prikhodko V.S., Gur'yanov V.A., Petukhova L.L., Perestoronin A.N. Sulfide Cu-Ni mineralization of paleo-proterozoic mafite-ultramafites on the South-East of the Aldan-Stanovoi shield. In: *The third international conference "Mafic-ultramafic complexes of folded regions and related deposits"*. Kachkanar, August 28–September 2, 2009 Yekaterinburg: Institute of Geology and Geochemistry named after Academician A.N. Zavaritsky, Ural Branch of the Russian Academy of Sciences. Pp. 111–114. (In Russ.)

143. Gurevich D.V., Belogub E.V., Petrov S.V. et al. Formation model of Cu-Pt-Pd mineralization in the Uralian-Alaskan-type Konder Pt-bearing pluton, Khabarovsk krai, Russia. In: *Rock, Mineral and Ore Formation: Achievements and Prospects of Research. Proceedings for the 90th Anniversary of the IGEM RAS*. Moscow: IGEM RAN; 2020. Pp. 87–90. (In Russ.)

144. Malyshev Y.F., Goroshko M.V., Kaplun V.B. et al. Geophysical characteristics and meallogeny of the eastern Aldan-Stanovoi shield, Far East. *Russian Journal of Pacific Geology*. 2012;6(4):263–274. https://doi.org/10.1134/S1819714012040033 (Orig. ver.: Malyshev Y.F., Goroshko M.V., Kaplun V.B. et al. Geophysical characteristics and meallogeny of the eastern Aldan-Stanovoi shield, Far East. *Tikhookeanskaya Geologiya*. 2012;31(4):3–16. (In Russ.))

145. Kutyrev E.I., Sobolev A.E., Tolstykh A.N., Shuleikin P.D. Copper sandstones and copper basalts from the southern part of the Bilyakcha zone. *Prospect and Protection of Mineral Resources*. 1986;(11):11–13. (In Russ.)

146. Mayboroda A.A. The copper sandstones of the Bilyakchan seam zone: their potential for platinum bearing and stratigraphic issues. *Regional Geology and Metallogeny*. 2007;(30–31):144–152. (In Russ.)

147. Khanchuk A.I. (ed.) *Geodynamics, magmatism and metallogeny of the East of Russia*. Vladivostok: Dalnauka; 2006. Book 1. 572 p. Book 2. Pp. 573–981. (In Russ.)

148. Glukhov A. N., Tyukova E. E. Geology and geochemistry of Oroyok sediment-hosted copper occurrence (Kolyma terrane, northeastern Russia). *Otechestvennaya Geologiya*. 2020;(1):52–65. (In Russ.)

149. Savva N.E., Volkov A.V., Galyamov A.L. et al. Copper shales of the Prikolymsky terrane (North-East of Russia): mineralogical and geochemical features and ore-forming conditions. *Tikhookeanskaya Geologiya*. 2023;42(6):20–38. https://doi.org/10.30911/0207-4028-2023-42-6-20-38 (In Russ.)

150. Kostin A.V. Mineral types of Fe-oxide-Cu-Au ores manifestations Jalkan, Rosomakha and Hurat (Sette-Daban, Eastern Yakutia). *Otechestvennaya Geologiya*. 2016;(6):11–15. (In Russ.)

151. Chitalin A.F., Usenko V.V., Fomichyov Y.V. The Baimskaya ore zone – a cluster of large deposits of non-ferrous and precious metals in the West of the Chukotka autonomous district. *Mineral Recourses of Russia. Economics and Management*. 2013;(6):68–73. (In Russ.)

152. Migachev I.F., Girfanov M.M., Shishakov V.B. The Peschanka copper porphyry deposit. *Ores and Metals*. 1995;(3):48–58. (In Russ.)

153. Nagornaya E.V., Baksheev I.A., Bryzgalov I.A., Yapaskurt V.O. Minerals of the Au-Ag-Pb-Te-Se-S system in copper-molybdenum porphyry deposits in the Nakhodka ore field, Chukotka. *Vestnik Moskovskogo Universiteta. Seria 4: Geologia*. 2012;(4):26–31. (In Russ.)

154. Sabelnikov I.S. Porphyry Cu-Mo miniralization in the eastern part of the Chukotka autonomous okrug. *Modern Problems of Science and Education*. 2013;(5):543–550. (In Russ.)

155. Avilova O.V., Girfanov M.M., Andreev A.V., Starostin I.A. Features of the material composition of ore of copper-porphyry occurrences of the Tanyurer and Olkhovsky districts (Central Chukotka). In: *Scientific and methodological bases of forecasting, exploration and evaluation of deposits of precious and non-ferrous metals, and diamonds. Abstracts of the VII Scientific and Practical Conference*. Moscow, 13–14 April 2017, Moscow: TSNIGRI; 2017. Pp. 56–57. (In Russ.)

156. Глухов А.Н., Тюкова Е.Э. Перспективы расширения минерально-сырьевой базы меди Магаданской области. *Руды и металлы*. 2013;(5):21–33.

Glukhov A.N., Tyukova E.E. Prospectives for development of resources of the copper in the Magadan region. *Ores and Metals*. 2013;(5):21–33. (In Russ.)

157. Kolova E.E., Glukhov A.N., Polzunenkov G.O., Akinin V.V. Porphyry-copper mineralization of Tal'nikovoye ore field (Okhotsk segment of the Okhotsk-Chukotka volcanogenic belt). *Tikhookeanskaya Geologiya*. 2023;42(6):39–61. (In Russ.) https://doi.org/10.30911/0207-4028-2023-42-6-39-61

158. Alekseenko A.V., Korobeynikov S.V., Sidorov V.A. New data on copper-molybdenum-porphyry mineralization in the Omolon Massif. In: *Ore formations of the North-East of the USSR*. Magadan: SVKNII FEB RAS; 1990. Pp. 157–162. (In Russ.)

159. Gorodinsky M.E., Gulevich V.V., Titov V.A. Copper manifestations of the North-East of the USSR. In: *Materials on geology and minerals of the North-East of the USSR*. Magadan: SVKNII DVNTs of the USSR Academy of Sciences; 1978. Pp. 151–158. (In Russ.)

160. Yarotskii G.P., Chotchaev Kh.O. Volcanogens of marginal orogenic belts of the northwestern sector of Northeast Asia. *Geology and Geophysics of Russian South*. 2019;9(3):18–35. (In Russ.) https://doi.org/10.23671/VNC.2019.3.36486

161. Ledneva G.V., Matukov D.I. Timing of crystallization of plutonic rocks from the Kuyul ophiolite terrane (Koryak highland): U-Pb microprobe (SHRIMP) zircon dating. *Doklady Earth Sciences*. 2009;424(1):11–14.

162. Novakov R.M., Sidorov M.D. Nickel-copper-pyrite ore occurrences in the serpentinites of the Eastern Kachatka. *Mining Informational and Analytical Bulletin*. 2016;(S31):13–26. (In Russ.)

163. Kutyev F.Sh., Baykov A.I., Sidorov E.G. et al. Metallogeny of mafic-ultramafic complexes of the Koryak-Kamchatka region. In: *Magmatism and ore content of volcanic belts*. Khabarovsk: ITiG; 1998. Pp. 73–74. (In Russ.)

164. Trukhin Yu.P., Stepanov V.A., Sidorov M.D., Kungurova V.Ye. Shanuch Cu-Ni ore field (Kamchatka). *The Bulletin of the North-East Scientific Center*. 2011;(1):20–26. (In Russ.)

165. Tararin I.A., Chubarov V.M., Moskaleva S.V., Ignat'ev E. K. Geology, mineralogy, and PGE mineralization of the copper-nickel occurrences of the Kvinum ore field, Sredinny range, Kamchatka. *Russian Journal of Pacific Geology*. 2007;1(1):82–97. https://doi.org/10.1134/S1819714007010095 (Orig. ver.: Tararin I.A., Chubarov V.M., Ignat'ev E.K., Moskaleva S.V. Geology, mineralogy, and PGE mineralization of the copper-nickel occurrences of the Kvinum ore field, Sredinny Range, Kamchatka. *Tikhookeanskaya Geologiya*. 2007;1(1):94–110. (In Russ.))

166. Sidorov M.D., Kungurova V.Ye. Determining productivity of ore-magmatic systems within the Quinum-Kuvalorog nickel-bearing zone by the density model (Kamchatka's Median Massif). *The Bulletin of the North-East Scientific Center*. 2019;(2):3–10. (In Russ.) https://doi.org/10.34078/1814-0998-2019-2-3-10

167. Soloviev S.G., Ezhov A.I., Voskresensky K.I. et al. The Kirganik alkalic porphyry Cu-Au prospect in Kamchatka, Eastern Russia: a shoshonite-related, silica-undersaturated system in a late cretaceous island arc setting. *Ore Geology Reviews*. 2021;128:103893. https://doi.org/10.1016/j.oregeorev.2020.103893

168. Gaskov I.V., Borisenko A.S., Babich V.V., Naumov E.A. The stages and duration of formation of gold mineralization at copper-skarn deposits (Altai-Sayan folded area). *Russian Geology and Geophysics*. 2010;51(10):1091–1101. https://doi.org/10.1016/j.rgg.2010.09.001 (Orig. ver.: Gaskov I.V., Borisenko A.S., Babich V.V., Naumov E.A. The stages and duration of formation of gold mineralization at copper-skarn deposits (Altai-Sayan folded area). *Geologiya i Geofizika*. 2010;51(10):1399–1412. (In Russ.))

169. Soloviev S.G., Kryazhev S.G., Dvurechenskaya S.S., Uyutov V.I. Geology, mineralization, fluid inclusion, and stable isotope characteristics of the Sinyukhinskoe Cu-Au skarn deposit, Russian Altai, SW Siberia. *Ore Geology Reviews*. 2019;112:103039. https://doi.org/10.1016/j.oregeorev.2019.103039

170. Soloviev S.G., Voskresensky K.I., Kryazhev S.G. et al. The Ulandryk and related Iron Oxide-Cu-Ree(-Au-U) prospects in the Russian Altai: a large emerging IOCG-type system in a phanerozoic continental setting. *Ore Geology Reviews*. 2022;146:104961. https://doi.org/10.1016/j.oregeorev.2022.104961

171. Han C., Xiao W., Sul B. et al. Mid-late paleozoic metallogenesis and evolution of the Chinese Altai and East Junggar orogenic belt, NW China, Central Asia. *Journal of Geosciences (Japan)*. 2014:59(3):255–274. https://doi.org/10.3190/jgeosci.173

172. Proskurnin V., Petrov O., Paderin P. Taimyr carbonatite province. In: *The 33rd International Geological Congress*. Oslo, Norway, 2008, 6–14 August.

173. Silaev V.I., Proskurnin V.F., Gavrish A.V. Carbonatite complex unusual rocks and mineralization in the Eastern Taimyr. In: *Problems of Mineralogy, Petrography and Metallogeny. Scientific readings in memory of P.N. Chirvinsky*. 2016;19:119–136. (In Russ.)

174. Ugryumov A.N., Dvornik G.P. Alkaline ore-bearing metasomatites of the Rowan massif (Aldan shield). *Sovetskaya Geologiya*. 1984;(9):84–94. (In Russ.)

175. Kochetkov A.Ya. Molybdenum-copper-gold-porphyry deposit Ryabinovoe. *Otechestvennaya Geologiya*. 1993;(7):50–58. (In Russ.)

176. Shatova N.V., Molchanov A.V., Terekhov A.V. Ryabinovoe copper-gold-porphyry deposit (Southern Yakutia): geology, noble gases isotope systematics and isotopic (U-Pb, Rb-Sr, Re-Os) dating of wallrock alteration and ore-forming processes. *Regional Geology and Metallogeny*. 2019;77:75–97. (In Russ.)

177. Bodouin A.Ya., Melnichuk M.S., Petrov G.V., Fokina S.B. Investigation of washability of copper-porphyritic ores of Aldan region. *International Research Journal*. 2018;(3):68–74. (In Russ.) https://doi.org/https://doi.org/10.23670/IRJ.2018.69.015

178. Petrov O.V., Molchanov A.V., Terekhov A.V., Shatov V.V. Morozkinskoe gold deposit (geological structure and short story of the exploration). *Regional Geology and Metallogeny*. 2018;75:112–116. (In Russ.)

179. Soloviev S.G., Kryazhev S.G., Dvurechenskaya S.S. Geology, mineralization, and fluid inclusion characteristics of the Agylki reduced tungsten (W-Cu-Au-Bi) skarn deposit, Verkhoyansk fold-and-thrust belt, Eastern Siberia: tungsten deposit in a gold-dominant metallogenic province. *Ore Geology Reviews*. 2020;120:103452. https://doi.org/10.1016/j.oregeorev.2020.103452

180. Zhegalov Yu.V. Commander Islands. In: *Geology of the USSR. Kamchatka, the Kuril Islands and the Commander Islands*. 1964;XXXI(I):645–660. (In Russ.)

Information about the authors

Grigory Yu. Boyarko – Dr. Sci. (Econ.), Cand. Sci. (Geol. and Min.), Professor, National Research Tomsk Polytechnic University, Tomsk, Russian Federation; ORCID 0000-0002-0715-7807, Scopus ID 56350674500; e-mail gub@tpu.ru

Anna M. Lapteva – Cand. Sci. (Geol. and Min.), Associate Professor, Head of the Department of Analysis of the Mineral Resource Complex, All-Russian Scientific Research Institute of Raw Mineral Synthesis (VNIISIMS), Moscow, Russian Federation; e-mail lapteva@vims-geo.ru

Liudmila M. Bolsunovskaya – Cand. Sci. (Philolog.), Assistant Professor, National Research Tomsk Polytechnic University, Tomsk, Russian Federation; ORCID 0000-0002-1499-8970, Scopus ID 56350747600; e-mail bolsunovskl@tpu.ru

Received 14.05.2024
Revised 07.06.2024
Accepted 10.06.2024

eISSN 2500-0632
https://mst.misis.ru/
2024;9(4):387–394

MINING ROCK PROPERTIES. ROCK MECHANICS AND GEOPHYSICS

Research paper

https://doi.org/10.17073/2500-0632-2023-09-160
UDC 622.023.23:556.16(470.21)

Effect of water inflows on the strength characteristics of the Lovozero rare-metal deposit rocks

A. I. Kalashnik ✉

Mining Institute of the Kola Scientific Center of the RAS, Apatity, Russian Federation

✉ *a.kalashnik@ksc.ru*

Abstract

The Lovozero rare-metal deposit is represented by a series of sheet-like ore bodies of small and medium thickness exposing on the northwestern slopes of the Lovozero massif. The purpose of the work is to assess the impact of water inflows on the strength characteristics of the rocks of the Lovozero rare-metal deposit developed by the Karnasurt mine. The data on water inflow into Karnasurt mine workings, which exploits two ore bodies of the Lovozero rare-metal deposit, are considered. Statistical processing of the data on water volumes collected by the mine over the latest 4 years was performed, with assessment of their changes during a calendar year. The peculiarities associated with calendar climatic changes were identified. The main purpose of the study was to assess the effect of water inflows on the strength characteristics of the rocks composing the support pillars. The analysis and calculations of precipitation accumulation within the mine allotment and water inflows into the mine workings were performed and compared with actual data on mine waters. The samples of the most representative rocks of the deposit were collected and tested for dry and water-saturated compressive and tensile strength. The quantitative indicators of the changes in the strength characteristics of rocks due to water saturation were determined. It was found that the water saturation led to a decrease in the rock strength by up to 10–20%, especially for compressive strength values.

Keywords

mine, extraction, water inflows, rocks, pillars, properties, strength, water saturation, rockburst hazard, Lovozero rare metal deposit, Karnasurt mine

Acknowledgments

The paper was written on the basis of initial data prepared by Alexander V. Lovchikov, Dr. Sci. (Eng.). For more than 60 years A.V. Lovchikov dealt with the issues of the geotechnical safety of the Lovozero deposit mining, and, in fact, the last task of his life was to study the effect of rock watering on the stability and rockburst hazard of the pillars of the Karnasurt mine.

For citation

Kalashnik A.I. Effect of water inflows on the strength characteristics of the Lovozero rare-metal deposit rocks. *Mining Science and Technology* (*Russia*). 2024;9(4):387–394. https://doi.org/10.17073/2500-0632-2023-09-160

СВОЙСТВА ГОРНЫХ ПОРОД. ГЕОМЕХАНИКА И ГЕОФИЗИКА

Научная статья

Влияние водопритоков на прочностные характеристики пород Ловозерского редкометалльного месторождения

А.И. Калашник ✉

Горный институт Кольского научного центра РАН, г. Апатиты, Российская Федерация

✉ *a.kalashnik@ksc.ru*

Аннотация

Ловозерское редкометалльное месторождение представлено свитой пластообразных пологопадающих рудных залежей малой и средней мощности, выходящих на поверхность на северо-западных склонах Ловозерского массива. Целью работы является оценка влияния водопритоков на прочностные характеристики пород Ловозерского редкометалльного месторождения, разрабатываемого рудником «Карнасурт». Рассмотрены данные о поступлении воды в горные выработки рудника «Карнасурт», отрабатывающего две согласно залегающие рудные залежи Ловозерского редкометалльного месторождения. Выполнена статистическая обработка объемов воды, собираемой рудником за последние 4 года, с оценкой динамики их поступления в течение календарного года. Выявлены особенности, связанные с календарными климатическими изменениями. Основной целью работы являлась оценка влияния водопритоков на прочностные характеристики пород, слагающие опорные целики. Выполнены анализ и расчеты осадконакопления в пределах горного отвода рудника и формирующихся водопритоков в горные выработки, а также сравнение их с фактическими данными по рудничной воде. Отобраны образцы наиболее представительных пород месторождения и выполнены испытания их на прочность на сжатие и растяжение в сухом и водонасыщенном состояниях. Определены количественные показатели изменения прочностных характеристик пород вследствие водонасыщения. Установлено, что водонасыщение привело к снижению прочности пород до 10–20 %, особенно для значений на сжатие. Полученные результаты дают основание для необходимости учета обводненности пород при расчете устойчивости как опорных целиков, так и обнажений пород в выработках рудника «Карнасурт».

Ключевые слова
рудник, добыча, водопритоки, горные породы, целики, свойства, прочность, водонасыщенность, удароопасность, Ловозерское редкометалльное месторождение, рудник «Карнасурт»

Благодарности
Статья написана на основе исходных данных, подготовленных доктором технических наук Ловчиковым Александром Васильевичем. А.В. Ловчиков более 60 лет занимался вопросами геомеханической безопасности отработки Ловозерского месторождения, и фактически последней задачей его жизни было исследование влияния обводненности пород на устойчивость и удароопасность целиков рудника Карнасурт.

Для цитирования
Kalashnik A.I. Effect of water inflows on the strength characteristics of the Lovozero rare-metal deposit rocks. *Mining Science and Technology* (*Russia*). 2024;9(4):387–394. https://doi.org/10.17073/2500-0632-2023-09-160

Introduction

The Lovozero rare-metal deposit is represented by a series of sheet-like ore bodies of small and medium thickness exposing on the northwestern slopes of the Lovozero massif [1]. At present, two ore bodies (I-4 (urtites) and II-4 (malignites)) with a thickness of 1.0–1.2 m each, occurring at a vertical distance of about 100 m from each other, are being mined by the Karnasurt mine. The mine applies room-and-pillar mining method with breast stoping and support of an undercut rock strata by chain pillars. Both bodies are mined by panels along their strike. The panels are cut at 20–40 m vertical intervals by drifts (adits at the upper levels), with leaving support chain pillars near the drifts. The panels are divided into blocks 60–120 m long, between which inter-block support chain pillars are left [1]. The deposit is classified as rockburst hazardous in mining conditions and characterized by increased seismicity and manifestations of tectonic rockbursts [2, 3].

At the current stage of the deposit mining, the support near-drift and inter-block pillars are 3 to 10 m wide. Their total area for each mined ore body can reach up to 25% of the mined out space. The mining depth is the lower ore body II-4 ranges from 30 m to the surface at the upper levels to 700 m at the deepest level +280 m.

The Karnasurt mine has a large mining allotment: the length along the lower ore body II-4 is about 8 km, with a maximum width of 2.6 km. Moreover, the issue of adding another 1.5 km to the west of the mining allotment is being considered [2]. Thus, the length of the mine field in the lower ore body at the final stage of development will reach 10 km with a width of up to 2.6 km, which in terms of area will amount to 26 km^2. The area of the upper ore body is slightly smaller, but of the same order of magnitude. This allows to confidently categorize the Karnasurt mine as one of the largest mines in the western part of the Russian sector of the Arctic.

At present, ore body II-4 within the mining allotment is only half mined-out, from the outcrops to the level +280 m. The dimensions of the mined out area are 6.5 km along the strike with a maximum width down dip of 1.3 km. In ore body I-4, mined out only in the Karnasurt area, the length of the mined-out space is 3.1 km along the ore body strike, with a maximum down dip width of 0.8 km and a depth of 50 to 350 m to the surface.

Water inflows into the Karnasurt mine workings are mainly due to surface precipitation. Water formed on the day surface due to rainfall, spring snowmelt and runoff from nearby mountains penetrates through numerous joints and structural heterogeneities in the overlying rock mass and enters the mine workings.

Water from mine workings of all mining areas is collected at the drifts' haulage levels and brought to the surface of the drifts – the drifts' floor – through the drifts' drainage channels. Thus, water flows through the floor of all mine drifts to lower levels. They are partially collected at the haulage levels and pumped from the mine workings to the surface by water pumping stations. As for the remaining volumes, both further water infiltration deep down into the underlying rock mass and abundant widespread water saturation of workings floor and pillar walls occur.

The issues of water inflow generation at coal seams mining by underground method were investigated in works [4, 5], including changes in surface natural sources [6, 7] and the mechanism of surface water infiltration into mine workings [8]. For ore deposits in hard rock masses, the effect of rock water content on the energy saturated state [9] and the manifestations of seismicity [10] has been considered. The peculiarities of rock water content were investigated in [11, 12], and the effect of the water content factor on the sustainable state and safety of the natural environment was studied in [13–15].

At the same time, taking into account that for the conditions considered in this work the water flows move directly along the lower parts of the support near-drift pillars of the rockburst-prone deposit, it is necessary to pay special attention to the effect of water content of rocks. Therefore, the purpose of the work is to assess the impact of water inflows on the strength characteristics of the rocks of the Lovozero rare-metal deposit developed by the Karnasurt mine.

Findings

According to the hydrogeological service of the Karnasurt mine, the volume of water collected by the mine is about 8 million m3 per year. At the same time, the dynamics of the volumes for the latest 4 years of observations remains practically monotonous: from January to May the volumes decrease, in June they increase significantly, followed by slightly lower values in July–September, and from October to December the volumes of water inflows decrease again (Fig. 1).

The histograms on the figure below show that the monthly water inflow into the mine workings ranges from 40 to 110 thousand m^3. The least amount of the water inflow, from 40 to 50 thousand m^3, is observed in May each year. This is due to the fact that from October to April precipitation falls as snow and due to negative temperatures accumulates on the surface without infiltration of water from the surface into the mine workings. The largest amount of the water inflows, between 70,000 and 110,000 m^3, occurs in June–September (summer–autumn period) of each year. It is obvious that the increase in the amount of water entering the mine during summer and autumn period is due to both intensive snow melting (in May–June) on the mountain slopes within the mine field surface and precipitation in the form of rain during this period (Fig. 2). Data on rain and snow precipitation volumes for the Karnasurt mine allotment area during the calendar year were obtained based on the analysis and processing of the information from the following sources[1].

[1] Atlas of the Murmansk region, 1971; Report on the environmental condition and protection in the Murmansk Region in 2022. 2023, 151 p. (In Russ.) URL: https://ru.weatherspark.com/y/98660/Обычная-погода-в-Ревда-Россия-весь-год

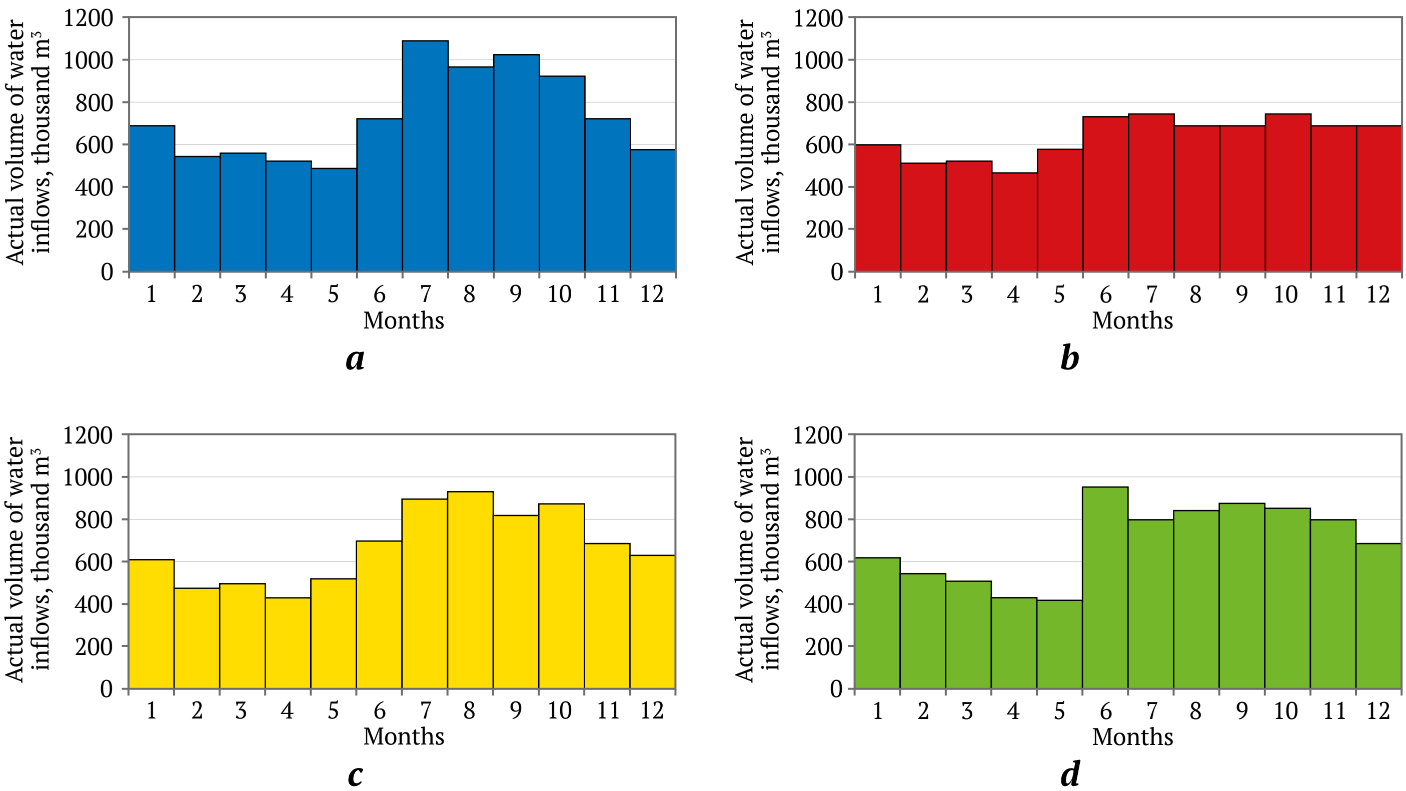

Fig. 1. Data on actual volumes of water collected and pumped out by the Karnasurt mine: *a* – 2017; *b* – 2018; *c* – 2019; *d* – 2020

For comparative analysis, the dynamics of total precipitation volumes on the surface of the mining allotment and actual volumes of water collected in the mine workings for 2017–2020 were considered (Fig. 3). The analysis of the data presented in Fig. 3 confirms the above mentioned opinion about the predominant effect of two periods: snow accumulation (approximately 2,400–3,000 thousand m^3/month from October to April) and snowmelt (May–June), as well as rainfall (approximately 1,200–1,800 thousand m^3/month from May to September).

The calculations have determined that during the period from October through April, snow accumulation on the mine allotment exceeds 21,700 thousand m. At the same time, the volume of actual water inflows into the mine workings decreases from 800 to almost 400 thousand m^3 due to reduced and virtually no water infiltration from the surface. The abundant snowmelt and rains in May–June lead to a sharp, more than 2-fold (from 400 to 850 thousand m^3/month) increase in water inflows into mine workings, reaching 70–80% of the surface precipitation. Such volumes of water inflows are recorded monthly from May until October, when rainfall is replaced by snowfall and negative ground temperature is established with subsequent decrease through April of the next year.

Thus, water inflows into the mine workings are generated by rainfall and snowmelt during periods with positive air and soil temperatures, as well as from natural surface water bodies and underground aquifers recharged by precipitation. The nature of their accumulation is more gradual than for the precipitation due to the above mentioned reasons. Visually, the boundary variations in the water inflow volumes clearly correlates with the identified climatic periods (see Fig. 3).

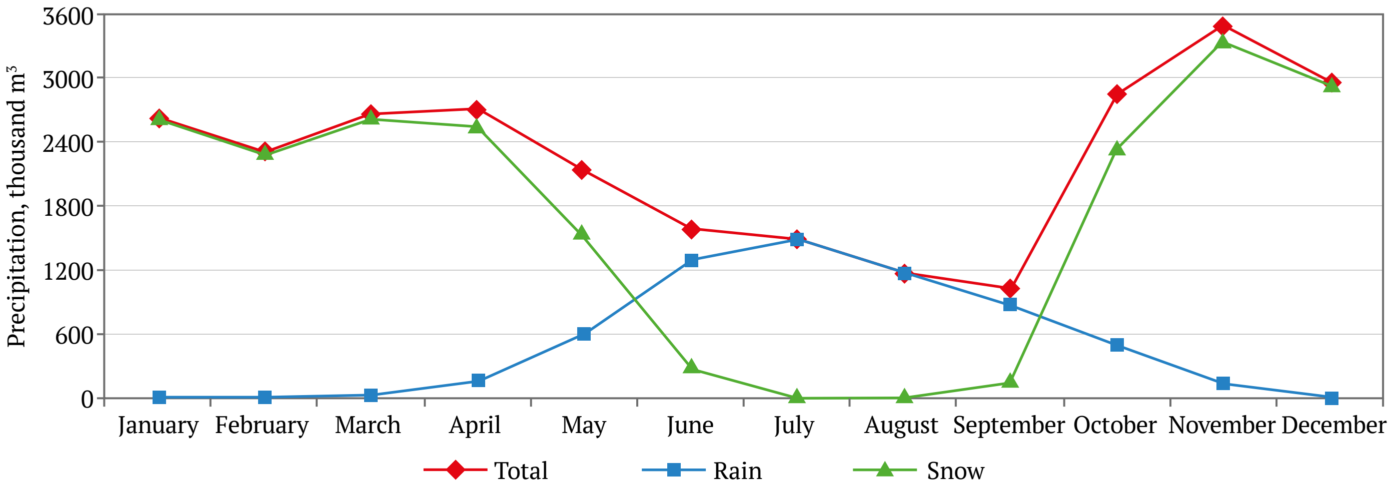

Fig. 2. Distribution of precipitation volumes on the surface of the Karnasurt mine allotment during a calendar year

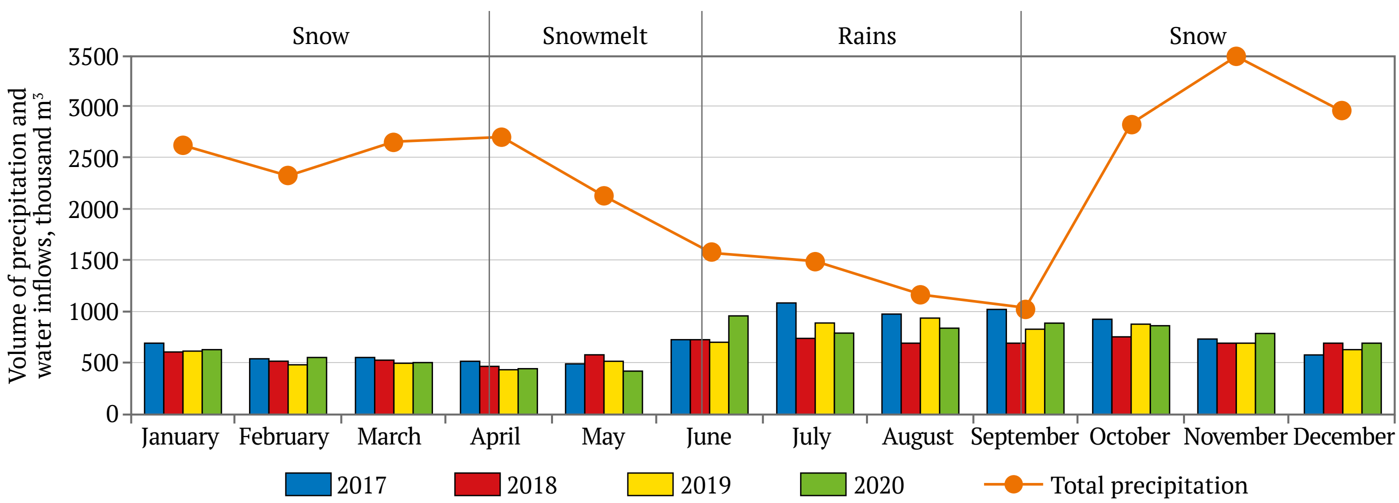

Fig. 3. Dynamics of total precipitation volumes on the surface of the mining allotment and actual volumes of water collected in the mine workings for 2017–2020

Special tests were conducted on rock samples to determine the effect of water saturation on the strength properties of the mine rocks. At ore body I-4, urtite rock hand specimens were taken as the most common rock variety in the drift at level +400 m (survey mark PK4), from which rock samples for testing were subsequently produced. For each type of test, 8–9 cube-shaped specimens (34 in total) with a cube face length of 4 cm were produced. The samples for tests in water-saturated condition were placed for a month into a vessel with water, and then tested for tension and compression. The specimens were tested for compression and tension in dry and water-saturated conditions in accordance with GOSTs[2].

The results of the specimens' compression and tensile tests in dry condition are given in Tables 1 and 2. As can be seen from these tables, the established value of compressive strength, which is σ_c = 181 MPa, and the value of tensile strength

[2] GOST 21153.2–84 Rocks. Methods for determining uniaxial compressive strength (Description update date: 01.07.2023); GOST 21153.3–85 Rocks. Methods for determining uniaxial tensile strength (Description update date: 01.07.2023).

Table 1

Results of dry rock specimens compression strength tests

Index	X, cm	Y, cm	Z, cm	Volume, cm^3	Weight, g	Bulk density, g/cm^3	Loading area, cm^2	Rupturing load, kN	Ultimate compressive strength, MPa
2	4.53	4.57	4.60	95.1	247.54	2.60	20.67	374.9	145
3	4.52	4.49	4.57	92.8	242.05	2.61	20.29	408.2	161
4	4.52	4.53	4.59	93.7	243.65	2.60	20.44	579.7	227
5	4.56	4.70	4.58	98.1	248.73	2.53	21.43	520.0	194
6	4.52	4.51	4.64	94.5	246.40	2.61	20.39	494.4	194
11	4.56	4.52	4.61	94.9	229.60	2.42	20.60	493.6	192
14	4.50	4.50	4.60	93.3	243.26	2.61	20.28	358.6	141
16	4.51	4.53	4.54	92.8	242.42	2.61	20.44	497.4	195
17	4.65	4.65	4.54	98.2	259.51	2.64	21.61	489.5	181
Min	4.50	4.49	4.54	92.8	229.60	2.42	20.28	358.6	141
Max	4.65	4.70	4.64	98.2	259.51	2.64	21.61	579.7	195
Average	4.54	4.56	4.59	94.82	244.80	2.58	20.68	468.48	181.11

Table 2

Results of dry rock specimens tensile strength tests

Index	X, cm	Y, cm	Z, cm	Volume, cm^3	Weight, g	Bulk density, g/cm^3	Loading area, cm^2	Rupturing load, kN	Ultimate compressive strength, MPa
1	4.56	4.67	4.56	97.1	254.92	2.26	21.30	39.4	19
7	4.66	4.56	4.62	98.2	245.20	2.50	21.27	31.9	15
8	4.55	4.50	4.59	94.1	247.63	2.63	20.50	26.9	13
9	4.63	4.56	4.62	97.4	244.90	2.52	21.08	30.1	14
10	4.55	4.56	4.61	95.5	248.27	2.60	20.72	42.5	21
12	4.56	4.56	4.60	95.7	250.62	2.62	20.82	31.5	15
13	4.62	4.55	4.59	96.4	242.00	2.51	20.98	19.3	9
15	4.57	4.53	4.59	95.1	231.85	2.44	20.72	17.7	9
18	4.54	4.54	4.63	95.4	250.47	2.62	20.59	29.3	14
Min	4.54	4.50	4.56	94.1	231.85	2.26	20.50	17.7	9
Max	4.66	4.67	4.63	98.2	254.92	2.63	21.30	42.5	21
Average	4.58	4.56	4.60	96.10	246.21	2.52	20.89	29.84	14.33

σ_t = 14.3 MPa correlate well with similar data of previous studies [1, 2].

The water-saturated specimens for the compression and tensile tests had the same dimensions as dry ones, but due to water saturation their weight increased slightly (3–5%). The results of their tests are presented in Tables 3 and 4.

Findings Discussion

For detailed analysis, the strength properties of all the tested specimens were plotted and ranked according to the values obtained (Fig. 4). The solid line indicates the mean value; the dotted line indicates a 20% decrease from the mean.

Fig. 4 shows that water saturation of the rocks reduced their compressive strength by 20% in general, and by 40% for two samples. At the same time, the lower compressive strength remained rather high, above 110 MPa.

The tensile strength of the water-saturated specimens also generally decreased, but to a lesser extent, and the lower limit did not fall below 10 MPa. For visual comparison, the data of statistical processing are shown in Fig. 5.

Table 3

Results of water-saturated rock specimens compression strength tests

Index	Loading area, cm²	Rupturing load, kN	Ultimate compressive strength, MPa
4	20.68	417.3	161
5	21.15	376.0	142
7	20.82	360.5	138
8	21.22	441.2	166
9	21.14	381.8	145
10	20.19	279.0	111
11	20.80	458.8	176
14	21.44	297.6	111
Min	20.19	297.6	111
Max	21.44	458.8	176
Average	20.93	376.525	143.75

Table 4

Results of water-saturated rock specimens tensile strength tests

Index	Loading area, cm²	Rupturing load, kN	Tensile strength, MPa
1	21.24	23.9	11
2	20.80	28.6	14
3	20.13	32.6	16
6	20.87	30.6	15
12	21.30	31.9	15
13	20.53	27.0	13
15	20.99	27.6	13
16	21.28	30.8	14
Min	20.13	23.9	11
Max	21.30	32.6	16
Average	20.89	29.13	13.88

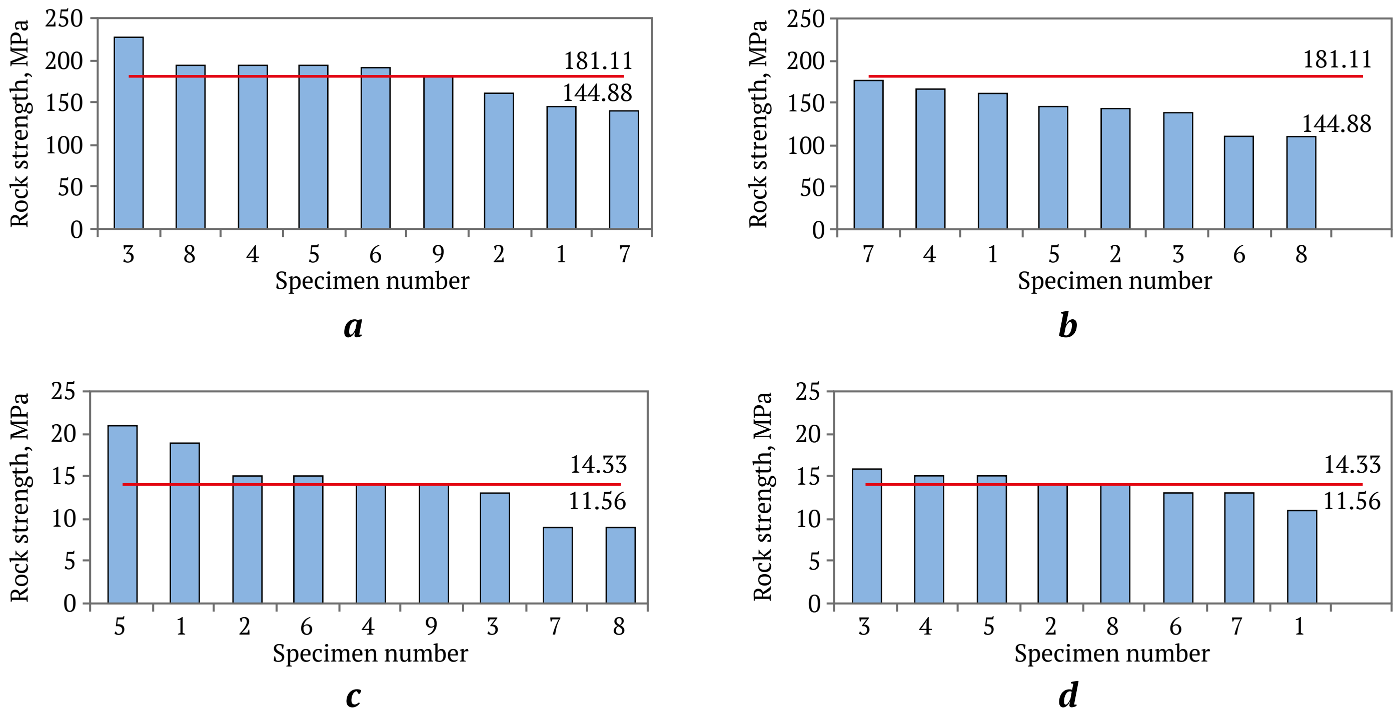

Fig. 4. Distribution of tested specimen compression (top row) and tensile strength values and tension tests: *a*, *c* – dry rock; *b*, *d* – water-saturated rock

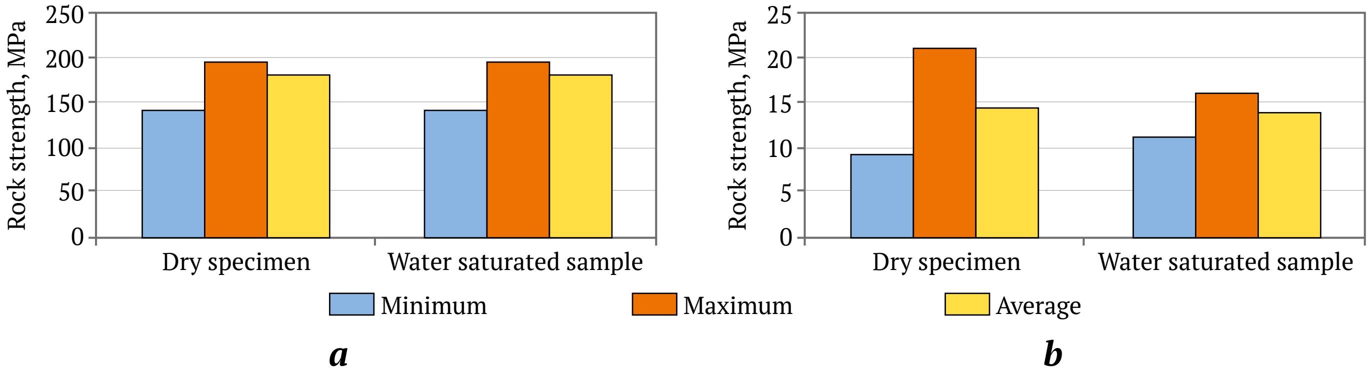

Fig. 5. Statistical distribution of strength characteristics of tested specimens: *a* – compression strength; *b* – tensile strength

Thus, the tests results showed that water saturation reduces compressive and tensile strength of rocks by 10 to 20% or more. This circumstance should be taken into account when calculating the stability of both support pillars and rock outcrops in the Karnasurt mine workings, which are subjected to abundant water saturation.

Conclusion

The data of actual water volumes collected in the workings of the Karnasurt mine over the latest 4 years were processed and analyzed. It was determined that the annual volume of the collected water reached 8 million m^3 with distribution by months in accordance with seasonal-climatic precipitation. The analysis and calculations of the precipitation within the mine allotment and the water inflows into the mine workings were performed. They were compared with the actual data on mine water regime. The specimens of the most representative rocks of the deposit were collected, from which 34 cubes with dimensions of 4×4×4 cm were produced, half of which were placed into water for a month. The specimens (8–9 for each condition and test) were tested for compressive and tensile strength in dry and water-saturated conditions. It was found that the water saturation led to a decrease in the rock strength by up to 10–20%, especially for compressive strength values. The results obtained give the grounds for the necessity to take into account the water content of rocks when calculating the stability of both support pillars and rock outcrops in the Karnasurt mine workings.

References

1. Bessonov I.I., Boborykin V.N., Kalashnik A.I. et al. *Improving the technology of underground mining of thin ore deposits of the Kola Peninsula*. Monograph. Apatity: Kola Science Centre AS SSSR Publ.; 1989. 156 p. (In Russ.)
2. Lovchikov A.V. *The strongest mining-tectonic impact in underground mines and mines in Russia: Umbozero mine, August 17, 1999* (*magnitude m = 5, energy class k = 11.8*). Monograph. Apatity: Kola Science Centre of the Russian Academy of Sciences Publ.; 2022. 127 p. (In Russ.) https://doi.org/10.37614/978.5.91137.456.3
3. Adushkin V.V., Lovchikov A.V., Goev A.G. The occurrence of a catastrophic rockburst at the Umbozero Mine in the Lovozero Massif, Central Part of the Kola Peninsula. *Doklady Earth Sciences*. 2022;504(1):85–90. (In Russ.) https://doi.org/10.31857/S2686739722050036
4. Purgina D.V., Kuzevanov K.I. Water inflow into mine under the influence of external boundary conditions at coal deposit exploitation (Kuzbass). *Izvestiya Tomskogo Politekhnicheskogo Universiteta. Inzhiniring Georesursov*. 2018;329(4):79–96. (In Russ.)
5. Gui H., Lin M., Song X. Identification and application or roof bed separation (water) in coal mines. *Mine Water and the Environment*. 2018;37(2):376–384. https://doi.org/10.1007/s10230-018-0518-0
6. Davis A., Zhan G., Sims N. et al. Is treatment of mine dewatering water necessary prior to rapid infiltration basin recharge? A case study. *Mine Water and the Environment*. 2022;41:58–73. https://doi.org/10.1007/s10230-021-00839-2
7. Enany P., Shevchenko O., Drebenstedt C. Experimental evaluation of airlift performance for vertical pumping of water in underground mines. *Mine Water and the Environment*. 2021;40:970–979. https://doi.org/10.1007/s10230-021-00807-w

8. Fan K., Li W., Wang Q. et al. Formation mechanism and prediction method of water inrush from separated layers within coal seam mining: A case study in the Shilawusu mining area, China. *Engineering Failure Analysis*. 2019;103:158–172. https://doi.org/10.1016/j.engfailanal.2019.04.057
9. Kuznetzov N.N. Study of watercut influence on the energy saturated state of hierarchically block geological medium. *Problemy Nedropol'zovaniya*. 2017;(1):64–71. (In Russ.) https://doi.org/10.18454/2313-1586.2017.01.064
10. Kozyrev A.A., Batugin A.S., Zhukova S.A. Influence of water content on seismic activity of rocks mass in apatite mining in Khibiny. *Gornyi Zhurnal*. 2021;(1):31–36. (In Russ) https://doi.org/10.17580/gzh.2021.01.06
11. Kalashnik A.I., Dyakov A.Yu. Evaluation of rock disturbance by GPR sensing using water saturation for contrast. *Vestnik MGTU. Trudy Murmanskogo Gosudarstvennogo Tekhnicheskogo Universiteta.* 2019;22(1):129–137. (In Russ.) https://doi.org/10.21443/1560-9278-2019-22-1-129-137
12. Auzina L.I. Water encroachment features of Vitim-Patom highland gold deposits. *Izvestiya Sibirskogo Otdeleniya Sekcii Nauk o Zemle Rossijskoj Akademii Estestvennyh Nauk. Geologiya, Razvedka i Razrabotka Mestorozhdenij Poleznyh Iskopaemyh*. 2017;40(1):127–136. (In Russ.)
13. Kalashnik A., Zaporozhets D. Information Technologies in Monitoring of Urbanized Territories in the Western Russian Arctic Sector. *Lecture Notes in Networks and Systems*. 2023;509:837–844. https://doi.org/10.1007/978-3-031-11058-0_84
14. Wu L., Bai H., Ma D. Prediction and Prevention of Water Inrush Hazards from Bed Separation Space. *Mine Water and the Environment*. 2021;40:657–670. https://doi.org/10.1007/s10230-020-00748-w
15. Melikhov M.V., Kalashnik A.I. Space monitoring of geological risks in the mining industry of the Barents Euro-Arctic region of Russia. *Russian Mining Industry.* 2023;(S1):128–134. (In Russ.) https://doi.org/10.30686/1609-9192-2023-S1-128-134

Information about the author

Anatoly I. Kalashnik – Dr. Sci.(Eng.), Head of Laboratory, Mining Institute of the Kola Scientific Center of the RAS, Apatity, Murmansk region, Russian Federation; ORCID 0000-0001-6567-2877, Scopus ID 7004943696, Researcher ID E-3197-2017; e-mail a.kalashnik@ksc.ru

Received 29.09.2023
Revised 20.03.2024
Accepted 01.04.2024

eISSN 2500-0632
https://mst.misis.ru/

SAFETY IN MINING AND PROCESSING INDUSTRY AND ENVIRONMENTAL PROTECTION

Research paper

https://doi.org/10.17073/2500-0632-2024-03-235
UDC 622.807:613.62:614.8.084

Assessing dust concentration at the workplace of a crushing and screening plant operator for special labor conditions evaluation

E. A. Korol[1], E. N. Degaev[1], D. S. Konyukhov[2,3] ✉
[1] National Research Moscow State University of Civil Engineering, Moscow, Russian Federation
[2] Mosinzhproekt JSC, Moscow, Russian Federation
[3] MIREA – Russian Technological University, Moscow, Russian Federation
✉ gidrotehnik@inbox.ru

Abstract
The mining industry is one of the key sectors of the Russian economy, supplying other industries with essential raw materials. However, this sector is characterized by harsh working conditions that may adversely affect workers' health. Exposure to harmful substances and significant physical workloads contribute to the development of occupational diseases. To ensure safety in production processes and protect the health of mining industry workers, it is necessary to conduct a special labor conditions assessment. This assessment allows for determining the level of harmfulness and hazard in workplaces, as well as developing measures to reduce the negative impact on workers' health. The purpose of this study is to assess dust concentration at the workplace of a crushing and screening plant operator as part of a special labor conditions evaluation. Dust concentration at the operator's workplace was measured using a standard gravimetric method. The testing was conducted in four stages and lasted 400 minutes, which is 83% of the total work shift duration. Data analysis revealed an exceedance of the permissible dust concentration by a factor of 1.28. The labor conditions class (subclass) was established as 3.1. It was found that the average dust concentrations varied by a factor of 3–4 across different testing stages due to the intensity and direction of air velocity at the production site. Based on the obtained data, dust concentrations at the workplace were predicted according to air velocity at the site, with an approximation accuracy of $R^2 = 0.95$. It was determined that the maximum allowable air velocity at the site should not exceed 2.6 m/s. Using approximated data, it was forecasted that, in the absence of air movement, the dust concentration at the operator's workplace would remain at 0.5 mg/m^3. To reduce dust concentration at the operator's workplace, comprehensive measures to minimize dust generation at the crushing plant are necessary, including washing vehicle wheels, installing dust suppression systems, and replacing the open belt conveyor with a closed one. To prevent the development of occupational diseases, operators are advised to use personal respiratory, skin, and eye protection throughout the shift.

Keywords
production, crushed stone, crushing and screening plant, dust, concentration, emissions, dust concentration, dust generation, operator, labor conditions, harm, forecasting, protection

For citation
Korol E.A., Degaev E.N., Konyukhov D.S. Assessing dust concentration at the workplace of a crushing and screening plant operator for special labor conditions evaluation. *Mining Science and Technology (Russia)*. 2024;9(4):395–405. https://doi.org/10.17073/2500-0632-2024-03-235

ТЕХНОЛОГИЧЕСКАЯ БЕЗОПАСНОСТЬ В МИНЕРАЛЬНО-СЫРЬЕВОМ КОМПЛЕКСЕ И ОХРАНА ОКРУЖАЮЩЕЙ СРЕДЫ

Научная статья

Определение запыленности рабочего места оператора дробильно-щебеночного завода в целях специальной оценки условий труда

Е. А. Король[1], Е. Н. Дегаев[1], Д. С. Конюхов[2,3] ✉
[1] *Национальный исследовательский Московский государственный строительный университет, г. Москва, Российская Федерация*
[2] *АО «Мосинжпроект», г. Москва, Российская Федерация*
[3] *МИРЭА – Российский технологический университет, г. Москва, Российская Федерация*
✉ gidrotehnik@inbox.ru

Аннотация
Горнодобывающая отрасль является одним из ключевых секторов экономики России, обеспечивая другие отрасли необходимым сырьем и материалами. Однако эта отрасль характеризуется тяжёлыми условиями труда, которые могут негативно сказаться на здоровье работников. Воздействие

вредных веществ и значительные физические нагрузки способствуют развитию профессиональных болезней. Для обеспечения безопасности производственных процессов и сохранения здоровья работников горнодобывающей отрасли необходимо проведение специальной оценки условий труда. Эта оценка позволяет определить уровень вредности и опасности на рабочих местах, а также разработать меры по снижению негативного воздействия на здоровье работников. Целью работы является определение запыленности рабочего места оператора дробильно-щебеночного завода в рамках специальной оценки условий труда. Определение концентрации пыли в воздухе рабочего места оператора дробильно-щебеночного завода производили в соответствии со стандартной весовой методикой. Испытания проводились в четыре этапа и длились 400 мин, что составляет 83% от общего времени рабочей смены. По результатам обработки данных выявлено превышение предельно допустимой концентрации пыли в 1,28 раза. Установлен класс (подкласс) условий труда – 3.1. Установлено, что средние концентрации пыли на разных этапах испытания различаются в 3–4 раза, что связано с интенсивностью и направлением ветра на производственной площадке. По полученным данным спрогнозированы концентрации пыли на рабочем месте в зависимости от скорости ветра на производственной площадке с величиной достоверности аппроксимации R^2 = 0,95. Установлено, что максимально допустимая скорость ветра на производственной площадке не должна быть выше 2,6 м/с. С помощью аппроксимированных данных спрогнозировано, что при отсутствии ветра на производственной площадке концентрация пыли в воздухе рабочего места оператора сохранится на уровне 0,5 мг/м³. Для снижения запыленности рабочего места оператора необходимы комплексные мероприятия по сокращению пылеобразования на дробильно-сортировочном заводе, включающие мойку колес автомобильного транспорта, установку систем подавления пыли и замену открытого ленточного конвейера на закрытый. Для предотвращения развития профессиональных заболеваний операторам рекомендуется использовать средства индивидуальной защиты органов дыхания, кожи и глаз на протяжении всей смены.

Ключевые слова
производство, щебень, дробильно-щебеночный завод, пыль, концентрация, выбросы, запыленность, пылеобразование, оператор, условия труда, вред, прогнозирование, защита

Для цитирования
Korol E.A., Degaev E.N., Konyukhov D.S. Assessing dust concentration at the workplace of a crushing and screening plant operator for special labor conditions evaluation. *Mining Science and Technology* (*Russia*). 2024;9(4):395–405. https://doi.org/10.17073/2500-0632-2024-03-235

Introduction

According to data from the Federal Labor and Employment Service of the Russian Federation[1], the mining industry remains the most hazardous sector of economic activity [1, 2]. This is primarily due to the specifics of production processes and the challenging climatic and geographical conditions. In 2023, crushed stone production exceeded 221 million tons, representing a 24.5% increase compared to 2017 (Fig. 1). Crushed stone is one of the primary materials used in construction and the production of building materials. A decline in extraction and production rates is not expected in the coming years due to the implementation of various large-scale federal projects. Consequently, the industry will need to expand its capacity and create more jobs [3, 4].

[1] Ministry of Labor and Social Protection of the Russian Federation. Results of Labor Conditions and Occupational Safety Monitoring in the Russian Federation, 2022. Moscow, 2022.

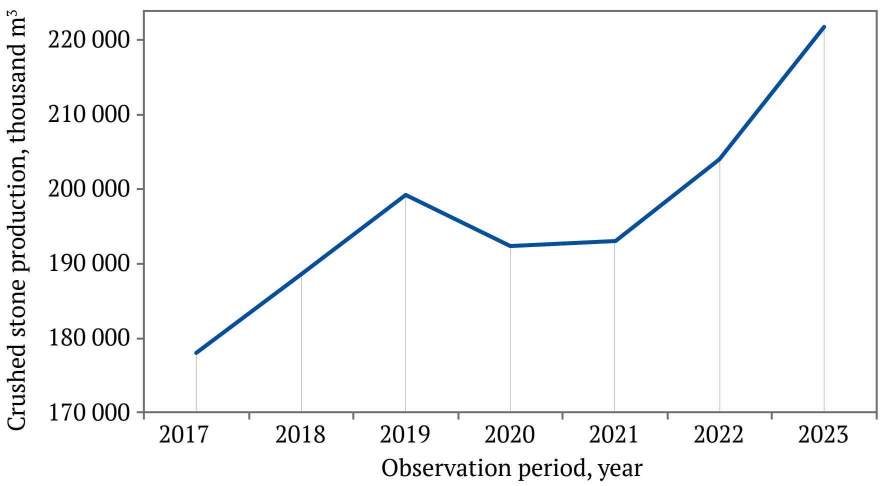

Fig. 1. Crushed stone production dynamics in Russia from 2017 to 2023

Crushed stone production involves a range of occupational risks and health hazards for workers [4, 5]. Various professions operate within crushing and screening plant, each with specific health risks. For example, dump truck and loader drivers are exposed to noise and vibration, which can lead to hearing loss and vibration disease. However, the most hazardous factor in crushed stone production is dust, which consists of 60% or more silicon dioxide (SiO_2). Crusher and screen operators work in high-dust environments, which can lead to silicosis and other lung diseases [6, 7].

Research in this area primarily focuses on the effects of silica dust on human health and on measuring dust concentration across the entire plant or quarry at various distances from pollution sources. This data is used for modeling and developing dust reduction methods. For instance, V.S. Kuznetsov and L.F. Sulamanidze note that during crushing and screening plant operations, dust concentration at the edge of the sanitary protection zone exceeds the permissible exposure limit (PEL) by 5–10 times [8]. Francis Ahadzi Dzifa investigated the effects of silica dust on quarry workers' health and reported their symptoms, recommending the use of personal protective equipment (PPE) for respiratory protection and eyewear [9]. In his studies, Frederick Anlimma highlights a rise in silicosis cases in several countries and questions the effectiveness of dust control methods in preventing exposure to inhalable crystalline silica [10]. Zhichao Liu proposed an optimized dust reduction method for a crushing station based on modeling results and simulated the dust diffusion pattern associated with this method [11].

Since 2014, Russia has implemented a special labor conditions assessment (SLCA), regulated by federal legislation[2] and aimed at identifying and evaluating hazardous and harmful production factors at individual workplaces, as well as developing measures to improve working conditions and prevent occupational diseases.

The **objective** of this study is to determine the dust concentration at the workplace of a crushing and screening plant operator within the framework of the SLCA.

To achieve this objective, the following tasks were set:

– conduct tests and determine the average shift dust concentration in the operator's working zone;

– identify factors affecting dust concentration at the operator's workplace;

– forecast dust concentration at the workplace based on approximated data under various wind speeds;

– evaluate the adequacy and accuracy of the obtained results;

– establish the labor conditions class (subclass) for the operator;

– develop recommendations to reduce dust concentration at the operator's workplace and improve working conditions.

The **novelty of this study** lies in its comprehensive approach to assessing dust concentration at the workplace of a crushing and screening plant operator, taking into account industry-specific factors and the effect of wind speed on dust concentration.

The **scientific significance of the study** is in the approximation of data for predicting dust concentration at the operator's workplace depending on wind speed at the production site.

The **practical value of the study** lies in forecasting dust concentration in the operator's workplace air based on wind speed at the production site and in developing recommendations to reduce dust concentration at the crushing and screening plant.

Research methods

To measure dust concentration in the air at the workplace of a crushing and screening plant operator, an aspiration method was applied. This method involves passing a specified volume of air through special filters, after which the dust mass is measured and the concentration calculated[3].

The mass concentration of total dust in the air, K_d, for each individual test is determined by the formula:

$$K_d = \frac{(m_n - m_0)\cdot 1000}{V_{20}}, \quad (1)$$

were K_d is the dust concentration in the air, mg/m³; m_0 is the mass of the clean filter, mg; m_n is the mass of the filter with deposited dust particles, mg; and V_{20} is the air volume, adjusted to standard conditions, dm³.

$$V_{20} = \frac{V_t \cdot 293P}{(273+T)\cdot 101.33}, \quad (2)$$

where V_t is the volume of air passed through the filter, dm³; P is atmospheric pressure, kPa; and T is the air temperature at the workplace, °C.

[2] Federal Law No. 426-FZ dated December 28, 2013, "On Special Labor Conditions Assessment".

[3] Methodology for measuring mass dust concentration by gravimetric method for special labor conditions assessment. MI APFD –18.01.2018; MUK 4.1.2468–09 Measurement of mass dust concentrations in workplace air in mining and non-metallic industry enterprises.

If the measurement times vary, the time-weighted average concentration is calculated by:

$$K_{oi} = \frac{K_{d1}t_1 + K_{d2}t_2 + \ldots + K_{dn}t_n}{t_1 + t_2 + \ldots + t_n}, \qquad (3)$$

where t_1, t_2, ..., t_n is the measurement times, min.

The average shift dust concentration at the workplace is calculated by:

$$K_{ash} = \frac{K_{ash1}T_{ash1} + K_{ash2}T_{ash2} + \ldots + K_{ashn}T_{ashn}}{\sum T}, \qquad (4)$$

where K_{ash1}, K_{ash2}, ... K_{ashn} are the time-weighted average dust concentrations for each technological operation, mg/m³; T_{ash1}, T_{ash2}, ... T_{ashn} are the durations of each technological operation, min; and $\sum T$ is the total duration of the work shift, min.

To assess data distribution, the median *Me* and the geometric standard deviation σ_g are determined:

$$Me = e^{\ln Me}, \qquad (5)$$

where

$$\ln Me = \frac{t_1 \ln K_{d1} + t_1 \ln K_{d1} + \ldots + t_n \ln K_{dn}}{\sum t}, \qquad (6)$$

$$\sigma_g = e^{\sqrt{2\ln \frac{K_{ash}}{Me}}}. \qquad (7)$$

The final result is recorded as:

$$K \pm 0.01\delta\tilde{K} \text{ for P = 0.95}, \qquad (8)$$

where $\tilde{K}$ is the arithmetic mean of the measurement results n, mg/m³, and δ is the relative error margins, %.

To assess the accuracy and reliability of the calculations, a probabilistic data processing method may also be used. In this case, the geometric standard deviation is calculated as follows:

$$\sigma_g = \left(\frac{K_{84}}{Me} + \frac{Me}{K_{16}}\right):2, \qquad (9)$$

where K_{84} and K_{16} are the concentration values corresponding to 84% and 16% probability levels, respectively, mg/m³.

The average shift dust concentration is then determined by:

$$K_{ash} = e^{\ln K_{ash}}, \qquad (10)$$

where

$$\ln K_{ash} = \ln Me + 0.5(\ln \sigma_g)^2. \qquad (11)$$

Research results

Dust measurements were conducted as part of the special labor conditions assessment procedure [12, 13] at a crushing and screening plant located in the Moscow region. The operator's workplace is housed in a standalone, container-type facility three meters above ground level, equipped with climate control for air conditioning.

Dust generation occurs throughout the entire production cycle at the crushing and screening plant (Fig. 2). The main factors contributing to dust generation at the site are as follows:

– movement of heavy-duty vehicles;

Fig. 2. Schematic of the crushing and screening plant illustrating the main sources of dust generation

– loading of raw materials into the receiving hopper;
– operation of the crusher;
– operation of the vibrating screen;
– piling of crushed stone.

The most intensive dust generation at the study site occurs when sorted crushed stone is piled. As it freely falls from the conveyor belt, lighter dust particles detach from the surface of the crushed stone due to air resistance. The greater the drop height, the more kinetic energy the crushed stone acquires, which transfers to dust particles, causing them to move and collide. This results in an increase in the number of collisions and particle fragmentation, generating a larger volume of dust. Another significant factor contributing to high dust concentration at the production site is air velocity, which not only intensifies dust movement but also lifts settled particles from stockpiles and equipment surfaces, thereby increasing dust concentration in the air. Therefore, in this study, air velocity measurements were taken and analyzed for their impact on dust concentration at the operator's workplace, in addition to the standard methodology.

As a mathematical model describing dust emissions, a system of equations can be used, which includes the following [14]:

– Navier–Stokes equation:

$$\begin{cases} \dfrac{\partial V_x}{\partial \tau} + V_x\dfrac{\partial V_x}{\partial x} + V_y\dfrac{\partial V_x}{\partial y} + V_z\dfrac{\partial V_x}{\partial z} = \\ = -\dfrac{1}{\rho}\dfrac{\partial \rho}{\partial x} + \dfrac{\eta}{\rho}\left(\dfrac{\partial^2 V_x}{\partial x^2} + \dfrac{\partial^2 V_x}{\partial y^2} + \dfrac{\partial^2 V_x}{\partial z^2}\right), \\ \dfrac{\partial V_y}{\partial \tau} + V_x\dfrac{\partial V_y}{\partial x} + V_y\dfrac{\partial V_y}{\partial y} + V_z\dfrac{\partial V_y}{\partial z} = \\ = -\dfrac{1}{\rho}\dfrac{\partial \rho}{\partial y} + \dfrac{\eta}{\rho}\left(\dfrac{\partial^2 V_y}{\partial x^2} + \dfrac{\partial^2 V_y}{\partial y^2} + \dfrac{\partial^2 V_y}{\partial y^2}\right) - g, \\ \dfrac{\partial V_z}{\partial \tau} + V_x\dfrac{\partial V_z}{\partial x} + V_y\dfrac{\partial V_z}{\partial y} + V_z\dfrac{\partial V_z}{\partial z} = \\ = -\dfrac{1}{\rho}\dfrac{\partial \rho}{\partial z} + \dfrac{\eta}{\rho}\left(\dfrac{\partial^2 V_z}{\partial x^2} + \dfrac{\partial^2 V_z}{\partial y^2} + \dfrac{\partial^2 V_z}{\partial y^2}\right); \end{cases} \quad (12)$$

– continuity equation:

$$\frac{\partial \rho}{\partial \tau} + \left(\frac{\partial V_x}{\partial x} + \frac{\partial V_y}{\partial y} + \frac{\partial V_z}{\partial z}\right)\rho = 0; \quad (13)$$

Table 1

Air sampling results for calculating average shift dust concentrations

Stage No.	Stage duration T, min	Filter mass m_0, mg	Filter mass m_n, mg	Airflow rate, L/min	Atmospheric pressure, kPa	Measurement time t, min	Air temperature at workplace, °C	Air velocity V, m/s	Dust concentration values K, mg/m³	Arithmetic mean concentration for stage K_{ol}, mg/m³	Average shift dust concentration K_{cc}, mg/m³	Median Me	Geometric standard deviation σ_g
I	120	62574.6	62577.0	20	102.0	25	21.4	1	4.79	3.70	7.7	6.22	1.92
		62020.2	62022.7			25	21.5	2	4.99				
		62828.1	62829.1			25	21.9	1	2.00				
		62532.8	62534.3			25	22.0	1	3.00				
II	120	64731.1	64737.2		102.2	25	22.3	4	12.19	14.21			
		60150.5	60159.4			25	22.5	5	17.80				
		60741.8	60750.1			25	22.7	5	16.61				
		61799.2	61804.3			25	23.5	4	10.23				
III	120	63384.4	63389.2		102.6	25	24.8	4	9.64	9.41			
		61474.8	61479.0			25	25.4	4	8.45				
		61696.4	61702.2			25	25.9	4	11.69				
		61495.3	61499.2			25	26.1	3	7.86				
IV	120	60473.5	60475.6		102.8	25	25.5	2	4.22	3.41			
		63826.8	63829.0			25	25.2	1	4.41				
		63638.6	63640.0			25	24.7	1	2.80				
		63937.4	63938.6			25	24.4	1	2.40				

– Mendeleev–Clapeyron equation:

$$P = \frac{\rho}{M} RT; \tag{14}$$

– heat conduction equation:

$$\frac{\partial T}{\partial \tau} + V_x \frac{\partial T}{\partial x} + V_y \frac{\partial T}{\partial y} + V_z \frac{\partial T}{\partial z} = \frac{1}{c(T)\rho}\left(\frac{\partial\left(\lambda(T)\frac{\partial T}{\partial x}\right)}{\partial x} + \frac{\partial\left(\lambda(T)\frac{\partial T}{\partial y}\right)}{\partial y} + \frac{\partial\left(\lambda(T)\frac{\partial T}{\partial z}\right)}{\partial z} \right); \tag{15}$$

– equation for dust concentration variation:

$$\frac{\partial C}{\partial \tau} + V_x \frac{\partial C}{\partial x} + (V_y + V_c)\frac{\partial C}{\partial y} + V_z \frac{\partial C}{\partial z} = F_c, \tag{16}$$

where *x, y, z* are the Cartesian coordinates; τ is the time; *V* is the air velocity; *P* is the air pressure; ρ is the material density; *T* is the air temperature; *M* is the molar volume; *R* is the universal gas constant (8.31 J/mol·K); η is the dynamic viscosity; *g* is the gravitational acceleration; $\lambda(T)$ is the thermal conductivity coefficient of the material; *C*(*T*) is the specific heat capacity of the material; *C* is the concentration of dust emissions; V_c is the dust settling velocity (0.04 m/s); F_c is the power of the dust source [14].

During the testing, the production process was conditionally divided into four stages of two hours each, evenly distributed throughout the shift. The measurement time for each individual sample was 25 minutes. The total measurement time was 400 minutes, covering 83% of the work shift. Sampling was conducted using AFA filters (analytical aerosol filters) with a PU-type aspirator. During testing, the wind was blowing toward the building housing the operator's workplace. Table 1 presents the measurement results and their subsequent processing according to the standard calculation methodology.

The results indicate a stable dust concentration in the air at the workplace, as the geometric standard deviation $\sigma_g < 3$. However, it should be noted that the average concentrations for each stage differ by a factor of 3–4, due to variations in air velocity and direction at the production site. An increase in air velocity up to 5 m/s was observed from 10:00 to 13:30, corresponding to the peak dust concentration levels at the workplace (Fig. 3).

Based on the data shown in Fig. 4, it is possible to predict the dust concentration K_{dw} at the workplace depending on air velocity V at the production site, with an approximation accuracy of $R^2 = 0.95$:

$$K_{dw} = 0.2185V^3 - 1.1571V^2 + 3.6493V + 0.4968. \tag{17}$$

Using the graph presented in Fig. 4, we determine the permissible air velocity at the study site:

$$V_{perm} = 2.6 \text{ m/s}.$$

To establish the relationship between dust generation and various factors – such as technological equipment, vehicle movement, loading of the receiving hopper, and the height of free-falling crushed stone – we calculate the dust concentration using formula (17) with $V = 0$ m/s:

$$K_{perm.0} = 0.5 \text{ mg/m}^3.$$

A probabilistic method was applied to assess the accuracy of measurements [15, 16]. This method provides a comprehensive view of all dust concentrations in the air within the workplace area using a logarithmic probability grid. To investigate the conformity of the data to a normal distribution, a frequency histogram method was employed as a graphical approach to data distribution (Fig. 5).

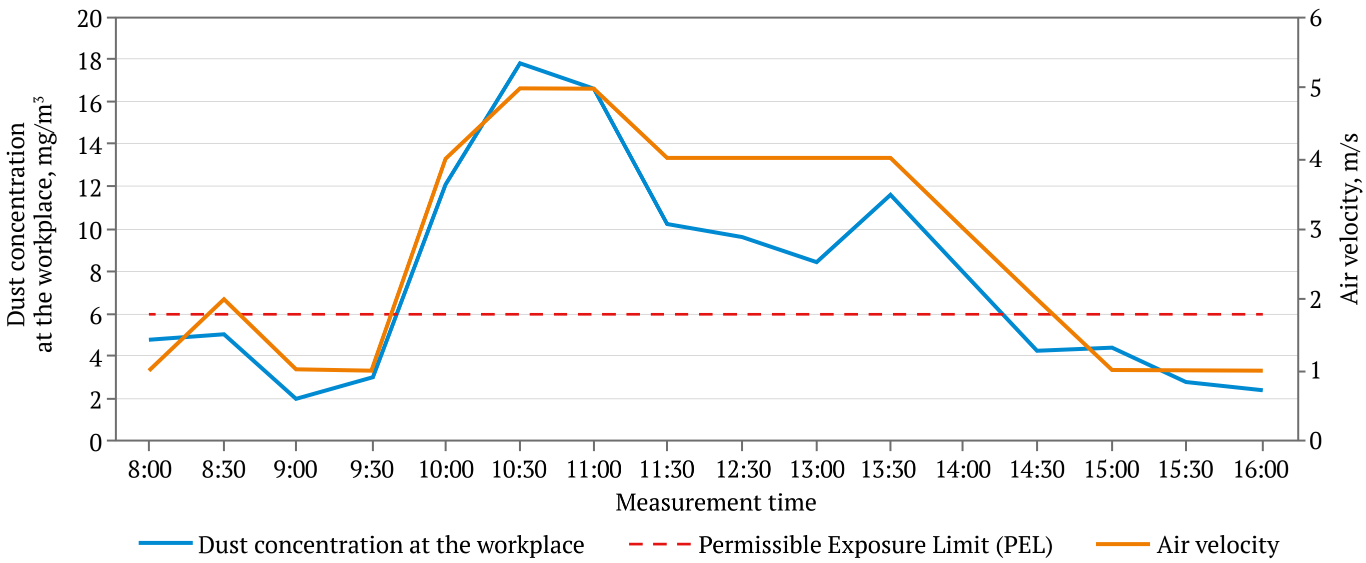

Fig. 3. Variation in dust concentration at the workplace across different testing stages

ПThe resulting histogram has a bell-shaped form, resembling a normal curve, which suggests that the data follow a normal distribution [17]. The data for probabilistic analysis are provided in Table 2, where individual dust concentration measurements have been ranked in ascending order with accumulated frequencies determined.

The probability grid (Fig. 6) shows the concentration results with corresponding cumulative frequencies, along with an integrated line drawn through the points. From this line, the following were determined: the median Me = 6 and concentration values for 84% and 16% (K_{84} = 12.1 mg/m³; K_{16} = 3.2 mg/m³).

To test the assumption of the model's conformity to a normal distribution, the Shapiro–Wilk test will be applied

$$W = \frac{\left(\sum_{i=1}^{n} a_i x_i\right)^2}{\sum_{i=1}^{n} (x_i - \tilde{x})^2} = 0.91, \quad (18)$$

where n is the number of observations; x_i is the values of the ordered sample; and a_i are tabulated coefficients depending on the number of trials.

Table 3 presents the intermediate calculations for the Shapiro–Wilk test.

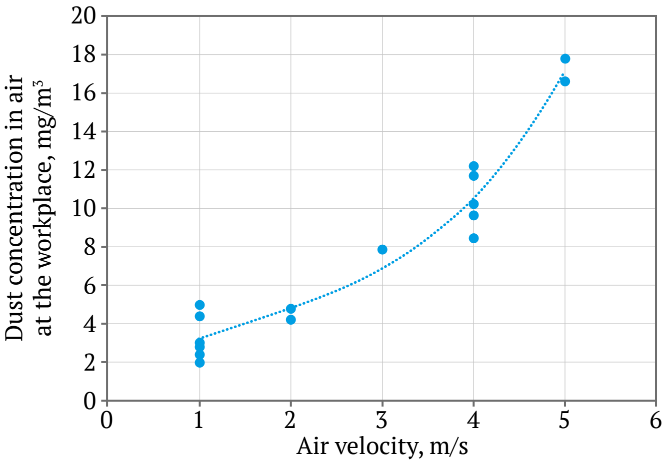

Fig. 4. Dependence of dust concentration at the workplace on air velocity

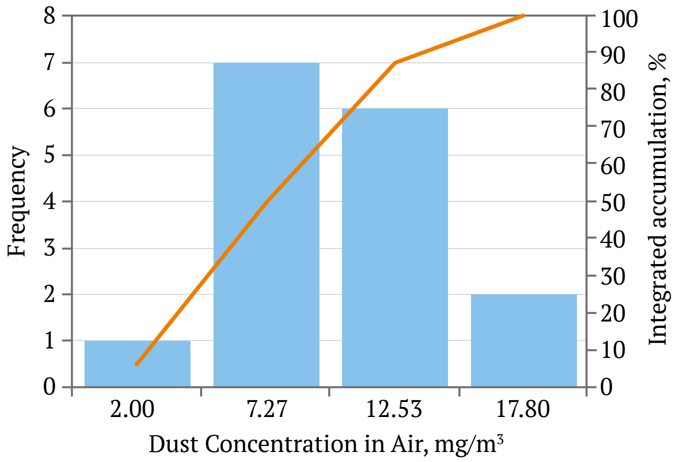

Fig. 5. Normal distribution graph for n = 16

Table 2

Calculation of average shift dust concentration in the workplace area using the probabilistic method

No.	Ranked dust concentration values K n Ascending Order, mg/m³	Measurement time T, min	Sampling duration as percentage of total testing time, %	Cumulative frequency, %	Average shift dust concentration K_{cc}, mg/m³	Median Me	Geometric standard deviation σ_g
1	2.00	25	6.25	6.25	7.6	6.00	1.94
2	2.40	25	6.25	12.50			
3	2.80	25	6.25	18.75			
4	3.00	25	6.25	25.00			
5	4.22	25	6.25	31.25			
6	4.41	25	6.25	37.50			
7	4.79	25	6.25	43.75			
8	4.99	25	6.25	50.00			
9	7.86	25	6.25	56.25			
10	8.45	25	6.25	62.50			
11	9.64	25	6.25	68.75			
12	10.23	25	6.25	75.00			
13	11.69	25	6.25	81.25			
14	12.19	25	6.25	87.50			
15	16.61	25	6.25	93.75			
16	17.80	25	6.25	100.00			

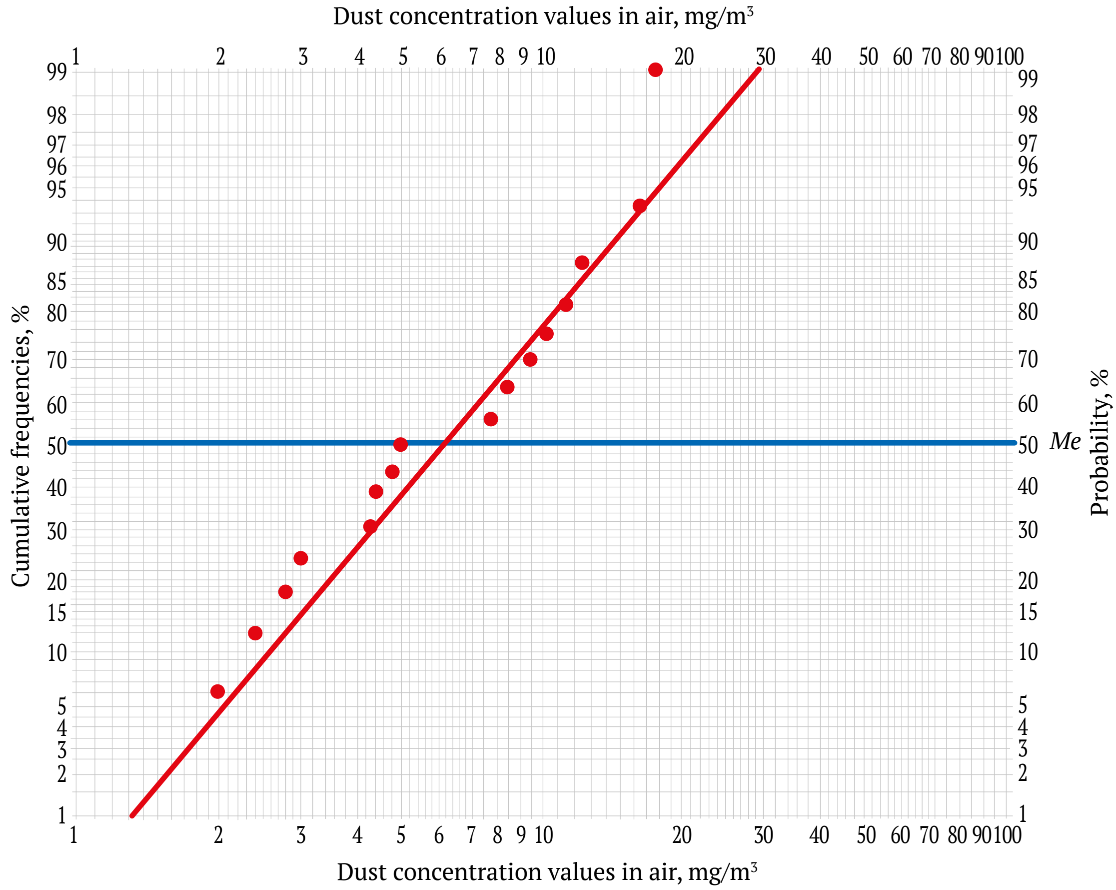

Fig. 6. Probability coordination grid

Table 3

Results of intermediate calculations for the Shapiro–Wilk Test

$\tilde{x}$	x_i	$(x_i - \tilde{x})^2$	a_i	$a_i \cdot x_i$
7.69	2.00	32.38	0.51	1.02
	2.40	27.98	0.33	0.79
	2.80	23.91	0.25	0.70
	3.00	22.00	0.19	0.57
	4.22	12.04	0.15	0.63
	4.41	10.76	0.10	0.44
	4.79	8.41	0.06	0.29
	4.99	7.29	0.02	0.10
	7.86	0.03	–0.02	–0.16
	8.45	0.58	–0.06	–0.51
	9.64	3.80	–0.10	–0.96
	10.23	6.45	–0.15	–1.53
	11.69	16.00	–0.19	–2.22
	12.19	20.25	–0.25	–3.05
	16.61	79.57	–0.33	–5.48
	17.80	102.21	–0.51	–9.08
Sum	–	373.66	–	–18.45

Table 4

Results of labor conditions assessment for the workplace

Occupation / position	PEL* or dust in workplace air, mg/m³	Hazard class	Health impact	Average daily dust concentration in workplace air, mg/m³	Deviation from PEL	Labor Conditions Class (Subclass)**
Crushing and screening operator	6	3	Crushing and screening operator	7.7	1.28	3.1

Source: * GN 2.2.5.3532–18 Permissible Exposure Limits (PEL) for harmful substances in workplace air; ** GOST P 54578–2011 Workplace air. Aerosols primarily with fibrogenic potential. General principles for hygienic control and impact assessment.

The calculated W statistic exceeds the tabulated value W_t = 0.887 at a significance level of α = 0.05, which confirms, providing 0.95 confidence that the data distribution conforms to a normal distribution.

The average shift dust concentration obtained using the probabilistic method was 7.6 mg/m³. A deviation of 0.1 mg/m³ demonstrates the accuracy and reliability of the tests, as the confidence interval, according to equation (8), is ±1.85 mg/m³. The calculated value is therefore accepted as the final result:

$$K_{ash} = 7.7 \pm 1.85 \text{ mg/m}^3.$$

The summary results for determining the labor conditions class (subclass) are presented in Table 4. Dust from crushed stone production is classified as an aerosol primarily with fibrogenic potential, which corresponds to hazard class 3. The obtained result exceeds the permissible exposure limit (PEL) by a factor of 1.28, which falls under labor conditions class 3.1 (subclass) and necessitates the establishment of a harmful exposure allowance.

Conclusion

The results of the dust concentration assessment at the workplace of a crushing and screening plant operator indicate an exceedance of the permissible exposure limit (PEL) by a factor of 1.28, corresponding to labor conditions class 3.1 (subclass). The average daily dust concentration at the operator's workplace is 7.7 mg/m³; however, it should be noted that the average concentrations across different stages vary by a factor of 3–4, influenced by the intensity and direction of air velocity at the production site.

Based on the obtained data, dust concentrations K_{dw} at the workplace were predicted as a function of air velocity V at the production site, with an approximation accuracy of R^2 = 0.95. It was determined that the maximum allowable air velocity at the site should not exceed 2.6 m/s.

When PEL values for dust concentration in workplace air are exceeded, legislation[4] requires the employer to halt production and take measures to reduce airborne dust to the lowest possible level.

To reduce dust concentration at the operator's workplace, comprehensive dust control measures are needed at the crushing and screening plant, including [18–22]:

– washing the wheels of vehicles upon entering and exiting the production site;

– installing stationary or mobile dust suppression systems that use water spray nozzles at low and medium pressure to create a mist;

– replacing the open belt conveyor with a closed conveyor system.

Additionally, it is recommended to replace the filters in the climate control equipment with carbon filters to enhance air purification.

Using approximated data, it was forecasted that, in the absence of air movement at the production site, the dust concentration at the operator's workplace would remain at 0.5 mg/m³. Inhaling crystalline silica can lead to the formation of nodules of connective tissue in the lungs and scarring around the particles. The body's natural defense cells cannot remove this toxic dust, leading to chronic inflammation and potential lung cell damage. Some individuals may experience allergic reactions, such as skin rashes and/or itching, when in contact with the dust. To prevent the development of occupational diseases, operators are advised to use personal protective equipment (PPE) for respiratory, skin, and eye protection throughout the shift.

The presented results can be used to predict dust concentrations at the workplaces of operators at other crushing and screening plants, taking into account individual empirical data collected at each site.

[4] Labor Code of the Russian Federation, dated December 30, 2001, No. 197-FZ.

References

1. Nikulin A., Nikulina A.Y. Assessment of occupational health and safety effectiveness at a mining company. *Ecology, Environment and Conservation*. 2017;23(1);351–335.
2. Korol E.A., Degaev E.N., Konyukhov D.S. Labor safety in laying of underground utilities. *Mining Informational and Analytical Bulletin*. 2024; (2):129–139. (In Russ.) https://doi.org/10.25018/0236_1493_2024_2_0_129
3. Lapshin N.S. Vinogradov I.P., Dzurich N.S. Analysis of development trend in the market of nonmetallic constructional materials in the Russian Federation. *Mining Informational and Analytical Bulletin*. 2018:(7):205–211. (In Russ.) https://doi.org/10.25018/0236-1493-2018-7-0-205-211
4. Butkevich G.R. Industry of non-metallic building materials. Prospection. *Building Materials*. 2019;(11):32–36. (In Russ.) https://doi.org/10.31659/0585-430X-2019-776-11-32-36

5. Balovtsev S.V. Monitoring of aerological risks of accidents in coal mines. *Mining Science and Technology* (*Russia*). 2023;8(4):350–359. https://doi.org/10.17073/2500-0632-2023-10-163

6. Rastanina N.K., Kolobanov K.A. Impact of technogenic dust pollution from the closed mining enterprise in the Amur Region on the ecosphere and human health. *Mining Science and Technology* (*Russia*). 2021;6(1):16–22. https://doi.org/10.17073/2500-0632-2021-1-16-22

7. Rathebe P. Occupational exposure to silicon dioxide and prevalence of chronic respiratory symptoms in the cement manufacturing industries: *Journal of Public Health Research.* 2023;12(4):1–10. https://doi.org/10.1177/22799036231204316

8. Sulamanidze L.F. Kuznetsov L.F. Assessment of dust pollution of the atmosphere during the processing of non-metallic materials. In: *Step into the future: theoretical and applied research of modern science: materials of the XVII Youth International Scientific and practical conference of students, postgraduates and young scientists.* St. Petersburg: Lulu Press; 2019. Pp. 38–41. (In Russ.)

9. Ahadzi D.F., Afitiri A.R., Ekumah B. et al. Self-reported disease symptoms of stone quarry workers exposed to silica dust in Ghana. *Health Science Reports.* 2020;3(4):189. https://doi.org/10.1002/hsr2.189

10. Anlimah F., Gopaldasani V., MacPhail C. et al. A systematic review of the effectiveness of dust control measures adopted to reduce workplace exposure. *Environmental Science and Pollution Research.* 2023:30(19);54407–54428. https://doi.org/10.1007/s11356-023-26321-w

11. Liu Z., Ao Z., Zhou W. et al. Research on the physical and chemical characteristics of dust in open pit coal mine crushing stations and closed dust reduction methods. *Sustainability*. 2023;*15*(16):12202. https://doi.org/10.3390/su151612202

12. Pakhomova L., Oleynik P. Selection and evaluation of work place certification parameters (special assessment of labor conditions). *Construction Production.* 2019:(1);49–52. (In Russ.) https://doi.org/10.54950/26585340_2019_1_49

13. Zanina I.A., Makeeva L.A., Zhabaeva M.U. et al. Identification of the causes of injuries in the coal industry and measures to reduce risks (using the example of Bogatyr Komir LLP). *Science & Reality*. 2023;4(16):90–95. (In Russ.)

14. Matyushinets T.V., Jatskevich Yu.V., Chychko A.N. Mathematical modeling of the distribution of dust emissions in the spatial structure of the workshop. *Foundry Production and Metallurgy*. 2018;(4):107–113. (In Russ.) https://doi.org/10.21122/1683-6065-2018-4-107-113

15. Verevkyna O.I. On the hybrid method of forecasting the risks on railway transport based on the general logical-and-probabilistic method. *Proceedings of Petersburg Transport University*. 2017;14(4):615–627.

16. Kuligin D., Shkoliar F. Influence of the probabilistic method to summarize loads on the reliability and material consumption of building structures. *Architecture and Engineering.* 2023:8(2):49–57. https://doi.org/10.23968/2500-0055-2023-8-2-49-57

17. Duplyakin V.M. Nuances of identification for normal distribution. Vestnik of Samara University. *Economics and Management*. 2020:11(3):176–183. https://doi.org/10.18287/2542-0461-2020-11-3-176-183

18. Zeng L.-M., Yang X.-Y., Wang L.-H. et al. Determination of weight concentration of free silicon dioxide for dust using X-ray diffraction technique and Rietveld refinement method. *Chinese Journal of Analytical Chemistry.* 2008;(36):599–603.

19. Jing D., Ma J., Dong Z. et al. Research on factors affecting the spread of dust pollution in conveyor belt workshop and research on wet dust reduction technology. *PLoS One*. 2024;19(2):e0299328. https://doi.org/10.1371/journal.pone.0299328

20. Jing D., Ma J., Zhang T. et al. Numerical simulation of the fine kinetics of dust reduction using high-speed aerosols. *PLoS One.* 2023;18(12):e0286101. https://doi.org/10.1371/journal.pone.0286101

21. Bajracharya N., Magar P., Karki S. et al. Occupational health and safety issues in the construction industry in south asia: a systematic review and recommendations for improvement. *Journal of Multidisciplinary Research Advancements.* 2023;1(1):27–31. https://doi.org/10.3126/jomra.v1i1.55101

22. Klimov I.Yu. Analysis of Soft Skills-Based Approach Effectiveness in Advanced Training Program for Mining Company. *Mining Science and Technology* (*Russia*). 2020;5(1):56-68. (In Russ.) https://doi.org/10.17073/2500-0632-2020-1-56-68

Information about the authors

Elena A. Korol – Dr. Sci. (Eng.), Professor, Head of the Department of Housing and Communal Services, Moscow State University of Civil Engineering (National Research University), Moscow, Russian Federation; ORCID 0000-0002-5019-3694, Scopus ID 57197844794, ResearcherID C-2635-2019, AuthorID 678276; e-mail KorolEA@mgsu.ru

Evgeniy N. Degaev – Cand. Sci. (Eng.), Associate Professor, Associate Professor of the Department of Housing and Communal Complex, Moscow State University of Civil Engineering (National Research University), Moscow, Russian Federation; ORCID 0000-0001-6384-8277, Scopus ID 57195225439, ResearcherID S-1854-2018, AuthorID 798266; e-mail degaev@inbox.ru

Dmitry S. Konyukhov – Dr. Sci. (Eng.), Mosinzhproekt JSC, Moscow, Russian Federation; MIREA – Russian Technological University, Moscow, Russian Federation; ORCID 0000-0001-8635-232X, Scopus ID 6507981388, AuthorID 350235; e-mail gidrotehnik@inbox.ru

Received 27.03.2024
Revised 23.05.2024
Accepted 01.06.2024

MINING SCIENCE AND TECHNOLOGY (RUSSIA)
ГОРНЫЕ НАУКИ И ТЕХНОЛОГИИ
2024;9(4):406–419

eISSN 2500-0632
https://mst.misis.ru/

SAFETY IN MINING AND PROCESSING INDUSTRY AND ENVIRONMENTAL PROTECTION

Research paper

https://doi.org/10.17073/2500-0632-2024-04-206
УДК 631.453:631.618:504.53:622

Chemical and ecological properties of soils and the NDVI analysis on reclaimed sulfide coal waste dumps in the boreal zone

N.V. Mitrakova ✉, **E.A. Khayrulina**, **A.A. Perevoshchikova**, **N.V. Poroshina**, **E.E. Malyshkina**, **E.S. Yakovleva**, **N.A. Kobelev**

Institute of Natural Science of Perm State National Research University, Perm, Russian Federation

✉ *mitrakovanatalya@mail.ru*

Abstract

Reclamation of coal waste dumps through the establishment of a stable soil and vegetation cover on their surface contributes to the restoration of ecological systems. Therefore, studying the properties of soils in technogenic landscapes is of current importance. The problem of biological reclamation was studied in the Kizel Coal Basin area. The effectiveness of reclamation was evaluated on several sulfide coal waste dumps. The reclamation methods, as well as the period of soil-vegetation cover formation, varied. Agrochemical properties of the dump soils were studied using unified methods. The NDVI (Normalized Difference Vegetation Index) was calculated based on Sentinel-2 and Landsat 7,8 images. To assess biological activity, phytotesting was used. The lithostrats ranged from slightly acidic to neutral ($pH–H_2O$ = 6.1–6.8); the embryonic soil showed a slightly alkaline reaction (7.9). The embryonic soil, due to the presence of coal particles, had the highest organic matter content (12–7.7%). Depending on the "age" of the soil, the amount of organic matter in the lithostrats varied: for the 7-year-old lithostrat, it ranged from 2.4 to 8.9%, while for the 4-year-old lithostrat, it was less than 1%. The absorption capacity of the lithostrats was similar to that of the background soil. The dump soils were characterized by low levels of nutrients (NPK), with the 4-year-old lithostrat having the lowest N content. The dump soils demonstrated favorable conditions for plant growth, as evidenced by the height and biomass of cress and oats. The calculated NDVI for all dumps ranged from 0.4 to 0.6, indicating the presence of a stable vegetation cover. The implemented reclamation measures proved to be effective.

Keywords

coal, dump, waste, reclamation, soil formation, lithostrat, soil, NDVI index, embryonic soil, Fe^{2+}, SO_4^{2-}, H^+, pH

Funding

The study was supported by the Russian Science Foundation grant No. 24-27-00324, https://rscf.ru/project/24-27-00324/.

For citation

Mitrakova N.V., Khayrulina E.A., Perevoshchikova A.A., Poroshina N.V., Malyshkina E.E., Yakovleva E.S., Kobelev N.A. Chemical and ecological properties of soils and the NDVI analysis on reclaimed sulfide coal waste dumps in the boreal zone. *Mining Science and Technology* (*Russia*). 2024;9(4):406–419. https://doi.org/10.17073/2500-0632-2024-04-206

ТЕХНОЛОГИЧЕСКАЯ БЕЗОПАСНОСТЬ В МИНЕРАЛЬНО-СЫРЬЕВОМ КОМПЛЕКСЕ И ОХРАНА ОКРУЖАЮЩЕЙ СРЕДЫ

Научная статья

Химико-экологические свойства почв и индекс NDVI на рекультивированных сернистоугольных отвалах бореальной зоны

Н.В. Митракова ✉, **Е.А. Хайрулина**, **А.А. Перевощикова**, **Н.В. Порошина**, **Е.Е. Малышкина**, **Е.С. Яковлева**, **Н.А. Кобелев**

Пермский государственный национальный исследовательский университет, г. Пермь, Российская Федерация

✉ *mitrakovanatalya@mail.ru*

Аннотация

Рекультивация угольных отвалов путем создания устойчивого почвенного и растительного покрова на их поверхности способствует восстановлению экологических систем. В связи с этим актуальным является изучение свойств почв техногенных ландшафтов. Проблема биологической рекультивации изучалась на территории Кизеловского угольного бассейна. Оценена эффективность рекультивации на нескольких сернистоугольных отвалах. Методы рекультивации, как и период формирования почвенно-растительного покрова, различались. Агрохимические свойства почв отвалов изучали стандартными методами. Индекс NDVI (нормализованный относительный индекс растительности) рассчитан по снимкам Sentinel-2 и Landsat 7,8. Для оценки биологической активности использовали фитотестирование. Литостраты варьировались от слабокислых до нейтральных (pH–H_2O = 6,1–6,8); эмбриозем имел слабощелочную реакцию (7,9). Эмбриозем благодаря наличию частиц угля имел наибольшее содержание органического вещества (12–7,7 %). В зависимости от «возраста» почвы количество органического вещества в литостратах варьировало: для 7-летнего литострата оно колебалось от 2,4 до 8,9 %, а для 4-летнего было меньше 1 %. Поглотительная способность литостратов была аналогична с фоновой почвой. Почвы отвалов характеризовались низким уровнем питательных элементов (NPK), а 4-летний литострат имел самое низкое содержание N. Почвы отвалов показали благоприятные условия для роста растений, о чем свидетельствуют высота и масса кресс-салата и овса. Рассчитанный индекс NDVI для всех отвалов имел значения от 0,4 до 0,6, что свидетельствует о наличии устойчивого растительного покрова. Реализованные рекультивационные мероприятия доказали свою эффективность.

Ключевые слова
уголь, отвалы, отходы, рекультивация, почвообразование, литострат, почва, индекс NDVI, эмбриозем, Fe^{2+}, SO_4^{2-}, H^+, pH

Финансирование
Исследование выполнено за счет гранта Российского научного фонда № 24-27-00324, https://rscf.ru/project/24-27-00324/.

Для цитирования
Mitrakova N.V., Khayrulina E.A., Perevoshchikova A.A., Poroshina N.V., Malyshkina E.E., Yakovleva E.S., Kobelev N.A. Chemical and ecological properties of soils and the NDVI analysis on reclaimed sulfide coal waste dumps in the boreal zone. *Mining Science and Technology* (*Russia*). 2024;9(4):406–419. https://doi.org/10.17073/2500-0632-2024-04-206

Introduction

The mining industry, particularly coal extraction, significantly contributes to the transformation of natural ecosystems. Underground mining causes changes in the landscape and surface subsidence. For instance, in a study [1], subsidence was determined based on the growth rings of European larch (*Larix decidua*), where the authors confirmed the highest subsidence activity during periods of intensive mineral extraction. As a result of mining operations, land is reclaimed for waste disposal. In the Kuznetsk Coal Basin alone, approximately 3.6 billion tons of waste are generated annually, and the area of land disturbed by open-pit mining has now increased to 16.4 hectares per million tons of extracted coal [2]. Soils adjacent to waste dumps exhibit high concentrations of polycyclic aromatic hydrocarbons (PAHs) [3], the sources of which are emissions from burning dumps. These emissions spread to nearby areas via atmospheric transport. Naphthalene has been detected in the emissions from burning dumps, with higher concentrations found in waste containing pyrogenic bitumen. Additionally, anthracene, phenanthrene, fluoranthene, and pyrene were identified, with the last three indicating intense oxidation of organic matter [4]. Soils in coal mining areas are frequently contaminated with heavy metals. In one study [5], elevated concentrations of Cr, Ni, and Hg were found in the soils of mining regions compared to regulatory standards. The presence of trace elements in coal contributes to soil and water contamination. For example, the authors of [6] found that during leaching, coal-bearing rocks release Se, Cd, Hg, As, Be, V, Cr, and Pb. High concentrations of Fe, Al, Mn, Be, and other elements in the rivers of the Kizel Coal Basin have been described in studies [7, 8]. The use of the *Igeo* coefficient revealed contamination by Co, V, Nb, Hg, Sn, Zn, Sm, Ni, Cr, and Gd in the bottom sediments of the Kosva River in the Kizel Coal Basin area [9]. In addition to environmental pollution, coal mining leads to changes in the hydrological regime. Research results [10] showed that runoff, runoff depth, and spring runoff decreased by approximately 25%, 30%, and 57%, respectively, as a result of coal mining, while the calculated soil erosion rates and soil loss increased by nearly 200%.

The coals and coal-containing rocks in large-scale mining waste dumps contain significant amounts of sulfides and organic sulfur as part of the mineral composition of the dumps, with the sulfur content in coals varying across different deposits. In the coals of the Kizel Coal Basin, sulfur content ranges from 5 to 8%, with sulfur primarily present in the form of pyrite [11]. A study by Singh and Narzary [12] on overburden and coal seams at the Tikok mine in India showed that sulfur content in different seams ranged from 0.02% to 2.5%, with the maximum sulfur content in the coal seam reaching 1.9%.

Pyrite and other sulfides in overburden dumps are chemically unstable under oxidizing conditions. Initially, when exposed to water and oxygen at a neutral pH, pyrite undergoes chemical oxidation, releasing Fe^{2+}, SO_4^{2-}, and H^+ [13]. In the presence of O_2, ferrous iron (Fe^{2+}) is oxidized to ferric iron (Fe^{3+}), leading to increased acidity in the water and enhanced activity of Fe^{3+} ions. Acidophilic microorganisms accelerate pyrite oxidation, resulting in the formation of acidic

MINING SCIENCE AND TECHNOLOGY (RUSSIA)
ГОРНЫЕ НАУКИ И ТЕХНОЛОГИИ
2024;9(4):406–419
eISSN 2500-0632
https://mst.misis.ru/

mine drainage [13]. These acidic waters, with a pH of 2.5–3, are saturated with heavy metals, trace elements, and sulfates [14], making coal waste dumps sources of environmental pollution.

Natural revegetation on coal dumps occurs slowly due to the high acidity caused by the oxidation of sulfide minerals in overburden rocks, nutrient deficiencies, and the unfavorable mechanical composition of the substrate. Reclamation significantly reduces the time required for soil and vegetation cover to form on dumps. Reclamation efforts on coal dumps raise soil pH values from ultra-acidic (pH-H_2O 2.7) to neutral levels (pH-H_2O 6.4) [15]. Changes in acidity promote vegetation recovery, improving soil quality by increasing the organic matter and nutrient (NPK) content. According to [16–18], both plant community density and biodiversity increased in older reclaimed areas.

Soil formation on coal mining waste dumps helps prevent the spread of contaminants into the environment [19, 20]. Reclamation of dumps and disturbed lands, along with vegetation and soil restoration, are essential for preserving the natural environment and preventing the negative consequences of resource extraction [21, 22].

The Kizel Coal Basin (KCB) is located in the eastern part of the Perm region (Fig. 1) and covers an area of approximately 1,500 km^2 [7]. Extensive surveys of surface waters and bottom sediments have been conducted in the KCB area [7, 8, 23]. However, the current condition of the soils on KCB dumps has not been sufficiently studied. While some coal dumps in the KCB have undergone reclamation, there have been no large-scale scientific studies. After the closure of the mines, there were attempts to study the soils formed on the dumps [24, 25], but these were isolated studies and did not include diagnostics, classification, or detailed chemical analyses.

The aim of this work is to study the chemical and ecological properties of anthropogenic soils formed as a result of coal dump reclamation, to classify the formed soils, and to assess the effectiveness of reclamation using the NDVI index and phytotesting.

Materials and Methods

Description of the study area

The study area is part of the Ural Geochemical Province, within the eluvial-transalluvial region of residual mountain ranges on the western slope of the Middle Urals. According to the landscape zoning, the study area belongs to the the VerkhneYaivinskiy high ridge-hummocky landscape which lies on Paleozoic carbonate and partially terrigenous rocks. The climate is moderately continental, with an average annual precipitation of 700 mm. In the system of modern soil-ecological zoning, the Kizel Coal Basin (KCB) area is classified within the Western Foothill District, characterized by heavy loam podzolic, sod-podzolic, and waterlogged soils. The region of the study is situated in the mid- and southern-taiga zones, dominated by fir-spruce and spruce-fir forests in the foothills.

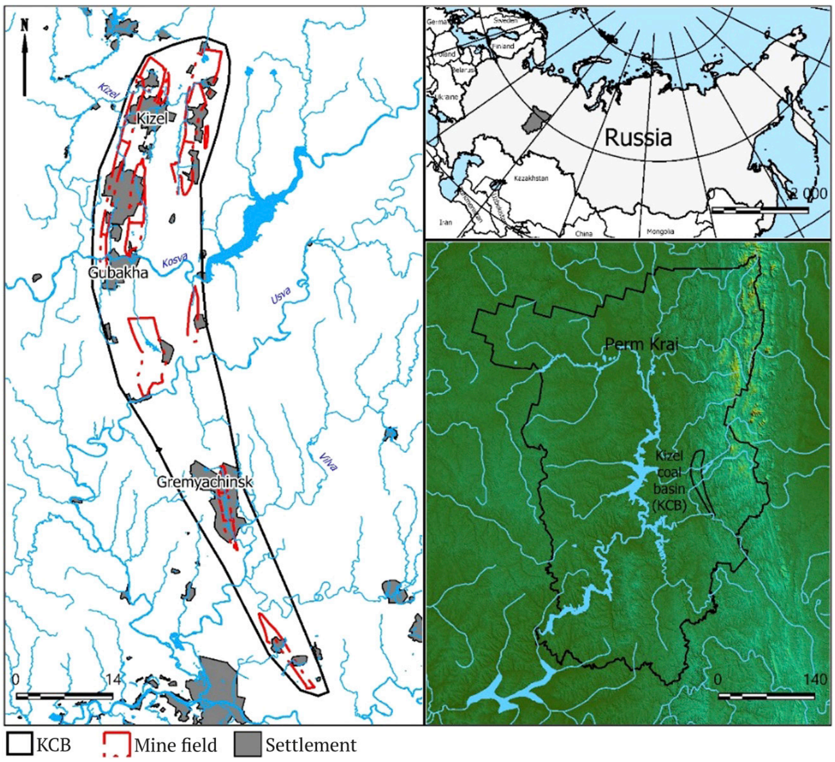

Fig. 1. Geographic location of the Kizel Coal Basin

Underground coal mining in this region took place from the late 18th century until the end of the 20th century, with the mines being closed in the early 2000s. There are approximately 100 spoil heaps in the KCB area [7]. According to satellite images from 2021, the area covered by these dumps reached 260 hectares. Over the course of mining operations, more than 35 million m^3 of rock waste accumulated. The lithology of the coal-bearing strata, mining technology, spoil heap storage methods, and the age of the heaps have all contributed to the heterogeneity of the dump material, which contains around 60 minerals [7]. The heaps consist of argillites, siltstones, sandstones, limestones, coal, pyrite, as well as wood and metal objects [26].

Soil sampling

In the summer of 2021 and 2022, soil samples were collected from three reclaimed waste dumps (Fig. 2) at a depth of 30 cm. The presence of a large amount of stony material made it difficult to collect samples from deeper layers. The soil samples were taken from the central part of the waste dumps, where the surface had been leveled prior to reclamation. In a 5×5 meter area, three pits were dug, and samples were collected from depths of 0–10 cm, 10–20 cm, and 20–30 cm. Before sampling, the vegetation at each collection site was cleared. The soil samples were extracted using a stainless steel trowel. Samples from each dump and corresponding depths were combined. The combined samples were then packed into polyethylene bags labeled with sample codes, dates, and collection locations. Each composite sample weighed at least 1 kg. As background samples, sod-podzolic soils were collected from a mixed forest.

Pit 1 was established on the waste dump of the Severnaya Mine in Shakhta settlement (Fig. 2(1)) (59°4'58.62"N 57°40'59.29"E). This dump was reclaimed in the early 2000s by leveling and adding slaked lime to the upper layer. Currently, the dump has a flat surface.

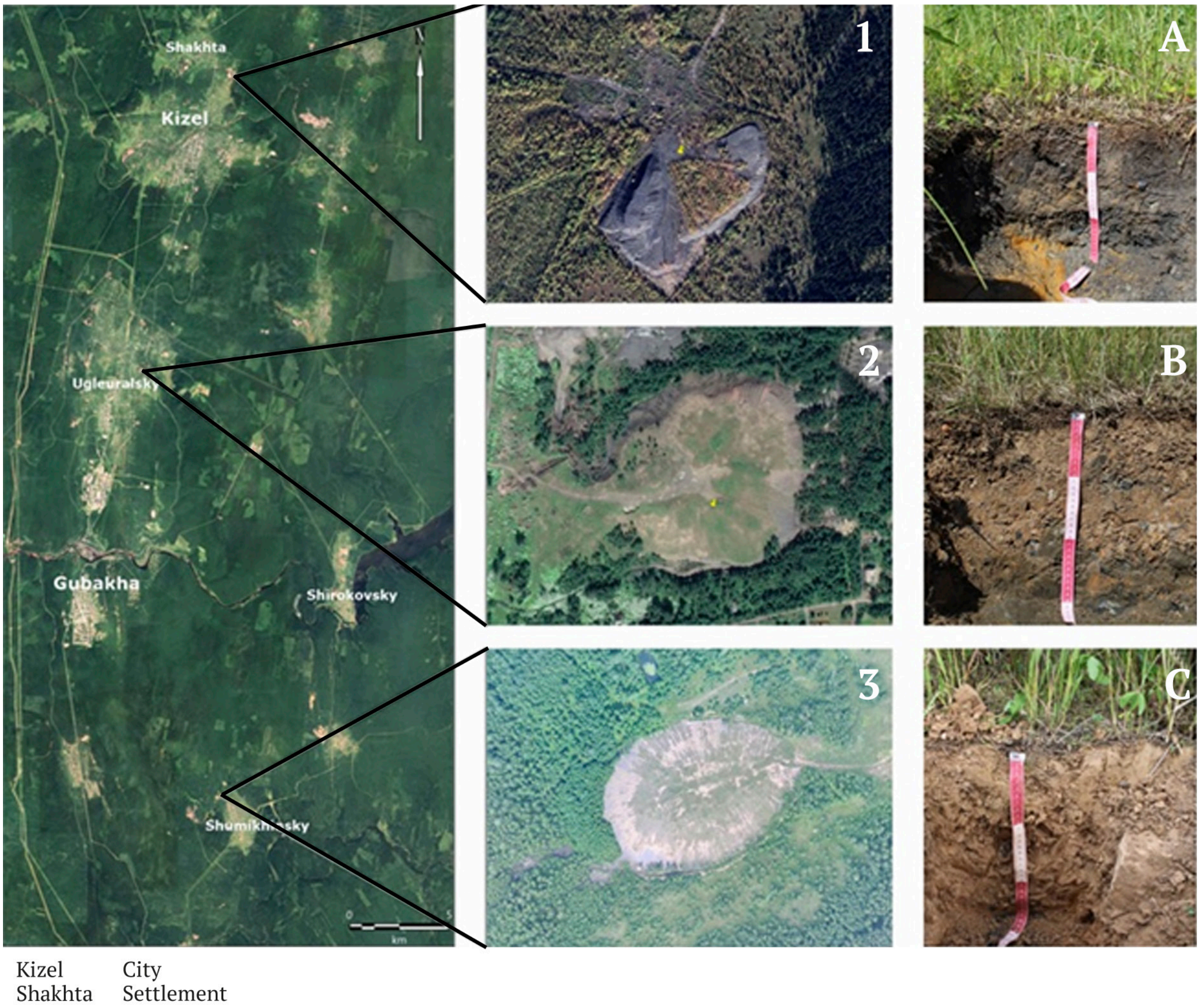

Fig. 2. Soil sampling locations and soil profiles:
1 – Severnaya Mine waste dump; *A* – soddy embryonic soil; *2* – Tsentralnaya Mine waste dump; *B* – clay lithostrat No. 1; *3* – Gorelovskaya Mine waste dump; *C* – clay lithostrat No. 2

Pit 2 was established on the waste dump of the Tsentralnaya Mine in Ugleuralsky settlement (Fig. 2(2)) (58°56'54.31"N 57°36'15.50"E). In 2016, the dump was reclaimed by leveling and covering it with a 0.3–0.5 m layer of clayey material. Sporadic mounds of construction debris are observed on the dump.

Pit 3 was established on the waste dump of the Gorelovskaya Mine in Shumikhinsky settlement (Fig. 2(3)) (58°45'21.25"N 57°40'17.25"E). In 2018, the dump was reclaimed by leveling and covering it with a layer of clayey material about 0.3 m thick.

Sod-podzolic soil samples from a secondary small-leaved forest were collected as background samples.

Research methods

Actual and exchangeable acidity in the soil samples was determined using the potentiometric method. Hydrolytic acidity was measured using the Kappen method (in a 1M CH_3COONa solution), which involves titration with a 1N alkali in the presence of phenolphthalein. Exchangeable acidity, exchangeable aluminum, and exchangeable hydrogen were determined by the Sokolov method, which is based on treating the soil with a 1M KCl solution, followed by titration. One part of the extract was titrated with alkali to determine the sum of exchangeable aluminum and hydrogen, while another part of the extract was titrated with alkali and fluoride to identify hydrogen ions. Acidity in hydrogen peroxide was determined to oxidize sulfide minerals present in the dumps; a pH lower than 2.5 in the peroxide solution indicates the presence of sulfide minerals.

The organic matter content was determined by the spectrophotometric method in accordance with GOST 26213–91. The cation exchange capacity (CEC) was determined using the Bobko-Askinazi-Aleshina method (GOST 17.4.4.01–84). The contents of exchangeable calcium and exchangeable (mobile) magnesium were measured using complexometric titration according to GOST 26487–85. The mobile sulfur content was determined by the turbidimetric method (GOST 26490–85), and mobile iron by the spectrophotometric method with o-phenanthroline according to GOST 27395–87. Sulfate ions were measured by the turbidimetric method (GOST 26426–85). Mobile phosphates and potassium were determined by the Kirsanov method, based on the extraction of mobile phosphates and potassium from the soil using a 0.2M HCl solution. Mobile phosphates were then measured as blue phosphorus-molybdenum complexes using a photoelectric colorimeter, while mobile potassium was determined using a flame photometer. The content of mobile potassium and phosphates in the dump soils was evaluated according to the criteria [27].

The biological activity of the soils was studied based on a patented method[1]. Phytotesting of the upper soil layers (0–10 cm) from the reclaimed waste dumps was conducted using cress (*Lepidium sativum*) and oats (*Avena sativa*). Cress was grown on both the waste dump soils and background soils for 7 days, and oats for 10 days. The height and biomass of the plants were measured in 25 replicates. A 10–30% reduction in cress growth indicates satisfactory soil conditions, while a reduction of 30–50% indicates unsatisfactory conditions. A reduction of more than 50% suggests environmentally hazardous soil conditions. As a control, plants were grown on vermiculite with Knop nutrient solution (1 g/l $Ca(NO_3)_2$, 0.25 g/l KH_2PO_4, 0.25 g/l $MgSO_4$, 0.125 g/l KCl, 0.0125 g/l $FeCl_3$).

To calculate the NDVI index for the dump areas, Sentinel-2 images (for lithostrat 2) and Landsat 7,8 images (for the embryonic soil and lithostrat 1) were used from the years 2000, 2007, 2014, 2018, 2020, and 2023. The necessary satellite images and spectral channels were obtained using the EOS LandViewer service.

The NDVI (Normalized Difference Vegetation Index) is an indicator of active biomass and is calculated as the ratio of the difference between the near-infrared and red spectral bands to their sum. NDVI values range from −1 to 1 and allow for the assessment of vegetation development during the growing season. Negative values of the index typically correspond to water bodies, clouds, or built-up areas. Low positive values (from 0 to 0.3) indicate either a complete absence of vegetation (approximately from 0 to 0.1) or sparse shrub or grass vegetation (up to 0.3). Values in the range of 0.3 to 0.5 correspond to moderate vegetation, while values between 0.5 and 1 indicate dense vegetation, often represented by forested areas.

Monitoring the dynamics of the NDVI index on reclaimed waste dump sites allows for an assessment of the success of reclamation efforts.

The NDVI was calculated using the Raster Calculator tool from the Spatial Analyst toolbox in ArcMap 10.4. To enhance the visual representation of the obtained rasters, the cubic convolution resampling method was applied.

Statistical parameters, such as the mean value and coefficient of variation (CV), were calculated using STATISTICA 7 and Microsoft Excel. For statistical processing of the data, regression and correlation analyses were conducted with a confidence level of 95%. Soil samples were compared based on agrochemical parameters using the non-parametric Kruskal-Wallis test. Significant differences between the compared

[1] Yeremchenko, O.Z., Mitrakova, N.V. Method for assessing the biological activity and toxicity of soils and technogenic soil substrates: RF patent. 2017. Bulletin No. 15. No. 2620555.

mean values were considered at a confidence level of 95% or higher ($P < 0.05$). The significance of differences between plant height and biomass was assessed using the Student's t-test ($P < 0.05$).

Results

Soil classification and vegetation changes

The background soils of the study area are zonal sod-podzolic loamy soils. Due to the exploitation of waste dumps, the natural soil cover has been altered. Overall, the soil cover of the dumps is heterogeneous, and technogenic soils or technogenic surface formations (TSF) have developed on the dumps.

The soddy embryonic soil was identified on the Severnaya Mine dump according to the classification proposed by [28]. According to the World Reference Base for Soil Resources (WRB), this soil can be classified as Epileptic Technosol (Densic, Carbonic, Skeletic) (Fig. 2, A). The surface soil has a dark gray color, with a sod layer of 2 cm thickness characterized by a cloddy structure. Beneath this layer is a dense material mixed with stones of various sizes, with fine earth observed in the upper 10 cm. The vegetation on the Severnaya Mine dump has a projective cover of approximately 25%. Tree cover consists of 10- to 15-year-old birches (*Betula*). A total of 9 plant species were recorded, including narrowleaf fireweed (*Chamaenerion angustifolium*), northern bedstraw (*Galium boreale*), green strawberry (*Fragaria viridis*), common haircap moss (*Polytrichum commune*), couch grass (*Elytrigia repens*), common yarrow (*Achillea millefolium*), sedge (*Carex*), and lady's mantle (*Alchemilla vulgaris*) (Table 1).

Table 1

List of vascular plants on reclaimed waste dumps

Family	Species name	Severnaya Mine Dump	Tsentralnaya Mine Dump	Gorelovskaya Mine Dump
Asteráceae	*Achilléa millefólium*	+	++	+
Rosaceae	*Alchemilla vulgaris*	+	++	–
Asteráceae	*Artemísia absínthium*	–	–	+
Asteráceae	*Artemísia vulgáris*	–	+	–
Gramíneae	*Brōmus inērmis*	–	++	–
Asteráceae	*Carduus crispus*	–	–	+
Cyperaceae	*Cárex sp*	++	+	-
Asteráceae	*Centaurea scabiosa*	–	–	+
Onagraceae	*Chamaenérion angustifolium*	+	–	+
Asteráceae	*Cichórium íntybus*	–	–	+
Asteráceae	*Cirsium arvense*	–	+	–
Gramíneae	*Dáctylis glomeráta*	–	+	–
Gramíneae	*Elytrígia répens*	+	+	–
Gramíneae	*Festuca pratensis*	–	+	–
Rosaceae	*Fragária víridis*	+	+	–
Rubiaceae	*Galium boreale*	+	+	+
Hyperiaceae	*Hypericum perforatum*	–	+	+
Fabaceae	*Lótus corniculátus*	–	+	+
Fabaceae	*Medicago falcata*	–	+	+
Fabaceae	*Medicágo satíva*	–	+	-
Fabaceae	*Melilótus officinális*	–	-	+
Gramíneae	*Phleum pratense*	–	+	+++
Asteráceae	*Picris hieracioides*	–	–	+
Gramíneae	*Poa praténsis*	–	+	+
Polytrichaceae	*Polýtrichum commúne*	+	–	–
Gramíneae	*Puccinellia distans*	–	–	+
Ranunculaceae	*Ranunculus repens*	–	–	+
Caryophylláceae	*Siléne vulgáris*	–	–	+
Asteráceae	*Tanacétum vulgáre*	–	+	+
Fabaceae	*Trifolium praténse*	n/a	n/a	+++
Plantaginaceae	*Veronica teucrium*	n/a	+	n/a
Fabaceae	*Vícia crácca*	n/a	+	n/a
Betulaceae	*Bétula péndula*	+	–20	–19

eISSN 2500-0632
https://mst.misis.ru/

According to the WRB, the clay lithostrat identified on the Tsentralnaya Mine dump is classified as Spolic Epileptic Technosol (Loamic, Densic, Skeletic) (Fig. 2, *B*). The lithostrat lacks distinct horizons or layers, and there is an abundance of stones and coal (about 40%). Up to a depth of 10 cm, the structure is cloddy with herbaceous roots. The soil is dense, clayey, and brownish-brown in color. The vegetation on the Tsentralnaya Mine dump includes 20 species from the families *Gramineae*, *Asteraceae*, *Rosaceae*, *Rubiaceae*, *Fabaceae*, *Plantaginaceae*, and *Cyperaceae* (see Table 1). The projective cover is about 35%.

The clay lithostrat was also diagnosed on the Gorelovskaya Mine dump. According to the WRB, this soil can also be classified as Spolic Epileptic Technosol (Loamic, Densic, Skeletic) (Fig. 2, *C*). The soil is light brown, with blocky soil aggregates and a clayey texture. The lower part of the profile is moist with a plastic consistency. The vegetation on the Gorelovskaya dump includes 19 species. The dominant species are Timothy grass (*Phleum pratense*) and red clover (*Trifolium pratense*), while 17 species from the families *Gramineae*, *Fabaceae*, *Asteraceae*, *Caryophyllaceae*, *Onagraceae*, *Ranunculaceae*, and *Rubiaceae* are found sporadically (see Table 1). The projective cover is about 50%

Vegetation changes were identified using the NDVI index based on Sentinel-2 and Landsat 7,8 satellite images (Figs. 3–5). Succession on the coal waste dumps was analyzed over several time periods: the initial period (untouched dump), a few years after reclamation, and the state of vegetation in 2023.

For the Severnaya Mine dump, four observation periods were considered (see Fig. 3): the initial state of the dump, two years after reclamation, seven years after reclamation, and the current state. The NDVI index for the Severnaya Mine dump in June 2000 (before reclamation) was approximately 0.3. After reclamation, the NDVI index increased to 0.5–0.6, indicating the development of a stable vegetation cover.

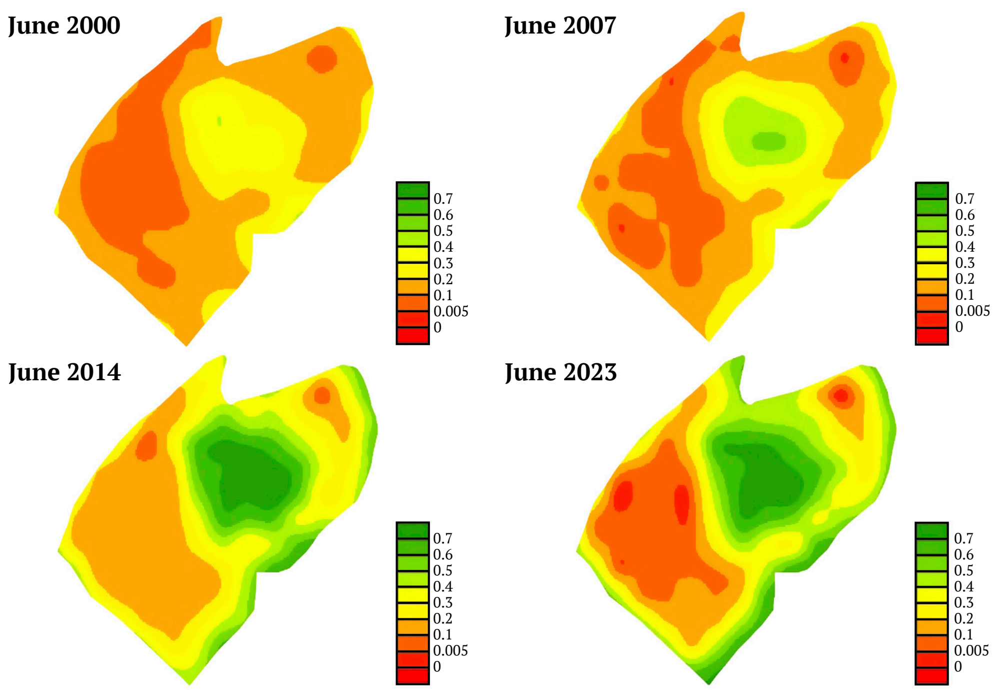

Fig. 3. NDVI Index for the Severnaya Mine Dump

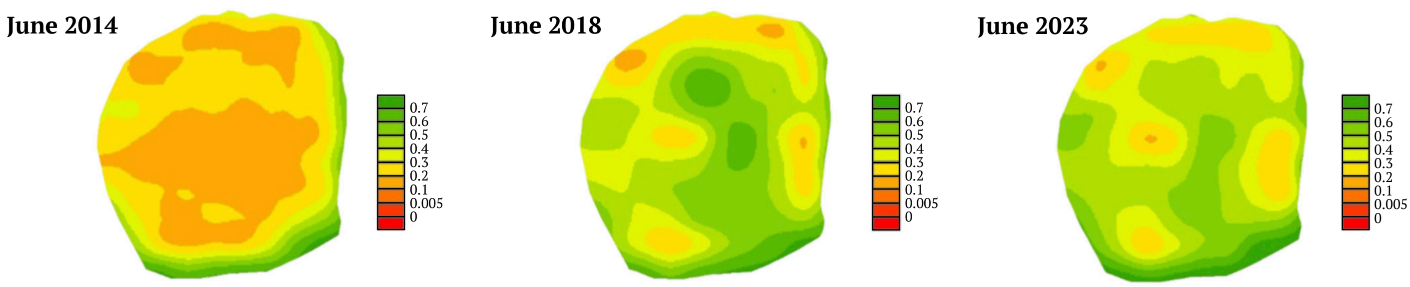

Fig. 4. NDVI Index for the Tsentralnaya Mine Dump

In June 2014 (before reclamation), the NDVI index for almost all areas of the Tsentralnaya Mine dump ranged from 0.1 to 0.3, indicating the absence of any vegetation (Fig. 4). Over the next 9 years, most of the dump area became covered by shrub vegetation, as reflected by an NDVI index value of around 0.4.

On the Gorelovskaya Mine dump, during the 5 years following reclamation, the NDVI index increased from 0.1–0.3 to 0.4–0.55, and even exceeded 0.6 in some areas (Fig. 5). The dynamics of the NDVI index across all three dumps indicate the success of reclamation efforts and the establishment of a stable vegetation cover.

Soil chemical properties

The surface layers of lithostrat 1 and the embryonic soil are characterized by a neutral pH, with pH–H_2O values of 6.8 and 7.9, respectively, and pH–KCl values of 4.4 in lithostrat 1 and 5.5 in the embryonic soil (see Table 2). At a depth of 20 cm, the soils become slightly acidic, with pH–H_2O decreasing to 3.3 in lithostrat 1 and to 5.0 in the embryonic soil. The surface layer of lithostrat 2 has a slightly acidic reaction (pH–H_2O = 6.1, pH–KCl = 4.1), with acidity increasing at depth, reaching pH–H_2O = 4.5 (see Table 1). The lower layers of lithostrat 1 contain sulfide minerals, as indicated by pH values in hydrogen peroxide (pH–H_2O_2 = 1.98) (see Table 2). This is due to the mixing of the lower soil layer with the upper layer of the dump material as a result of physical and chemical migration of substances.

Lithostrat 2 exhibits the highest exchangeable acidity among all the dump soils, attributed to the fact that the soil is formed from the middle horizons of local clay soils. Hydrolytic acidity in lithostrat 1 and the embryonic soil is significantly lower than in the background soil (see Table 2), which is explained by the neutral to slightly alkaline nature of the dump soils. The results of the Kruskal-Wallis test showed that the acidity of the embryonic soil differs from that of the background soil and lithostrats.

The content of mobile iron in the dump soils is 1.5–2 times lower than in the background soil (see Table 2). Sulfate ions dominate in the aqueous extracts of the soils, with the highest concentration found in lithostrat 1. The increase in mobile sulfur content with depth in the lithostrats is associated with the presence of overburden material at depths of 20–30 cm. In contrast, the content of mobile sulfur in the embryonic soil decreases with depth, while it increases in the lithostrats.

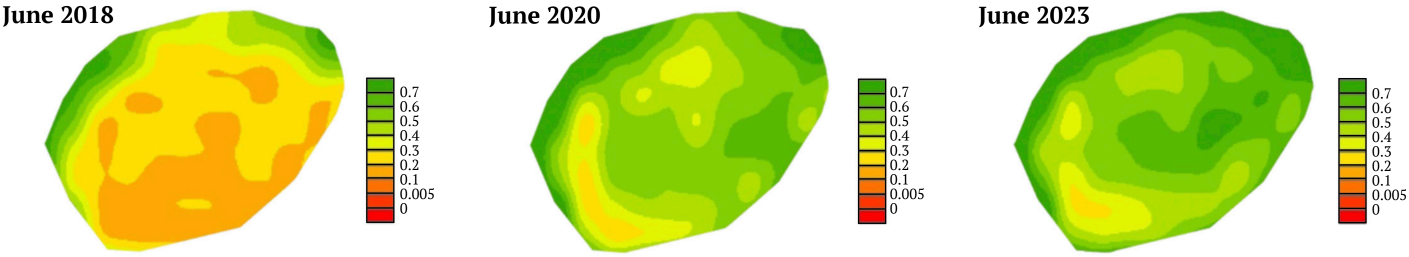

Fig. 5. NDVI Index for the Gorelovskaya Mine Dump

Table 2

Soil chemical properties

Parameters	Depth, cm	pH–H_2O	pH–H_2O_2	pH–KCl	$H_{гк}$*	OK** (Al^{3+}+ H^+)	Al_{exch}	Fe_{mobile}	S_{mobile}	SO_4^{2-}
					mmol/100 g			mg/kg		
Soddy embryonic soil	0–10	7.9	5.47	6.9	1.2	0	0.05	90	211.0	384.0
	10–20	7.4	5.41	6.3	1.2	0	0.05	220	163.0	480.0
	20–30	5.0	3.83	4.3	2.5	0.06	0.05	110	53.6	480.0
Lithostrat 1	0–10	6.8	4.41	5.3	3.9	0.08	0.05	250	17.0	312.0
	10–20	6.1	4.04	4.7	4.7	0.07	0.05	200	109.0	288.0
	20–30	3.3	1.97	2.6	16.3	2.33	3.98	260	253.0	816.0
Lithostrat 2	0–10	6.1	4.10	4.0	4.2	0.60	0.35	70	5.19	168.0
	10–20	5.1	3.80	3.7	15.2	8.40	9.37	110	20.8	240.0
	20–30	4.5	3.30	3.5	21.3	13.60	14.75	250	93.8	230.0
Background sod-podzolic soil	0–10	4.5	3.71	3.5	26.4	5.00	43.00	430	12.90	240.0
	10–20	4.6	3.88	3.5	21.4	5.90	52.00	430	4.60	240.0
	20–30	4.7	4.05	3.6	20.8	5.90	52.00	360	0.20	240.0

Note: * H_{ha} – hydrolytic acidity, ** *EA* – exchangeable acidity.

The organic matter content varies across soil types and layers (Table 3). The highest organic matter content was observed in the embryonic soil. The high organic matter content in the lower layer of lithostrat 1 is attributed to the abundance of coal, while the upper layers of lithostrat 1 contain 2–3 times less organic matter. In comparison to lithostrat 1 and the embryonic soil, lithostrat 2 exhibits the lowest organic matter content.

The cation exchange capacity of the soils is generally moderate, with the highest values in the upper 10 cm layer. The absorption capacity of the background soil is slightly lower, likely due to the presence of exchangeable calcium and magnesium cations. The exchangeable calcium content in the dump soils shows no significant variation and decreases with depth.

The phosphate content in the dump soils is lower than in the background soil and is classified as "low" according to the Kirsanov scale (see Table 3). The highest mobile potassium content is found in lithostrat 1, while the lowest is in the embryonic soil. The nutrient content in the soils is influenced by the duration of soil formation and the vegetation cover. The greatest variety of herbaceous plant species was observed in lithostrat 1 at the Tsentralnaya Mine dump, which may contribute to higher nutrient availability. All soils exhibit similar nitrogen content, except for lithostrat 2 (Table 3).

The upper soil layers of the dumps demonstrate more favorable conditions for test crops compared to the background soil (Fig. 6). Cress grown on lithostrat 1 and the embryonic soil showed significantly better results in terms of height and biomass compared to the control plants grown on vermiculite.

Oats grown in the control group on vermiculite reached the same height as those grown on the dump soils (Fig. 6, *b*). However, the biomass of oats grown in the control group was significantly higher than that of the plants grown on both the dump soils and the background soil.

Table 3

Agrochemical soil properties

Parameters	Depth, cm	Organic matter	Ca_{exch}	Mg_{exch}	EKO	K_{mobile}	$P_2O_{5mobile}$	N_{total}
		%	mmol/100 g			mg/100 g		
Soddy embryonic soil	0–10	12.1	5.75	0.56	37.0	7.0	2.5	311
	10–20	7.7	6.06	0.56	22.0	7.2	0.7	143
	20–30	9.2	4.25	1.00	19.0	2.8	0.09	70
Lithostrat 1	0–10	2.43	10.00	1.25	23.0	20.5	2.2	166
	10–20	3.11	7.60	1.13	24.0	10.4	3.1	93
	20–30	8.90	1.75	0.50	27.0	5.3	0.09	143
Lithostrat 2	0–10	1.04	16.75	6.25	27.0	10.4	3.0	47
	10–20	0.81	5.62	3.62	24.0	10.8	1.9	48
	20–30	1.01	4.75	1.12	28.0	12.0	3.0	49
Background sod-podzolic soil	0–10	5.04	3.25	1.25	13.0	15.4	29.7	187
	10–20	5.07	2.25	1.00	21.0	10.7	22.6	240
	20–30	6.10	2.75	1.25	19.0	8.8	7.5	228

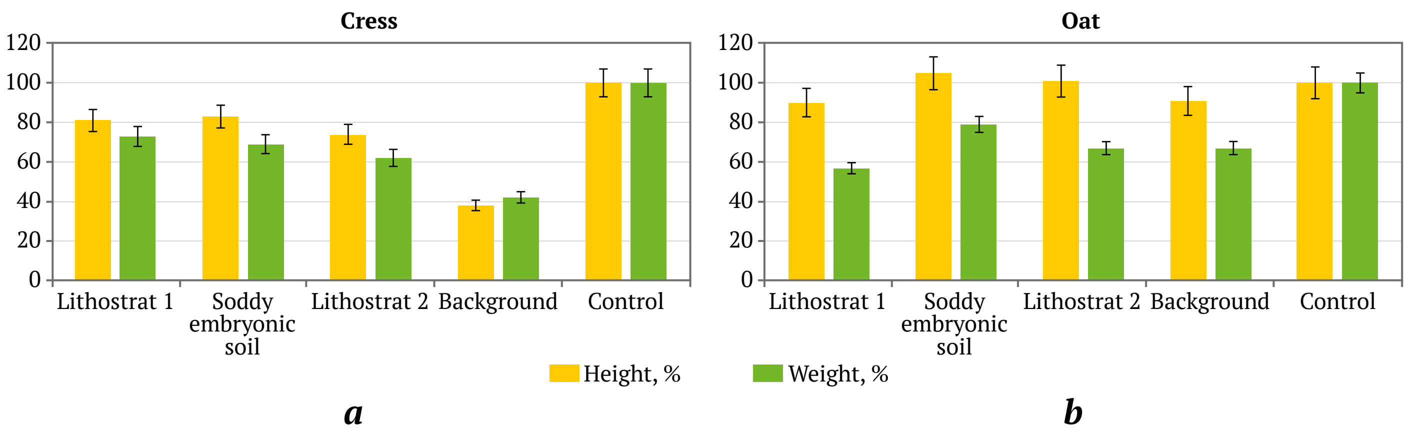

Fig. 6. Phytotesting of the upper soil layers

Discussion

The lithostrats formed as a result of covering the flattened top of the coal waste dump with a layer of clay material, which appears to originate from the subsurface layers or parent material of the local soils. This is evidenced by the similar granulometric and aggregate composition. Iron coatings were observed on soil aggregates (peds) down to a depth of 20 cm. The profile depth of the lithostrats ranges from 30 to 40 cm, which is determined by the thickness of the clay deposit, the slope steepness of the dump, and the degree of fragmentation of the dump's overburden material.

The differences in acidity between the lithostrats can be explained by the fact that the reclamation of lithostrat 2 was completed several years later, and construction debris from former mining operations remained on the Tsentralnaya Mine dump, which may have led to the reduction of acidity in lithostrat 1. However, the strong acidity of the lower layer of lithostrat 1 is attributed to the presence of sulfides in the dump's overburden.

The embryonic soil formed on the crushed overburden of the leveled coal dump. To create favorable conditions for plant growth, slaked lime was added to the surface layer of the dump, making the soil slightly alkaline. The use of lime in waste dump reclamation is a common practice, as is the use of activated sludge as a fertile layer.

For instance, the combined use of beet lime and composted biological materials helped neutralize active and exchangeable acidity in soils and improve soil fertility at a copper mine site [15]. During the biological reclamation phase of the Kapitalnaya Mine in the Kuznetsk Coal Basin, sewage sludge from urban wastewater treatment plants was used as a fertile layer [29].

Primary soil formation processes are actively taking place in the soils of the Kizel Coal Basin (KCB) dumps. Vegetative cover, plant roots, and the annual formation of dead plant matter contribute to the loosening of the upper soil layer and the accumulation of organic matter.

Similar types of technogenic soils are formed under comparable conditions in other regions with coal mining, similar climates, and vegetation [3, 30, 31]. Technogenic soils on waste dumps are pedogenically immature and inherit the negative physicochemical properties of coal mine dumps [32], as well as containing a significant amount of artifacts.

The relatively high mobility of iron in the background soil compared to the dump soils may be due to the acidity and high content of iron hydroxides in the clay minerals of sod-podzolic soils [33, 34].

The low organic matter content in lithostrat 2 is due to the absence of fertilizer application during reclamation. Its organic layer has not yet developed because of the immaturity of the phytocenosis. The high organic matter content in lithostrat 1 can potentially be explained by the presence of coal inclusions throughout the profile, as well as a stable herbaceous community. The presence of coal particles in the overburden [35] could explain the high organic matter content in the embryonic soil (7.7–12.1%) and the lower layer of lithostrat 1(8,9%).

The amount of total nitrogen and mobile potassium increases with the age of the lithostrat, as confirmed by [36, 37]. Overall, the total nitrogen content in the lithostrats is significantly lower than in the background sod-podzolic soil and embryonic soil.

The coefficient of variation (CV) is explained by the influence of technogenic and anthropogenic processes on soil formation. Notably, the coefficient of variation for exchangeable acidity, organic matter, total iron, and mobile sulfur in the lithostrats exceeds 40%. In contrast, the range of CV for these indicators is significantly lower in the embryonic soil. This is due to the homogeneity of the parent material in the embryonic soil, while the lithostrats consist of a mixture of clay and the upper layer of the dump. As a result, the properties of the lower layers of the lithostrats do not correspond to either the characteristics of the overburden or the clay material. The coefficient of variation for most chemical indicators of the background soil does not exceed 25%, except for mobile sulfur content, where the CV reaches 110%, similar to the values for mobile sulfur in the lithostrats and embryonic soil.

Correlation analysis revealed a direct and significant relationship between hydrolytic acidity, exchangeable aluminum content, and mobile iron. The sources of iron in the studied technogenic soils are minerals from zonal soils and the overburden of the dumps. The amount of mobile phosphates is proportional to these indicators, possibly due to the ability of phosphates to form complexes with aluminum and iron under acidic conditions. At the same time, a negative correlation was found between absorption capacity and mobile iron.

Based on the growth indicators of oats, the embryonic soil showed the best biological conditions, as it has a neutral pH and is characterized by a high organic matter content.

Reclamation of coal dumps through the creation of a clay barrier or the addition of fertilizers to stimulate the growth of herbaceous or woody vegetation is critical for preventing water and wind erosion, as well as the spread of pollutants. It is also essential for establishing stable plant communities. The chemical properties of technogenic soils vary significantly across the profile compared to the background soil in the study area, as well as among themselves.

Reclamation activities at the Severnaya Mine dump, conducted 25 years ago, have resulted in the formation of soddy embryonic soil, and soil evolution continues. Reclamation activities at the Severnaya Mine dump, conducted 25 years ago, have resulted in the formation of soddy embryonic soil, and soil evolution continues. Reclamation with the addition of slaked lime has reduced soil acidity to neutral levels and increased organic matter content and absorption capacity. Given that a stable herbaceous-woody plant community has developed on the reclaimed soils, this reclamation method can be considered effective. The modification of the substrate by adding ash, slag, and sewage sludge has been studied on coal dumps in Brazil, showing promising results for growing bristle oat (*Avena strigose*) and corn (*Zea mays*) [38].

Covering dumps with clay material neutralizes the sulfide minerals in the overburden by creating a barrier that prevents water and oxygen from contacting the minerals and forming acid mine drainage. The studied lithostrats formed similarly but differ in age. The effectiveness of reclamation using clay to cover the dump can be assessed by comparing the initial condition of the dump soil (lithostrat 2) with the more mature soil (lithostrat 1). The number of plant species in the vegetation community increases over time. A diverse herbaceous community promotes the accumulation of organic matter in the upper soil layer and the formation of soil aggregates, which improves the physical properties of the dump soils, reduces acidity, and increases NPK content.

In the study by [39], soils were compared 5, 10, and 25 years after mining. In the soils of degraded coal mining lands, carbon and nitrogen reserves increased with the length of the reclamation period. This may also be attributed to the input of organic matter from the waste dumps. The physical properties of the soil improved over time. Finer fractions became dominant in the older dump soils. [18] reported an increase in plant biodiversity in long-reclaimed areas. [17] noted the beneficial effects of herbaceous plants on the physicochemical properties of soils during the reclamation of mining areas. Soil properties on reclaimed dumps, such as organic matter content, nitrogen, and phosphorus levels, improved over time following reclamation [40].

Overall, plant growth on sulfide coal dumps after reclamation prevents wind and water erosion, spontaneous combustion, and the spread of contaminants [41]. Based on a comparison of lithostrats of different ages, it is recommended that organic and mineral fertilizers be applied to the reclaimed soil. Agroamelioration measures (soil layer formation for plant growth, fertilizer application, and planting of herbaceous crops) help achieve optimal results [42].

Conclusions

Various soil types have been identified on the reclaimed waste dumps of the Kizel Coal Basin. The classification is based on the reclamation activities carried out and the technogenic soil-forming materials. Clay lithostrats, or Spolic Epileptic Technosol (Loamic, Densic, Skeletic), were found on the dumps reclaimed by surface leveling and covering with clay material. The embryonic soil, classified as Epileptic Technosol (Densic, Carbonic, Skeletic), formed over a nearly 25-year period after the coal dump was leveled and lime was applied to the upper layer.

The absence of horizons and a well-defined soil aggregate structure, along with the presence of numerous artifacts (fragments of overburden of various sizes) in the soils formed on coal dumps, indicates their technogenic origin and immature stage of development.

The acidity levels in the lithostrats ranged from acidic to neutral, with hydrolytic acidity decreasing over time following reclamation. The embryonic soil exhibits a slightly alkaline reaction, and exchangeable acidity is absent. Statistical analysis showed no differences between the pH in water and the pH in KCl of the lithostrats and the background soil. However, the level of exchangeable acidity in lithostrat 1 was lower than that in the background soil and lithostrat 2.

Since the embryonic soil formed from crushed overburden of coal dumps, it contains the highest amount of organic matter. The organic matter content in lithostrat 1 is higher than in lithostrat 2, which is attributed to the presence of coal inclusions throughout the profile.

Herbaceous vegetation contributes to the formation of soil structure, the accumulation of organic matter, exchangeable calcium and magnesium ions, and, as a result, the reduction of acidity. The nutrient content (NPK) also depends on the time of soil formation and plant species diversity. Phytotesting using cress and oats showed that the dump soils provide more favorable environmental conditions for plant growth compared to the background soil.

Overall, reclamation accelerates soil formation and the development of stable plant communities on waste dumps, while minimizing the spread of contaminants to other environmental components. According to the NDVI index, stable herbaceous vegetation was observed on the sulfide dump just two years after reclamation. During the reclamation period, it is essential to implement measures such as plowing and the application of organic and mineral fertilizers to create optimal conditions for plant communities.

References

1. Tichavsky R., Lenart J., Fabiánová A., Tolasz R. Tree-ring records of surface displacements in a coal-mining subsided region and their links to hypsometric changes and extreme precipitation. *Catena*. 2023;221(Part A):106758. https://doi.org/10.1016/j.catena.2022.106758
2. Kutepov Yu.I., Kutepova N.A., Mukhina A.S., Moseykin V.V. Geological, geotechnical and geoecological problems of reclamation of land disturbed by dumping in open pit coal mining in Kuzbass. *Mining Informational and Analytical Bulletin*. 2022;(5):5–24. (In Russ.) https://doi.org/10.25018/0236_1493_2022_5_0_5
3. Bragina P.S., Tsibart A.S., Zavadskaya M.P., Sharapova A.V. Soils on overburden dumps in the forest_steppe and mountain taiga zones of the Kuzbass. *Eurasian Soil Science*. 2014;(47):723–733. https://doi.org/10.1134/S1064229314050032
4. Nádudvari A., Kozielska B., Abramowicz A. et al. Heavy metal- and organic-matter pollution due to self-heating coal-waste dumps in the Upper Silesian Coal Basin (Poland). *Journal of Hazardous Materials*. 2021;(412):125244. https://doi.org/10.1016/j.jhazmat.2021.125244
5. Tozsin G. Hazardous elements in soil and coal from the Oltu coal mine district, Turkey. *International Journal of Coal Geology*. 2014;(131):1–6. https://doi.org/10.1016/j.coal.2014.05.011
6. Shan Y., Wang W., Qin Y., Gao L. Multivariate analysis of trace elements leaching from coal and host rock. *Groundwater for Sustainable Development*. 2019;8:402–412. https://doi.org/10.1016/j.gsd.2019.01.001
7. Maksimovich N.G., Pyankov S.V. *The Kizel Coal Basin: ecological problems and solutions*. Perm: Perm State National Research University; 2018. 288 p. (In Russ.)
8. Ushakova E., Menshikova E., Blinov S. et al. environmental assessment impact of acid mine drainage from Kizel coal basin on the Kosva Bay of the Kama Reservoir (Perm Krai, Russia). *Water*. 2022;14(5):727. https://doi.org/10.3390/w14050727
9. Ushakova E., Menshikova E., Blinov S. et al. Distribution of trace elements, rare earth elements and ecotoxicity in sediments of the Kosva bay, Perm region (Russia). *Journal of Ecological Engineering*. 2022;23(4):1–16. https://doi.org/10.12911/22998993/146269
10. Yang J., Wei H., Quan Z. et al. A global meta-analysis of coal mining studies provides insights into the hydrologic cycle at watershed scale. *Journal of Hydrology*. 2023;617(Part B):129023. https://doi.org/10.1016/j.jhydrol.2022.129023
11. Imaykin A.K., Imaykin K.K. *Hydrogeological conditions of the Kizelovsky coal basin during and after the end of its operation, forecast of their changes*. Perm: Perm State National Research University; 2013. 112 p. (In Russ.)
12. Singh K.N., Narzary D. Geochemical characterization of mine overburden strata for strategic overburden-spoil management in an opencast coal mine. *Environmental Challenges*. 2021;(3):100060. https://doi.org/10.1016/j.envc.2021.100060
13. Welch C., Barbour S.L., Hendry M.J. The geochemistry and hydrology of coal waste rock dumps: A systematic global review. *Science of the Total Environment*. 2021;(795):148798. https://doi.org/10.1016/j.scitotenv.2021.148798
14. Jiao Y., Zhang C., Su P. et al. A review of acid mine drainage: Formation mechanism, treatment technology, typical engineering cases and resource utilization. *Process Safety and Environmental Protection*. 2023;(170):1240–1260. https://doi.org/10.1016/j.psep.2022.12.083
15. Fernández-Caliani J.C., Giráldez M.I., Waken W.H. et al. Soil quality changes in an Iberian pyrite mine site 15 years after land reclamation. *Catena*. 2021;(206):105538. https://doi.org/10.1016/j.catena.2021.105538
16. Ahirwal J., Maiti S.K. Development of Technosol properties and recovery of carbon stock after 16 years of revegetation on coal mine degraded lands, India. *Catena*. 2018;(166):114–123. https://doi.org/10.1016/j.catena.2018.03.026
17. Li Y., Zhou W., Jing M. et al. Changes in reconstructed soil physicochemical properties in an opencast mine dump in the Loess Plateau Area of China. *International Journal of Environmental Research and Public Health*. 2020;19(2):706. https://doi.org/10.3390/ijerph19020706
18. Arshi A. Reclamation of coalmine overburden dump through environmental friendly method. *Saudi Journal of Biological Sciences*. 2017;24(2):371–378. https://doi.org/10.1016/j.sjbs.2015.09.009
19. Rahmonov O., Czajka A., Nádudvari Á. et al. Soil and vegetation development on coal-waste dump in Southern Poland. *International Journal of Environmental Research and Public Health*. 2022:(19):9167. https://doi.org/10.3390/ijerph19159167
20. Lei H., Peng Z., Yigang H., Yang Z. Vegetation and soil restoration in refuse dumps from open pit coal mines. *Ecological Engineering*. 2016:(94):638–646. https://doi.org/10.1016/j.ecoleng.2016.06.108

21. Feng Y., Wang J., Bai Z. Reading Lucy Effects of surface coal mining and land reclamation on soil properties: A review. *Earth-Science Reviews*. 2019;(191):12–25. https://doi.org/10.1016/j.earscirev.2019.02.015
22. Guan Y., Wang J., Zhou W. et al. Identification of land reclamation stages based on succession characteristics of rehabilitated vegetation in the Pingshuo opencast coal mine. *Journal of Environmental Management*. 2022;(305):114352. https://doi.org/10.1016/j.jenvman.2021.114352
23. Pyankov S.V., Maximovich N.G., Khayrulina E.A. et al. Monitoring acid mine drainage's effects on surface water in the Kizel Coal Basin with Sentinel-2 Satellite Images. *Mine Water and the Environment*. 2021;(40):606–621. https://doi.org/10.1007/s10230-021-00761-7
24. Karakulieva A.A., Kondrateva M.A. Properties of embryoses of coal mines dumps of the Kizelovsky Basin. Anthropogenic Transformation of Nature. 2018;(4):156–159. (In Russ.)
25. Berdinskikh S.Yu., Botalov V.S., Romanov A.V., Zaytsev A.G. Agrochemical characteristics of the top layer of soil on coal waste heaps and the effect of claying on their natural overgrowth on the example of the Kizelovsky Coal Basin. In: *Ecological Safety in the Conditions of Anthropogenic Transformation of the Natural Environment. Collection of papers of the All-Russian School-Seminar Dedicated to the Memory of N. F. Reimers and F. R. Shtilmark*. Perm: Perm State National Research University; 2022. Pp. 437–441. (In Russ.)
26. Menshikova E., Osovetsky B., Blinov S., Belkin P. Mineral formation under the influence of mine waters (the Kizel Coal Basin, Russia). *Minerals*. 2020;10(4):364. https://doi.org/10.3390/min10040364
27. Motuzova G.V., Bezuglova O.S. *Ecological monitoring of soils*. Moscow: Academic Project, Gaudeamus; 2007. (In Russ.)
28. Androkhanov V.A. Specificity and genesis of the soil cover of man-made landscapes. *Siberian Journal of Forest Science*. 2005;(5):795–800. (In Russ.)
29. Nekrasova A.E., Bobrenko E.G., Knych A.I., Sologaev V.I. Reclamation of waste dump open joint-stock company "Mine "Capital" of the Kemerovo Region. *Vestnik of Omsk SAU*. 2016;(1):154–160. (In Russ.)
30. Uzarowicz Ł., Zagórski Z., Mendak E. et al. Technogenic soils (Technosols) developed from fly ash and bottom ash from thermal power stations combusting bituminous coal and lignite. Part I. Properties, classification, and indicators of early pedogenesis. *Catena*. 2017;(157):75–89. https://doi.org/10.1016/j.catena.2017.05.010
31. Krupskaya L.T., Androkhanov V.A., Belanov I.P. Technogenic surface formations within the limits of mining-industrial system of the Dalnegorsky District of the Primorsky Krai as the reclamation site. *IOP Conference Series: Earth and Environmental Science*. 2020;459:032046. https://doi.org/10.1088/1755-1315/459/3/032046
32. Filcheva E., Hristova M., Haigh M. et al. Soil organic matter and microbiological development of technosols in the South Wales Coalfield. *Catena*. 2021;(201):105203. https://doi.org/10.1016/j.catena.2021.105203
33. Kozlova A.A., Khalbaev V.L., Aysueva T.S. et al. Contents of different forms of iron in the soils of Southern Predbaikal'ye. *International Journal of Applied and Fundamental Research*. 2014;(5):56–61. (In Russ.)
34. Litvinovich A.V., Lavrishchev A.V., Bure V.M. et al. Studying the dynamics of mobile iron contentin sod-podzolic light loam soil ameliorated by dolomite. *Agrohimia*. 2019;(3):44–53. (In Russ.) https://doi.org/10.1134/S0002188119030098
35. Menshikova E.A. Technogenical formation of mining areas in the Perm region. *Geology and mineral resources of Western Urals*. 2020;(3):277–281. (In Russ.)
36. Li X., Lei S., Liu F., Wang W. Analysis of plant and soil restoration process and degree of refuse dumps in open-pit coal mining areas. *International Journal of Environmental Research and Public Health*. 2020;17(6):1975. https://doi.org/10.3390/ijerph17061975
37. Zhang N., Huang S., Lei H. et al. Changes in soil quality over time focusing on organic acid content in restoration areas following coal mining. *Catena*. 2022;(218):106567. https://doi.org/10.1016/j.catena.2022.106567
38. Firpo B.A., Weiler J., Schneider I.A.H. Technosol made from coal waste as a strategy to plant growth and environmental control. *Energy Geoscience*. 2021;2(2):160–166. https://doi.org/10.1016/j.engeos.2020.09.006
39. Bandyopadhyay S., Novo L.A.B., Pietrzykowski M., Maiti S.K. Assessment of forest ecosystem development in coal mine degraded land by using Integrated Mine Soil Quality Index (IMSQI): the evidence from India. *Forests*. 2020;11(12):1310. https://doi.org/10.3390/f11121310
40. Liu X., Bai Z., Zhou W. et al. Changes in soil properties in the soil profile after mining and reclamation in an opencast coal mine on the Loess Plateau, China. *Ecological Engineering*. 2017;(98):228–239. https://doi.org/10.1016/j.ecoleng.2016.10.078

41. Zheng S., Bai D.-S., Yang X. et al. Changes in soil microecology of gangue reclamation areas after 10 years of in situ restoration with herbaceous plants (Artemisia sacrorum and Imperata cylindrica) and trees (Populus spp.). *Ecological Engineering*. 2022;182:106719. https://doi.org/10.1016/j.ecoleng.2022.106719

42. Xu D., Li X., Chen J., Li J. Research progress of soil and vegetation restoration technology in open-pit coal mine: a review. *Agriculture*. 2023;13(2):226. https://doi.org/10.3390/agriculture13020226

Information about the authors

Natalya V. Mitrakova – Cand. Sci. (Biol.), Senior Researcher at the Laboratory of Biogeochemistry of Man-made Landscapes, Natural Science Institute, Perm State National Research University, Perm, Russian Federation; ORCID 0000-0002-5571-7725, Scopus ID 57208284684, ResearcherID ABC-8334-2021; e-mail mitrakovanatalya@mail.ru

Elena A. Khayrulina – Dr. Sci. (Geograph.), Leading Researcher at the Laboratory of Biogeochemistry of Man-made Landscapes, Natural Science Institute, Professor of the Department of Cartography and Geoinformatics, Faculty of Geography, Perm State National Research University, Perm, Russian Federation; ORCID 0000-0002-9074-8551, Scopus ID 56029238900, ResearcherID J-8411-2014; e-mail elenakhay@gmail.com

Anna A. Perevoshchikova – Junior Researcher at the Laboratory of Biogeochemistry of Man-made Landscapes, Natural Science Institute, Perm State National Research University, Perm, Russian Federation; ORCID 0000-0003-1769-7740, Scopus ID 57694899800; e-mail aaperevoshchikova@yandex.ru

Natalya V. Poroshina – Cand. Sci. (Chem.), Senior Researcher at the Laboratory of Biogeochemistry of Man-made Landscapes, Natural Science Institute, Perm State National Research University, Perm, Russian Federation; ORCID 0000-0002-1761-6720, Scopus ID 57694163400; e-mail navit1@yandex.ru

Elizaveta E. Malyshkina – Research Engineer at the Laboratory of Biogeochemistry of Man-made Landscapes, Natural Science Institute, Perm State National Research University, Perm, Russian Federation; ORCID 0000-0002-7251-7637, Scopus ID 58017742100; e-mail thelionofcintra@gmail.com

Evgenia S. Yakovleva – Research Engineer at the Laboratory of Biogeochemistry of Man-made Landscapes, Natural Science Institute, Perm State National Research University, Perm, Russian Federation; ORCID 0009-0005-5344-7361; e-mail evyakovlevaa@gmail.com

Nikita A. Kobelev – Research Engineer at the Laboratory of Biogeochemistry of Man-made Landscapes, Natural Science Institute, Perm State National Research University, Perm, Russian Federation; ORCID 0009-0007-3129-5568; e-mail amst3rz@gmail.com

Received 13.04.2024
Revised 08.06.2024
Accepted 22.06.2024

MINING SCIENCE AND TECHNOLOGY (RUSSIA)
ГОРНЫЕ НАУКИ И ТЕХНОЛОГИИ
2024;9(4):420–432
eISSN 2500-0632
https://mst.misis.ru/

MINING MACHINERY, TRANSPORT, AND MECHANICAL ENGINEERING

Research article

https://doi.org/10.17073/2500-0632-2023-10-175
УДК 622.734:658.58

Vibration metrics for informational support in assessing the technical condition of ball mills

V.F. Borisenko [1], **V.A. Sidorov**[1] ✉, **A.E. Sushko**[2], **V.N. Rybakov** [3]

[1] *Donetsk National Technical University, Donetsk, Russian Federation*
[2] *SPA DIATECH LLC, Moscow, Russian Federation*
[3] *PromTEK R&D LLC, Samara, Russian Federation*
✉ *sidorov_va58@mail.ru*

Abstract
The technical condition of ball mills, employed in the fine grinding of minerals, ores, coal, cement clinker, and other materials, is dictated by both the operational load and the actual physical state of the equipment. Vibration metrics serve as the most versatile diagnostic parameter for developing an informational profile of equipment in active use. The distinct operational environments of high-powered ball mills with frequency-controlled drive systems – one with an induction motor (FC-IM) and the other with a synchronous motor (FC-SM) – necessitate the development of universal approaches to assessing vibration loading that consider each mill's unique design features and operational modes. This study presents the first analysis of the key interrelated technical characteristics of industrial ball mills, including drum volume, diameter, rotational speed, ball load, total weight, and drive power, enabling a more substantiated approach to selecting technical parameters and operational modes. The installation of a permanent vibration control system on ball mills used for grinding mineral raw materials required the individual determination of technical condition category thresholds for the motor, gear-shaft, and drum. The category thresholds were determined individually for each shaft using statistical classification, under the assumption that coupled components are in a state influenced by the energy potential of damage during staged progression. Standard 'reference' ratios of vibration values across three mutually perpendicular directions were established. Characteristic patterns and sequences of damage progression were identified based on the direct spectra of vibration velocity and acceleration. During the analysis of vibration signal time series, a beat frequency mode was detected, indicating potential damage development within gear elements. Effective informational support for the operational condition of ball mills is achieved through the analysis of overall vibration levels, direct trends in vibration velocity and acceleration, time series of the vibration signal, and both long-term and short-term trend analyses. Vibration velocity trends provide insights into technical condition by assessing operational stability, startup frequency, and maintenance intervals.

Keywords
ball mill, electric drive, electric engine, gear unit, design, shaft, bearing, operation, operational capacity, damage, failures, control, diagnostics, vibration, signal, vibration analyzer, vibration velocity, vibration acceleration, frequency, amplitude, harmonic, spectrum, analysis, correlation, forecasting, trend analysis

For citation
Borisenko V.F., Sidorov V.A., Sushko A.E., Rybakov V.N. Vibration metrics for informational support in assessing the technical condition of ball mills. *Mining Science and Technology* (*Russia*). 2024;9(4):420–432. https://doi.org/10.17073/2500-0632-2023-10-175

ГОРНЫЕ МАШИНЫ, ТРАНСПОРТ И МАШИНОСТРОЕНИЕ

Научная статья

Вибрационные показатели для информационного обеспечения оценки технического состояния шаровых мельниц

В.Ф. Борисенко[1], **В.А. Сидоров**[1] ✉, **А.Е. Сушко**[2], **В.Н. Рыбаков**[3]

[1] *Донецкий национальный технический университет, г. Донецк, Российская Федерация*
[2] *ООО НПО «ДИАТЕХ», г. Москва, Российская Федерация*
[3] *ООО НПП «ПромТЭК» г. Самара, Российская Федерация*
✉ *sidorov_va58@mail.ru*

Аннотация
Техническое состояние шаровых мельниц, используемых в процессе подготовки минералов, руд, угля, цементного клинкера и др. для тонкого измельчения материалов, определяется технологической нагрузкой и фактическим состоянием. Вибрационные показатели в данном случае являются наиболее

универсальным диагностическим показателем при формировании информационной картины работающего оборудования. Уникальность условий эксплуатации мощных агрегатов шаровых мельниц с регулированием частоты вращения на базе систем ПЧ – АД (преобразователь частоты – асинхронный двигатель), ПЧ – СД (преобразователь частоты – синхронный двигатель) требует разработки универсальных подходов к оценке вибрационной нагруженности с учётом индивидуальных конструкторских особенностей и режимов работы. В статье впервые выполнен анализ основных взаимосвязанных технических характеристик промышленных шаровых мельниц: объём барабана, диаметр, частота вращения, шаровая нагрузка, общий вес, мощность привода, что позволит более обоснованно подойти к выбору технических параметров и режимов работы. Установка стационарной системы вибрационного контроля на шаровых мельницах размола минерального сырья потребовала индивидуального определения границ категорий технического состояния отдельно для двигателя, вал-шестерни и барабана. Границы категорий определялись индивидуально для каждого вала методом статистической классификации в предположении, что сопрягаемые узлы находятся в состоянии, формируемом энергетическим потенциалом повреждения при ступенчатом развитии. Определены «эталонные» соотношения между значениями вибрации в трёх взаимно перпендикулярных направлениях. Установлены характерные образы и последовательность развития повреждений по прямым спектрам виброскорости и виброускорения. При анализе временных реализаций вибрационного сигнала выделен режим биений как признак развития повреждения элементов зубчатых передач. Информативное обеспечение технического состояния шаровых мельниц в достаточной степени достигается анализом общего уровня вибрации, прямых трендов виброскорости и виброускорения, анализом временных реализаций вибрационного сигнала, длительным и краткосрочным анализом трендов. Тренды виброскорости позволяют оценить техническое состояние по стабильности работы, частоте запусков, времени ремонтов.

Ключевые слова
шаровая мельница, электропривод, электродвигатель, редуктор, конструкция, вал, подшипники, эксплуатация, работоспособность, повреждения, отказы, контроль, диагностика, вибрация, сигнал, виброанализатор, виброскорость, виброускорение, частота, амплитуда, гармоника, спектр, анализ, корреляция, прогнозирование, тренд

Для цитирования
Borisenko V.F., Sidorov V.A., Sushko A.E., Rybakov V.N. Vibration metrics for informational support in assessing the technical condition of ball mills. *Mining Science and Technology* (*Russia*). 2024;9(4):420–432. https://doi.org/10.17073/2500-0632-2023-10-175

Introduction

The operational condition of ball mills used for preparing minerals, ores, coal, cement clinker, and other materials for fine grinding to sizes ranging from 0.074 to 0.4 mm is determined by the operational load, actual physical state, and the quality of maintenance and repairs. In this context, vibration metrics serve as the most versatile diagnostic indicator for creating an informational profile of equipment in active operation.

Literature Review

Vibration measurements of ball mill components in certain industrial sectors have shown that unique characteristics, large dimensions, low rotational speeds, and other factors limit the application of traditional approaches commonly used in vibration diagnostics. The issues of vibration diagnostics presented in the monograph [1] are undoubtedly classical; however, discrepancies arise in the evaluation of technical condition categories when assessing overall vibration levels. Differences also emerge when analyzing time series of vibration signals, unlike those discussed in [2]. The vibration spectra examples provided in [3] should also be supplemented with results obtained from diagnostics of this equipment. According to the standard[1], ball mills are classified as Class III – large machines mounted on rigid foundations without differentiation by drive type. The standard[2] specify vibration limits for machinery operating at "nominal speeds between 120 and 15,000 rpm". Certain general provisions related to vibration measurement and analysis, as outlined in various standards[3], served as the foundation for this study, which aims to refine specific aspects of vibration analysis for assessing the condition of ball mills.

[1] GOST ISO 10816-1-97. Vibration. Machine condition monitoring based on vibration measurements of non-rotating parts. Part 1. General requirements.

[2] GOST R ISO 10816-3-99. Machine condition monitoring based on vibration measurements of non-rotating parts. Part 3. Industrial machines with a nominal power above 15 kW and nominal speeds from 120 to 15,000 rpm.

[3] GOST R ISO 13373-1-2009. Condition monitoring and diagnostics of machines. Vibration condition monitoring. Part 1. General methods; GOST R ISO 13373-2-2009. Condition monitoring and diagnostics of machines. Vibration condition monitoring. Part 2. Processing, analysis, and presentation of vibration measurement results.

The design, calculations, and operational conditions of ball mills have been actively studied over an extended period, spanning both the 20th and 21st centuries. Primary attention has been given to technological aspects [4]; however, the quality of grinding is proposed to be assessed by the vibration of the drum walls [5]. The grinding patterns within ball mills [6] can also be validated by the vibration characteristics of an operating mill [7] based on a simulated model of wall vibration. Issues related to the modernization of horizontal ball mill drives [8] indicate efforts to enhance the durability of this equipment. The operational practice of ball mills necessitates information on the vibration profile based on experimental research [9] and the identification of diagnostic indicators of damage to specific components, such as gear transmissions, using digital twin technology [10]. This brief literature review confirms the relevance of vibration diagnostics for ball mills and the application of resulting data to support technical condition assessment. It also underscores the timeliness of discussing industrial research data that define the vibration profile of ball mills.

General provisions

Currently, significant attention is focused on optimizing drive systems, automation, and control in grinding processes[4]. For the first time, an analysis of the primary interrelated technical characteristics of industrial ball mills (Fig. 1) has been conducted, including parameters such as drum volume – V_b, m³, drum diameter – D_b, m, rotational speed – W, rad/s, ball load – Q_{mel}, t, total weight – Q, t, and drive power – P, kW. By comparing the correlation dependencies $Q = f(V_b)$ and $P = f(V_b)$, their similarity can be

[4] ham Van Bien. Switched reluctance drive for ball mills. Dissertation abstract for the Candidate of Technical Sciences. Institution of defense: South-Russian State Polytechnic University (NPI) named after M.I. Platov, Novocherkassk; 2019; Zakamalden A.A. Optimal control of the grinding process in a ball mill using a predictive model. Dissertation and Abstract for the Candidate of Technical Sciences. Institution of defense: Tomsk State University of Control Systems and Radioelectronics, Tomsk; 2022; Khanin S.I. Development of scientific foundations for designing ball mills with energy exchange and classifying devices. Dissertation abstract for the Doctor of Technical Sciences. Institution of defense: Orel State University named after I.S. Turgenev, Belgorod; 2016.

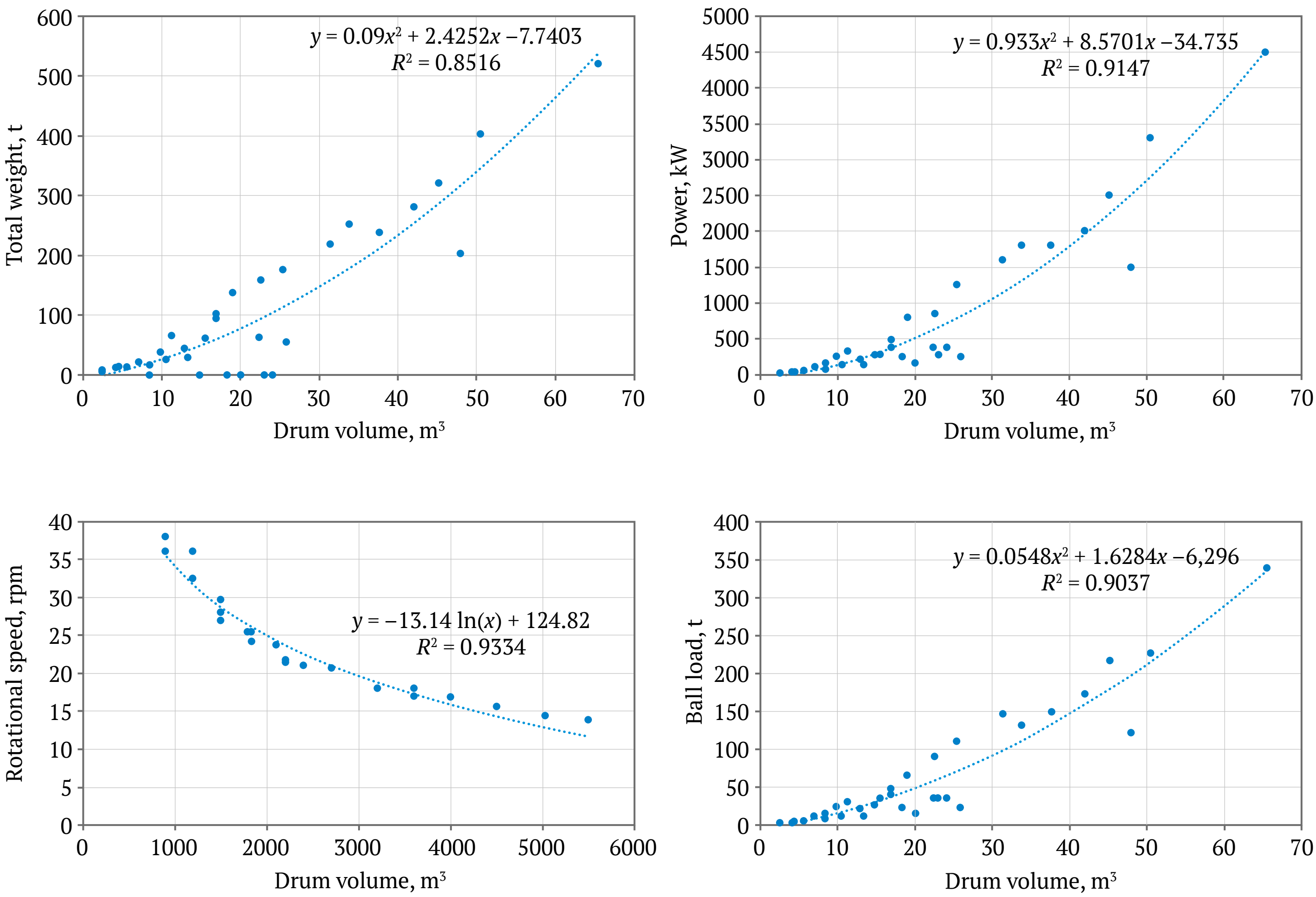

Fig. 1. Correlations between key characteristics of available ball mill size classifications

noted; conversely, for the dependencies $W = f(D_b)$ and $Q_{mel} = f(V_b)$, an inverse similarity is observed. The established correlation dependencies for the graphs:

$$Q = f(V_b): y = 0.09x^2 + 2.4252x - 7.7403, R^2 = 0.8516; \quad (1)$$

$$P = f(V_b): y = 0.933x^2 + 8.5701x - 34.735, R^2 = 0.91474; \quad (2)$$

$$W = f(D_b): y = -13.14 \ln x + 124.82, R^2 = 0.9334; \quad (3)$$

$$Q_{mel} = f(V_b): y = 0.0548x^2 + 1.6284x - 6.296, R^2 = 0.9037, \quad (4)$$

will enable specialists in design and operation to make more informed decisions regarding the selection of technical parameters and operational modes for both existing and planned-for-commissioning ball mills.

The wide variability in technical specifications should be factored in when setting vibration standards, as these mills are often manufactured as customized units or in limited production runs for specialized orders. The prolonged operational cycle for crushing and grinding raw materials allows for the use of either synchronous or induction motors as ball mill drives. A synchronous motor with a rotational speed of 75 rpm or 150 rpm, to achieve a drum rotation speed of 13–16 rpm, requires the use of a single-stage gear unit with a gear ratio of 5.4–9.0, with the drum's ring gear acting as the drive wheel of the gear unit.

The use of an induction motor requires installing either a cylindrical gear unit[5] [8] (with one or two low-speed gears) or a planetary gear unit[6] with a high gear ratio. A direct drive configuration from the low-speed shaft of the gear unit, without using the drum's ring gear as the drive wheel of the gear unit, is also possible. Implementing a dual-gear unit drive reduces overall system reliability due to the increased number of components or insufficient motor load. In the event of a motor failure, the remaining motor is expected to complete the current stage of the technological process. To ensure continuous grinding operation when using multiple ball mills, partial redundancy is employed, allowing maintenance on one or more machines. Transitioning to a predictive maintenance strategy should be supported by data on individual stiffness characteristics and specific drive type features.

Options for diagnosing the technical condition of mills with synchronous and induction drive motors

The arrangement of vibration measurement control points (Fig. 2) was determined according to the recommendations of the GOST ISO 10816-1–97 standard: *1* – free bearing of the electric motor; *2* – motor bearing near the coupling; *3* – drive gear bearing; *4* – non-drive side bearing of the drive gear; *5* – drum bearing on the drive side; *6* – drum bearing on the non-drive side. The sensor was mounted using a magnetic attachment. The monitored frequency ranges were 2–800 Hz and 10–4000 Hz. Measurements were taken along three mutually perpendicular directions: *V* – vertical, *T* – transverse (horizontal), and *A* – axial.

The ball mill's structure includes three shafts (each mounted on two bearing supports) that are kinematically connected, with variations in rotational speed, bearing support design, and stiffness:

– synchronous drive motor shaft – points *1* and *2*;

– drive gear shaft – points *3* and *4*;

– mill drum – a hollow shaft with a gear wheel, mounted on sliding bearings– points *5* and *6*.

[5] FLSmidth company website Gear Units for Horizontal Mills. URL: www.FLSmidthMaagGear.com

[6] FLENDER company website. PLANUREX 3 standard series. URL: https://www.flender.com/de/Produkte/Getriebe/PLANUREX-3-Standardbaureihe/p/ATN319

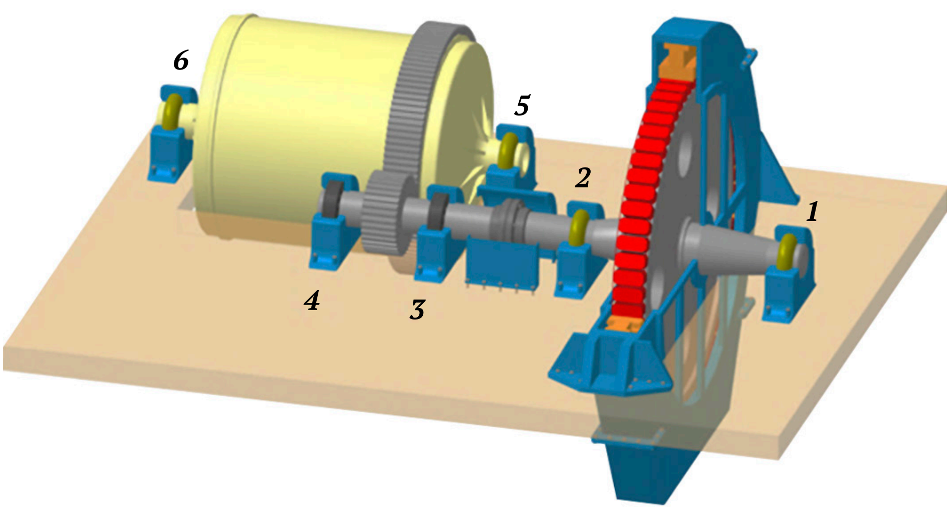

Fig. 2. Arrangement of control points on the ball mill

Table 1

Vibration parameter values for control points of the ball mill

Measurement point	RMS vibration displacement, μm	RMS vibration velocity, mm/s	Vibration acceleration, a-rms/a-peak m/s²
1H	26/1	0.7/0.6	0.4/1.6/0.4/1.3
2H	36/1	0.7/0.5	0.5/2.7/0.6/3.2
3H	398/60	10.6/8.3	5.4/28.7/14/93
4H	470/48	20.6/18.2	8.7/19.8/9/42
5H	145/8	2.9/1.5	1.6/6.3/4.2/24
6H	54/6	2.1/1.3	1.0/3.4/1.5/8.7

Note: frequency range: 2–800 Hz / 10–4000 Hz.

Measurements conducted on coal grinding mills revealed instability in vibration displacement readings within the frequency range of 10–4000 Hz, stable values for vibration velocity, and high values of vibration acceleration in the same frequency range (Table 1). The localization of elevated vibration values at points *3* and *4* suggests misalignment between the gear teeth of the pinion and the wheel, loosening of threaded connections, or damage to the foundation of the drive gear bearing supports.

The installation of a stationary vibration monitoring system on ball mills for grinding mineral raw materials required the individualized determination of technical condition category thresholds based on overall vibration levels for control points. The diagnostic task sequence required the inclusion of the following provisions.

Study of object characteristics

The mill's motor shaft connects to the drive pinion shaft through an intermediate shaft equipped with flexible couplings and measuring 3800 mm in length and 450 mm in diameter. This design allows for up to 1° of angular misalignment compensation, equating to 17.6 mm per meter of length. Asymmetrical wear of the flexible coupling elements may occur.

The torque generated by the motor is 533 kN·m. The pinion shaft is a two-support shaft with the drive gear mounted between supports. The supports are double-row spherical roller bearings (type 3680), housed in cups or mounted directly in the casing. The fixed support is positioned on the gear unit side of the re-lining drive.

The gear diameter is 1220 mm, with a linear tooth speed of 4.5 m/s. Lubrication is provided by liquid oil supplied from an oil station. Sealing is non-contact labyrinth type. Nozzles are installed for lubricating the gear wheel, differing from the original design. Technical specifications: high-speed shaft rotation frequency is 75 rpm; the pinion shaft has 46 teeth.

Vibration represents the response of a system with unknown stiffness, damping both the calculated and parasitic forces [11]. The calculated forces in the gear mesh are:

– tangential $F_t = 2M_{ct}/D_0 = 2\times533/1.156 = 922.1$ kN;

– radial $F_r = F_t\times \mathrm{tg}\alpha/\cos\beta = 922.1\times0.364/0.9945 = 337.5$ kN;

– axial $F_a = F_t\times\mathrm{tg}\beta = 922.1\times0.105 = 96.8$ kN,

where $\alpha = 20°$, $\mathrm{tg}20° = 0.364$; $\beta = 6°$, $\cos6° = 0.9945$, $\mathrm{tg}6° = 0.105$.

The pinion shaft has a mass of 11,000 kg.

During operation, the pinion shaft is pressed against the bearing support. The wear rate of the pinion shaft teeth is 5.47 times faster than that of the wheel teeth. This differential wear leads to a mismatch in the gear pairing, necessitating adjustment of the pinion shaft's position while keeping the motor stationary. This wear process is accompanied by increased wear and vibration. Gaps in the gear teeth with varying inclination angles result in the appearance of harmonic and subharmonic components in the gear mesh.

The frequency range includes:

– harmonics of the rotation frequency at 1.25 Hz;

– tooth mesh frequency at 57.5 Hz and its harmonics up to the 5th harmonic at 287.5 Hz;

– subharmonics and 1.5 harmonics are observed in centrifugal ball mill (CBM) 5.5×6.5 at 28.75 Hz (tooth subharmonic), 86.25 Hz (1.5 tooth mesh), 143.75 Hz (2.5 tooth mesh), 201.25 Hz (3.5 tooth mesh):

– bearing frequencies are nearly undetectable, except for frequencies at 8.13, 8.28, 27.81, 28.28, 29.69, 34.22, and 35.16 Hz.

The rotational motion implies that axial vibration has the lowest values, and the ratio between vertical and horizontal components is 0.8.

Vibration velocity values in the axial direction increase in the presence of axial clearances, non-parallel alignment between the gear teeth of the pinion and gear wheel, loosened threaded connections, or a "soft foot". Vibration velocity values in the horizontal direction are the highest, and increased vertical vibration may indicate loosened threaded connections or a "soft foot".

Horizontal vibration velocity values exceed vertical values by 20%. The supports, like the pinion shaft, are symmetric, so:

$$3V \approx 4V,\ 3H \approx 4H,\ 3A \approx 4A.$$

The thresholds for technical condition categories were determined for each shaft individually through statistical classification, under the assumption that coupled components are in a state defined by the damage energy potential in progressive development stages. Technical condition categories indicate the necessity and urgency of repairs. The "emergency" category signifies a loss of control over the condition. An example histogram for determining technical condition category thresholds based on overall vibration acceleration (m/s²) is provided in Fig. 3.

Based on the hypothesis of a minimal number of instances at the thresholds of technical condition categories, as shown in Fig. 3 for the pinion shaft bearings, we established the following condition thresholds: satisfactory – up to 2.0 m/s²; requires correction – 2.0–4.8 m/s²; emergency – above 4.8 m/s².

Similarly, condition category thresholds for overall vibration velocity levels were determined individually for each shaft bearing support.

Technical condition thresholds for the synchronous drive motor bearing supports are as follows: satisfactory – up to 1.8 mm/s; requires maintenance intervention – 1.8–3.0 mm/s; emergency – above 3.0 mm/s.

Technical condition thresholds for the mill drum bearing supports are as follows: good – up to 0.6 mm/s; satisfactory – 0.6–1.5 mm/s; requires maintenance intervention – 1.5–3.0 mm/s; emergency – above 3.0 mm/s.

Technical condition thresholds for the drive pinion shaft bearing supports are as follows: satisfactory – up to 4.5 mm/s; requires maintenance intervention – 4.5–11.2 mm/s; emergency – above 11.2 mm/s. These thresholds align with the recommendations of GOST ISO 10816-1–97.

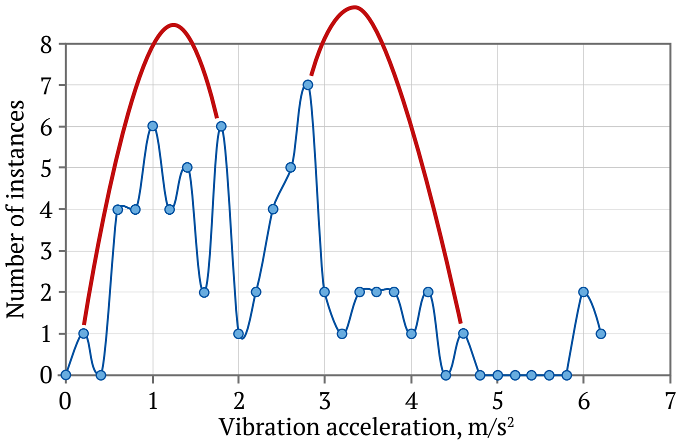

Fig. 3. Histogram of vibration acceleration instances for points *3* and *4* (pinion shaft bearings)

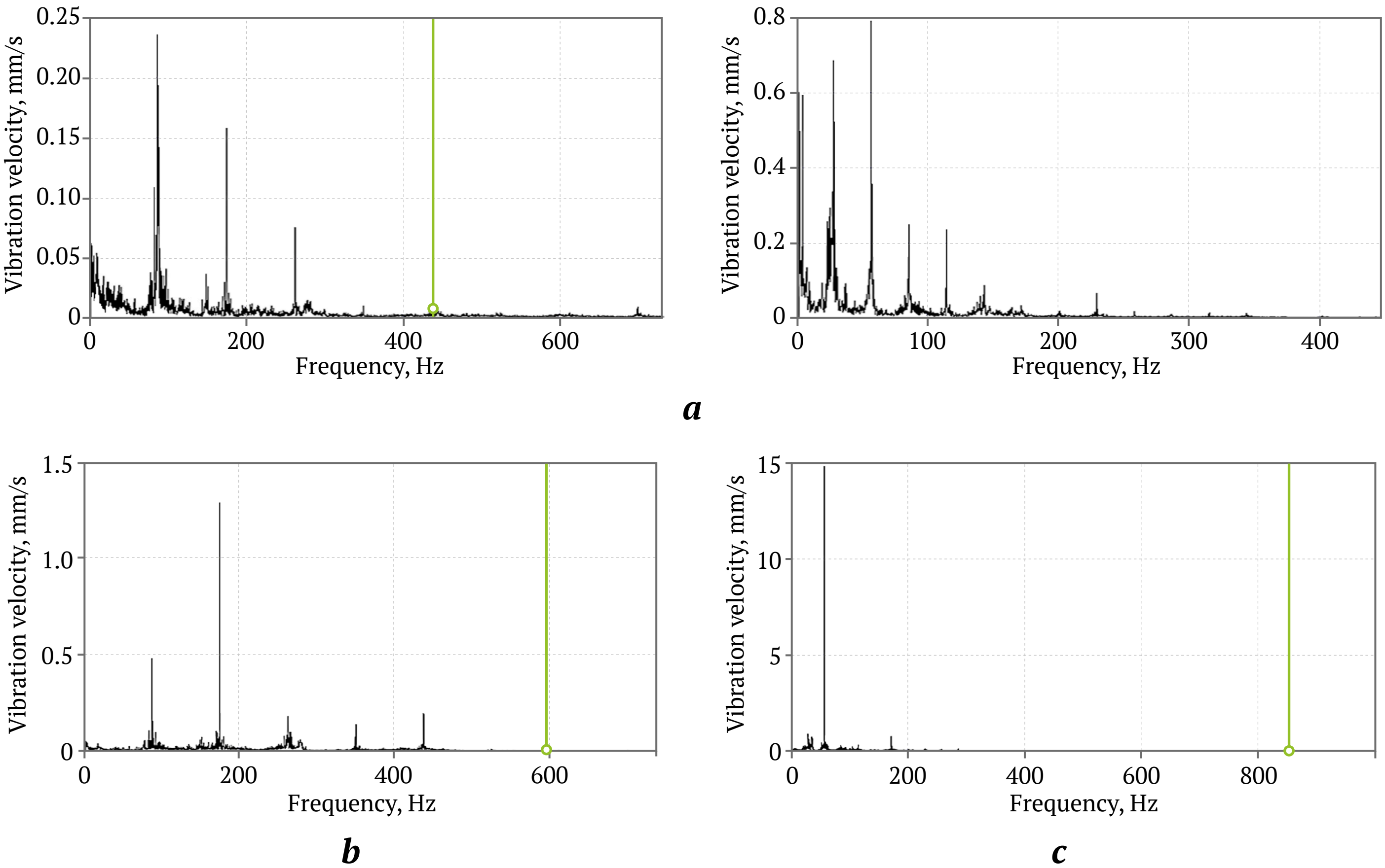

Fig. 4. Damage progression in the direct spectra of vibration velocity at points *3* and *4*:
a – good condition – harmonics with low component levels of 0.2–0.8 mm/s; *b* – satisfactory condition – increase in the amplitude of higher harmonics up to 2.0 mm/s; *c* – correction required – increase in the amplitude of the first harmonic above 4.5 mm/s, decrease in the amplitude of higher harmonics

Based on the analysis of failures and maintenance work, conclusions were drawn regarding:

– the extent of damage and possible actions;

– principles for analyzing overall vibration levels;

– the nature of damage as vibration velocity values increase in specific directions;

– diagnostic guidelines for differentiating damage types based on direct spectra.

Characteristic patterns and the sequence of damage progression were established using the direct spectra of vibration velocity (Fig. 4) and vibration acceleration.

The time-domain vibration signal allows for the observation of the emerging beat frequency mode (Fig. 5). For example, in the operation of the gear mechanism of ball mills, beats occur with a period of approximately 1.1 seconds. The beat period is determined by the formula:

$$T_{beat} = 2 \times \frac{\pi}{\Delta\omega}. \quad (5)$$

From this, we get:

$$\Delta n = \frac{60}{T_{beat}} = 54.5 \text{ rpm}.$$

Beats may arise under the following condition:

$$\Delta n = n_{motor} - n_{mill} - 0{,}5 \times n_{mill} = 54.5 \text{ rpm}.$$

This corresponds to the development of clearances in the sectors of the gear mesh.

The advantage of a permanent vibration control system lies in its continuous recording of vibration parameters. In this context, one key diagnostic criterion is the stability of the vibration profile. These profiles are unique to each mechanism at a given point in time. For a well-functioning mechanism, spectral pattern changes occur without an increase in component

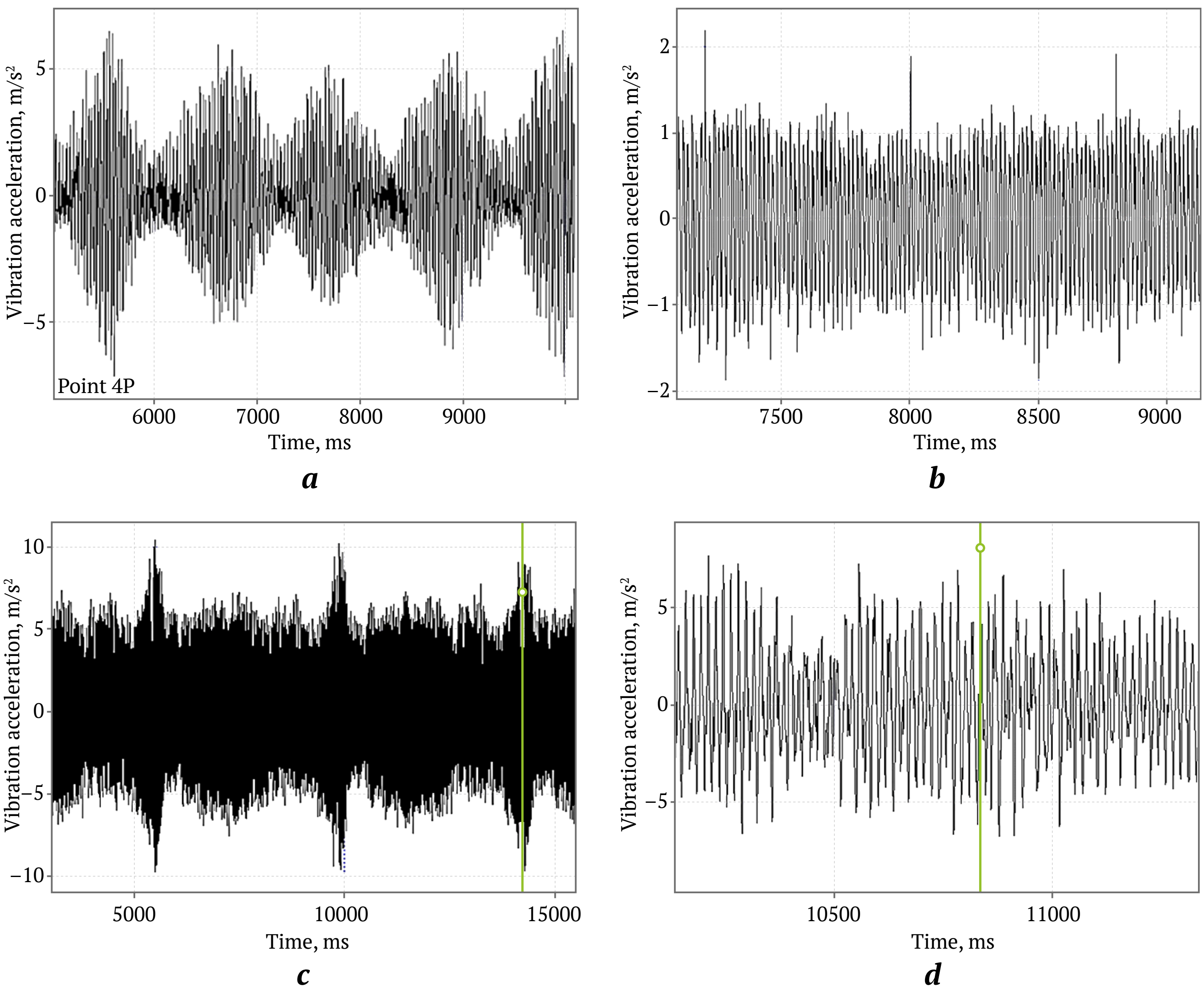

Fig. 5. Beat phenomena: *a* – clearances in gear mesh sectors; *b* – tooth spalling; *c* – bearing damage; *d* – instability in gear operation

amplitudes; only the frequencies shift. In contrast, a faulty condition is indicated by amplitude growth – first in the higher harmonics, followed by the primary rotational harmonic. Establishing standards for acceptable rates of vibration increase is essential.

The roles of portable and permanent vibration control systems differ significantly. Diagnosis with single-channel or multi-channel portable vibration analyzers provides a static assessment of the equipment's current state. This method uses the most informative control points and supplements them with additional data from visual inspection, noise analysis, localized temperature measurements, the overall thermal profile, and other organoleptic and instrumental assessments.

A permanent system, however, continuously tracks variations in diagnostic values at control points, offering a dynamic picture of the system's condition. The absence of visual inspection data, load program details, and maintenance history cannot be fully compensated by even advanced expert modules. Data from permanent systems should therefore complement, rather than compete with, the capabilities of portable systems. Any lack of maintenance history is offset by trend analysis. Here, the analysis duration depends on the diagnostic objectives and the feasibility of acquiring supplementary data. The analysis period is typically limited to the interval between major maintenance events, comparable in scope to overhauls involving key element replacements and restoring operational capacity to at least 80% of its original state.

In this case, trend analysis becomes the primary source of additional information. The following examples pertain to mechanisms like ball mills (Fig. 6), where the motor has a power of 4000 kW, a rotational speed of 75 rpm, and a drum with a diameter of 5.5 m and a length of 6.5 m, rotating at an angular speed of 13.68 rpm. The objective was to identify certain logical rules and dependencies by analyzing trends in the RMS vibration velocity within a frequency range of 10–1000 Hz at control points. The baseline interval is one month.

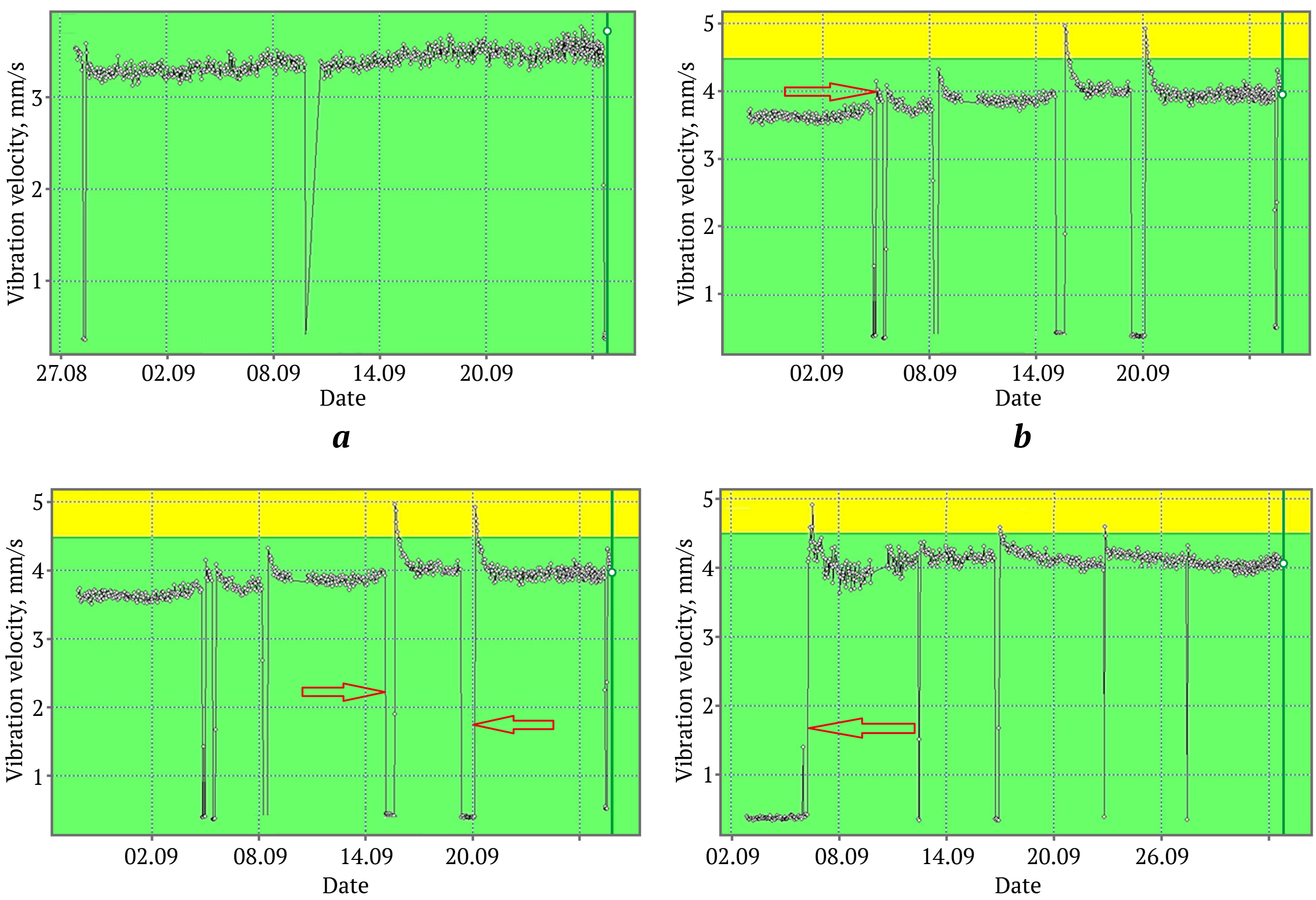

a *b* *c* *d*

Fig. 6. Stop types: *a* – short-term stops; *b* – brief startups; *c* – preventive stops; *d* – extended stops

The number of equipment stops within a month may vary randomly and can reflect certain trends in the technological process or maintenance activities.

It is important to distinguish between short-term stops (Fig. 6, *a*), brief startups (Fig. 6, *b*) resulting from disruptions in operational or maintenance processes, preventive stops (Fig. 6, *c*), and extended stops (Fig. 6, *d*). An additional parameter is the stop type, classified by downtime duration: short-term or extended. These data are used to calculate the availability factor Ka, one of the key reliability indicators of the technical system:

$$K_a = \frac{T}{T+\tau}, \tag{6}$$

where T is the operating time, and τ is the recovery time.

A high number of stops indicates either a persistent issue that is difficult to resolve or the use of these mechanisms as a 'hot' standby. In trend analysis (Fig. 7), signs emerge of brief startups and exponential decreases in vibration velocity after startup. These are accompanied by downtimes lasting several days.

In extended operation, several modes can be identified (Fig. 8): stable operation (Fig. 8, *a*), decreasing vibration velocity (Fig. 8, *b*), increasing vibration velocity (Fig. 8, *c*), and unstable operation (Fig. 8, *d*). To assess instability, it is essential to consider the range of peak values, as well as the causes of increases and decreases in vibration velocity, recorded at the sensor polling interval of 20 minutes. Analyzing long-term trends can be used to address operational challenges and optimize the operating mode.

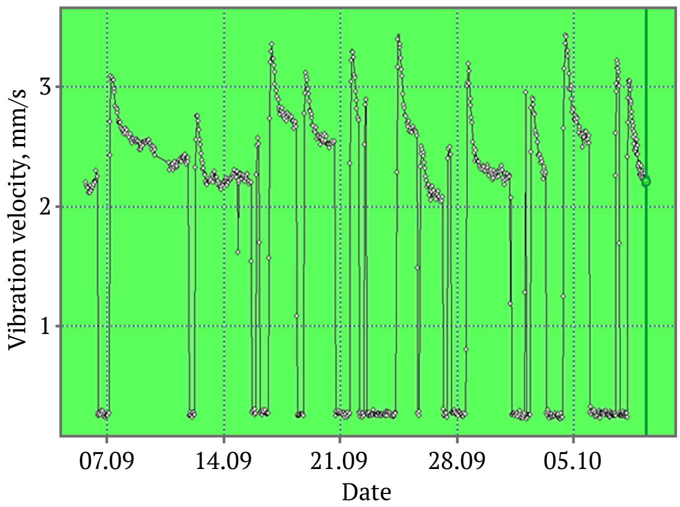

Fig. 7. Vibration velocity trend at point 4P of the ball mill

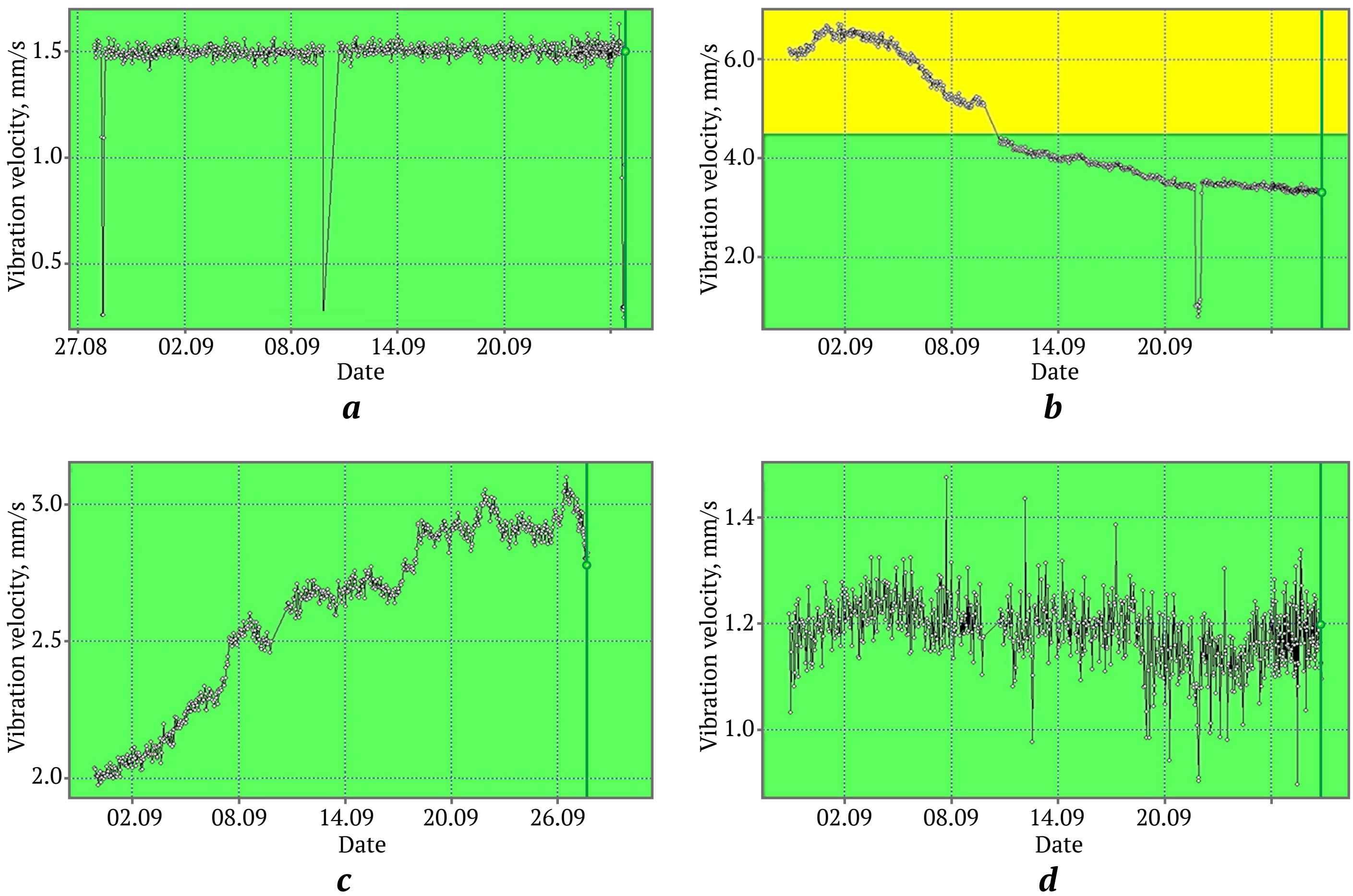

Fig. 8. Operating modes: *a* – stable; *b* – decreasing vibration velocity; *c* – increasing vibration velocity; *d* – unstable

MINING SCIENCE AND TECHNOLOGY (RUSSIA)
ГОРНЫЕ НАУКИ И ТЕХНОЛОГИИ
2024;9(4):420–432
eISSN 2500-0632
https://mst.misis.ru/

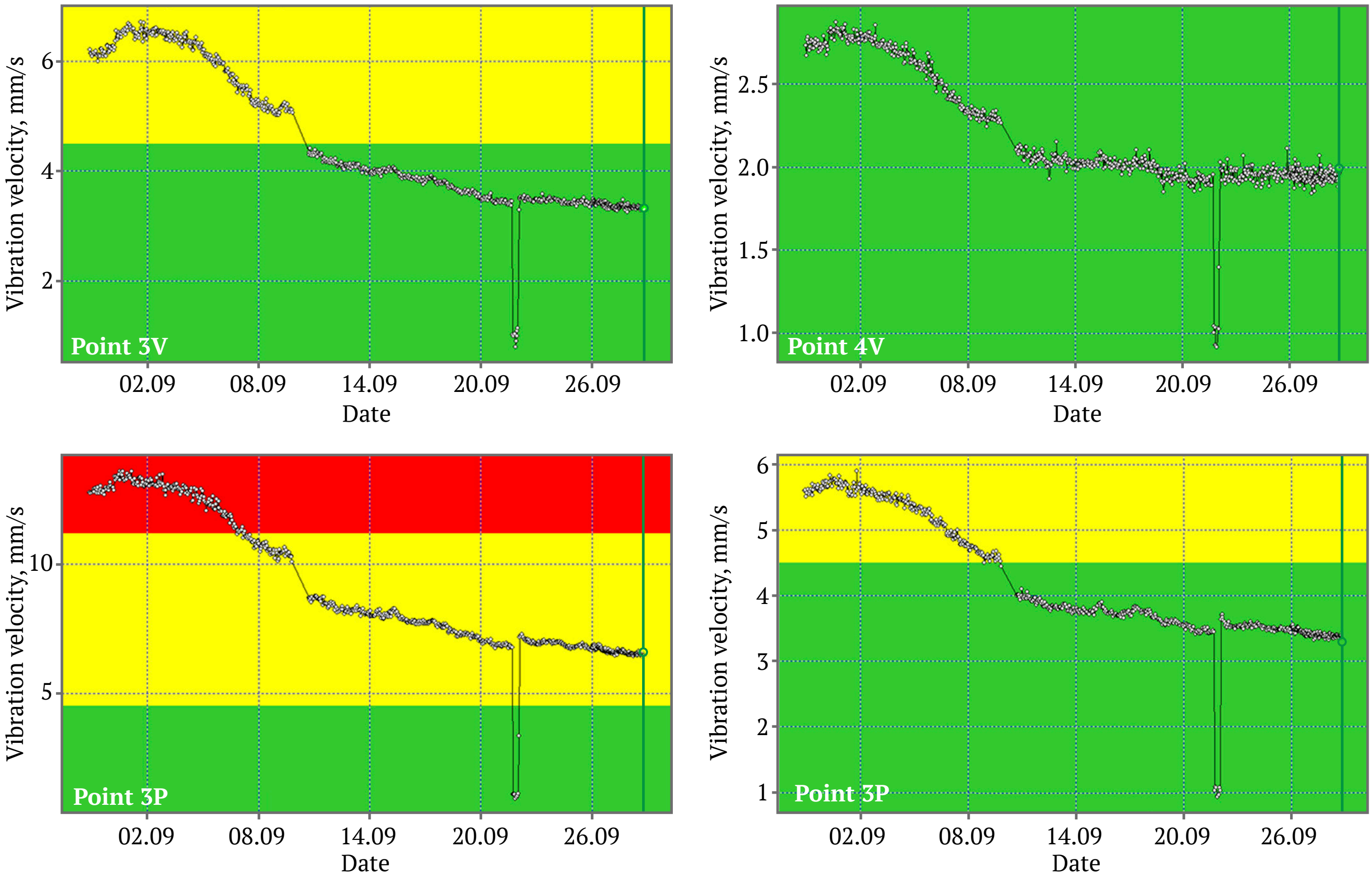

Fig. 9. Vibration velocity trends for the pinion shaft bearing assemblies in September

Each operating mode clearly has its own causes. Stable operation corresponds to the stability of the technical condition and does not require any additional maintenance or repair actions. Decreasing vibration velocity may occur due to ball wear and the resulting decrease in the unbalanced force acting on the mill. Increasing vibration velocity indicates the presence of additional forces or a reduction in bearing support stiffness due to loosening of threaded connections.

General trends may be observed across the entire machine or within specific assemblies. Fig. 9 shows long-term vibration velocity trends at the pinion shaft bearings of the ball mill over an extended observation period (more than two weeks) for several key points, such as 3*V*, 4*V*, 3*P*, and 4*P*. As seen in Fig. 9, there is a positive trend of decreasing vibration velocity during the observation period.

In the vibration velocity trends, two segments can be identified. The first segment is a descending line, and the second is a sharp drop in vibration velocity readings, which can be attributed to a temporary shutdown of the ball mill's electromechanical system (EMS). After the EMS is restored, the downward trend in vibration velocity resumes. Another diagnostic indicator is the transition of vibration velocity values: from the red zone to the yellow, from the yellow to the green, or remaining within the green zone – the zone of permissible values.

The examples provided illustrate possible realizations of vibration velocity values over time in a technical system. Key indicators must be formalized and integrated into expert modules to support decision-making. For instance, accumulating data on instances of brief vibration velocity exceedances, introducing a stability indicator, and assessing the post-repair condition. To evaluate the motor's condition, a vibration sensor should be installed on its housing.

Diagnosis of a ball mill driven by an induction motor

The presence of a gear unit in the design of this mill increases the number of control points for vibration measurement (Fig. 10). Varying replacement intervals for gear wheels[7] necessitate high-quality

[7] Troshina A.G. Modernization of the drive system of operated horizontal cement mills. Dissertation Abstract for the Candidate of Technical Sciences. Defense Institution: Tula State University, Tula; 2013.

eISSN 2500-0632
https://mst.misis.ru/

spare part production on equipment from a single manufacturer. The results of overall vibration level measurements are presented in Table 2. Despite the substantial size of the gear unit, vibration levels are relatively high across the entire assembly (acceptable limit: 11.2 mm/s), which may be due to increased compliance of the foundation or the gear pair being manufactured by two different companies.

The analysis of the overall vibration velocity measurement results indicates that the gear unit is in an emergency state, and operation should cease until the identified defects are resolved. Increased axial vibration suggests the presence of bending during rotation. This is further confirmed by uneven vibration velocity values in two mutually perpendicular directions.

Determining the informative frequencies of potential damage is feasible with a simple calculation, given the known kinematic scheme. We identify the rotational and gear mesh frequencies as follows:

– high-speed shaft: first harmonic – 16.6 Hz, gear mesh frequency – 612 Hz;

– intermediate shaft: first harmonic – 7.6 Hz, gear mesh frequencies – 613 Hz / 174 Hz;

– low-speed shafts: first harmonic – 2.1 Hz, gear mesh frequencies – 174 Hz / 65 Hz.

In examining the direct spectra (Fig. 11), the developed diagnostic rules for identifying spectral patterns were confirmed, though the appearance of a 729 Hz frequency generating a harmonic series was unexpected. The exceeded amplitude of higher harmonics at the 612 Hz gear mesh frequency clearly indicates damage progression. High foundation compliance was confirmed by contour diagram analysis. The 729 Hz frequency was identified as a resonant frequency.

Table 2

Vibration parameter values for the gear unit control points of the ball mill

Measurement point	RMS vibration velocity by direction (frequency range 10–1000 Hz), mm/s		
	Vertical	Horizontal	Axial
1	6.89	9.91	12.18
2	12.73	9.55	7.01
3	7.17	5.96	10.74
4	7.36	9.45	10.54
5	5.64	8.00	9.54
6	13.73	8.41	8.16
7	4.81	7.77	–
8	9.35	7.04	11.25

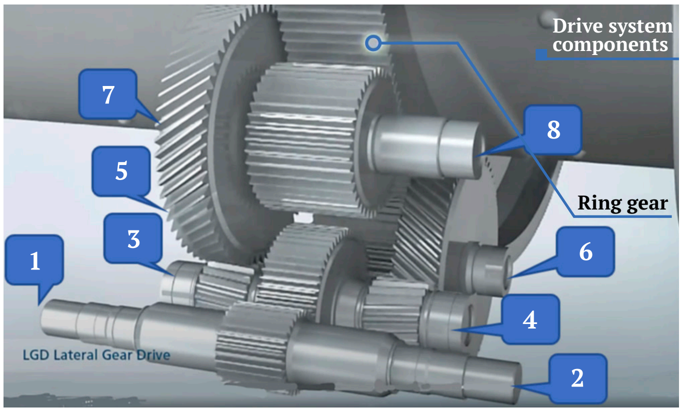

Fig. 10. Arrangement of control points for measuring vibration in the gear unit

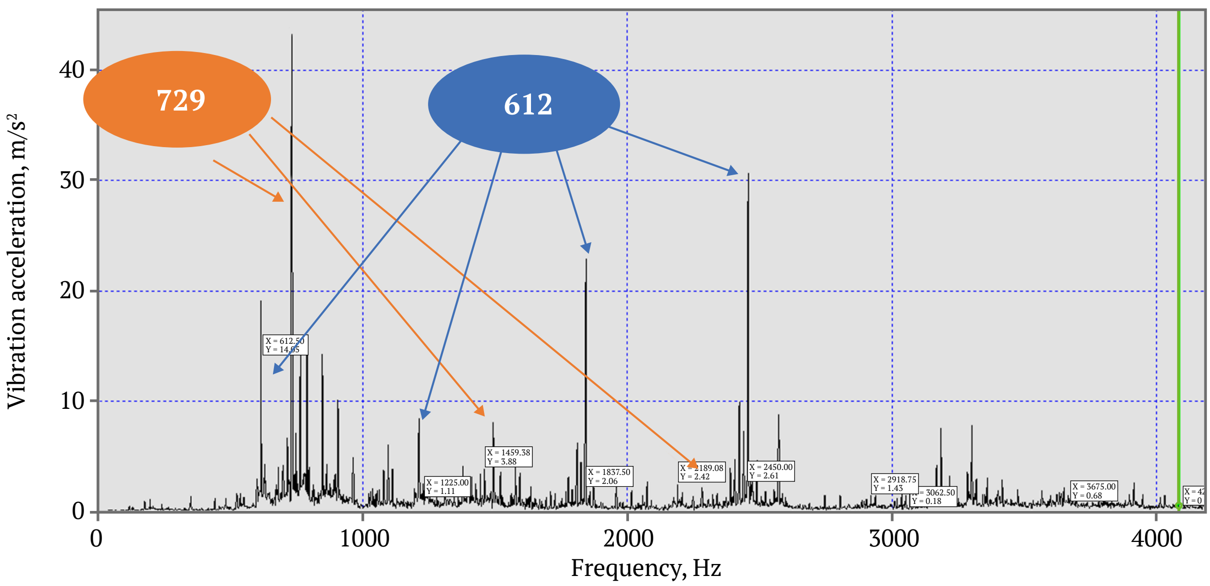

Fig. 11. Direct spectrum of vibration acceleration in the frequency range 10–4000 Hz

Over 10 days of operation, critical increases in vibration were observed at specific frequencies:

– 65 Hz – amplitude 2.0 mm/s, second harmonic at 130 Hz with amplitude 1.5 mm/s: This indicates increased vibration in the gear mesh zone (third and fourth stages), with progressively worsening misalignment;

– 612 Hz – amplitude 9.5 mm/s: A 2.5-fold increase over a short period, suggesting a shift in the technical condition category;

– 1224 Hz (second harmonic of the 612 Hz frequency) – component amplitude rose over 12-fold, from 0.79 mm/s to 9.4 mm/s, indicating increased misalignment or eccentricity in the gear mesh zone;

– 726 Hz – component amplitude remained unchanged, confirming this frequency's resonant nature.

Conclusions

1. For the first time, an integrated analysis of the key interrelated parameters of ball mills – Q, P, W, Q_{mel}. The analysis of correlation dependencies for the graphs $Q = f(V_b)$; $P = f(V_b)$; $W = f(D_b)$; and $Q_{mel} = f(V_b)$ enables equipment design and operations specialists to make more informed choices regarding the technical parameters and operating modes of both current and planned-for-commissioning ball mills.

2. The combination of shafts with varying rotational frequencies and stiffness in ball mill designs requires individualized determination of technical condition category thresholds. Based on vibration velocity and acceleration trends over time, an analysis is performed to assess the electromechanical system (EMS) components' susceptibility to damage and operational feasibility under current loads.

3. The technical condition of ball mills can be adequately assessed through overall vibration level analysis, direct trends in vibration velocity and acceleration, analysis of time-domain realizations of the vibration signal, and both short-term and long-term trend analysis. Vibration velocity trends displayed in color-coded zones (red, yellow, green) at any given time allow for the assessment of the system's condition and decision-making regarding potential repair actions.

4. Combining the capabilities of permanent vibration monitoring with multi-channel portable diagnostic tools provides timely information on equipment condition, allowing for effective planning of maintenance and repair work. Comprehensive conclusions on technical condition require data on production load, electrical load, thermal fields, visual inspections, and completed maintenance and repair activities.

5. The examples provided demonstrate the need to classify key trend types and establish logical decision rules for consideration by the expert system in decision-making. To avoid resonant and sub-resonant frequencies in the ball mill EMS, it is recommended to use frequency-controlled drives (FC-IM, FC-SM) for material grinding of specific fractions.

References

1. Rozenberg G.Sh., Madorskij E.Z., Golub E.S. et al. *Vibration diagnostics*. Monograph. Rosenberg G.Sh. (Ed.) St. Petersburg: St. Petersburg Energy Institute for Advanced Studies; 2003. 284 p. (In Russ.)
2. Shirman A.R., Solovyov A.D. *Practical vibration diagnostics and monitoring of the condition of mechanical equipment*. Moscow; 1996. 276 p. (In Russ.)
3. Rusov V.A. *Spectral vibration diagnostics*. Perm: Vibro-Center; 1996. 176 p. (In Russ.)
4. Sharapov R.R. *Closed-cycle ball mills*. Belgorod: BSTU Publ. House; 2008. 269 p. (In Russ.)
5. Huang P., Jia M., Zhong B. Study on the method for collecting vibration signals from mill shell based on measuring the fill level of ball mill. *Mathematical Problems in Engineering*. 2014;2014:72315. https://doi.org/10.1155/2014/472315
6. Amosov E.A. Some regularities of ball mills work. *Vestnik of Samara State Technical University. Technical Sciences Series*. 2012;(1):219–222. (In Russ.)
7. Yoshida T., Kuratani F., Ito T. Taniguc K. Vibration characteristics of an operating ball mill. *Journal of Physics Conference Series*. 2019;1264(1):012016. https://doi.org/10.1088/1742-6596/1264/1/012016
8. Troshina A.G. Modernisation of drives of horizontal ball mills. *Journal Cement and Its Applications*. 2009;(3):26–31. (In Russ.)
9. Su Zh., Wang P., Yu X., Lv Zh. Experimental investigation of vibration signal of an industrial tubular ball mill: Monitoring and diagnosing. *Minerals Engineering*. 2008;21(10):699–710. https://doi.org/10.1016/J.MINENG.2008.01.009
10. Gauthier N.K., Chiementin X., Rasolofondraibe L., Boujelben A. *Diagnostic de défauts d'engrenages assisté par jumeau numérique "Application à la surveillance des broyeurs à boulets"*. May 2022. https://doi.org/10.13140/RG.2.2.28847.41129
11. Logov A.B., Zamaraev R.Yu. *Mathematical models for diagnosing unique objects*. Novosibirsk: Publ. House SB RAS; 1999. 228 p. (In Russ.)

Information about the authors

Vladimir F. Borisenko – Cand. Sci. (Eng.), Associate Professor of the Department of Electric Drive and Automation of Industrial Installations, Donetsk National Technical University, Donetsk, Russian Federation; AuthorID 850557; e-mail borissenko.vp@gmail.com

Vladimir A. Sidorov – Dr. Sci. (Eng.), Professor of the Department of Mechanical Equipment of Ferrous Metallurgy Plants, Donetsk National Technical University, Donetsk, Russian Federation; ORCID 0000-0001-6794-7838, Scopus ID 55424503900; e-mail sidorov_va58@mail.ru

Andrey E. Sushko – Cand. Sci. (Eng.), General Director, SPA DIATECH LLC, Moscow, Russian Federation; ORCID 0009-0003-3113-5194; e-mail as@diatechnic.ru

Vyacheslav N. Rybakov – vibration diagnostics of the 3rd level, Head of the Diagnostics Service, PromTEK R&D LLC, Samara, Russian Federation; e-mail rvn@npp-promtek.com

Received 25.10.2023
Revised 24.01.2024
Accepted 25.03.2024